THESE DE DOCTORAT DE L'UNIVERSITE PARIS 6

Spécialité :

Physique des solides

présentée par

Philippe LAFARGE

pour obtenir le grade de **DOCTEUR de l'UNIVERSITE PARIS 6**

Sujet de la thèse :

MACROSCOPIC CHARGE QUANTIZATION IN METALLIC NANOSTRUCTURES

Soutenue le 30 novembre 1993

devant le jury composé de MM:

M. DEVORET
H. GRABERT
P. MARTINOLI
J. E. MOOIJ
B. PANNETIER
J.-F. PETROFF

à Françoise et Claude

REMERCIEMENTS

Je tiens à remercier tout particulièrement Michel Devoret, Daniel Esteve et Cristian Urbina. Au sein du groupe "Quantronique", ils ont su créer une ambiance de travail unique, à la fois amicale et stimulante, et j'ai pu y trouver les conditions idéales pour un travail de thèse.

J'exprime mes profonds remerciements à Pief Orfila non seulement pour sa contribution technique multiforme à toutes les étapes des expériences mais aussi pour sa disponibilité permanente et son soutien amical.

Ma reconnaissance va également à Philippe Joyez, mon compagnon de thèse pendant un peu plus de deux ans. Durant notre travail en commun, j'ai apprécié sa collaboration sans faille qui fut aussi agréable qu'efficace. Je remercie aussi Hugues Pothier avec qui j'ai partagé ma première année de thèse et qui m'a initié aux secrets de l'électronique à un électron, Emmanuel Turlot qui m'a fait découvrir le laboratoire et Edwin Williams pour sa collaboration lors de la première expérience de boîte à électrons.

Pour de nombreuses et fructueuses discussions, je désire remercier Vincent Bouchiat, Andrew Cleland, Thorsten Holst, Antoine Filipe, Morvan Salez et Denis Vion. A plusieurs occasions, j'ai bénéficié des connaissances et des conseils avisés de Hermann Grabert, John Martinis et Hans Mooij, qu'ils en soient ici remerciés.

Je remercie Daniel Beysens de m'avoir permis d'effectuer ce travail de thèse dans le Service de Physique de l'Etat Condensé.

Je remercie Hermann Grabert, Piero Martinoli, Hans Mooij, Bernard Pannetier et Jean-François Petroff d'avoir accepté de faire partie du jury.

TABLE OF CONTENTS

1. INTRODUCTION 1

2. REVIEW OF THEORETICAL PREDICTIONS ON MACROSCOPIC CHARGE QUANTIZATION IN THE SINGLE ELECTRON BOX 13
    2.1 The normal electron box 13
        2.1.1 The Coulomb staircase and the Coulomb sawtooth at T=0 13
        2.1.2 Macroscopic charge quantization at finite temperature 17
        2.1.3 Quantum fluctuations of the island charge 21
        2.1.4 Tunneling rate in the electron box 27
    2.2 The normal/superconducting electron box 34
        2.2.1 Odd-even symmetry breaking and 2e-quantization in the normal/superconducting electron box at T=0 35
        2.2.2 Effect of finite temperature 38
        2.2.3 Calculation of the odd-even free energy difference $D(T,H)$ 40
        2.2.4 Influence of the magnetic field 42
        2.2.5 Observability of the 2e-quantization of the macroscopic charge 47
    2.3 The superconducting electron box 48
        2.3.1 Josephson coupling between the charge states of the box 48
        2.3.2 Effect of the electromagnetic environment 52

3. EXPERIMENTAL RESULTS ON THE ELECTRON BOX 59
    3.1 Normal case 59
        3.1.1 Paper 1: direct observation of macroscopic charge quantization 59
    3.2 Superconducting case 77
        3.2.1 Paper 2: measurement of the even-odd free energy difference of an isolated superconductor 77
        3.2.2 Paper 3: 2e-quantization of the charge on a superconductor 89

4. CHARGE TRANSFER ACCURACY 101
    4.1 Theoretical Predictions 101
        4.1.1 Paper 4: passing electrons one by one: is a 10^{-8} accuracy achievable? .. 101
        4.1.2 Paper 5: nondivergent calculation of unwanted high-order tunneling rates in single-electron devices 118

4.2 Experimental results 141
4.2.1 Paper 6: Direct observation of macroscopic charge quantization: a Millikan experiment in a submicron solid state device 141

5. CONCLUSION 151

APPENDIX 1: total energy of a general tunnel junctions circuit 155
APPENDIX 2: fabrication of the superconducting/normal tunnel junctions 163
APPENDIX 3: the single electron transistor 171

1. INTRODUCTION

The aim of this work is to demonstrate experimentally the quantization of the charge on a metallic electrode connected to an electron reservoir by a tunnel junction and to show that this phenomenon can be used to transfer electrons one by one from one electrode to another with metrological accuracy.

From the famous Millikan's experiment performed in 1911 [1], we know that the electrical charge on an isolated body is quantized. To demonstrate charge quantization, Millikan used small charged oil droplets. The principle of the experiment was to measure the speed of a single droplet in a gravitational field combined with a variable vertical electrical field. These measurements give access to the mass and the charge of the oil droplet. Millikan showed that this charge is an integer multiple of an elementary electrical charge, $e \cong 1.6\ 10^{-19}$ C. In his experiment, the charge carried by the oil droplets resulted from the irradiation with α particles produced by a Radium source. Although the charge deposited on the droplet was quantized, it was not controlled. Is it possible to transpose such an experiment in a solid state device and, moreover, to control the stored charge with an externally applied voltage?

Surprisingly, the discreteness of the charge carriers does not appear in the usual behavior of electronic circuits. One may think the reason is that any electronic signal involves too large a number of electrons but there is in fact a more profond reason: the conduction electrons are delocalized and form a quantum fluid. To illustrate this effect, let us consider the simple circuit consisted of a capacitor C_S to which we apply a voltage U by perfect leads (see Fig. 1.1a). The charge Q stored on the capacitor is equal to $C_S U$ and can be precisely adjusted to any arbitrarily small value by varying the applied voltage. Although a charge is transferred from the source to the surface of the capacitor plate, this quantity is a continuous variable. It corresponds to the collective displacement of the charge carriers in the metal with respect to the ionic background. Hence, the charge on the capacitor is not constrained to be an integer number of electrons. The charge quantization can only appear if the circuit includes an isolated piece of metal. This can be done by opening a switch placed between the voltage source and the capacitor (see Fig. 1.1b). One of the capacitor plates is then disconnected from the circuit and forms an isolated electrode. Like the oil droplet of the Millikan's experiment, this electrode contains a well defined number of electrons and its total charge q is equal to an integer multiple of the electron charge $-e$. As soon as one wants to change this charge, a difficulty arises. Since there is no possibility to transfer electrons from the source to the isolated electrode, the charge q remains constant and cannot be tuned subsequently with the applied voltage U. Obviously, we can connect the switch again to modify q, but simultaneously, we will suppress the quantization of the electrode charge.

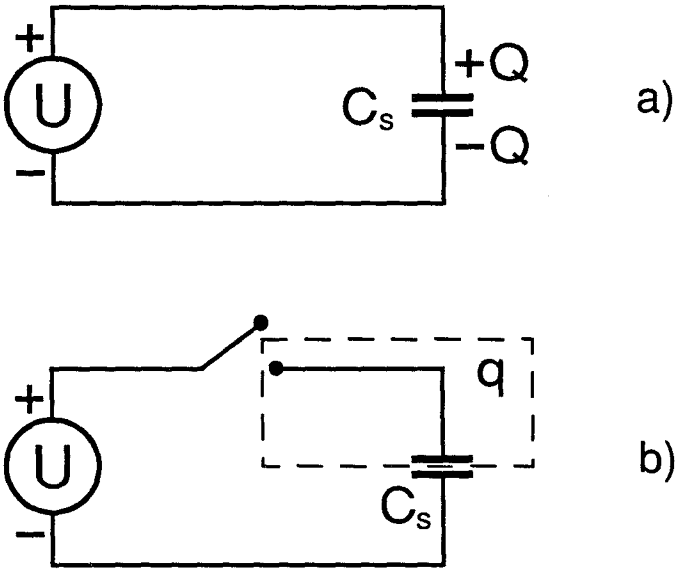

Fig. 1.1 a) *Capacitor connected to a voltage source. The charge* $Q = C_s U$ *on the capacitor plate is not quantized.* b) *If one opens a switch between the voltage source and the capacitor, the portion of the circuit inside the dashed line box contains a charge q which is quantized but fixed.*

How can we combine charge quantization and charge transfer? We certainly need a more elaborate device than a usual switch. A highly resistive tunnel junctions provides a way to maintain both the quantization of the electrode charge and the possibility to vary it.

A tunnel junction consists of two metallic electrodes separated by a thin insulating layer (see Fig. 1.2). In such a device, the mechanism of conduction is the tunnel effect of electrons through the insulating barrier. A tunnel junction is characterised by two parameters, its capacitance C and its tunnel resistance R_t. This latter quantity is determined experimentally by the current $I = V/R_t$ which flows through the device when a voltage V is imposed to the junction. The tunnel resistance is a phenomenological macroscopic parameter which depends on the area and the thickness of the insulating layer. Although it has the dimension of a resistance, R_t does not correspond to any dissipative process like the resistance value in a usual resistor. The tunnel resistance can be expressed through the relation $R_t^{-1} = \left(2e^2/h\right)N\mathcal{T}$, where N is the number of conduction channels and $\mathcal{T}$ is the transmission coefficient of the barrier for each channel, assumed to be independent of the channel index.

Elaborate theoretical considerations [2,3] show that if the junction tunnel resistance R_t is much larger than the resistance quantum $R_K = h/e^2 \cong 25.8\ \mathrm{k\Omega}$, electrons are localised on either side of the insulating barrier and electron tunneling through the barrier is a stochastic Poisson process with a rate given, at zero temperature, by $\Delta E/R_t e^2$, where ΔE is the energy difference before and after the tunnel event. Thus, provided $R_t >> R_K$, the charge of an isolated electrode connected to an external electron reservoir by such a tunnel junction will remain quantized. Apart from its tunneling properties, the junction behaves like a capacitor with a capacitance C.

Let us replace, in the simple circuit of Fig. 1.1b, the switch by a tunnel junction with a tunnel resistance such that $R_t >> R_K$. Therefore, we maintain the quantization of the charge of the isolated electrode but the transfer of electrons from the voltage source is now allowed by tunnel events across the junction. We have called "electron box" [4] this basic circuit consisting of a tunnel junction and a capacitor placed in series with a voltage source (see Fig. 1.3). Since the electrons can enter and leave the electrode formed between the junction and the capacitor, this electrode is isolated in the sense that it is surrounded everywhere by insulating material. We call "island" this particular kind of electrode for which the instantaneous charge only varies by tunnel events and remains quantized in units of e.

Although the instantaneous number n of excess electrons on the island is quantized, the average number $\langle n \rangle$ may vary smoothly with the gate voltage U. The really observable quantity is the macroscopic charge of the island $\langle -ne \rangle$. If we want $\langle n \rangle$ itself to be quantized, we must

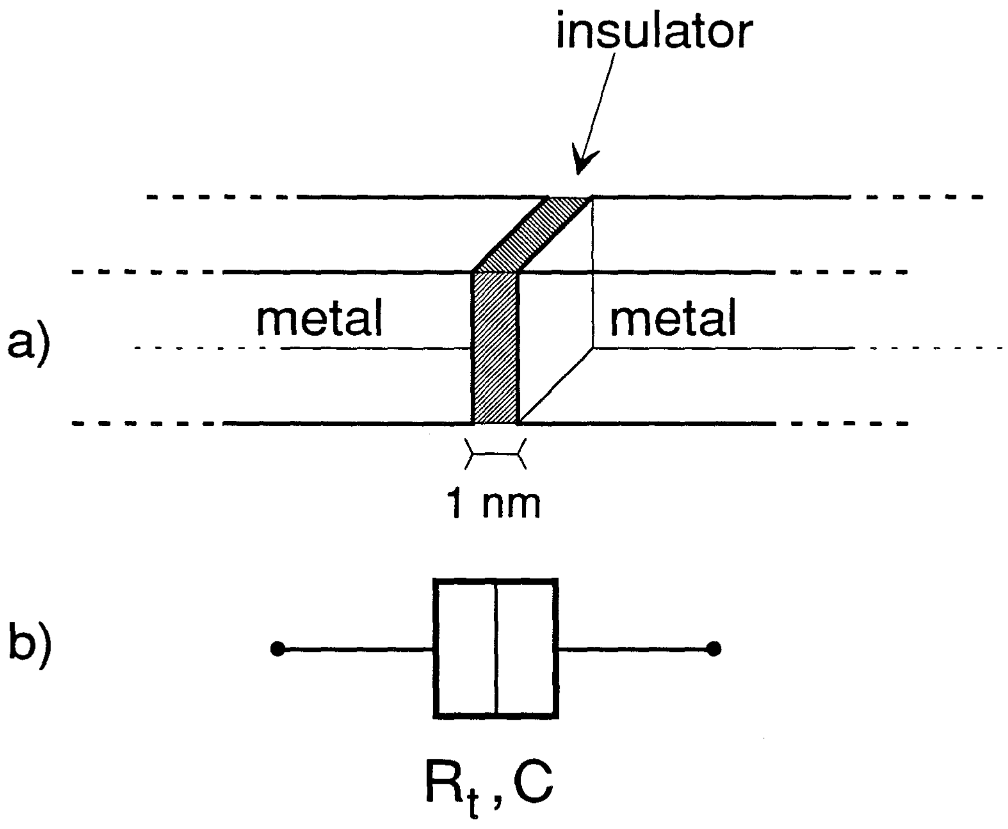

Fig 1.2 a) *A tunnel junction consists of two metallic electrodes separated by a thin insulating layer.* b) *In circuit schematics, a tunnel junction is represented by a double box symbol and characterized by its tunnel resistance R_t and its capacitance C.*

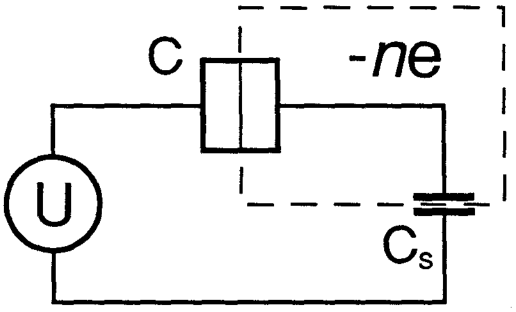

Fig. 1.3 *Circuit diagram of the electron box which consists of a tunnel junction and a capacitor placed in series with a voltage source. The metallic electrode between the junction and the capacitor forms an "island" which contains a well defined number of excess electrons.*

suppress the thermal fluctuations of the island charge. The characteristic energy of the charge quantization phenomenon is the charging energy $E_c = e^2/2(C+C_s)$ equal to the energy cost of putting one excess electron in the island when there is no voltage applied. Charge quantization requires that the charging energy E_c is much larger than the characteristic energy $k_B T$ of the thermal fluctuations where k_B is the Boltzmann constant. The condition $E_c >> k_B T$ ensures that the thermal fluctuations of the island charge are negligible. A circuit temperature of about $T \approx 30$ mK is attainable with a dilution refrigerator. This implies that the island capacitance $C_{island} = C + C_s$ must be lower than 1 fF to satisfy the latter inequality. Such low capacitance is achieved by using tunnel junctions with a typical area of 100 nm × 100 nm. We have fabricated this type of nanoscale junctions using a combination of electron beam lithography and shadow evaporation through a suspended mask [5]. The junctions are located at the overlap between two metallic thin films. A scanning electron microscope photograph of such a junction is shown on Fig. 1.4. The bottom metallic electrode is made of aluminum, the insulating layer is obtained by oxidizing the surface of the aluminum layer, and the top electrode is made either of aluminum or copper alloyed with 3 % of aluminum in weight. We have thus fabricated two different types of nanostructures: Al/AlOx/Al or Al/AlOx/Cu. To measure the charge increment of the island, we have used a single-electron transistor [6] as an electrometer. This device is fabricated together with the box and is capacitively coupled to the island of the box. The coupling capacitance C_c is sufficiently small not to affect the behavior of the single-electron box and we assume that the temporal average charge $\overline{n}$ measured by the electrometer is equal to the thermal ensemble average $\langle n \rangle$.

When plotted versus the gate voltage U, the average number $\langle n \rangle$ of excess electrons in the island takes the form of a staircase: the "Coulomb staircase" depicted on Fig. 1.5. The number of electrons adjusts itself to minimize the total energy of the circuit given by $E = E_c(n - C_s U/e)^2$. At $T = 0$, the staircase steps are perfectly flat and each one corresponds to a fixed number of electrons inside the island. At high temperature ($k_B T >> E_c$), one finds $\langle n \rangle = C_s U$, the island macroscopic charge quantization is suppressed and the junction acts as a short circuit. Note that the instantaneous charge of the island is still quantized; only the average charge takes non integer values. At lower temperature ($E_c << k_B T$), the staircase is

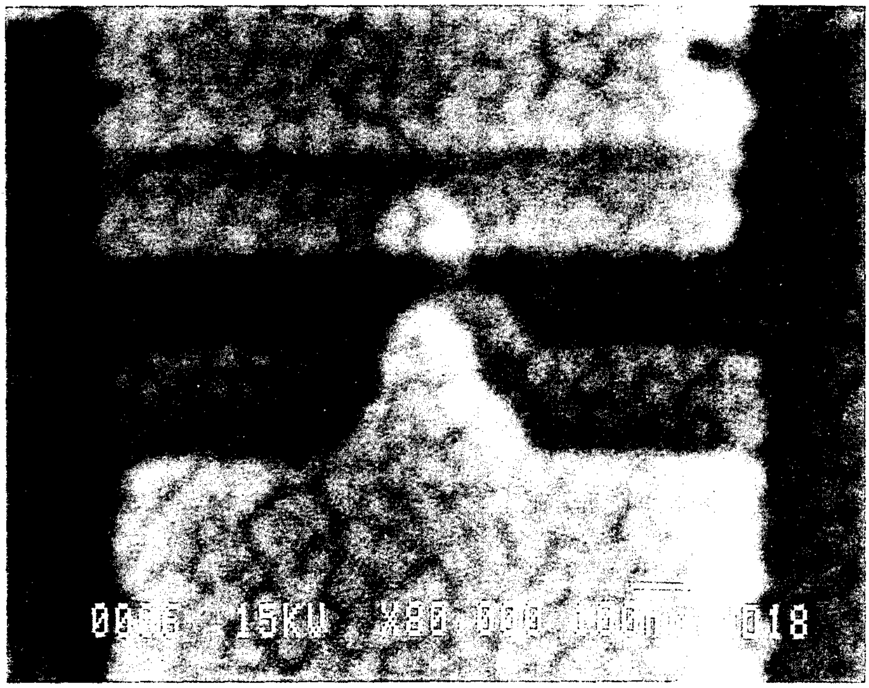
15KU
X80,000
018

Fig. 1.4 *Scanning electron microscope photograph of an aluminum/aluminum-oxide/copper tunnel junction.*

just slightly rounded (see Fig. 1.5) and the central part of the steps corresponds to a well defined number of electrons inside the island. The voltage required to inject one electron in the island is equal to the period of the staircase given by e/C_s. This latter quantity is in the mV range for the gate capacitance C_s of the order of 100 aF. Hence, provided $E_c << k_B T$, one can precisely control the number of electrons inside the island with a macroscopic voltage. We have called this effect "macroscopic charge quantization" because the island charge is distributed over a macroscopic number of atoms. It is important to note that unlike the usual charge quantization of an isolated piece of matter, the macroscopic charge quantization defined above is only exact in the limit $T \rightarrow 0$, $R_t/R_K \rightarrow \infty$. While the former limit corresponds to the suppression of thermal fluctuations, the latter limit corresponds to the suppression of the quantum fluctuations due to the tunnel process itself [3].

If we consider now a single-electron box with an island made of superconducting material, the previous analysis must be modified since electrons are paired in a superconductor. If we assume that the island is a perfect superconductor following the BCS theory [7], all the electrons are paired and the energy cost of an unpaired electron is at least equal to the superconducting energy gap Δ [8]. For $\Delta > E_c$ and at low temperature, electrons should be transferred two by two from the electron reservoir into the superconducting island by creating or suppressing Cooper pairs in the island. As we have shown, the superconducting electron box indeed exhibits a $2e$-quantization of the island charge [9]. In this regime, the height and the length of the staircase steps are twice as large as in the non-superconducting case, as shown in Fig. 1.6. However, if the charging energy E_c is sufficiently large with respect to Δ, Cooper pairs can be broken and electrons enter the island one by one [10]. In that case, we observe that the staircase is asymmetric with long steps corresponding to the states with an even number of electrons inside the island and short steps corresponding to an odd number of electrons (see Fig. 1.6). This odd-even asymmetry [10,11,12] will persist when the temperature is increased until the odd-even free energy difference $D(T)$ vanishes. This quantity $D(T)$ depends strongly on the temperature through the relation $D(T) \approx \Delta - k_B T \ln N_{eff} + O\left(T^2\right)$ [11] where N_{eff} is the effective number of states available for excitations in the island. From the staircase asymmetry we can measure the odd-even free energy difference [10]. In this regime,

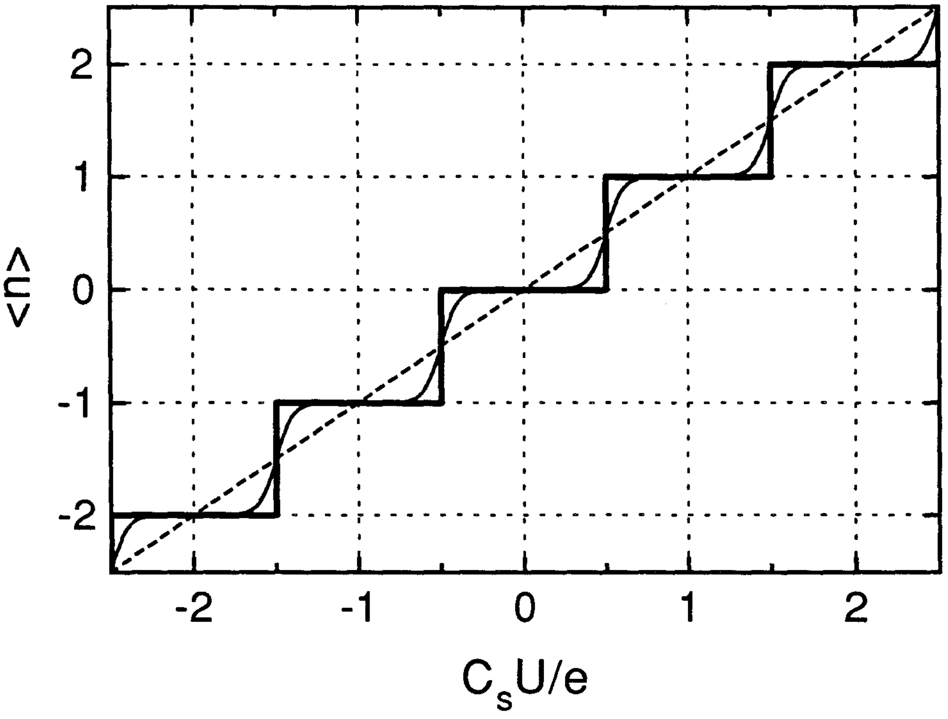

Fig. 1.5 a) *Theoretical variations of the average number* $\langle n \rangle$ *of excess electrons in the island of the electron box as a function of the reduced charge* C_sU/e *when* $T = 0$ *(solid line), when* $k_BT/E_c = 0.1$ *(thin line), and in the limit* $k_BT >> E_c$ *(dashed line).*

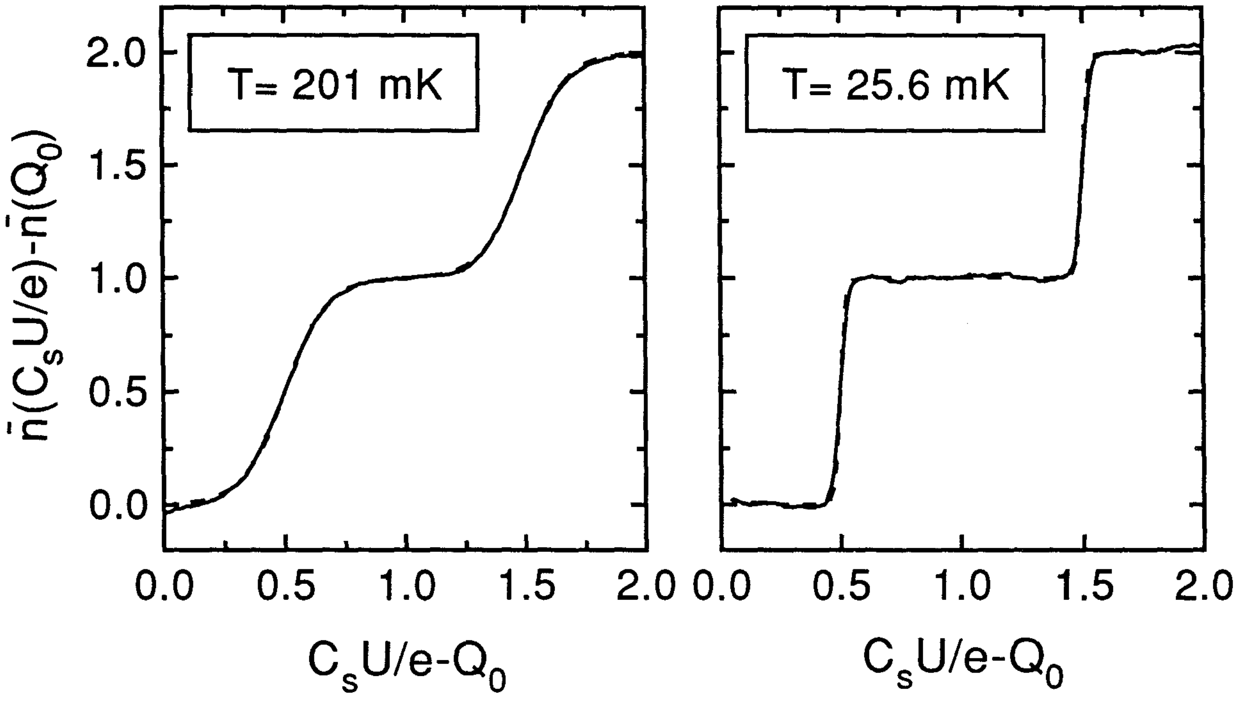

Fig. 1.5 b) *Solid lines: experimental variations of the average number* $\bar{n}$ *of excess electrons in in the island of an electron box. Dashed lines: theoretical calculations for an island capacitance* $C_\Sigma = 0.8$ fF. *The experimental parameters of the circuit are* $C_s = 74$ aF *and* $C_c = 21$ aF. *The quantity* Q_0 *denotes the random offset charge in the island.*

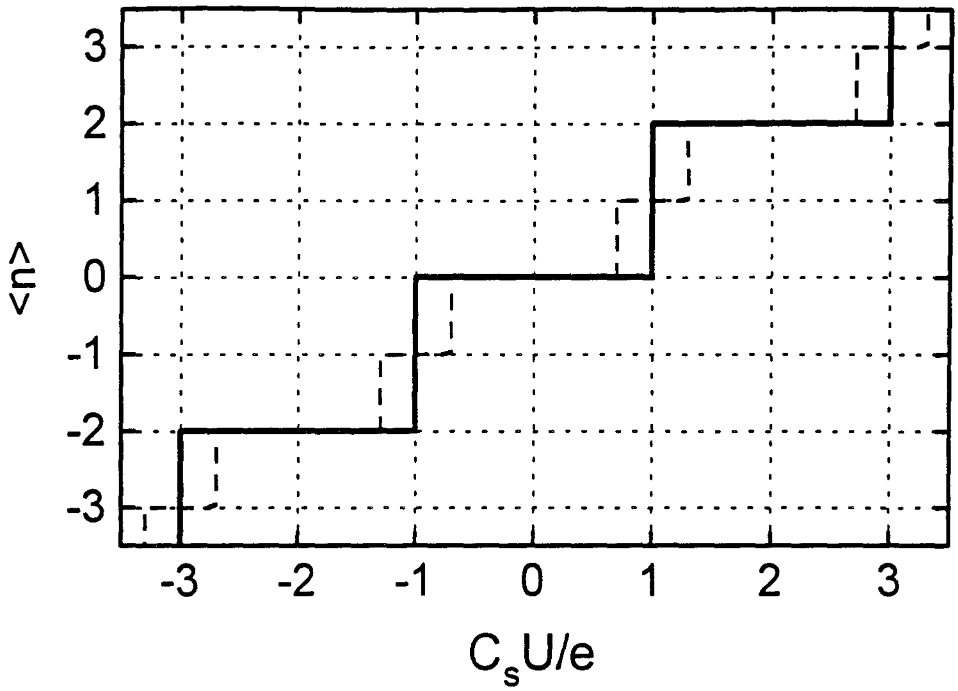

Fig. 1.6 a) *Theoretical variations of* $\langle n \rangle$ *as a function of* C_sU/e *for a superconducting island at zero temperature. Inside the 2e-quantization regime (*$\Delta > E_c$*), the height and the length of the steps are twice as large as in the non-superconducting case (solid line). When* $\Delta < E_c$*, the incremental charge is equal to e (dashed line, calculation done for* $\Delta/E_c = 0.4$*).*

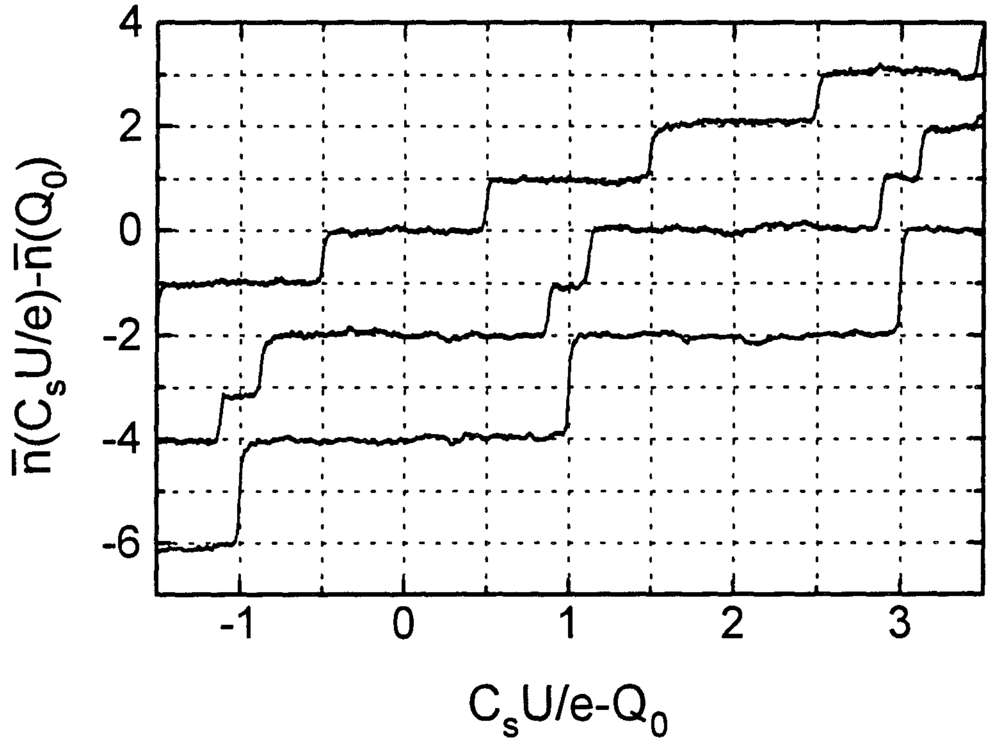

Fig. 1.6 b) *Experimental variations of the average number* $\bar{n}$ *of excess electrons in a superconducting island at* $T = 40$ mK *when* $\Delta = 0$ *(top), when* $\Delta/E_c = 0.83$ *(middle), and when* $\Delta/E_c = 1.22$ *(bottom). For the sake of clarity, the two lowest curves have been shifted vertically. The experiment is described in Sec. 3.2.2.*

the island charge quantization provides an energy scale E_c with which $D(T)$ can be directly compared. A similar effect arises if one depresses the superconducting gap Δ by applying a magnetic field to the sample.

Finally, the electron box, which consists of one island, can be seen as the basic element of more complex circuits which include several islands. In the charge transferring devices [13,14] such as the "turnstile" [15] or the "electron pump" [16], gate voltages are used to transfer electrons from an island to another in order to build a current electron by electron which circulates in an external current-measuring apparatus. The electron pump circuit, for example, can be described as two electron "boxes" connnected through a third junction. For this device, there is a two-dimensional stability diagram analogous to the Coulomb staircase of the single-electron box [16]. As a current source, the electron pump is a potential candidate for a current standard. However, higher order tunneling processes [17-22] can directly transfer a single charge across two or more tunnel junctions although single electron tunneling across each junction is forbidden. These processes, usually referred to as cotunneling processes, reduce the accuracy of the electron pump and must be take into account to evaluate the metrological applications of such a device [23-25].

In this work, we present experiments based on nanoscale tunnel junctions, which both demonstrate that the macroscopic charge, i.e. the mean value of the total charge, of a metallic electrode is quantized and that we are able to control this charge at the single-electron level. In chapter 2, we review the theoretical foundations and the limits of the macroscopic charge quantization. We present in chapter 3 experimental results on the electron box, both in the non-superconducting and the superconducting state. Chapter 4 is devoted to the accuracy of the charge transferring devices. We report experimental results performed on a four junctions device and calculations of the transfer accuracy of the pump. Appendix 1 presents the calculation of the total electrostatic energy of a general circuit consisting of junctions, capacitances and voltage sources. The fabrication techniques of the superconducting/normal tunnel junctions used in the superconducting electron box are described in appendix 2 and the measurement device, the SET electrometer, is presented in appendix 3.

REFERENCES

[1] R. A. Millikan, Phys. Rev. **32**, 349 (1911).

[2] K. A. Matveev, Zh. Eksp. Teor. Fiz. **99**, 1598 (1991) [Sov. Phys. JETP **72**, 892 (1991)].

[3] H. Grabert, Proceedings of the LT20 conference (1993).

[4] P. Lafarge, H. Pothier, E. R. Williams, D. Esteve, C. Urbina, and M. H. Devoret, Z. Phys. **B 85**, 327 (1991).

[5] G. J. Dolan and J. H. Dunsmuir, Physica **B 152**, 7 (1988).

[6] T. A. Fulton and G. J. Dolan, Phys. Rev. Lett. **59**, 109 (1987).

[7] J. Bardeen, L. N. Cooper and J. R. Schrieffer, Phys. Rev. **108**, 1175 (1957).

[8] D. V. Averin and Yu. V. Nazarov, Phys. Rev. Lett. **69**, 1993 (1992).

[9] P. Lafarge, P. Joyez, D. Esteve, C. Urbina, and M. H. Devoret, Nature **365**, 422 (1993).

[10] P. Lafarge, P. Joyez, D. Esteve, C. Urbina and M. H. Devoret, Phys. Rev. Lett. **70**, 994 (1993).

[11] M. T. Tuominen, J. M. Hergenrother, T. S. Tighe and M. Tinkham, Phys. Rev. Lett. **69**, 1997 (1992).

[12] T. M. Eiles, J. M. Martinis and M. H. Devoret, Phys. Rev. Lett. **70**, 1862 (1993).

[13] D. Esteve, in *Single Charge Tunneling*, edited by H. Grabert and M. H. Devoret (Plenum, New York, 1992), Chap. 3.

[14] M. H. Devoret, D. Esteve and C. Urbina, Nature **360**, 547 (1992).

[15] L. J. Geerligs, V. F. Anderegg, P. A. M. Holweg, J. E. Mooij, H. Pothier, D. Esteve, C. Urbina and M. H. Devoret, Phys. Rev. Lett. **64**, 2691 (1990).

[16] H. Pothier, P. Lafarge, D. Esteve, C. Urbina and M. H. Devoret, Europhys. Lett. **17**, 249 (1992).

[17] D. V. Averin and A. A. Odintsov, Phys. Lett. **A 149**, 251 (1989).

[18] D. V. Averin and Yu. V. Nazarov, Phys. Rev. Lett. **65**, 2446 (1990).

[19] L. J. Geerligs, D. V. Averin and J. E. Mooij, Phys. Rev. Lett. **65**, 3037 (1990).

[20] D. V. Averin and Yu. V. Nazarov, in *Single Charge Tunneling*, edited by H. Grabert and M. H. Devoret (Plenum, New York, 1992), Chap. 6.

[21] T. M. Eiles, G. Zimmerli, H. D. Jensen, and John M. Martinis, Phys. Rev. Lett. **69**, 148 (1992).

[22] V. I. Mel'nikov, Phys. Lett. A **176**, 267 (1993).

[23] H. D. Jensen and J. M. Martinis, Phys. Rev. B **46**, 13407 (1992).

[24] D. V. Averin, A. A. Odintsov and S.V. Vyshenskii, J. Appl. Phys. **73**, 1297 (1993).

[25] H. Pothier, P. Lafarge, D. Esteve, C. Urbina and M. H. Devoret, IEEE Trans. Instrum. Meas. **42**, 324 (1993).

2. Review of Theoretical Predictions on Macroscopic Charge Quantization in the Single-Electron Box

In this chapter we review the theoretical predictions concerning macroscopic charge quantization of a metallic island. We first treat the case of an electron box consisting only of normal metal elements. We will afterwards treat the case of a box with a superconducting island and a normal metal reservoir. Finally, we will treat the case where both the island and the reservoir are superconducting.

2.1 The normal electron box.

2.1.1 The Coulomb staircase and the Coulomb sawtooth at T=0.

The electron box circuit consists of a small tunnel junction of capacitance C and a capacitor C_s placed in series with a voltage source U (Fig. 2.1). The "island", which is the metallic electrode common to the junction and the capacitor, is free to exchange electrons with the charge reservoir consisting of the "lead", i.e. the electrode common to the junction and the voltage source. Since the lead wave impedance Z_t is much less than the resistance quantum $R_K = h/e^2 \cong 25.8\ \mathrm{k}\Omega$, the charge q of the island is the sole degree of freedom of the system whose states can be indexed by the number n of excess electrons on the island [1]. For the moment, we assume that the junction tunnel resistance R_t is much larger than the resistance quantum R_K. Under this condition, as we will see in Sec. 2.1.3, n is a good quantum number [2,3].

At $T = 0$, the charge $q = -ne$ is fixed and determined by the integer number n for which the total energy of the circuit is minimal. The total energy of the electron box including the work done by the voltage source is (see appendix 1):

$$E_{total} = \frac{1}{2}\frac{(ne - C_s U)^2}{C + C_s} - \frac{C_s U^2}{2} . \tag{1}$$

Since we want to compare the energy of the different n-states for a given value of the voltage U, we can retain only the first term of the right hand side of Eq. (1) and define:

$$E_n = E_c\left(n - C_s U/e\right)^2 . \tag{2}$$

Here, we have introduced the charging energy $E_c = e^2/2C_\Sigma$, $C_\Sigma = C + C_s$ being the total capacitance of the island. The quantity E_c is the cost of putting one excess electron on the island when $U = 0$. Expression (2) clearly shows that the minimum of E_n corresponds to a number n of excess electrons equal to the integer closest to $C_s U/e$. Consequently, at $T = 0$, the equilibrium value of n as a function of $C_s U/e$ takes the form of a staircase function (Fig. 2.2b) which we have called the Coulomb staircase. We must mention that the expression "Coulomb staircase" is also used [4,5] to denote the steplike structure in the current-voltage characteristic of a double junction circuit. However, there is no conflict since both staircases originate from the same basic effect.

We have plotted in Fig. 2.2a the energies E_n versus $C_s U/e$ for different values of n. They are represented by a set of parabolas, each parabola being shifted from its neighbors by 1 along the x axis. The system has in general a non-degenerate ground state, which fixes the equilibrium value of n at $T = 0$, except when the two lowest n-states have the same energy E_n. This latter situation corresponds to the crossings of parabolas and occurs for the half integer values of the reduced variable $C_s U/e$. At these threshold points, the ground state is degenerate and transitions between the n-state and the $(n+1)$-state of the box can occur. Such a transition corresponds to a single tunnel event across the junction, transferring one electron in or out the island.

The charge Q on the junction capacitance, the charge Q_s on the capacitor C_s and the number n of electrons stored in the island are related as follows:

$$\begin{cases} Q = \dfrac{C}{C_\Sigma}\left(-ne + C_s U\right) \\[2ex] Q_s = \dfrac{C_s}{C_\Sigma} ne + \dfrac{C}{C_\Sigma} C_s U \end{cases} \tag{3}$$

Let us examine the evolution of these three quantities as we sweep the voltage U (Fig. 2.3). At $U = 0$, the $n = 0$ state is the ground state and the energy cost of one excess electron is exactly equal to the charging energy E_c. Then, the energy difference between the $n = 0$ state and the $n = 1$ state decreases with increasing U. At the same time, the charge Q on the junction

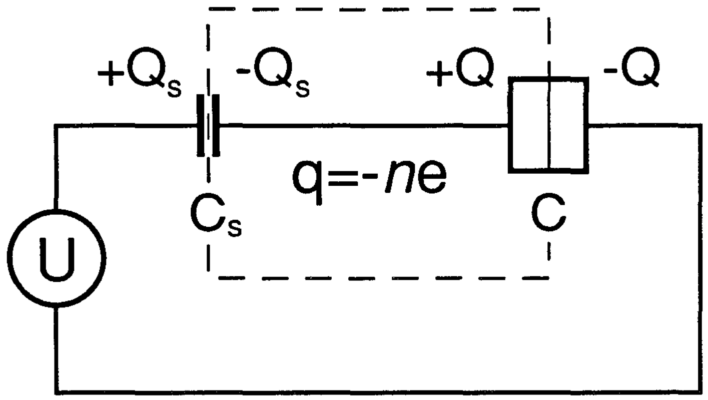

Fig. 2.1 *Schematic of the single-electron box circuit consisting of a capacitor and a tunnel junction placed in series with a voltage source. The symbol in form of a double box represents the tunnel junction. The part of circuit inside the dashed line is the "island" which contains a number n of excess electrons.*

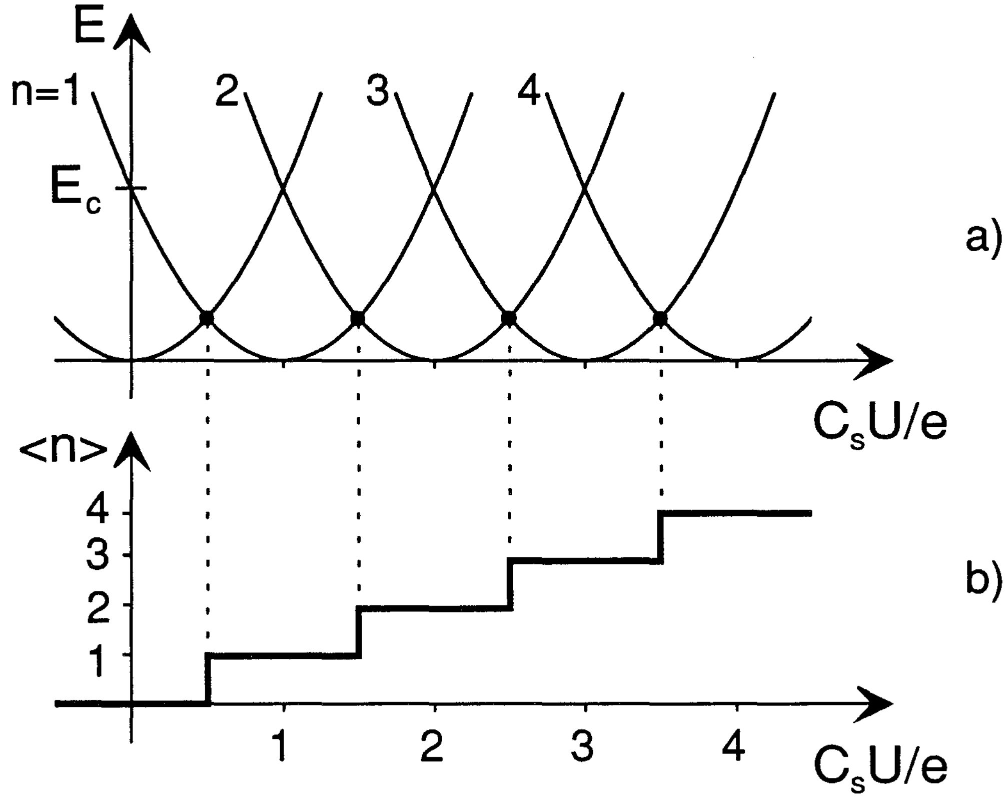

Fig. 2.2 a) *Energy of the circuit versus C_sU/e for several values of the number n of excess electrons in the island. The charging energy E_C is the electrostatic energy of one extra electron in the island when $C_sU/e = 0$. The solid dots correspond to level crossings between parabolas where one electron can tunnel into and out the island.* b) *The Coulomb staircase which displays the equilibrium value of n as a function of C_sU/e.*

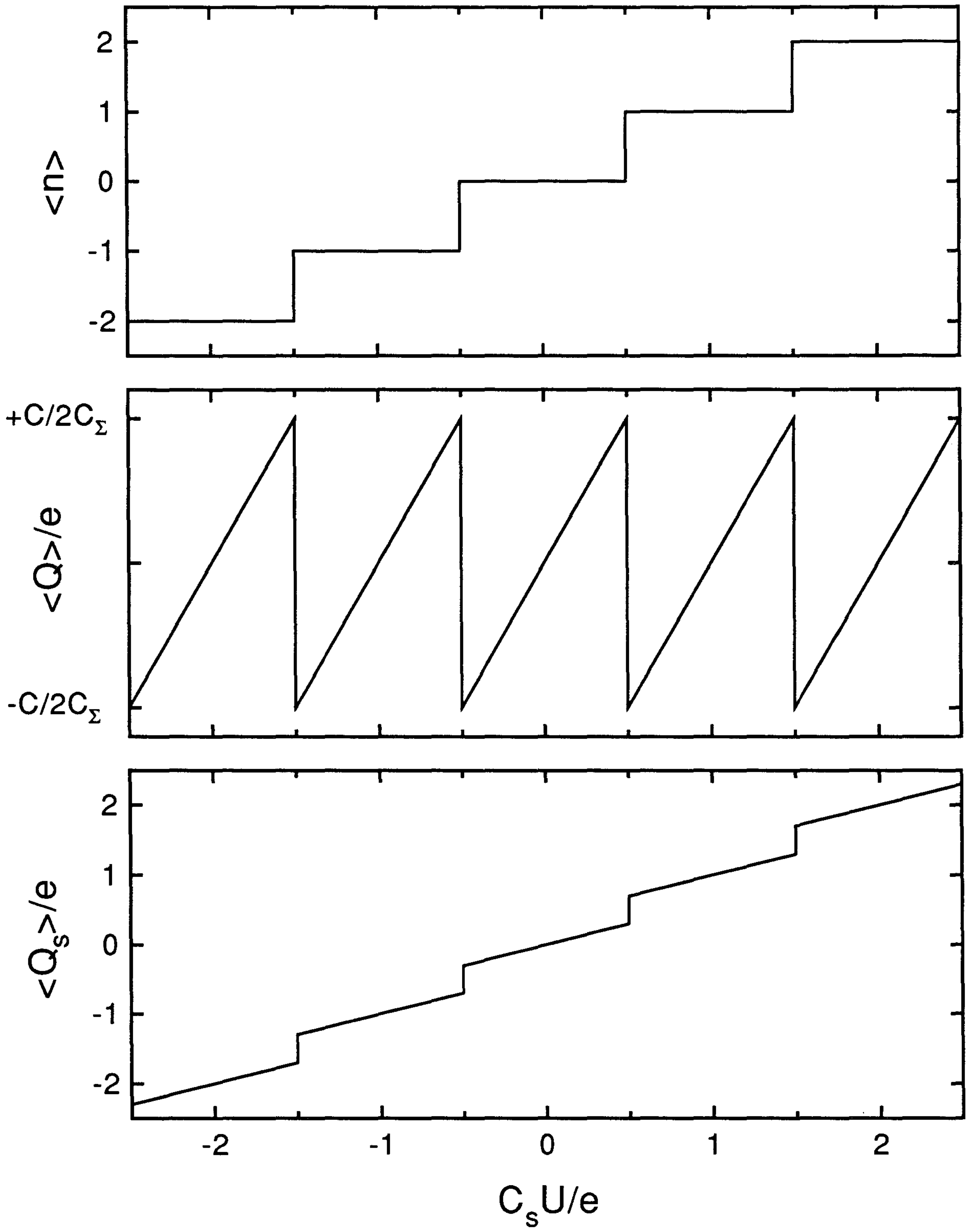

Fig. 2.3 *Average value at* $T = 0$ *of the number n of excess electrons in the island (top), of the charge Q on the junction (middle) and of the charge* Q_s *on the capacitor (bottom) versus* C_sU/e. *The bottom curve is plotted for* $C_s/C_\Sigma = 0.4$.

capacitance grows linearly with U. When $C_sU/e = 1/2$, the two states $n = 0$ and the $n = 1$ have the same energy and the transition $n = 0 \rightarrow n = 1$ can occur. The charge of the electron entering the island is distributed over the two capacitances C and C_s. Thus, the charge Q on the junction exhibits a negative jump equal to $-e(C/C_\Sigma)$ while the capacitor charge Q_s exhibits a positive jump equal to $e(C_s/C_\Sigma)$. After the transition, the $n = 1$ state becomes the new ground state and Q grows again from a negative value. The variations of the charge Q on the junction as a function of the reduced variable C_sU/e are periodic sawtooth oscillations: we call them the Coulomb sawtooth.

The three discontinuous curves depicted in Fig. 2.3 are actually three different manifestations of the same effect: the steplike variations of the equilibrium number of excess electrons on the island. The charge increment is fixed by the charge quantum e and the periodicity of the phenomenon is set by e/C_s.

2.1.2 Macroscopic charge quantization at finite temperature.

According to the previous electrostatic calculation, the charge q on the island of the electron box at $T = 0$ is fixed when $C_sU/e \neq 1/2 \bmod 1$ and the steps of the resulting Coulomb staircase are thus perfectly flat. The question now arises of the robustness of the steps to thermal fluctuations of the island charge. At finite temperature, the system can be found in excited states corresponding to the various n-states of the box. The quantity of interest is the thermal average $\langle q \rangle = -\langle n \rangle e$, hereafter referred to as the "macroscopic" charge of the island.

Using expressions (2) and (3), the charge Q on the junction can be expressed as:

$$Q = \frac{C}{C_s}\frac{\partial E_n}{\partial U}. \tag{4}$$

At finite temperature, this relation is transposed to average values. The average junction charge $\langle Q \rangle$ and the free energy F are related by:

$$\langle Q \rangle = \frac{C}{C_s}\frac{\partial F}{\partial U}, \tag{5}$$

where $F = -k_B T \ln Z$. Here T is the temperature of the system, k_B is the Boltzmann constant and Z is the partition function of the system given by:

$$Z = \sum_{n=-\infty}^{n=+\infty} \exp\left(-E_n/k_BT\right). \tag{6}$$

Combining Eq. (3) and Eq. (5), we can express the thermal average number $\langle n \rangle$ of excess electrons in the island as:

$$\langle n \rangle = C_sU/e + \frac{k_BT}{2E_c}\frac{\partial \ln Z}{\partial\left(C_sU/e\right)}. \tag{7}$$

This expression is particularly useful at high temperatures. For large values of the reduced parameter $\theta = k_BT/E_c$, the series (6) does not converge numerically and one computes the partition function Z using the following identity [6]:

$$Z = \sum_{n=-\infty}^{n=+\infty} \exp\left[-\left(n - C_sU/e\right)^2/\theta\right] = \sqrt{\frac{\theta}{4\pi}}\left[1 + 2\sum_{p=1}^{+\infty}\cos\left(2\pi p\, C_sU/e\right)\exp\left(-\theta\pi^2p^2\right)\right]. \tag{8}$$

When $\theta >> 1$, we can keep only the first term of the sum in the right hand side of Eq. (8). In this limit, using Eq. (7) the average $\langle n \rangle$ is thus approximately given by:

$$\langle n \rangle = C_sU/e - 2\pi\theta\sin\left(2\pi\, C_sU/e\right)e^{-\theta\pi^2}. \tag{9}$$

At low temperature, we have to go back to the definition of $\langle n \rangle$. We calculate directly the Boltzmann average of the number n of excess electrons. Each n state is weighted by its Boltzmann factor $\exp\left(-E_n/k_BT\right)$ and the average $\langle n \rangle$ is given by:

$$\langle n \rangle = \frac{\sum_{n=-\infty}^{n=+\infty} n \exp\left(-E_n/k_BT\right)}{\sum_{n=-\infty}^{n=+\infty} \exp\left(-E_n/k_BT\right)}. \tag{10}$$

When $\theta << 1$, a useful approximation is obtained by keeping in Eq. (10) only the two terms corresponding to the lowest energies. Within this approximation, if we consider C_sU/e in the neighborhood of $m + 1/2$, one readily shows that $\langle n \rangle$ takes the form:

$$\langle n \rangle = m + \frac{1}{2}\left\{1 + \tanh\left[-\left(m + 1/2 - C_sU/e\right)/\theta\right]\right\}. \tag{11}$$

The two quantities $\langle n\rangle$ and $\langle Q\rangle$ are plotted versus C_sU/e in Fig. 2.4 for three different values of the reduced parameter θ. A quantitative measurement of the effect of temperature on the Coulomb staircase is its slope at the half integer values of C_sU/e:

$$\begin{aligned}\frac{\partial\langle n\rangle}{\partial(C_sU/e)}(C_sU/e=m+1/2) &= \frac{1}{2\theta} && \text{for } \theta<<1 \\ &= 1+4\pi^2\theta e^{-\theta\pi^2} && \text{for } \theta>>1.\end{aligned} \tag{12}$$

These two expressions give the same value of the slope for $\theta \approx 0.34216$. Finally, in the limit $T\rightarrow 0$, we recover the perfect Coulomb staircase since Eq. (7) reduces to:

$$\langle n\rangle = \frac{C_sU}{e} - \frac{C_\Sigma}{C_se}\frac{\partial E_G}{\partial U}\ , \tag{13}$$

where E_G refers to the ground state energy.

At high temperature, Eq. (9) shows that the quantization of the macroscopic charge $\langle q\rangle = -\langle n\rangle e$ is completely suppressed. Although the instantaneous charge q remains always quantized, the mean value $\langle q\rangle$ becomes equal to $-C_sU$ in the limit $k_BT >> E_c$. In that case, the tunnel junction behaves as a short circuit and its average charge $\langle Q\rangle$ is zero. The macroscopic charge quantization occurs in the opposite limit:

$$E_c >> k_BT\ . \tag{14}$$

This condition ensures that the Coulomb staircase is just slightly rounded by thermal fluctuations and that in the central part of the steps the mean value $\langle n\rangle$ remains equal to an integer number (Fig. 2.4a).

Like the Coulomb staircase, the Coulomb sawtooth is also rounded at $T\neq 0$ and the amplitude of the oscillations is less than $(C/C_\Sigma)e$ (Fig 2.4b). The Coulomb sawtooth is similar but not identical to the single electron tunneling (SET) oscillations which are expected to occur for a small tunnel junction biased with a perfect current source [7]. In that latter effect, the voltage across the junction oscillates between $+e/C$ and $-e/C$ at frequency $f=I/e$, where I is the current applied to the junction. However, the Coulomb sawtooth arises from the macroscopic charge quantization and is an equilibrium effect while the SET oscillations involve a dynamic blockade of tunneling.

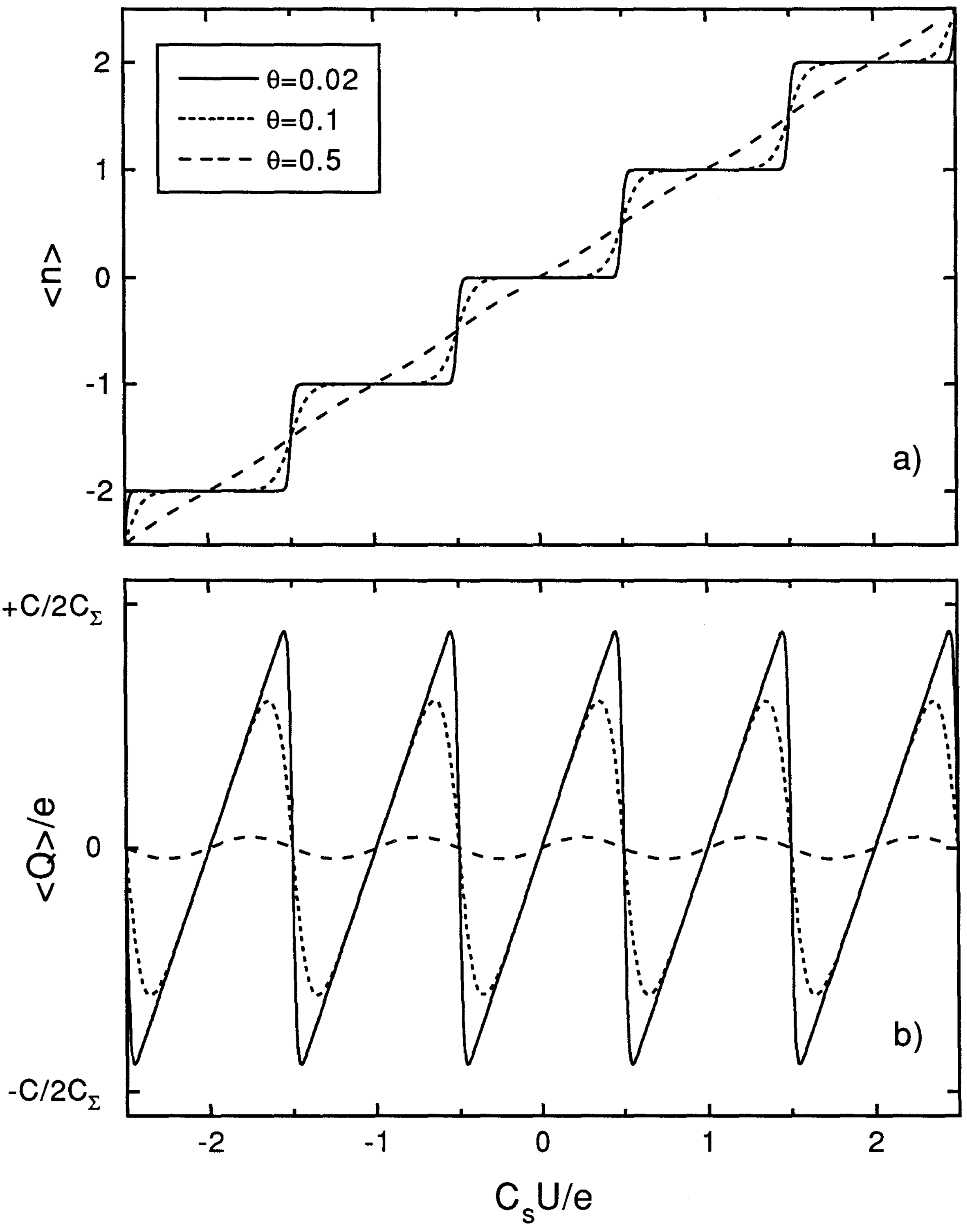

Fig. 2.4 a) *Average value* $\langle n\rangle$ *of the number of excess electrons in the island and* b) *average charge* $\langle Q\rangle$ *on the junction versus* C_sU/e *for three different values of the reduced parameter* $\theta = k_BT/E_c$. *Note that when* $\theta = 0.5$ *(dashed lines) the Coulomb staircase has been reduced to an almost linear ramp while the modulation of the average junction charge* $\langle Q\rangle$ *is still visible.*

Experimentally, a sample can be reliably cooled down to about 30 mK. It means that the island capacitance C_Σ must be in the fF range to satisfy condition (14). This is achieved using ultrasmall tunnel junctions with typical area of $100\,\text{nm} \times 100\,\text{nm}$ fabricated by nanofabrication techniques. Since the capacitance C_s can be made smaller than 1 fF, the period e/C_s of the Coulomb sawtooth will be a voltage (> 1 mV) sufficiently large to be easily controlled. The experimental observation of the Coulomb sawtooth and its temperature dependence are described in the next chapter (see section 3.1.1).

In summary, provided an adequate tunnel junction is used, the number of electrons stored in the island does not fluctuate at low temperature and is entirely determined by the externally applied voltage. The Coulomb staircase reveals the macroscopic charge quantization arising from the electrostatic energy gap between the different n states of the island. At finite temperature the aspect of the staircase depends on two external parameters: the capacitance C_s and the charging energy E_c. The former one determines the length of the steps of the staircase, the latter one determines the sharpness of the charge jumps.

2.1.3 Quantum fluctuations of the island charge.

We now discuss the case where the transmission coefficient of the insulating barrier of the junction is finite. The finite tunnel conductance of the junction, which has been neglected so far, makes the island charge subject to quantum fluctuations. Even at $T = 0$, the ground state is not a pure n state and we expect the charge of the island not to be strictly quantized. We shall now discuss the correction to the staircase dependence of the island charge on U and treat the tunnel hamiltonian as a perturbation.

Quantum mechanically, the single electron box is described by the following hamiltonian:

$$H = H_0 + H_t\,, \tag{15}$$

where H_0 describes the system in the absence of tunneling and H_t is the perturbing tunnel hamiltonian. The unperturbed hamiltonian H_0 is given by

$$H_0 = E_c\left(\hat{n} - C_g U/e\right)^2 + \sum_{k_L} \varepsilon_{k_L} a_{k_L}^{+} a_{k_L} + \sum_{k_R} \varepsilon_{k_R} a_{k_R}^{+} a_{k_R}\,, \tag{16}$$

where $\hat{n}$ is the operator associated with n the number of excess electrons stored in the island, a_{k_L} and a_{k_R} are the quasiparticle annihilation operator in the island and in the lead respectively, ε_{k_L} and ε_{k_R} being the kinetic energies of the quasiparticles measured from the Fermi energy. Note that in Eq. (16) the a_k's are purely kinetic degrees of freedom while $\hat{n}$ is the sole electrical degree of freedom. In the limit of large electrodes, $\hat{n}$ and the a_k's are independent. In the one-dimensional model of the tunnel junction, the tunnel hamiltonian [8] H_t is written:

$$H_t = \sum_{k_L,k_R} t a_{k_L}^{+} a_{k_R} e^{i\hat{\delta}} + h.c. \ , \tag{17}$$

where t is the matrix element which characterises the tunneling across the junction and $\left[\hat{\delta},\hat{n}\right] = i$. In Eq. (17) we have assumed that the tunnel matrix element t is independent of the energy of the ingoing and outgoing quasiparticle. One can show that the tunnel resistance R_t of the junction and the tunnel matrix element t are related by

$$\rho_L \rho_R t^2 = R_K \big/ \left(4\pi^2 R_t\right) \ , \tag{18}$$

where ρ_L and ρ_R are the density of states at the Fermi level on each side of the junction. Since the pattern of the Coulomb staircase is periodic in $C_s U/e$, we will restrict our calculation to the range $-1/2 < C_s U/e < 1/2$, inside which the unperturbed ground state is given by $n = 0$.

At the lowest order in H_t, the $n = 0$ state is coupled to the states $n = 1$ and $n = -1$. The corresponding corrections $\delta E_{\pm 1}$ to the ground state energy take the form

$$\delta E_{\pm 1} = \int_0^{\infty} \int_0^{\infty} \frac{t^2 \rho_L \rho_R}{E_0 - E_{\pm 1} - \varepsilon_L - \varepsilon_R} \mathrm{d}\varepsilon_L \mathrm{d}\varepsilon_R \ , \tag{19}$$

where $E_{\pm 1}$ refers to the total electrostatic energy of the $n = \pm 1$ state defined by Eq. (2). Using (18) and making a change of variable $\varepsilon = \varepsilon_L + \varepsilon_R$, we get:

$$\delta E_{\pm 1} = \frac{R_K}{4\pi^2 R_t} \int_0^{\infty} \frac{\varepsilon}{E_0 - E_{\pm 1} - \varepsilon} \mathrm{d}\varepsilon \tag{20}$$

Inserting this result in Eq. (13), we obtain the average number of excess electrons [9] in the island:

$$\langle n \rangle = g \ln\left[\frac{1/2 + C_s U/e}{1/2 - C_s U/e}\right], \tag{21}$$

where $g = R_K / 4\pi^2 R_t$. This expression diverges at $C_s U/e = \pm 1/2$.

Grabert [2] has calculated the correction to $\langle n \rangle$ up to second order in g and has obtained:

$$\langle n \rangle = g \ln\left[\frac{1/2 + C_s U/e}{1/2 - C_s U/e}\right] + g^2 c_2(C_s U/e) + O\left(g^3\right), \tag{22}$$

where

$$\begin{aligned} c_2(x) = &-x\left(\frac{4\pi^2}{3} + \ln^2\frac{1-2x}{1+2x}\right) - \frac{16\left(1+2x-2x^2\right)}{(3-2x)(1+2x)}\ln(1-2x) \\ &-2(1-x)\left(\ln^2\frac{1-2x}{4(1-x)} + 2\,\mathrm{Li}_2\left(\frac{3-2x}{4(1-x)}\right) - \frac{8(1-x)}{(1-2x)(3-2x)}\ln(4(1-x))\right) - s.t.(-x). \end{aligned} \tag{23}$$

Here $s.t.(-x)$ refers to the same sum of terms with x replaced $-x$, and $\mathrm{Li}_2 = \int_0^x dz \ln(1-z)/z$. For $R_t = 0.5 R_K$, Grabert shows that the second order calculation is sufficient to describe the variations of $\langle n \rangle$ in 98% of the interval $-1/2 < C_s U/e < +1/2$ (see Fig. 2.5b). At the threshold values $C_s U/e = \pm 1/2$, the second order expression (22) diverges logarithmically like (21). In order to remove the divergence, Matveev [3] has used an analogy with the Kondo problem and has re-summed the most diverging logarithmic terms. Grabert has done a systematic diagrammatic expansion and has obtained after re-summation for $C_s U/e \to 1/2$:

$$\langle n \rangle = \frac{-g^* \ln \delta^*}{1 - 2g^* \ln \delta^*} + O(\delta), \tag{24}$$

where the renormalized parameters g^* and δ^* are given by $g^* = g\left[1 + 6g + O\left(g^2\right)\right]$, $\delta^* = \delta\left[1 - ag + O\left(g^2\right)\right]$, $\delta = 1/2 - C_s U/e$, and $a = -9.7726...$.

This calculation predicts that the island charge is not strictly quantized and varies approximately linearly with the voltage U in the center of the flat part of the staircase. Fig. 2.5 shows the two effects of a finite tunneling conductance on the Coulomb staircase: a finite slope in the middle of the steps and a weak rounding as $C_s U/e \to \pm 1/2$. However, the slope at $C_s U/e = \pm 1/2$ remains infinite like in the $R_t / R_K \to \infty$ limit. We must mention that, using a

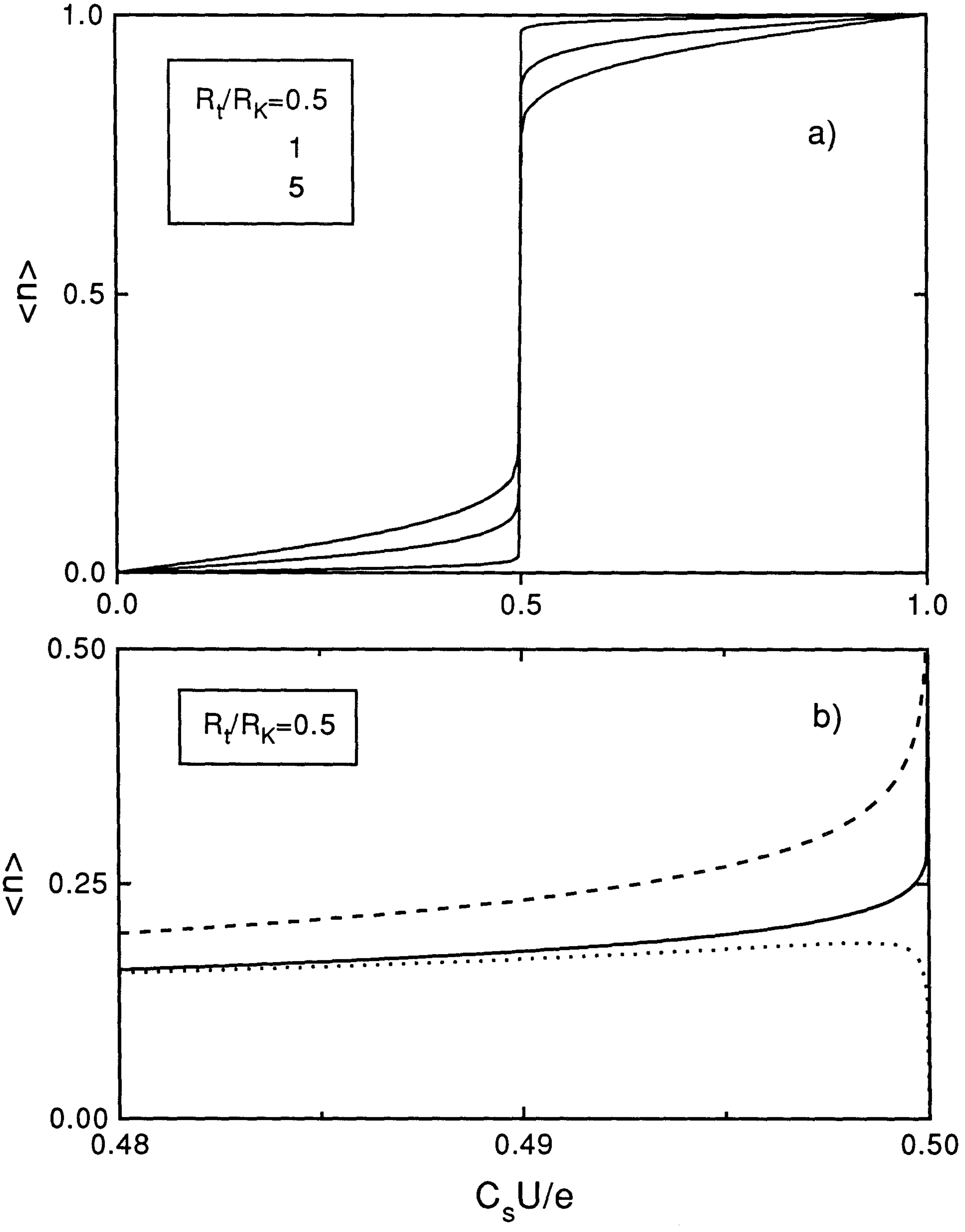

Fig. 2.5 a) *Average value* $\langle n \rangle$ *of the number of excess electrons in the island versus* C_sU/e *calculated using Eq. (22) and Eq. (24) for three different values of the ratio* R_t/R_K. b) *Enlargement of the preceeding curve in the vicinity of* $C_sU/e = 0.5$ *for* $R_t/R_K = 0.5$. *The solid line is the non divergent result, the dashed line is the first order calculation given by Eq. (21) and the dotted line is the second order result given by Eq. (22).*

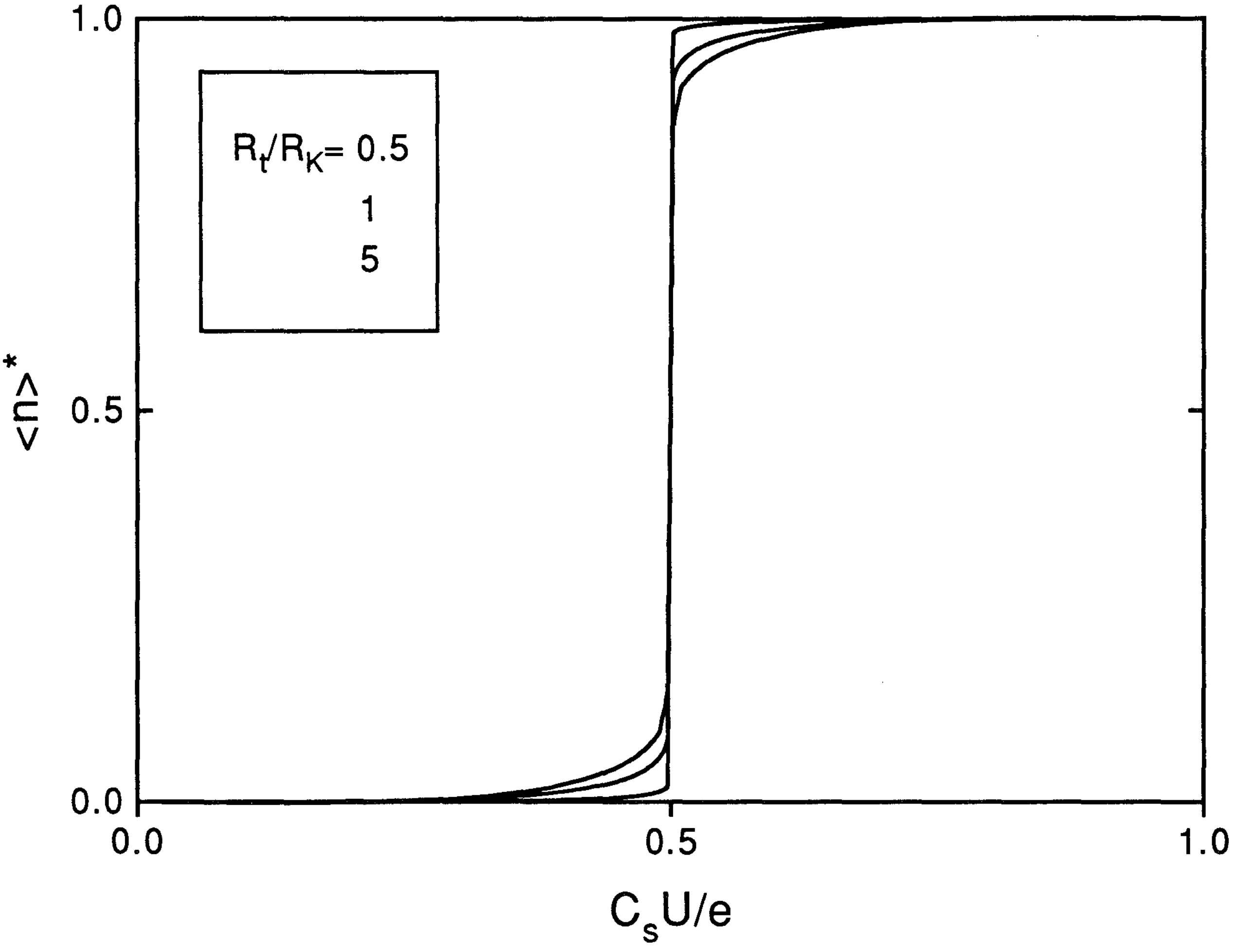

Fig. 2.6 *Renormalized average number* $\langle n \rangle^*$ *of excess electrons in the island as a function of* C_sU/e *calculated using Eq. (24) and Eq. (25) for three different values of the ratio* R_t/R_K .

different approach, Zwerger [10] has predicted a finite slope of the staircase at $C_sU/e = \pm 1/2$, in contradiction with the preceeding analysis.

A word of caution is necessary at this point. Because we cannot perform an absolute measurement of the island charge, the curves plotted in Fig. 2.5 cannot be directly compared with experimental results. The experiments are only sensitive to the relative variations of $\langle n \rangle$. In Fig. 2.6, we have plotted the staircase calculated with (22) and (24) in a "canonical form", i.e. with flat steps and normalized charge increment. This can be done by substracting the steps slope and rescaling of the curve. We obtain for the renormalized average charge $\langle n \rangle^*$:

$$\langle n \rangle^* = \frac{\langle n \rangle - 4g(C_sU/e)}{1-4g} . \tag{25}$$

The curves plotted in Fig. 2.6 show that, even for tunneling resistances of the order of R_K, the charge quantization is experimentally a good approximation and that the charge jumps are always well defined. Nevertheless, the effective incremental charge is always smaller than the charge quantum. The reduction factor equal to $(1-4g)$ can reach 10 % for $R_t \approx R_K$. If we assume that quantum and thermal fluctuations can be treated separately, the charging energy which can be extracted from the staircase at finite temperature is only a renormalized quantity E_c^* given by:

$$E_c^* = E_c/(1-4g) . \tag{26}$$

Finally, we must mention that Büttiker *et al.* [11] have considered the quantum corrections to the capacitance of a mesoscopic capacitor. They emphasize the fact that one cannot describe a mesoscopic capacitor simply with its geometrical capacitance but that the experimentally relevant capacitance is an electrochemical capacitance. This distinction is valid only if the density of states of the capacitor plates are small compared to C_e/e^2, where C_e denotes the geometrical capacitance. However, for the typical dimensions of the metallic islands used in electron box experiments, this condition is not satisfied and we can neglect the corrections to the geometrical capacitances.

2.1.4 Tunneling rate in the electron box.

In this section, we will calculate the tunneling rate across the junction of the electron box, taking into account the effect of the electromagnetic environment [8,12].

In this approach, we include in the description of the circuit the impedance $Z(\omega)$ which models the electromagnetic environment of the electron box and which is placed in series with the junction (see Fig. 2.7a). The impedance $Z(\omega)$ takes into account the finite resistance of the bias circuitry as well as radiation losses in the lead. The junction itself is represented by a pure tunnel element in parallel with a capacitance C. The equivalent circuit seen by the pure tunnel element is an effective voltage source V_{eff} in series with an impedance $Z_t(\omega)$ (Fig 2.7b). The effect of the environment on the tunneling rate is contained in the real part of the total impedance $Z_t(\omega)$.

The total impedance $Z_t(\omega)$ can be described as a capacitance $C_\Sigma = C + C_s$ in series with an impedance $\kappa^2 Z_c(\omega)$ [13], where $\kappa = C_s/C_\Sigma$ and $Z_c(\omega) = Z(\omega)[1 + j\kappa C\omega Z(\omega)]^{-1}$ (Fig 2.7c). If the low frequency behavior of the impedance $Z(\omega)$ corresponds to that of a resistance R, then $\lim_{\omega\to 0} Z_c(\omega) = \lim_{\omega\to 0} Z(\omega) = R$. Denoting the junction temperature by T, the rate Γ of a tunneling event across the junction is [8,12]

$$\Gamma = \frac{1}{R_t e^2}\int_{-\infty}^{+\infty} \frac{E}{1-\exp[-E/k_B T]} P(\Delta E - E)\,dE \ , \tag{27}$$

where R_t is the tunnel resistance of the junction, ΔE is the difference between the total energy of the circuit **before** and **after** the tunneling event, and the function $P(E)$ is the probability that the tunneling electron creates an excitation of the electromagnetic environment with energy E. The function $P(E)$ is a functional of the real part of $Z_t(\omega)$.

If p electrons have already passed through the junction and if $\lim_{\omega\to 0} Z(\omega) = R$, the energy difference ΔE associated with a tunneling event which increases p is

$$\Delta E = \kappa e U - (p + 1/2)\frac{e^2}{C_\Sigma} \ . \tag{28}$$

The function $P(E)$ is given [8] by

$$P(E) = \frac{1}{2\pi\hbar}\int_{-\infty}^{+\infty} \exp[J(t) + i\,Et/\hbar]\,dt \ , \tag{29}$$

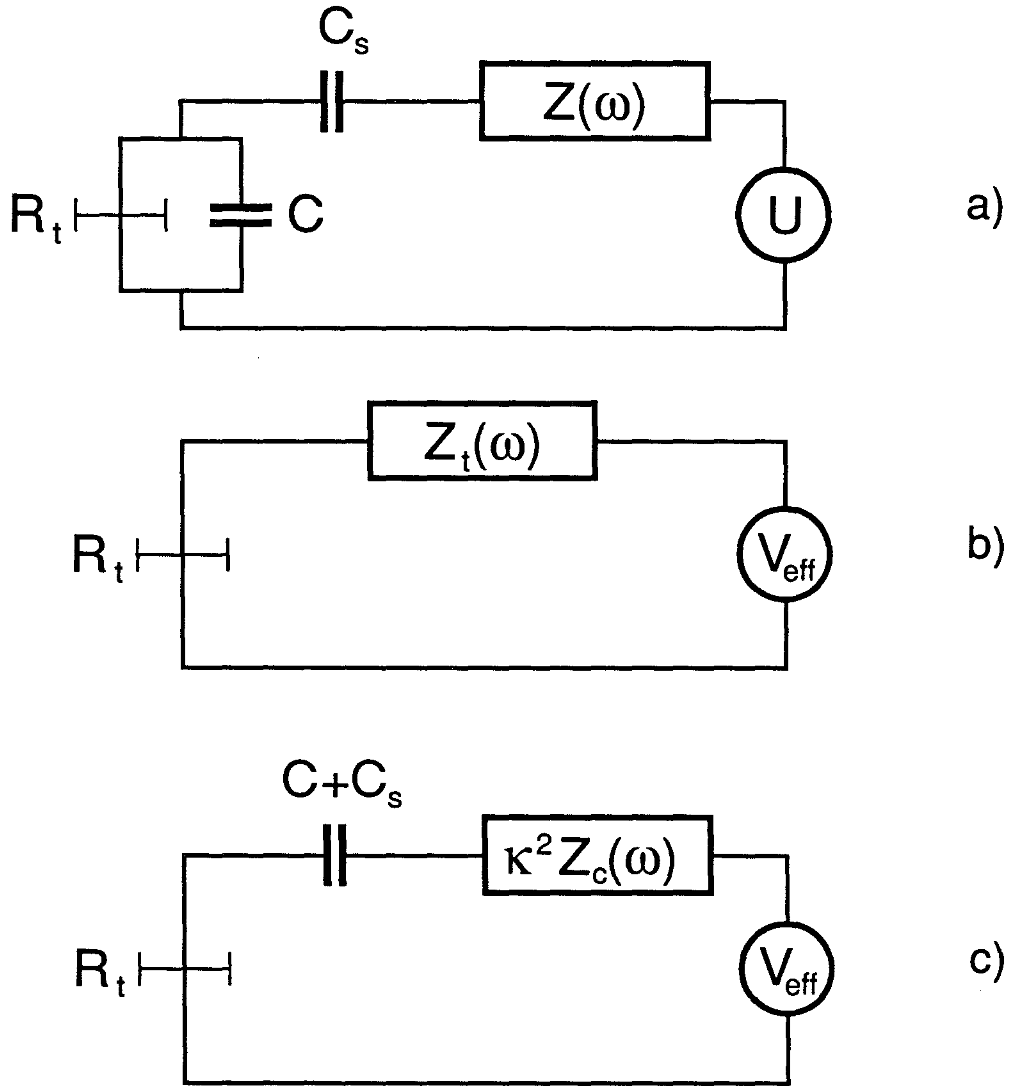

Fig. 2.7 a) *Schematic of the single-electron box circuit coupled to its electromagnetic environment. The junction is represented by a pure capacitor of capacitance C in parallel with a pure tunnel element of resistance* R_t *symbolized by a double T. The electromagnetic environment of the circuit is modeled by an impedance* $Z(\omega)$ *in series with the voltage source.* b) *The circuit seen by the pure tunnel element is the total impedance* $Z_t(\omega)$ *in series with an effective voltage source* V_{eff}. c) *The total impedance* $Z_t(\omega)$ *can be described as a capacitance* $C + C_s$ *in series with an impedance* $\kappa^2 Z_c(\omega)$, *where* $\kappa = C_s/(C + C_s)$.

where $$J(t)=2\int_0^{\infty}\frac{\mathrm{d}\omega}{\omega}\frac{\mathrm{Re}[Z_t(\omega)]}{R_K}\left(\coth\left(\tfrac{1}{2}\beta\hbar\omega\right)(\cos\omega t-1)-i\sin\omega t\right). \tag{30}$$

In this expression $\beta=1/k_B T_e$, where T_e is the temperature of the environment which can be different from the temperature of the junction T involved in Eq. (27). Under common experimental conditions, the real part of the environmental impedance $\mathrm{Re}[Z_t(\omega)]$ is small compared with the resistance quantum R_K, particularly in the electron box. This can be seen from $\mathrm{Re}[Z_t(\omega)]=\kappa^2\,\mathrm{Re}[Z_c(\omega)]$. Typically $\kappa<0.1$, hence we can evaluate the function $P(E)$ by making a linear expansion of $\exp[J(t)]$ in Eq. (29). At zero-th order in $\mathrm{Re}[Z_t(\omega)]/R_K$, $P(E)$ reduces to a delta function $\delta(E)$ and the rate Γ is simply given by

$$\Gamma=\frac{1}{R_t e^2}\frac{\Delta E}{1-\exp[-\Delta E/k_B T]}. \tag{31}$$

Eq. (31) constitutes the so-called "global" rule formula of the tunneling rate [14]. The limit $P(E)=\delta(E)$ corresponds to an electron box completely decoupled from its electromagnetic environment.

We now develop $\exp[J(t)]$ to first order in $\mathrm{Re}[Z_t(\omega)]/R_K$. The function $P(E)$ can be expanded as

$$\mathrm{P}(E)\approx\frac{1}{2\pi\hbar}\int_{-\infty}^{+\infty}(1+J(t))\exp[iEt/\hbar]\mathrm{d}t. \tag{32}$$

Rewriting Eq. (30) as

$$J(t)=2\int_{-\infty}^{+\infty}\frac{\mathrm{d}\omega}{\omega}\frac{\mathrm{Re}[Z_t(\omega)]}{R_K}\frac{e^{-i\omega t}-1}{1-e^{-\beta\hbar\omega}}, \tag{33}$$

we obtain

$$\mathrm{P}(E)=\delta(E)\left[1-2\int_{-\infty}^{+\infty}\frac{\mathrm{d}\omega}{\omega}\mathrm{r}(\omega)\frac{1}{1-e^{-\beta\hbar\omega}}\right]+\frac{2\,\mathrm{r}(E/\hbar)}{E}\frac{1}{1-e^{-\beta E}}, \tag{34}$$

where $\mathrm{r}(\omega)=\mathrm{Re}[Z_t(\omega)]/R_K$. The first order expansion made in Eq. (32) is equivalent to considering that a tunnel event can create or annihilate only one energy quantum in one of the oscillators modelling the environment [12].

If $E>0$ $(E<0)$, the function $P(E)$ given by Eq. (34) can thus be interpreted as the probability for the environment to emit (absorb) one quantum of energy E $(-E)$. Introducing the Bose factor $n(\omega)=1/[\exp(\beta\hbar\omega)-1]$ and the coupling coefficient $c(\omega)=2r(\omega)/\hbar\omega$, one can relate the function $P(E)$ to the probabilities of emission or absorption of an energy quantum $h\omega$. The probability $P(\hbar\omega)$ to emit one quantum of energy $h\omega$ by a single tunneling event is given by $P(\hbar\omega)=c(\omega)(n(\omega)+1)$. On the other hand, the probability $P(-\hbar\omega)$ to absorb one quantum is given by $P(-\hbar\omega)=c(\omega)n(\omega)$.

We consider finally a general type of environment where the impedance $Z(\omega)$ is a 1-port network consisting of several impedances $Z_1(\omega), Z_2(\omega),\ldots, Z_m(\omega)$ at different temperatures $T_1, T_2,\ldots, T_m$ (Fig 2.8a). We denote by $a_i(\omega)$ the attenuation coefficient of a voltage source placed in the branch of the circuit which contains the impedance $Z_i(\omega)$ and measured at the port of the network. From circuit theory, $a_i(\omega)$ is also the attenuation coefficient of a current source placed at the port of the network and measured in series with the impedance $Z_i(\omega)$. The theory of networks only consisting of impedances yields the three following relations:

$$\begin{cases} a_i^2=\dfrac{\partial Z}{\partial Z_i} \\ Z(\omega)=\displaystyle\sum_{i=1}^{m} a_i^2(\omega)Z_i(\omega) \\ \mathrm{Re}[Z(\omega)]=\displaystyle\sum_{i=1}^{m}|a_i(\omega)|^2\,\mathrm{Re}[Z_i(\omega)] \end{cases} \tag{35}$$

The impedance $Z_c(\omega)=Z(\omega)/[1+j\kappa C\omega Z(\omega)]$ and the impedances $Z_{ci}(\omega)$ given by $Z_{ci}(\omega)=Z_i(\omega)/[1+j\kappa C\omega Z(\omega)]$ (Fig. 2.8b) obey the same set of relations as $Z(\omega)$ and the impedances $Z_i(\omega)$. Assuming that each impedance $Z_{ci}(\omega)$ is at thermodynamic equilibrium at T_i', we can generalize Eq. (34) to

$$\begin{aligned} P(E)=\delta(E)&\left[1-\int_{-\infty}^{+\infty}\kappa^2\sum_{i=1}^{m}|a_i(\omega)|^2\frac{2r_i(\omega)}{\omega}\frac{d\omega}{1-e^{-\beta_i\hbar\omega}}\right] \\ &+\kappa^2\sum_{i=1}^{m}|a_i(E/\hbar)|^2\frac{2r_i(E/\hbar)}{E}\frac{1}{1-e^{-\beta_i E}} \end{aligned} \tag{36}$$

where $\beta_i=1/k_BT_i$ and $r_i(\omega)=\mathrm{Re}[Z_{ci}(\omega)]/R_K$.

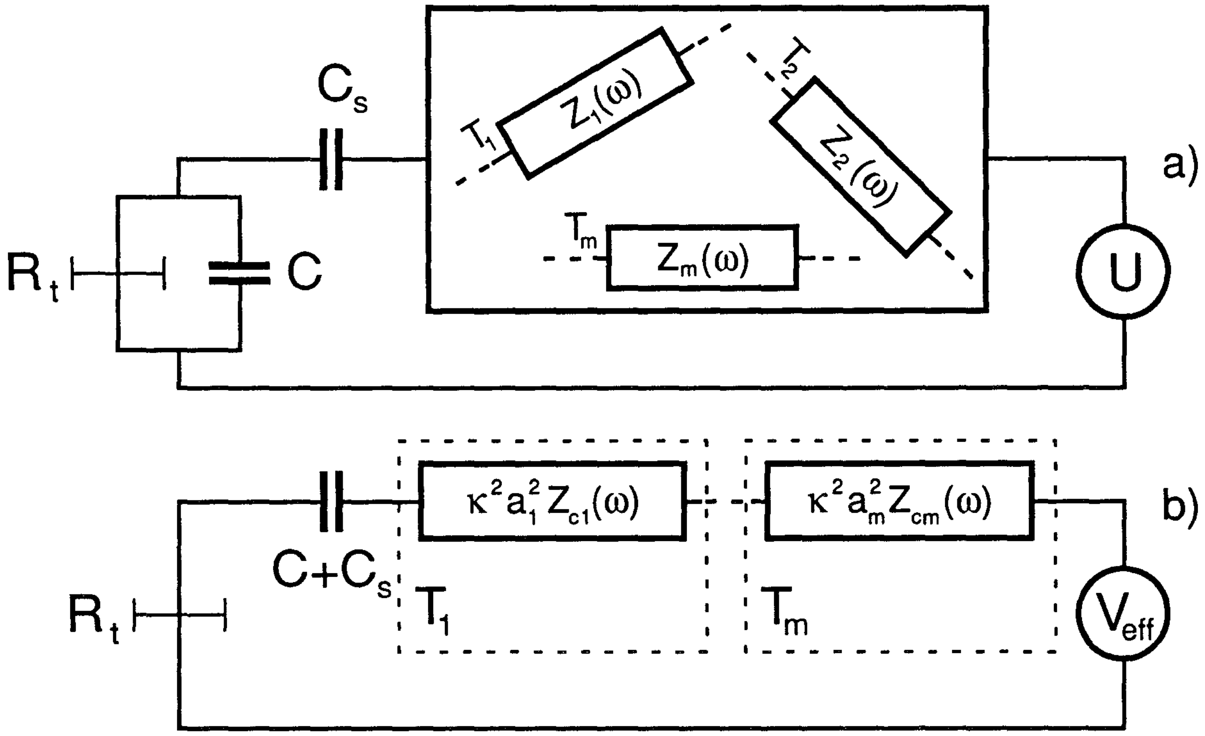
Cs
Rt
C
T1
Z1(ω)
T2
Z2(ω)
Tm
Zm(ω)
U
a)
κ²a₁²Zc1(ω)
κ²am²Zcm(ω)
b)
C+Cs
Rt
T1
Tm
Veff

Fig 2.8 a) *Schematic of a single-electron box circuit connected to an environmental impedance* $Z(\omega)$ *consisting of a 1-port network of impedances at different temperatures.* b) *The impedance* $Z_c(\omega)$ *(see* Fig. 2.7c*) can be represented by m impedances at different temperatures placed in series. The coefficient* $a_i(\omega)$ *is the attenuation of a current source placed at the port of the network and measured in series with the impedance* $Z_i(\omega)$.

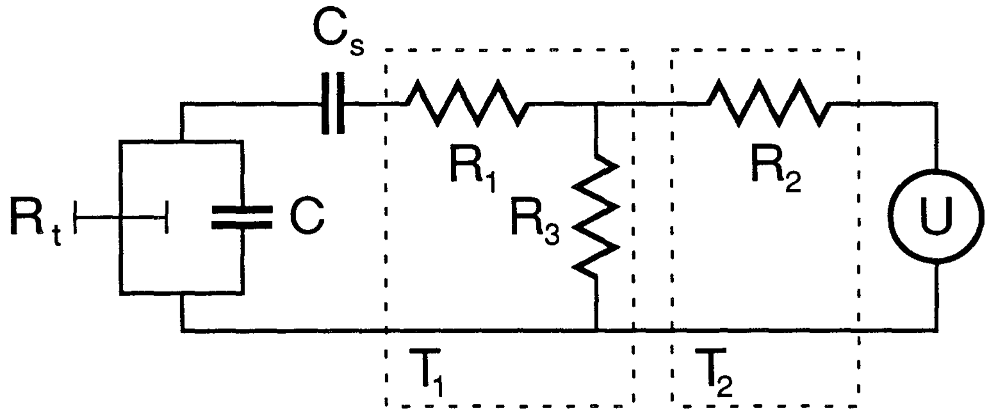
Cs
Rt
C
R1
R3
R2
U
T1
T2

Fig. 2.9 *Example of an environmental impedance* $Z(\omega)$ *consisted of two parts at temperature* T_1 *and* T_2.

At high positive energy ($E > 0$) the spontaneous emission is the dominant decay process and the effect of the temperatures T_1, T_2,..., T_p of the environment on the tunneling rate is negligible. In that case, $P(E)$ is well approximated by $P(E) \approx \kappa^2 2\,\mathrm{Re}\left[Z_c(E/\hbar)\right]/ER_K$. The situation is very different in the case of absorption processes ($E < 0$) for which the function $P(E)$ and consequently the tunneling rate are strongly affected by the environmental temperatures. In that case, one can regard each impedance $Z_{ci}(\omega)$ as a voltage noise source [15] at temperature T_i. The effect of the impedance $Z_{ci}(\omega)$ is characterized by a spectrum density of voltage noise $S_{vi}(\omega)$ such that $P(E)$ can be expressed as:

$$P(E) = \delta(E)\left[1 - \int_{-\infty}^{+\infty} \kappa^2 \sum_{i=1}^{m} \frac{\pi\left|a_i(\omega)\right|^2}{R_K \omega^2} S_{vi}(\omega) \mathrm{d}\omega\right] + \kappa^2 \sum_{i=1}^{m} \frac{\pi\left|a_i(E/\hbar)\right|^2}{R_K E^2} S_{vi}(E/\hbar)\,, \qquad (37)$$

where

$$S_{vi}(E/\hbar) = 2/\pi\,\mathrm{Re}\left[Z_{ci}(E/\hbar)\right]\frac{E}{1-\exp(-\beta_i E)}\,. \qquad (38)$$

When $E = -\hbar\omega < 0$, the spectrum density of voltage noise $S_{vi}(E/\hbar)$ is given by $S_{vi}(-\omega) = 2/\pi\,\mathrm{Re}\left[Z_{ci}(\omega)\right] n_i(\omega)\hbar\omega$. Here $n_i(\omega)$ corresponds to the distribution of photons in the impedance $Z_i(\omega)$ at temperature T_i.

More generally, we can define a spectral density $S_v(\omega)$ for the whole environment given by $S_v(\omega) = \sum_i \left|a_i(\omega)\right|^2 S_{vi}(\omega)$. Since the spectral density $S_v(\omega)$ is a sum involving different temperatures it cannot be described by a constant equivalent noise temperature. Finally combining Eq. (27) and Eq. (37) we obtain

$$\Gamma = \frac{1}{R_t e^2}\frac{\Delta E}{1-e^{-\Delta E/k_B T}}\left[1 + \int_{-\infty}^{+\infty} \kappa^2 \frac{\pi S_v(E/\hbar)}{E^2}\left(\frac{\Delta E - E}{\Delta E}\frac{1-e^{-\Delta E/k_B T}}{1-e^{-(\Delta E - E)/k_B T}} - 1\right)\mathrm{d}E\right]. \qquad (39)$$

As an example, we consider the circuit depicted in Fig. 2.9. The environmental impedance $Z(\omega)$ is separated in two parts at temperatures T_1 and T_2 and is given by $Z(\omega) = a_1^2 R_1 + a_2^2 R_2 + a_3^2 R_3$ with $a_1 = 1$, $a_2 = R_3/(R_2 + R_3)$ and $a_3 = R_2/(R_2 + R_3)$. In the center of a step at $C_s U/e = 0$, the ground state of the box corresponds to $n = 0$ and the energy difference with the first excited states $n = 1$ and $n = -1$ is equal to $-E_c$. A log-log plot of the

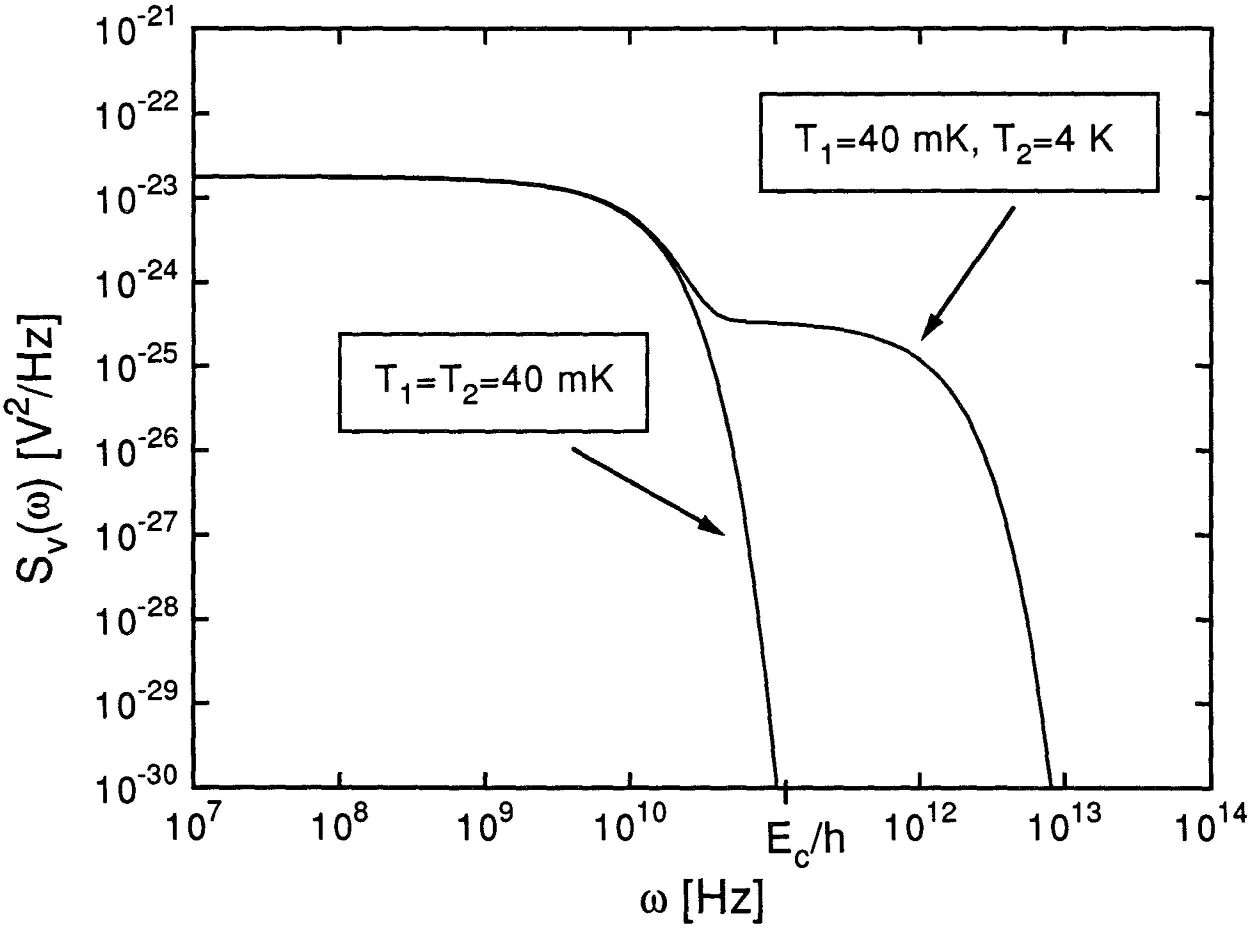

Fig 2.10 *Spectral density of the voltage noise as a function of the frequency calculated for the circuit of* Fig. 2.9, *in the case where* $R_1 = 49\ \Omega$, $R_2 = 100\ \Omega$, $R_3 = 1\ \Omega$ *and* $C_\Sigma = C + C_s = 1$ fF.

function $S_V(-\omega)$ is shown schematically in Fig. 2.10 when $R_1 = 49\ \Omega$, $R_2 = 100\ \Omega$, $R_3 = 1\ \Omega$, and $C_\Sigma = 1$ fF for two cases $T_1 = T_2 = 40$ mK and $T_1 = 40\text{ mK} << T_2 = 4$ K. When $T_1 << T_2$, the dominant noise at frequency $\omega_c = E_c/\hbar$ comes from the resistor R_2 at T_2. This off-equilibrium tunneling rate calculation shows how crucial low temperature filtering is to prevent the activation of tunnel events from parts of the measuring circuit at higher temperatures.

2. 2 The normal/superconducting electron box.

In this section, we consider the case of a superconducting electron box where the island is made of a superconducting metal and connected to a non-superconducting lead through a superconducting/normal tunnel junction. We can regard the island as a small piece of superconductor free to exchange charges with an electron reservoir. According to the BCS theory of superconductivity, electrons are paired in the ground state of a superconductor [16]. The pairing of electrons clearly breaks the invariance of the ground state with respect to the parity of the total number N of conduction electrons. Since, in the island of the electron box, this number N is fixed, we must distinguish two cases depending on the parity of N. If N is even, all the electrons can be paired in the island and there is a unique superconducting ground state. If N is odd, one electron should remain unpaired as a quasiparticule excitation with an energy at least equal to the BCS energy gap Δ and the superconducting ground state is degenerate. As pointed out by Averin and Nazarov [17], this odd-even asymmetry should result in a parity dependence of the ground state energy of the box. We will discuss in this section how the electron box experiment can reveal this odd-even asymmetry. We will also show under which conditions the macroscopic charge on a superconductor is quantized in units of $2e$.

2. 2. 1 Odd-even symmetry breaking and 2e-quantization in the normal/superconducting electron box at T=0.

For the sake of simplicity, we first assume that the total number N of conduction electrons in the island and the number n of excess electrons have the same parity. At $T = 0$ and in absence of magnetic field, the total energy E of the superconducting box is given by

$$E = E_c(n - C_s U/e)^2 + D_0 p_n , \tag{40}$$

where D_0 is the energy difference at $T = 0$ between the odd-n and the even-n ground states of the system, and $p_n = n \bmod 2$. The first term in the right-hand side of Eq. (40) is the usual total electrostatic energy E_n of the circuit of the non-superconducting case, hereafter referred to as the normal case. The second term is a parity dependent energy which corresponds to the fact that an unpaired electron must remain when the number of electrons stored in the island is odd. If N and n have opposite parities, p_n is given by $p_n = (n+1) \bmod 2$.

The BCS theory predicts that in zero field the excitation energy D_0 is equal to Δ, the superconducting energy gap of the island. Nevertheless, a finite magnetic field or the presence of paramagnetic impurities inside the sample can induce pair-breaking effects [18]. As we shall see in section 2.2.4, these effects modify the quasiparticles energy spectrum of a superconductor. Thus the excitation energy D_0 involved in the ground state energy of the box is not necessarily equal to the pair potential Δ in the superconducting island.

In Fig. 2.11, we plot the energy E versus $C_s U/e$ and we get a set of parabolas indexed by n. The odd-n parabolas are shifted up with respect to the even-n parabolas by an amount equal to D_0. Therefore, at $T = 0$, the energy cost of adding one extra electron in the island will depend crucially on the relative magnitude of the charging energy E_c and the excitation energy gap D_0. Two cases must be distinguished:

i) When $D_0 < E_c$ (Fig. 2.11b), the incremental charge of the Coulomb staircase is still equal to e but the even-n steps are longer than the odd-n steps. The experimental observation of such an asymmetric staircase is reported in Sec. 3.2.1. In comparison with the normal case, when U increases, it is now more "difficult" for the system to attain an odd-n state but "easier" to leave it. If n is even, the energy cost of the addition of one electron in the island is the **sum**

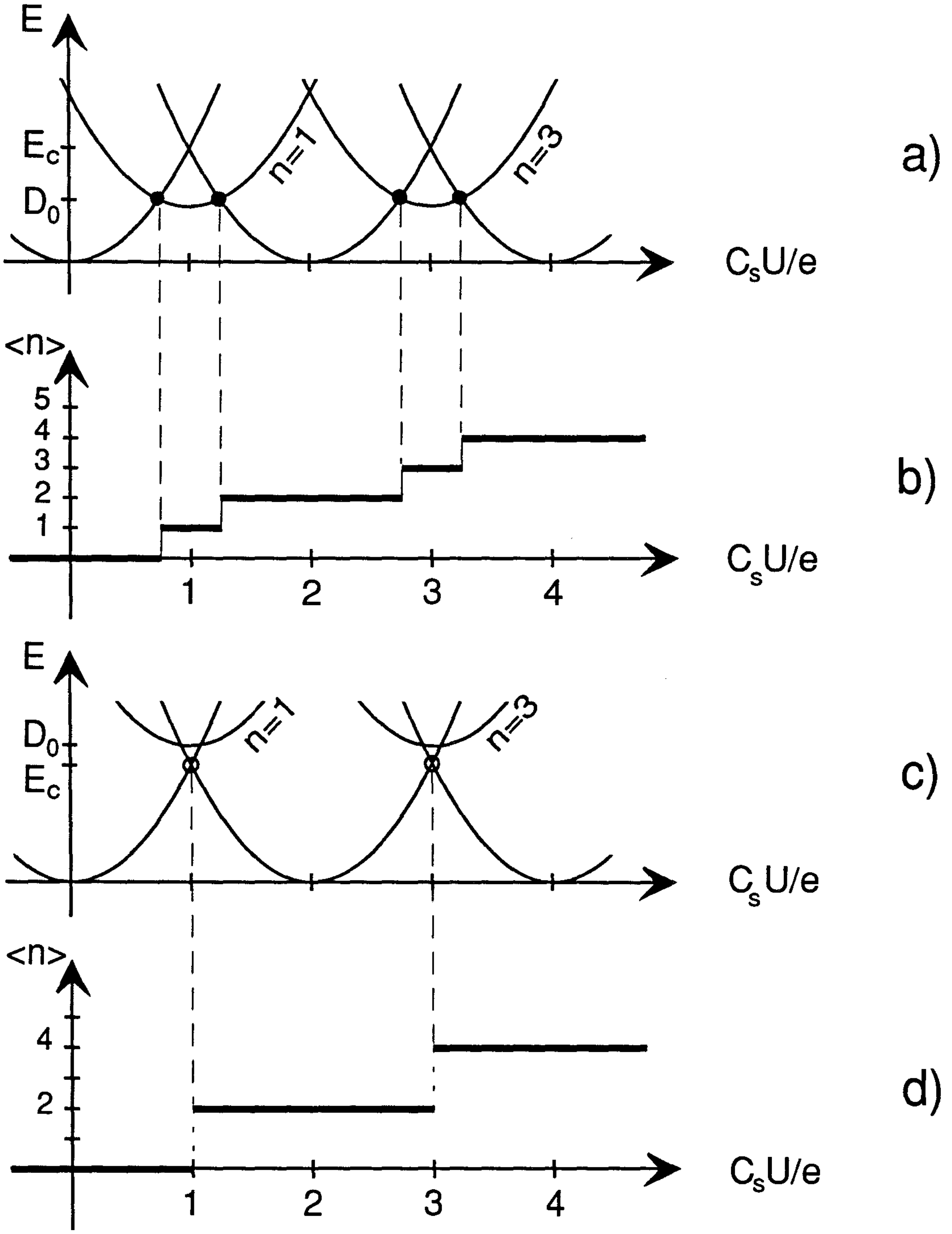

Fig 2.11 *Energy of the normal/superconducting electron box as a function of* C_sU/e *for several values of the number n of excess electrons in the island when* $E_c > D_0$ (a) *and when* $E_c < D_0$ (c). *The black dots* (a) *correspond to level crossings where one electron tunnels into and out of the island* (b). *The open dots* (c) *correspond to level crossings where two electrons tunnel into the island to form a Cooper pair* (d).

of the electrostatic energy cost of one extra charge and the superconducting energy gap required for creating one quasiparticle excitation. If n is odd, however, the energy cost of the addition of one electron is the **difference** between the electrostatic energy cost of one extra charge and the superconducting energy gap. From Eq. (40), the ratio between the excitation energy D_0 and the charging energy E_c can be expressed in terms of the length S of the odd-n steps and the length L of the even-n steps of the staircase through the relation:

$$D_0/E_c = (L-S)/(L+S). \tag{41}$$

ii) When $D_0 > E_c$ (Fig. 2.11c), the ground state of the island is always an even-n state, the island can only contain an even number number of electrons. Consequently, the staircase is symmetric with an incremental charge equal to $2e$ and the step length is twice as large as in the normal case. The superconducting electron box is in the $2e$-quantization regime. The direct observation of the $2e$-quantization of the incremental charge of a superconducting island is described in Sec. 3.2.2.

When $D_0 > E_c$, the transition which occurs between two even-n states of the island involves the simultaneous tunneling of two electrons into the island which form a Cooper pair. This mechanism, identical to the so-called Andreev reflection [19] of an electron into a hole, is a second order process in the tunnel hamiltonian. The two-electron tunneling conductance G_{NS} associated with this process has been calculated by Eiles *et al.* [20]. At $C_s U/e = 1$, the conductance G_{NS} of the normal/superconducting junction of the box is given by

$$G_{NS} = \frac{R_K}{4M_{eff}R_t^2}\,\mathrm{f}^2(E_c/D_0), \tag{42}$$

where M_{eff} is the number of effective conduction channels through the barrier of the junction, R_t is the normal state tunnel resistance of the junction and where $\mathrm{f}(\mathrm{E_c}/D_0) = (2/\pi)\arccos(-E_c/D_0)\Big/\sqrt{1-(\mathrm{E_c}/D_0)^2}$ is a factor equal to $\mathrm{f}=1$ in the limit $E_c \ll D_0$. Since $R_t/R_K \gg 1$, the junction conductance is reduced in comparison with the normal case but the time G_{NS}/C is still sufficiently short to ensure that the normal/superconducting electron box stays in thermodynamic equilibrium under common sweep rate conditions.

2.2.2 Effect of finite temperature.

In practice, the Coulomb staircase is modified by the thermal fluctuations. As in the normal case, thermal fluctuations can change the number of electrons in the island, but they can also break Cooper pairs and create quasiparticle excitations in the island without changing the total number of electrons. The different states of the island are now characterized not only by the number n of excess electrons but also by the filling factors of the various quasiparticles states of the island.

We will calculate the average number $\langle n \rangle$ using Eq. (7). When the island is superconducting, the partition function Z of the system takes the following form:

$$Z = \sum_n Z_n e^{-E_n/k_B T}, \tag{43}$$

where Z_n is the partition function for quasiparticle excitations above the ground state in the superconducting island with n excess electrons. For a given value of n, the conservation of the number of electrons in the island requires that excitations must be always created two at a time by substracting a Cooper pair from the condensate. We thus set the parity of the number of quasiparticles equal to the parity of n and we assume otherwise that the quasiparticle excitations can be simply described as independent fermions. This last assumption neglects corrections of order $1/N$ on the thermodynamic quantities [21] which is acceptable here since $N \sim 10^9$. Following Ref [22], we first introduce:

$$Z_\pm = \Pi_q\left[1 \pm \exp\left(-\beta\varepsilon_q\right)\right], \tag{44}$$

where $\beta = 1/k_B T$ and where the subscript q denotes a generic quasiparticle with an energy ε_q. Then we obtain

$$Z_n = \left[Z_+ + (-1)^n Z_-\right]/2 . \tag{45}$$

This quantity can only take two different values Z_{even} or Z_{odd} depending on the parity of n. Combining Eq. (7) and Eq. (43) we can express the average number of electrons in the superconducting island as:

$$\langle n \rangle = \frac{\sum_{n=-\infty}^{n=+\infty} n \exp[-\beta(E_n + F_n)]}{\sum_{n=-\infty}^{n=+\infty} \exp[-\beta(E_n + F_n)]}, \tag{46}$$

where $F_n = -k_B T \ln Z_n$ is defined as the free energy of the superconducting island with n excess electrons. Multiplying the numerator and the denominator of the right hand side of Eq. (46) by $\exp(\beta F_{even})$, we get:

$$\langle n \rangle = \frac{\sum_{n=-\infty}^{n=+\infty} n \exp[-\beta(E_n + p_n D(T,H))]}{\sum_{n=-\infty}^{n=+\infty} \exp[-\beta(E_n + p_n D(T,H))]}, \tag{47}$$

where $D(T,H) = F_{odd} - F_{even}$ is the odd-even free energy difference of the island, first introduced by Tuominen *et al.* [22]. Expression (47) shows that, at finite temperature, $D(T,H)$ is the relevant quantity for the energy shift between the even-n and the odd-n parabolas.

If we consider an asymmetric Coulomb staircase at finite temperature, the length of the steps can be defined by the values of U where $\langle n \rangle$ is a half integer. From Eq. (46), one readily shows that a half integer values of $\langle n \rangle$ means that the sum $E_n + F_n$ is equal for two neighbouring n states of the island. The lengths S of the odd-n steps and L of the even-n steps are thus given by $S = 1 - D(T,H)/E_c$ and $L = 1 + D(T,H)/E_c$. Compared to an asymmetric staircase at $T = 0$, the relative length of the odd-n and the even-n steps is now determined by $D(T,H)$. Consequently, when the normal/superconducting box is not in the $2e$-quantization regime ($D_0 < E_c$), the staircase asymmetry is a direct measurement of the ratio $D(T,H)/E_c$ through the relation:

$$\frac{D(T,H)}{E_c} = \frac{L-S}{L+S}. \tag{48}$$

By measuring the asymmetry of the Coulomb staircase at various temperatures, we have determined experimentally the odd-even free energy difference of a small aluminum island (see section 3.2.1).

As in the normal case, the incremental charge staircase is rounded at finite temperature because the system can reach various n-states by thermal excitations. Nevertheless, in the limit $k_B T << E_c$, the most important effect of the temperature is a reduction of the odd-even asymmetry. This effect originates in the entropy contributions to the free energy F_n as we will see in next section.

2.2.3 Calculation of the odd-even free energy difference *D*(*T*,*H*).

We will now derive a general expression of the odd-even free energy difference $D(T,H)$ in terms of the temperature T and the density $\rho(\varepsilon)$ of quasiparticle states in the island. The dependence of $D(T,H)$ on the magnetic field H enters only through the density of quasiparticle states $\rho(\varepsilon)$. Using Eq. (45), $D(T,H)$ is written:

$$D(T,H) = -k_B T \ln \frac{Z_{odd}}{Z_{even}} = -k_B T \ln \frac{Z_+ - Z_-}{Z_+ + Z_-}. \tag{49}$$

If we know $\rho(\varepsilon)$, we can express $Z_\pm$ in the integral form:

$$Z_\pm = \exp\left[\int_0^{+\infty} \rho(\varepsilon) \ln\left(1 \pm e^{-\beta\varepsilon}\right) d\varepsilon\right]. \tag{50}$$

We express the ratio Z_+/Z_- as:

$$\frac{Z_+}{Z_-} = \exp\left[\int_0^{+\infty} \rho(\varepsilon) \ln\left(\frac{1+e^{-\beta\varepsilon}}{1-e^{-\beta\varepsilon}}\right) d\varepsilon\right]. \tag{51}$$

Then introducing the integral transform $\tilde{\rho}(T,H)$ given by

$$\tilde{\rho}(T,H) = \int_0^{\infty} \rho(\varepsilon) \ln\left[\coth(\beta\varepsilon/2)\right] d\varepsilon/2, \tag{52}$$

we obtain:

$$D(T,H) = -k_B T \ln\left[\tanh \tilde{\rho}(T)\right]. \tag{53}$$

Formula (52) and (53) show that the odd-even free energy difference is a functional of the density of quasiparticle states $\rho(\varepsilon)$.

At $H=0$, we can assume for the superconducting island a continuous BCS density of quasiparticle states given by $\rho(\varepsilon)=0$ for $\varepsilon<\Delta$ and $\rho(\varepsilon)=2\rho_A N_A\,\varepsilon\big/\sqrt{\varepsilon^2-\Delta^2}$ for $\varepsilon>\Delta$. Here ρ_A is the density of states at the Fermi level per atom when the metal is in the normal state, N_A is the number of atoms in the island and the factor of 2 is inserted to count both quasielectrons and quasiholes excitations. Over the temperature range we will consider ($T<300\text{mK}$), Δ can be taken as constant and we assume also that $e^{-\beta\Delta}<<1$. With these approximations, the integral transform $\tilde{\rho}(T,0)$ can be evaluated analytically. We rewrite Eq. (52) as

$$\tilde{\rho}(T,0)\approx e^{-\beta\Delta}\int_{\Delta}^{+\infty}2\rho_A N_A\varepsilon\left(\varepsilon^2-\Delta^2\right)^{-1/2}e^{-\beta(\varepsilon-\Delta)}\,d\varepsilon\,. \tag{54}$$

Then one obtains

$$\tilde{\rho}(T,0)\approx N_{eff}(T)e^{-\beta\Delta}, \tag{55}$$

where

$$N_{eff}(T)=N_0\left(2\pi k_B T/\Delta\right)^{1/2}+O\left[(T/\Delta)^{3/2}\right] \tag{56}$$

is the effective number of quasiparticle states available for excitations and where $N_0=\rho_A N_A\Delta$. Finally, at temperatures such that $N_{eff}\,e^{-\beta\Delta}<<1$, $D(T,0)$ is approximately given by

$$D(T,0)\approx\Delta-k_B T\ln N_0\,. \tag{57}$$

This expression defines a cross-over temperature $T_0=\Delta\big/\left(k_B\ln N_0\right)$ above which the odd-even free energy difference rapidly vanishes. At $T\geq T_0$, the island of the box is still in the superconducting state but the Coulomb staircase has the same aspect as in the normal state. The cross-over temperature T_0 corresponds roughly to the temperature at which the number of thermally induced quasiparticles in the island is equal to 1. The expression of T_0 is approximately equal to the temperature T^* defined in Ref [22]. The threshold temperature T^* has been introduced to separate the regions where the current-voltage characteristic of a superconducting double junction circuit is a $2e$-periodic or an e-periodic function of the gate-induced charge.

More generally, if discrete quasiparticles states are present inside the gap of the energy spectrum at energies ε_{q_i} with degeneracies g_{q_i}, they each contribute to $\tilde{\rho}(T,H)$ by $g_{q_i} e^{-\beta \varepsilon_{q_i}}$. Therefore the odd-even free energy difference in the limit $T \to 0$ is given by

$$D(T,0) = \varepsilon_{q_0} - k_B T \ln g_{q_0} \ , \tag{58}$$

where q_0 denotes the discrete quasiparticle state of lowest energy.

2.2.4 Influence of the magnetic field.

For a "small" superconductor in a magnetic field, we can use the density of states calculated by Skalski *et al* [23]. Here "small" means that the superconductor has dimensions normal to the field less than the London length λ_L so that screening currents can be neglected. It has been shown [24] that this calculation of the density of states is valid only in the "dirty" limit, i.e., when $\ell << \xi_0$, where ℓ is the electronic mean free path and ξ_0 is the coherence length. This latter quantity is given by $\xi_0 = \hbar v_F / \pi\Delta$, where v_F is the Fermi velocity and Δ is the BCS energy gap at $T = 0$ and $H = 0$. In aluminum $\xi_0 = 1.6 \mu m$ and in our sample, under the assumption of surface scattering, ℓ is expected to be less than 100 nm (see section 3.2.1). We can thus assume that the condition $\ell << \xi_0$ is satisfied.

In Ref [23], the effect of the magnetic field or magnetic impurities is completely included in a single parameter, the pair breaking energy Γ which has to be calculated separately from the geometry of the problem (see below). Using the Abrikosov-Gor'kov theory [25], Skalski *et al.* associate to a quasiparticle of energy ε in the normal state a reduced complex energy u given by:

$$u = \frac{\varepsilon}{\Delta(T,\Gamma)} + i \frac{\Gamma}{\Delta(T,\Gamma)} \frac{u}{\sqrt{u^2 - 1}} \ , \tag{59}$$

where $\Delta(T,\Gamma)$ is the pair potential satisfying the following self-consistent equation:

$$\Delta(T,\Gamma) = N(0)V \int_0^{\omega_{D'}} d\omega \, \mathrm{Re}\left[\frac{1}{\sqrt{u^2 - 1}}\right] \tanh\left(\tfrac{1}{2}\beta\omega\right) . \tag{60}$$

Here $N(0)$ is the density of states at the Fermi energy per unit volume in the normal state, V is the volume of the sample, $\omega_{D'}$ is a cut-off energy and $\beta = 1/k_B T$. The quantity $\Delta(T,\Gamma)$ must now be distinguished from the minimum energy for excitations, or spectral gap, which we denote by $\Omega_G(T,\Gamma)$. These two quantities are related by

$$\Omega_G(T,\Gamma) = \Delta(T,\Gamma)\left[1-(\Gamma/\Delta(T,\Gamma))^{2/3}\right]^{3/2} . \tag{61}$$

The second term of the right hand side of Eq. (59) corresponds to a complex energy shift of the energy of a quasiparticle state. This shift is proportional to a complex density of states $\tilde{N}(u)$ defined as

$$\tilde{N}(u) = u\big/\sqrt{u^2-1} , \tag{62}$$

the pair breaking energy Γ being the proportionality coefficient. The quasiparticle density of states $\rho(\varepsilon)$ which enters in Eq. (52) is expressed as

$$\rho(\varepsilon) = \rho_N(\varepsilon)\,\mathrm{Re}\left[\tilde{N}(u)\right] , \tag{63}$$

where $\rho_N(\varepsilon) = 2\rho_A N_A$ refers to the quasiparticle density of states in the normal state. In the limit $\Gamma \to 0$, one recovers the BCS formulas since Eq. (63) reduces to $\rho(\varepsilon) = \rho_N(\varepsilon)\varepsilon\big/\sqrt{\varepsilon^2-\Delta^2}$ and Eq. (60) reduces to the BCS self-consistent equation for the energy gap. For a finite value of the ratio $\Gamma/\Delta(T,\Gamma)$, Eq. (59) and Eq. (63) must be solved simultaneously to determine $\rho(\varepsilon)$.

In Fig. 2.12, we have plotted the density $\rho(\varepsilon)$ versus $\varepsilon/\Delta(T,\Gamma)$ for several values of the ratio $\Gamma/\Delta(T,\Gamma)$. From Eq. (61), one can show that the superconductor is gapless, i.e. the spectral gap is zero, when $\Gamma = \Delta(T,\Gamma)$. If $\Gamma < \Delta(T,\Gamma)$, calculations made in Ref [23] show also that the pair potential $\Delta(T,\Gamma)$ can be taken as a constant at low temperature. At $T = 0$, one has $\Gamma/\Delta = \Gamma/\Delta(0,\Gamma)\exp\left[-(\pi/4)\Gamma/\Delta(0,\Gamma)\right]$.

The odd-even free energy difference $D(T,H)$ of an aluminum island is plotted versus the temperature in Fig. 2.13 for several values of $\Gamma/\Delta(T,\Gamma)$, assuming a realistic value of the island volume. At $T = 0$, $D(0,H) = D_0$ is equal to the spectral gap $\Omega_G(0,H)$ given by Eq. (61), a quantity which is smaller than the pair potential $\Delta(0,H)$.

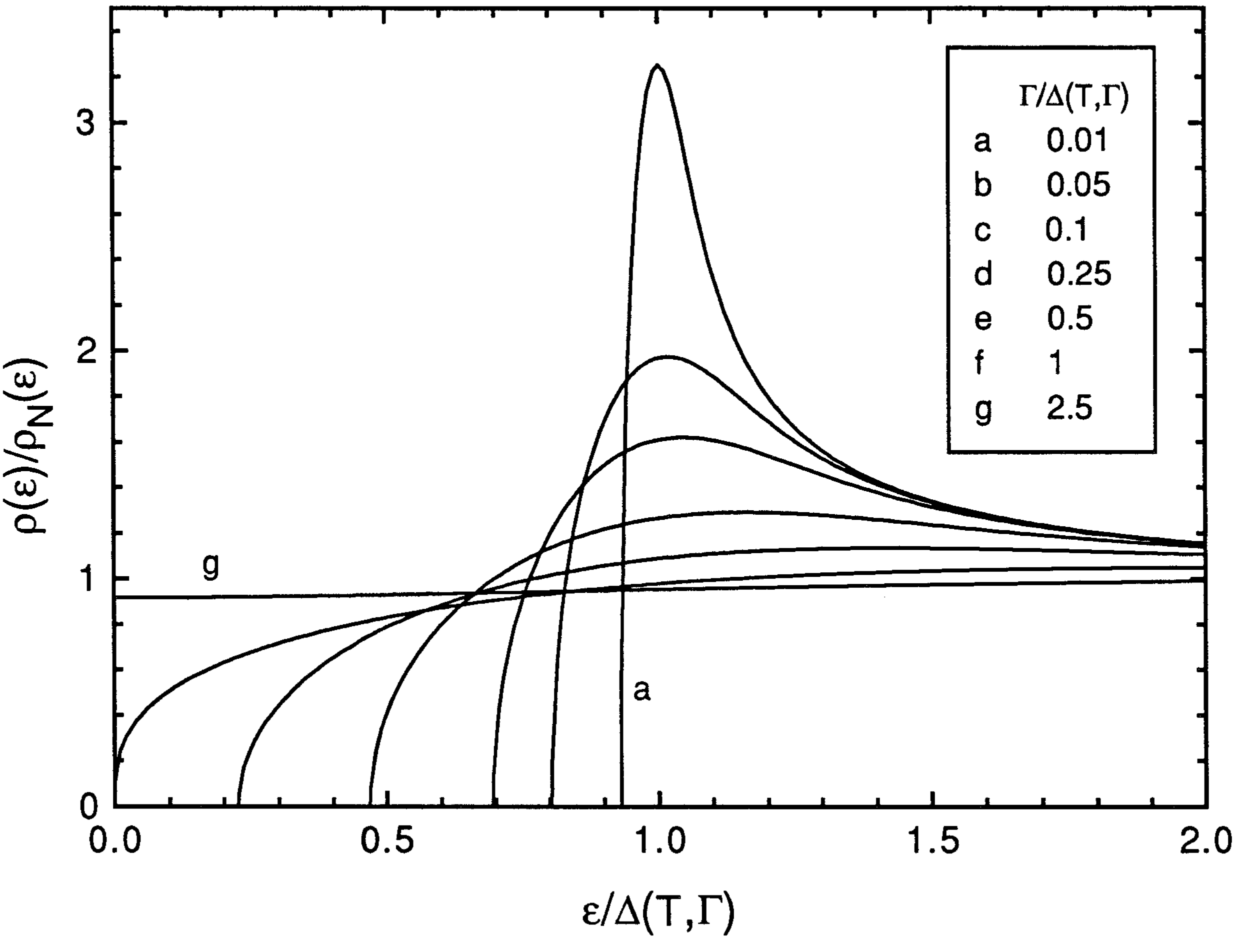

Fig 2.12 *Density of quasiparticle states in a superconductor versus reduced energy as computed by Skalski et al. for several values of the ratio* $\Gamma/\Delta(T,\Gamma)$, *where* Γ *is the pair breaking energy and where* $\Delta(T,\Gamma)$ *is the pair potential. Here* $\rho_N(\varepsilon)$ *denotes the density of quasiparticle states in the non-superconducting state.*

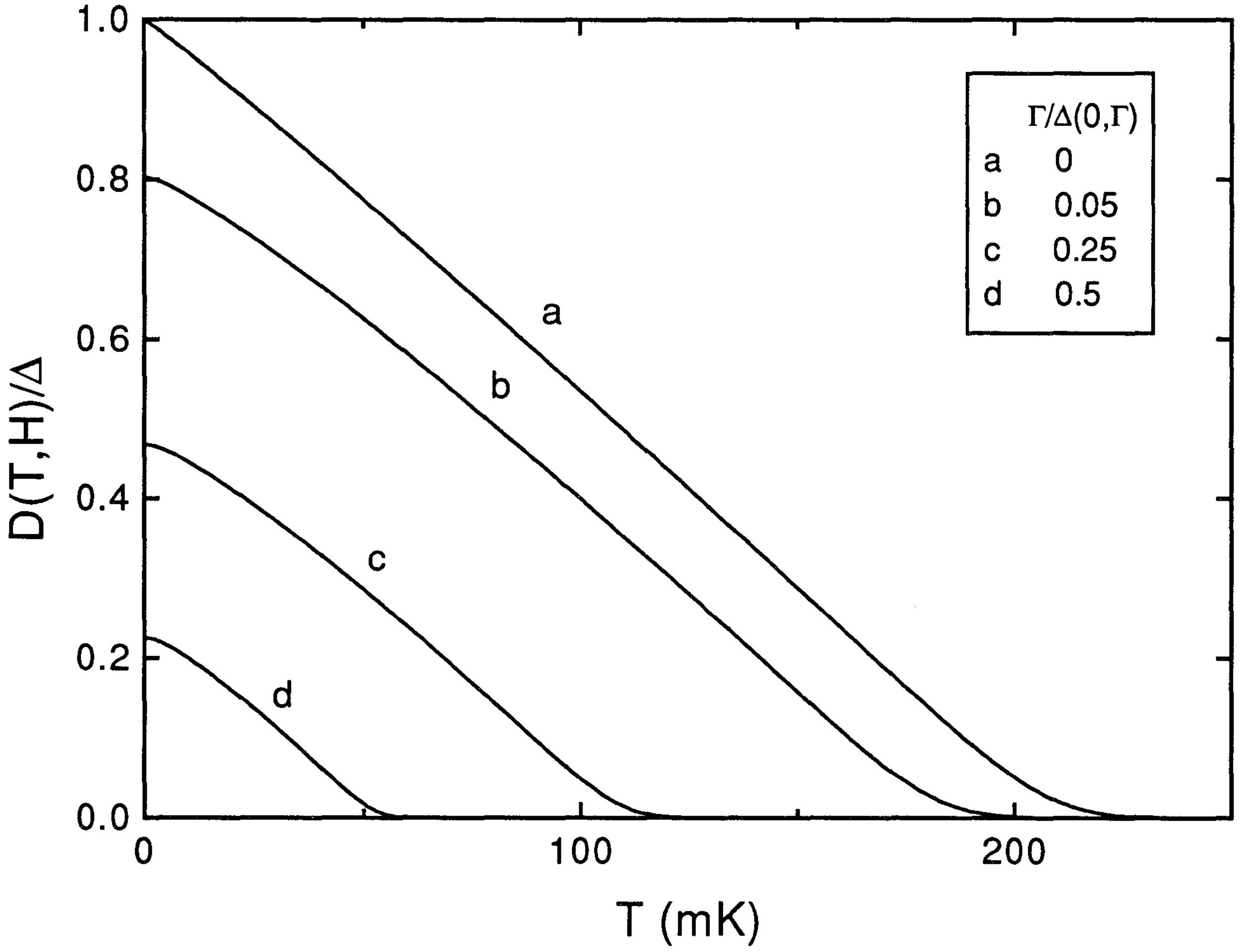

Fig 2.13 *Odd-even free energy difference* $D(T,H)$ *of an aluminum island as a function of the temperature T for four values of the ratio* $\Gamma/\Delta(0,\Gamma)$. *The quantity* Δ *is the BCS energy gap at* $T=0$ *and* $H=0$. *All the curves are calculated for an aluminum island of volume* $V=10^{-20}$ m^3, *with a normal density of state* $\rho=2.15\ 10^{47}$ J^{-1}m^{-3} *and a BCS energy gap* $\Delta=180\ 10^{-6}$ eV.

Finally, the relation between the pair breaking energy Γ and the applied magnetic field H can be calculated using a theory by De Gennes and Tinkham [26,27]. They have shown that the calculation of the critical field of small superconducting particles or thin films as a function of the magnetic field is reduced to the study of the flux Φ enclosed by all classical one electron trajectories in the normal state. Thus the magnetic behavior of such a sample is essentially governed by the geometric properties of the trajectories. These authors have classified the magnetic properties of thin films as a function of the value of the bulk mean free path ℓ. They essentially distinguish two types of magnetic behavior: ergodic and non-ergodic depending on the electron scattering properties of the sample. In the island of the box, the elastic mean free path ℓ is expected to be smaller than the width d of the metallic strip and thus the magnetic behavior of the superconducting island is "ergodic".

In the calculation of de Gennes and Tinkham, the quantity of interest is the limit of the average $\left\langle e^{i\phi(t)}\right\rangle$ at large times, where the phase ϕ is given $\phi = 2\pi\Phi/\Phi_0$, Φ_0 being the flux quantum. If the system is "ergodic", the phase ϕ has a gaussian distribution and $\lim_{t\to\infty}\left\langle e^{i\phi(t)}\right\rangle = e^{-t/\tau_K}$. In a dirty superconductor, the effect of a magnetic field is equivalent to the effect of paramagnetic impurities [27,28]. The equality $1/\tau_K = 2\Gamma/\hbar$ [29,18], where Γ is the pair breaking energy, gives the connection between de Gennes and Tinkham's analysis and the calculation of Skalski *et al.*. We can reasonably assume that in our sample $d^2/\xi_0 < \ell$ (Maki case) and following Ref [26] we write:

$$\frac{1}{\tau_K} = \frac{1}{3}\tau\left(\frac{2ev_F}{\hbar c}\right)^2\left\langle \mathbf{A}^2\right\rangle = D\left(\frac{2\pi}{\Phi_0}\right)^2\left\langle \mathbf{A}^2\right\rangle , \tag{64}$$

where $\tau = v_F\ell$, $D = \frac{1}{3}v_F^2\tau = \frac{1}{3}v_F\ell$ is the diffusion constant and $\mathbf{A}$ is the vector potential. For the particular case of a strip of width d in a perpendicular magnetic field H, the gauge invariant average $\left\langle \mathbf{A}^2\right\rangle$ is given by:

$$\left\langle \mathbf{A}^2\right\rangle = \frac{H^2 d^2}{12} . \tag{65}$$

The coherence length ξ_0 and the gap $\Delta = \Delta(T=0,\Gamma=0)$ are related by $\xi_0 = \hbar v_F/\pi\Delta$. Using this latter relation, the pair breaking energy Γ is finally given by:

$$\Gamma/\Delta = \left(\pi^3/18\right) H^2 d^2 \ell \xi_0 / \Phi_0^2 \ . \tag{66}$$

Our experimental measurement of the odd-even free energy difference as a function of the temperature and the magnetic field is reported in Sec. 3.2.2. The data are well fitted by the theoretical $D(T,H)/E_c$ calculated using the general expression (53) of the odd-even free energy difference, the density of states calculated by Skalski *et al* [23] and the magnetic field dependence of the pair breaking energy given by Eq. (66).

2.2.5 Observability of the 2e-quantization of the macroscopic charge.

The above calculation shows that in the $T \otimes H$ plane there are three concentric domains corresponding to three different behaviors of the superconducting electron box: i) when $D(T,H) = 0$, the staircase is symmetric with an incremental charge equal to e, ii) when $0 < D(T,H) < E_c$, the staircase is asymmetric with an incremental charge equal to e, iii) finally, when $D(T,H) > E_c$, the staircase displays the $2e$-quantization of the island charge.

The $2e$-periodicity of the symmetric or asymmetric staircase originates in the pairing of electrons in the island but an e-periodicity of the staircase does not mean that the island is in the non-superconducting state. The cross-over temperature T_0, which determines the boundary of the asymmetric staircase domain at $H = 0$, depends only logarithmically on the island volume. For an aluminum island fabricated by nanolithographic techniques, T_0 will be always of the order 200-300 mK. Provided $E_c >> k_B T$, the observation of an assymetric staircase is actually not constrained by the size of the sample or the junctions.

This is not the case for the $2e$-symmetric staircase. From Eq. (57), one can show that the boundary of the $2e$-quantization domain intersects indeed the T-axis at a threshold temperature T_{2e} given by

$$T_{2e} = T_0\left(1 - E_c/\Delta\right) \ . \tag{67}$$

We already know that T_0 weakly depends on the sample parameters, and thus T_{2e} is fixed essentially by the charging energy E_c and hence by the island capacitance C_Σ. Eq. (12) and Eq. (67) show that the sharpness of the staircase and the area of the $2e$-quantization domain have opposite variations with the charging energy E_c. In contrast with the usual charging effects, the smaller the junction size, the lower is the temperature required to observe the $2e$-quantization of the island charge. This is due to the fact that this phenomenon is subject to the double inequality $k_B T << E_c < D(T,H)$.

In order to observe the $2e$-quantization of the macroscopic charge one must therefore find a compromise between these two opposite effects. Note that the thermal rounding of the staircase is not as important as in the normal case because a carrier with charge equal to $2e$ yields a staircase four times sharper than in the normal case at the same temperature. Finally Eq. (58) predicts that only one quasiparticle state inside the energy gap can strongly diminish the odd-even free energy difference. It can go below the charging energy and completely suppres the $2e$-quantization even at very low temperature. In that sense, the $2e$-quantization of the island charge constitutes a sensitive test of the ideality of the superconductivity of an isolated superconductor.

2.3. The Superconducting Electron Box

2.3.1 Josephson coupling between the charge states of the box

We now consider an electron box in which both sides of the junction are superconducting (Fig. 2.14). The tunnel junction establishes a Josephson coupling between the island and the lead. We assume that $T = 0$ and $\Delta > E_c$. We also assume that there is no out of equilibrium quasiparticle in the island and in the lead attached to the junction. Under these conditions, the island only contains an even number of electrons and the states of the system are characterized by the number of excess Cooper pairs in the island.

We restrict our analysis to the interval $0 < C_s U/e < 2$. Since $T = 0$, we can consider only the Hilbert space spanned by the two states $|0\rangle$ and $|1\rangle$, which correspond respectively to the ground state of the superconducting island with zero and one excess Cooper pair. It is convenient to measure the energy of these states relatively to a reference set at $E_c(1 - C_s U/e)^2$. The energies of the states $|0\rangle$ and $|1\rangle$ are then respectively equal to $-E/2$ and

$+E/2$, where $E = 4E_C(1 - C_s U/e)$. These two energies are represented on Fig. 2.15 by two straight lines which cross at the threshold value $C_s U/e = 1$.

Because of Josephson tunneling, the states $|0\rangle$ and $|1\rangle$ are not eigenstates of the system. In the bidimensional Hilbert space $\{|0\rangle, |1\rangle\}$, the Josephson tunnel hamiltonian H_t can be written as [12]:

$$H_t = -\frac{E_J}{2}\left(|0\rangle\langle 1| + |1\rangle\langle 0|\right), \tag{68}$$

where E_J is the Josephson energy of the junction. Since there are no quasiparticles in the island or in the lead, the total hamiltonian H is simply the sum of the total electrostatic energy and the Josephson tunnel hamiltonian. Consequently, the system can be seen as an effective spin ½ with the following hamiltonian:

$$H = -\frac{E}{2}\sigma_z - \frac{E_J}{2}\sigma_x \tag{69}$$

where σ_z and σ_x are the Pauli matrices. This hamiltonian corresponds to a magnetic field making an angle $\gamma = \arctan(E_J/E)$ with the z axis. The eigenstates of H are linear superpositions of $|0\rangle$ and $|1\rangle$ given by:

$$\begin{aligned} |\Psi_s\rangle &= \cos\frac{\gamma}{2}|0\rangle + \sin\frac{\gamma}{2}|1\rangle \\ |\Psi_a\rangle &= \sin\frac{\gamma}{2}|0\rangle - \cos\frac{\gamma}{2}|1\rangle \end{aligned} \tag{70}$$

The energies E_s and E_a of the two eigenstates $|\Psi_s\rangle$ and $|\Psi_a\rangle$ are given by

$$E_{a/s} = \pm\frac{1}{2}\sqrt{E^2 + E_J^2} \tag{71}$$

As shown in Fig 2.15, the Josephson coupling results in an anticrossing of the levels. At $C_s U/e = 1$, the energy splitting $E_a - E_s$ is equal to the Josephson energy E_J. Since the ground state $|\Psi_s\rangle$ is a superposition of two states with a well defined number of Cooper pairs in the island, the mean value $\langle n\rangle$ of the number of excess electrons is no longer an integer. Assuming that the system stays in its ground state when we sweep the voltage U, $\langle n\rangle$ is simply given by $\langle n\rangle = 2\sin^2(\gamma/2)$ and we obtain:

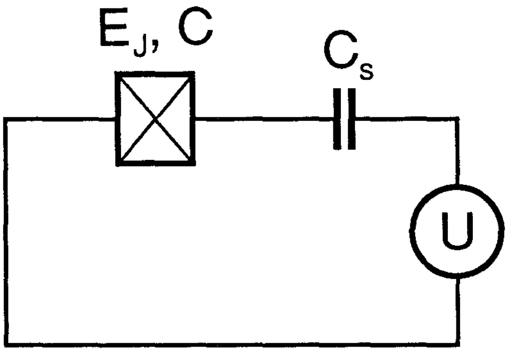

Fig 2.14 *Schematic of a superconducting electron box where the tunnel junction is a Josephson junction characterized by its capacitance C and its Josephson energy* E_J.

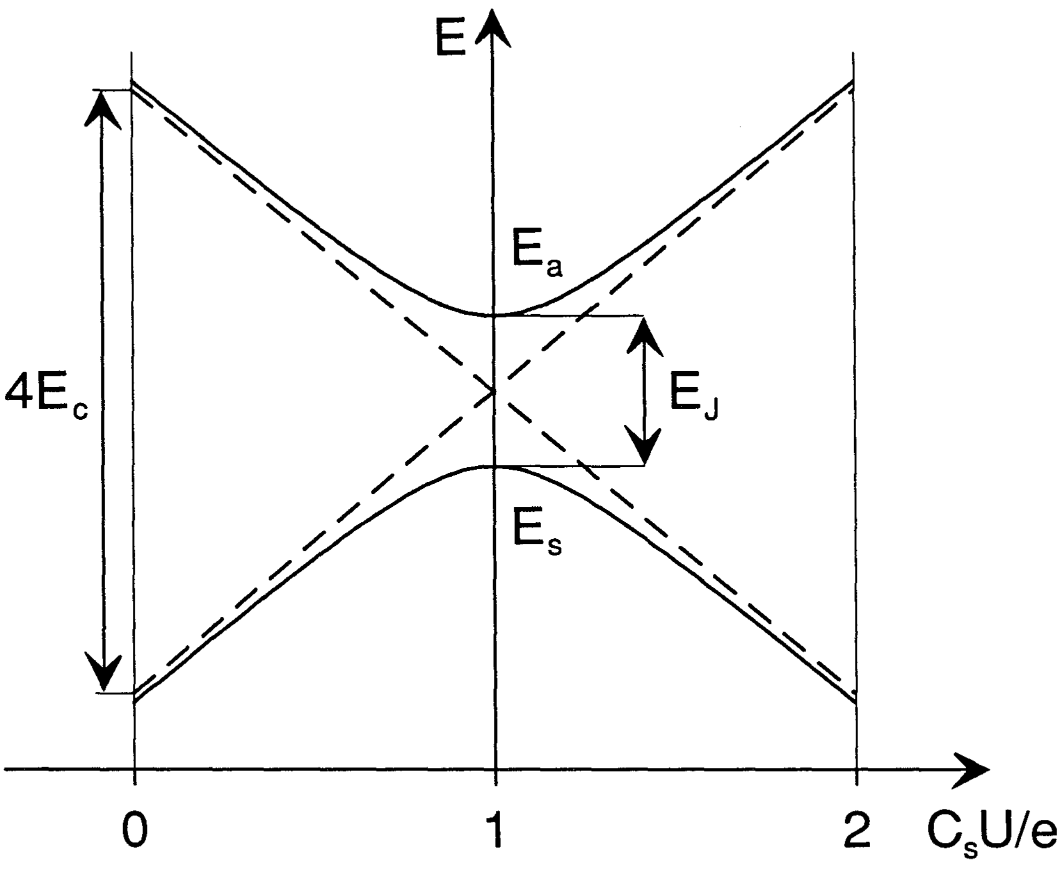

Fig 2.15 *Energies of the two eigenstates* $|\Psi_s\rangle$ *and* $|\Psi_a\rangle$ *of the system versus* C_sU/e. *Dashed lines are the energies of the unperturbed states* $|0\rangle$ *and* $|1\rangle$. *At* $C_sU/e = 1$, *the energy splitting between the two eigenstates is equal to* E_J.

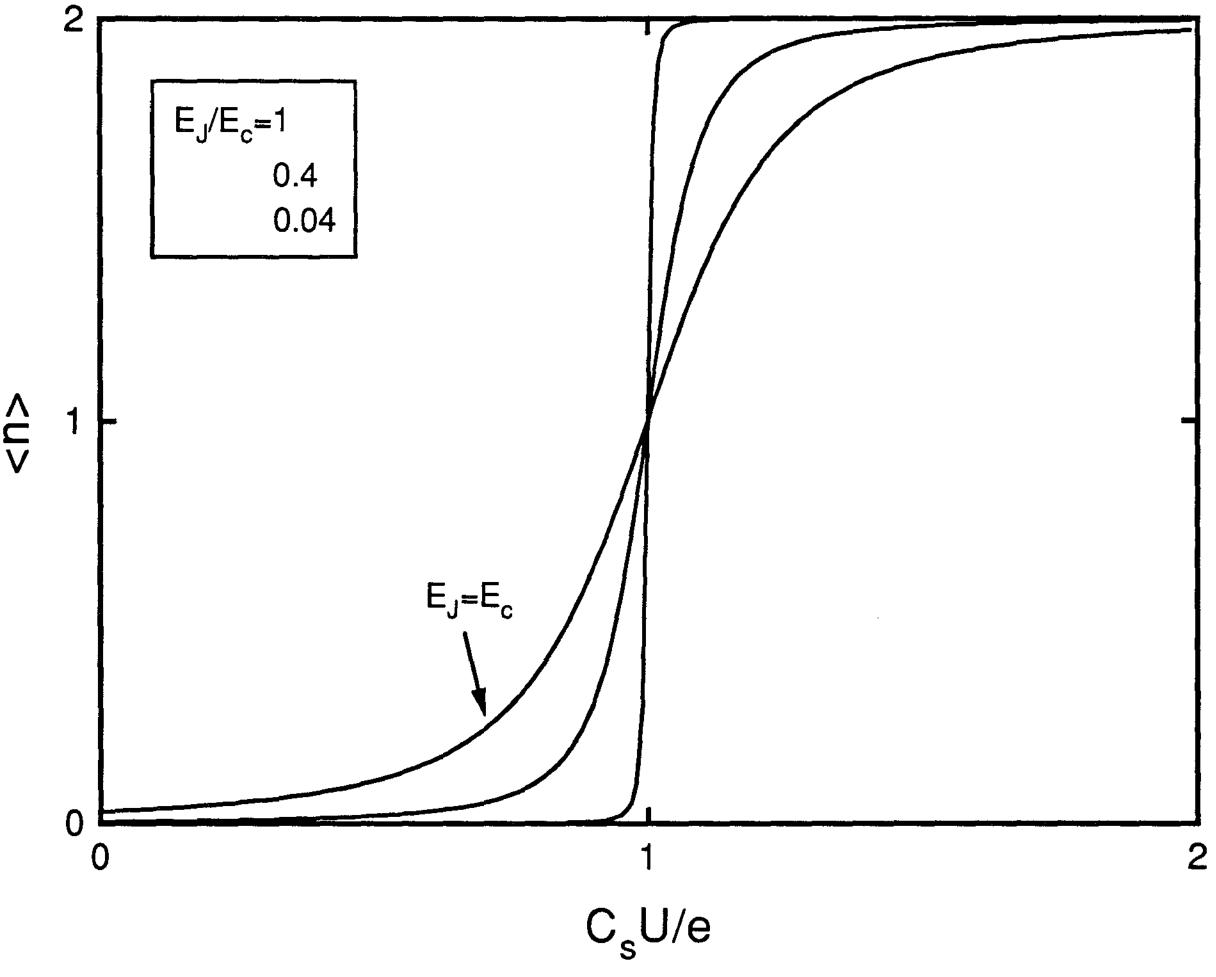

Fig 2.16 *Average number* $\langle n \rangle$ *of excess electrons in the island of the superconducting electron box as a function of* C_sU/e *calculated from Eq. (72) for three values of the ratio* E_J/E_c .

$$\langle n\rangle = 1 + \frac{C_s U/e - 1}{\sqrt{(C_s U/e - 1)^2 + (E_J/4E_c)^2}} \; . \tag{72}$$

The charge jump of the staircase exhibits a finite slope (see Fig. 2.16) given by

$$\frac{\partial\langle n\rangle}{\partial(C_s U/e)}(C_s U/e = 1) = \frac{4E_c}{E_J} \, , \tag{73}$$

which is equal to the ratio between the charging energy associated with a Cooper pair and the Josephson energy. This quantity has to be compared to the slope $2E_c/k_BT$ arising from the thermal rounding of a $2e$ staircase.

2.3.2 Effect of the Electromagnetic Environment

The question now arises as to whether the coherent quantum superposition of charge states leading to (72) and (73) will survive in the presence of dissipation in the leads which has been neglected so far. We will thus evaluate the effect of the electromagnetic environment of the junction on the box considered as an effective two-state system. We model the electromagnetic environment as an impedance $Z(\omega)$ in series with the superconducting electron box (Fig. 2.17a). As in the normal case, the circuit is equivalent to a pure tunnel element in series with an effective impedance $Z_t(\omega)$ and an effective voltage source. $Z_t(\omega)$ is the total impedance seen by the pure tunnel element of the junction and its the real part is given by

$$\mathrm{Re}[Z_t(\omega)] = \kappa^2 \,\mathrm{Re}\left[\frac{1}{Z^{-1}(\omega) + j\kappa C\omega}\right] , \tag{74}$$

where $\kappa = C/C_\Sigma$. The impedance $Z_t(\omega)$ is equivalent to a set of L-C oscillators of frequency $\omega_j = 1/\sqrt{L_j C_j}$ (see Fig. 2.17c) such that:

$$\mathrm{Re}[Z_t(\omega)] = \sum_j \pi/C_j \,\delta(\omega - \omega_j) \, . \tag{75}$$

The hamiltonian H_{env} of the electromagnetic environment is thus the hamiltonian of the set of harmonic oscillators:

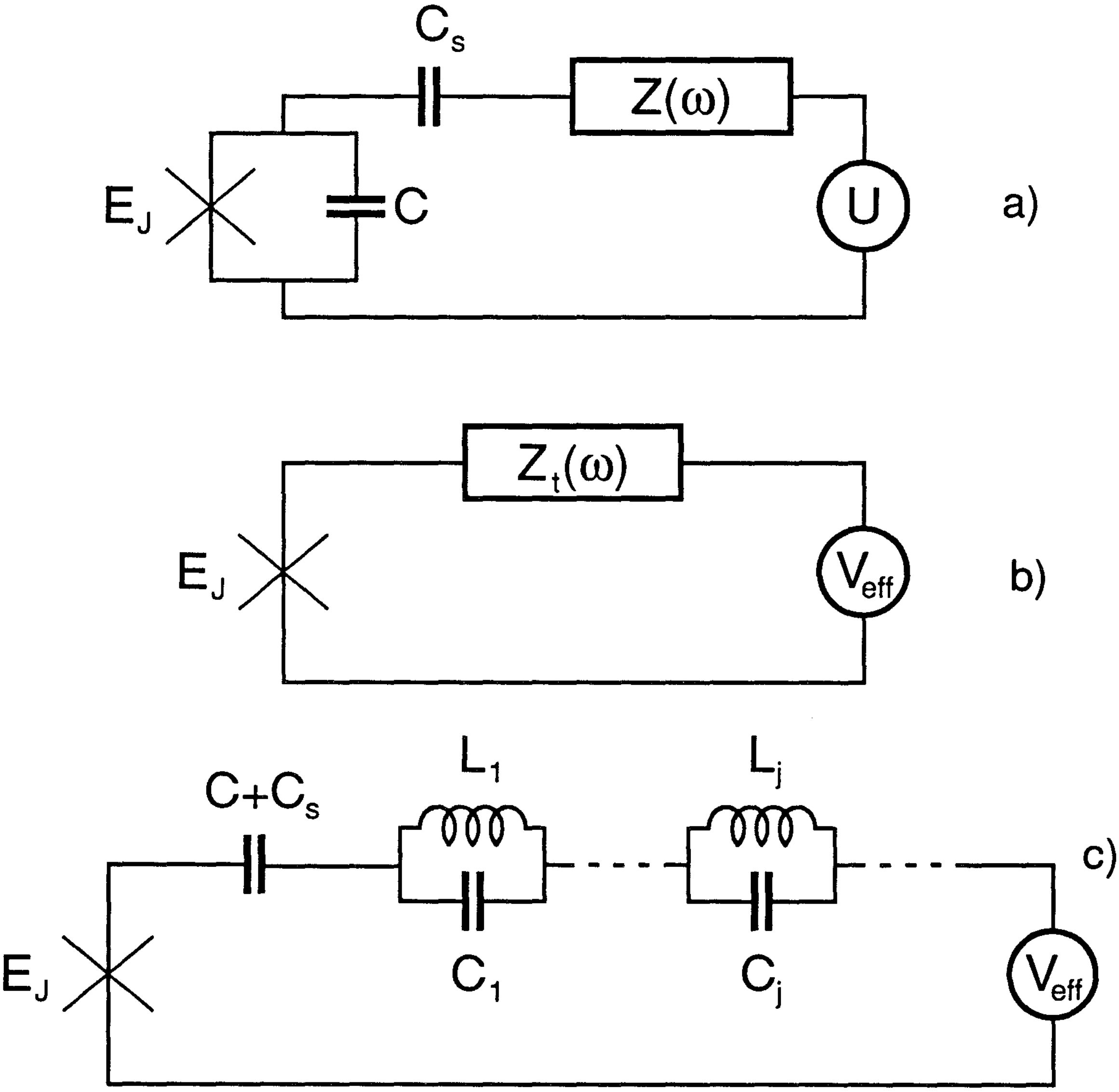

Fig. 2.17 a) *Schematic of the superconducting electron box circuit coupled to its electromagnetic environment. The junction is represented by a pure capacitor of capacitance C in parallel with a Josephson tunnel element characterized by* E_J*. The electromagnetic environment of the circuit is modeled by an impedance* $Z(\omega)$ *in series with the voltage source.* b) *Equivalent circuit seen by the Josephson element.* c) *The total impedance* $Z_t(\omega)$ *can be described as a capacitance* $C+C_S$ *in series with a set of L-C oscillators.*

$$H_{env} = \sum_j \left(\frac{\Phi_j^2}{2L_j} + \frac{Q_j^2}{2C_j} \right). \tag{76}$$

The unperturbed hamiltonian H_0 is now:

$$H_0 = -\frac{E}{2}\sigma_z + H_{env} . \tag{77}$$

Finally, the coupling between the environment and the two-state system is contained in the tunneling hamiltonian [12] which is now written in terms of projectors:

$$H_t = -\frac{E_J}{2}\left[e^{i\varphi}\sigma_+ + h.c.\right], \tag{78}$$

where $\sigma_+ = \left(\sigma_x - i\sigma_y\right)/2 = \begin{pmatrix} 0 & 1 \\ 0 & 0 \end{pmatrix}$ and where $\varphi = 2e/\hbar \sum_j \Phi_j$. The translation operator $e^{i\varphi}$ acts only the environmental degrees of freedom. It shifts the charge of each L-C oscillator of the environment by an amount equal to $-2e$:

$$e^{-i\varphi} Q_j e^{i\varphi} = \left(Q_j - 2e\right) \tag{79}$$

The total hamiltonian $H = H_0 + H_t$ is:

$$H = -\frac{E}{2}\sigma_z - \frac{E_J}{2}\left(\sigma_+ e^{i\varphi} + \sigma_- e^{-i\varphi}\right) + \sum_j \left(\frac{\Phi_j^2}{2L_j} + \frac{Q_j^2}{2C_j} \right), \tag{80}$$

where $\sigma_+ = \begin{pmatrix} 0 & 1 \\ 0 & 0 \end{pmatrix}$ and $\sigma_- = \begin{pmatrix} 0 & 0 \\ 1 & 0 \end{pmatrix}$.

In order to diagonalize the interaction between the set of the oscillators and the two-state system, we proceed a canonical transformation $\tilde{H} = UHU^{-1}$, where

$$U = \exp\left[-i\sigma_z \, \varphi/2\right]. \tag{81}$$

Thus, we obtain

$$\tilde{H} = -\frac{E}{2}\sigma_z - \frac{E_J}{2}\sigma_x + \sum_j \left(\frac{\Phi_j^2}{2L_j} + \frac{Q_j^2}{2C_j} \right) - \frac{1}{2}\sigma_z \sum_j 2e\frac{Q_j}{C_j} + \sum_j \frac{e^2}{2C_j} . \tag{82}$$

The problem of the superconducting box coupled to an arbitrary impedance is now reduced to the study of a well known dissipative two-state system [30,31]. The hamiltonian $\tilde{H}$ has indeed the same form as the so-called "spin-boson" hamiltonian H_{SB}. This hamiltonian H_{SB} is usually written in the following form:

$$H_{SB} = \frac{1}{2}\hbar\varepsilon\sigma_z - \frac{1}{2}\hbar\Delta\sigma_x + \sum_j \frac{1}{2}\left(\frac{P_j^2}{m_j} + m_j\omega_j^2 x_j^2\right) + \frac{1}{2}q_0\sigma_z \sum_j c_j x_j . \tag{83}$$

Here Δ refers to the tunneling matrix element which corresponds to $E_J/\hbar$, m_j is the mass of the j–th harmonic oscillator and corresponds to L_j. The quantity c_j is the strength of coupling of the system to the j–th oscillator. Identifying x_j as Q_j, we obtain $c_j = 1/C_j$, where C_j is the capacitance of the j–th L-C oscillators, and $q_0 = -2e$. All the effects of the environment are contained in the spectral density function $J(\omega) = \pi/2 \sum_j (c_j/m_j\omega_j)\delta(\omega - \omega_j)$ which is given by $J(\omega) = \omega\,\mathrm{Re}[Z_t(\omega)]/2$ for the electron box circuit.

We consider now the simple case where the impedance $Z(\omega)$ is a pure resistance R. In this case, $\mathrm{Re}[Z_t(\omega)] = \kappa^2 R\,\mathrm{Re}[1/(1 + j\kappa RC\omega)]$. This situation corresponds to the ohmic case [32] defined by $J(\omega) = \eta\omega$, for $\omega << \omega_c$, ω_c being the cut-off frequency $\omega_c = (\kappa RC)^{-1}$. In order to characterize the dissipation, Chakravarty *et al.* [32] have introduced a dimensionless dissipation coefficient $\alpha = \eta q_0^2/2\pi\hbar$ and a renormalized tunneling frequency Δ/ω_c. For the electron box circuit, these two quantities are given by:

$$\begin{aligned} \alpha &= 2\kappa^2 \frac{R}{R_K} \\ \frac{\Delta}{\omega_c} &= \kappa\pi \frac{E_J}{E_c}\frac{R}{R_K} \end{aligned} \tag{84}$$

At $T = 0$, when $\Delta << \omega_c$, and $0 < \alpha < 1/2$, the effective tunneling frequency Δ_{eff} [32] is

$$\Delta_{eff} = (\Gamma(1-2\alpha)\cos\pi\alpha)^{1/2(1-\alpha)} (\Delta/\omega_c)^{\alpha/(1-\alpha)} \Delta\ , \tag{85}$$

Typically $\kappa < 0.1$ and the resistance R of the lead is of order $50\ \Omega << R_K$. The dissipation coefficient α and the renormalized tunneling frequency Δ/ω_c are thus both much smaller than 1. For $\alpha << 1$, Δ_{eff} is of order Δ. Hence, we can conclude that the staircase rounding arising from the Josephson coupling between two charge states of the island will be affected by the electromagnetic environment only if we design a box with a high impedance lead as in the experiment by Kuzmin *et al.* [33] and with a large C_s capacitor to make $\kappa \approx 1$.

REFERENCES

[1] M. H. Devoret and H. Grabert, in *Single Charge Tunneling*, edited by H. Grabert and M. H. Devoret (Plenum, New York, 1992), Chap. 1.

[2] H. Grabert, Proceedings of the LT20 conference (1993).

[3] K. A. Matveev, Zh. Eksp. Teor. Fiz. **99**, 1598 (1991) [Sov. Phys. JETP **72**, 892 (1991)].

[4] K. Mullen, E. Ben Jacob, R. C. Jaklevic, and Z. Schuss, Phys. Rev. B **37**, 98 (1988).

[5] B. Laikhtman, Phys. Rev. B **43**, 2731 (1991).

[6] M. Goldman, private communication.

[7] D. V. Averin and K. K. Likharev, in *Mesoscopic Phenomena in Solids*, ed. by B. Al'tshuler, P. Lee, and R. Webb (Elsevier, Amsterdam, 1991), Chap. 6.

[8] M. H. Devoret, D. Esteve, H. Grabert, G.-L. Ingold, H. Pothier, and C. Urbina, Phys. Rev. Lett. **64**, 1824 (1990).

[9] D. Esteve, in *Single Charge Tunneling*, edited by H. Grabert and M. H. Devoret (Plenum, New York, 1992), Chap. 3.

[10] W. Zwerger, to be published.

[11] M. Büttiker, H. Thomas, and A. Prêtre, Phys. Lett. **A180**, 364 (1993).

[12] G.-L. Ingold and Yu. V. Nazarov, in *Single Charge Tunneling*, edited by H. Grabert and M. H. Devoret (Plenum, New York, 1992), Chap. 2.

[13] H. Pothier, Ph.D. Thesis, Université Paris 6 (1991), unpublished.

[14] U. Geigenmüller and G. Schön, Europhys. Lett. **10**, 765 (1989).

[15] J. Martinis and M. Nahum, Phys. Rev. B **48**, 18316 (1993).

[16] J. Bardeen, L. N. Cooper and J. R. Schrieffer, Phys. Rev. **108**, 1175 (1957).

[17] D. V. Averin and Yu. V. Nazarov, Phys. Rev. Lett. **69**, 1993 (1992).

[18] M. Tinkham, *Introduction to Superconductivity* (McGraw-Hill, New York, 1975), Chap. 8.

[19] A. F. Andreev, Zh. Eksp. Teor. Fiz. **46**, 1823 (1964) [Sov. Phys. JETP **19**, 1228 (1964)].

[20] T. M. Eiles, J. M. Martinis, M. H. Devoret, Physica **B 189**, 210 (1993).

[21] Yu. Gefen, private communication.

[22] M. T. Tuominen, J. M. Hergenrother, T. S. Tighe and M. Tinkham, Phys. Rev. Lett. **69**, 1997 (1992).

[23] S. Skalski, O. Betbeder-Matibet and P. R. Weiss, Phys. Rev. **136**, A1500 (1964).

[24] S. Strässler and P. Wyder, Phys. Rev. **158**, 319 (1967).

[25] A. A. Abrikosov and L. P. Gor'kov, Zh. Eksp. Teor. Fiz. **39**, 1781 (1960) [Sov. Phys. JETP **12**, 1243 (1961)].

[26] P. G. de Gennes and M. Tinkham, Physics **1**, 107 (1964).

[27] P. G. de Gennes, *Superconductivity of Metals and Alloys* (W. A. Benjamin, New York, 1966), Chap. 8.

[28] K. Maki, in *Superconductivity*, edited by R. D. Parks (Marcel Dekker, New York, 1969), Chap. 18.

[29] P. G. de Gennes and G. Sarma, J. Appl. Phys. **34**, 1380 (1963).

[30] A. J. Leggett, S. Chakravarty, A. T. Dorsey, M. P. A. Fisher, A. Garg, and W. Zwerger, Rev. Mod. Phys. **59**, 1 (1987).

[31] U. Weiss, *Quantum Dissipative Systems* (World Scientific, Singapore, 1993), Chap. 4.

[32] S. Chakravarty and A. J. Leggett, Phys. Rev. Lett. **52**, 5 (1984).

[33] L. S. Kuzmin and D. B. Haviland, Phys. Rev. Lett. **67**, 2890 (1991).

3. Experimental results on the electron box

3.1.1 Paper 1:

Direct Observation of Macroscopic Charge Quantization

Originally published as:

P. Lafarge, H. Pothier, E. R. Williams, D. Esteve, C. Urbina, and M. H. Devoret, Direct observation of macroscopic charge quantization, Z. Phys. **B 85**, 327 (1991).

This paper presents the experimental observation of the macroscopic charge quantization in a normal electron box circuit theoretically described in Sec. 2.1.2. We report also the temperature dependence of the Coulomb sawtooth. We would like to thank Prof. Hipolito for showing us an error in the caption of Fig. 5 in the original paper which is corrected in this version. In this first experiment, below 100 mK there is a discrepancy between the measured temperature and the temperature that would fit the data. Further experiments performed with an improved filtering of the electron box gate line have shown a good agreement between theory and experiment from 200 mK to 35 mK (see Fig. 1.5b).

DIRECT OBSERVATION OF MACROSCOPIC CHARGE QUANTIZATION

P. Lafarge, H. Pothier, E.R. Williams$^+$, D. Esteve, C. Urbina and M.H. Devoret
Service de Physique de l'Etat Condensé, Centre d'Etudes de Saclay
91191 Gif-sur-Yvette Cedex, France

ABSTRACT: The circuit formed by a nanoscale tunnel junction in series with a capacitance and a voltage source is the building block of most multi-junction circuits of single electronics. The state of this "single electron box" is entirely determined by the number n of extra electrons on the intermediate "island" electrode between the junction and the capacitance. We have fabricated such a system and measured the charge on the junction capacitance, which is directly related to the average value of n, as a function of the bias voltage using a Fulton-Dolan electrometer. At low temperature, the junction charge followed the $e-$periodic sawtooth function expected from the theory of macroscopic charge quantization. Strikingly, e-periodic variations were also observed when the box was superconducting. The thermal rounding of the sawtooth function is well explained by a simple model, except at the lowest temperatures.

PACS: 73.40.G, 06.20.H, 73.40.R.

$^+$Permanent address: Electricity Division, National Institute of Standards and Technology, Gaithersburg, MD 20899, USA.

One way to observe Coulomb blockade, i.e. the suppression of the tunneling of electrons due to their discrete charge, is to place a small capacitance tunnel junction in series with a large resistor R, as was originally proposed by Averin and Likharev [1]. For $R \gg R_K$, where R_K is the resistance quantum $h/e^2 \simeq 25.8$ kΩ, the fluctuations of the charge Q on the junction capacitance C due to its electromagnetic environment are much less than the charge quantum e and tunneling takes place only if $\mid Q \mid > e/2$. This approach, which is very difficult experimentally because the resistor must provide a large resistance up to the Coulomb gap frequency $e^2/2C\hbar$ [2], has been realized only recently [3]. Another way to observe Coulomb blockade has been clearly demonstrated by Fulton and Dolan [4]. These authors fabricated two small junctions in series, thereby forming a metallic "island" which could only exchange electrons with the rest of the circuit by tunnel events through the junctions. Although, in this type of experiment, the two junctions are connected to a voltage bias V which induces the charges on the junction capacitances to fluctuate by an amount much larger than e [5], the total number of electrons on the island is a good quantum number. The increase in Coulomb energy due to the presence of one extra electron on the island acts as an effective energy barrier for the tunneling of electrons through this "SET transistor" [1] as long as V is smaller than the Coulomb gap e^2/C_i where C_i is the total capacitance of the island. The Fulton-Dolan experiment was the basis for more elaborate experiments involving larger numbers of junctions [6] as well as microwave irradiation which revealed correlations between tunnel events [7]. These experiments ultimately led to the controlled transfer of single electrons level with a precision better than one percent [8,9]. In multi-junction circuits, of which the SET transistor is the basic example, the relevant degrees of freedom are the discrete island charges rather than the continuous junction capacitance charges. The simplest such circuit is a tunnel junction connected to a voltage source via a capacitance. In this circuit, which we have nicknamed the "single electron box", the island is the intermediate electrode between the junction tunnel barrier and the dielectric of the capacitance, and the island charge is the sole degree of freedom of the system.

In order to understand the roles of the capacitor and the tunnel junction, let us first consider a metal electrode with self-capacitance C_s connected via a wire with negligible capacitance to an electron reservoir. We call Q_s the charge on the electrode. This charge is the integral of the surface charge density over the electrode surface. The variable Q_s is continuous since it just represents a displacement of the electron density with respect to the background ion density. Simple statistical mechanics show that the equilibrium fluctuations of Q_s have mean square amplitude $\Delta Q_s^2 =< Q_s^2 > - < Q_s >^2$ at temperature T given by $\Delta Q_s^2 = C_s k_B T$, where k_B is the Boltzmann constant. For example, if $C = 0.5$ fF and $T = 20$ mK, then $(\Delta Q_s^2)^{1/2} = 0.07e$. The typical fluctuations can thus be less than the charge of the electron for sufficiently small capacitances C_s; nevertheless the amplitude decreases only as the square root of the temperature. However, if the electrode is connected to a charge reservoir via a tunnel junction and thus becomes the island of an electron box, the fluctuations of the total charge q of the island can be radically different from the fluctuations of either the capacitor charge Q_s or the junction charge $Q = q - Q_s$. A necessary condition though, is that the tunnel barrier be sufficiently opaque, i.e. there are no quantum fluctuations of the number $n = q/(-e)$ of excess electrons on the island due to tunneling. It is generally accepted that this condition is fulfilled if $R_T \gg R_K$ [10]. Under these circumstances, the thermal fluctuations of q can be greatly reduced from their value for Q_s in the case of the wire. This reduction is due to the energy gap associated with the the island charge having discrete values.

To see this, consider a box consisting of a junction with capacitance C placed in series with a capacitor C_s and a voltage source U (see Fig. 1). If n electrons from the source have tunneled through the junction onto the island, the equilibrium electrostatic energy of the whole circuit including the work performed by the voltage source is

$$E_n = \frac{[n(-e) + \tilde{Q}]^2}{2(C_s + C)} - \frac{\tilde{Q}^2}{2C_s}, \tag{1}$$

where $\tilde{Q} = C_s U$ and where $-e$ denotes the electron charge. The average number $< n >$ of extra electrons in the island at thermal equilibrium is given by

$$< n >= \frac{\sum_{n=-\infty}^{n=+\infty} n \exp\left(\frac{-E_n(\tilde{Q})}{k_B T}\right)}{\sum_{n=-\infty}^{n=+\infty} \exp\left(\frac{-E_n(\tilde{Q})}{k_B T}\right)}. \tag{2}$$

This quantity has already been considered by Glazman and Shekhter [11] in the context of quantum dots. It is plotted as a function of $\tilde{Q}/e$ in Fig. 2(a) for three values of the parameter $\theta = C_i k_B T/e$, where $C_i = C + C_s$ is the total capacitance of the island. For small

θ, expression (2) can be evaluated directly, while for large θ one can get rapid convergence using the identity

$$\sum_{n=-\infty}^{n=+\infty} \exp(-\sigma(x-n)^2) = \sqrt{\frac{1}{4\pi\sigma}}[1+2\sum_{p=1}^{p=+\infty} \cos(2\pi px)\exp(-\pi^2p^2/\sigma)]. \quad (3)$$

We see that at low temperature (small θ), the average number of electron $< n >$ is a staircase function of the charge bias $\tilde{Q}$. We call this effect "macroscopic charge quantization" since the charge is distributed over a macroscopic number of atoms. [This effect is reminiscent of the flux quantization through a superconducting ring. In this latter phenomenon, however, the energy gap which anchors the flux on an integer number of flux quanta involves a macroscopic number of electrons]. In the central part of each of the steps of $< n >$ versus $\tilde{Q}$, the fluctuations of n are suppressed. This is shown in Fig. 2(b), where we plot $\sigma_n/\theta^{1/2} = (< n^2 > - < n >^2)/\theta^{1/2}$ as a function of $\tilde{Q}/e$. This quantity is related to the zero-bias conductance of the SET transistor as a function of gate voltage. The normalizing factor $\theta^{1/2}$ is the root mean square average of the thermal charge fluctuations, in units of e, on a capacitor C_i connected to a voltage source. Another quantity of interest is the average charge $< Q >$ on the junction capacitance, which, as we will see, is directly measurable. It is given by the expression

$$< Q >= \frac{C}{C_i}[< n > (-e) + \tilde{Q}]. \quad (4)$$

The variations of $< Q > /e$ versus $\tilde{Q}/e$ are plotted in Fig. 2(c). Note that in the limit where $C_s \ll C$, which was considered by Büttiker [12] in the context of Bloch oscillations, the oscillations shown in Fig. 2(c) are analogous to the SET oscillations [1] of Q versus It for the junction biased with a current I. It is worth noting that even when $C_s \simeq C$, the sawtooth variations of $< Q >$ versus $\tilde{Q}$ stay sharp at $T = 0$; they differ from SET oscillations in that they have an amplitude less than e.

We have measured the charge variations of Fig. 2(c) using an electrometer based on a SET transistor [4]. The experimental set-up [shown schematically in Fig. 3(a)] consists of a dual junction version of the "electron box" circuit of Fig. 1, with the island b connected by a coupling capacitor C_c to the island m of an electrometer (we explain below why we have used two junctions in parallel rather than one). The electrometer consists of two junctions with capacitances $C'/2$ placed in series. The island between the junctions is coupled to a voltage bias U_0 through the capacitance C_0 as well as to the electron box through C_c. The capacitors have nominal values $C_s = C_c = C_0 = \frac{1}{10}C$ and $C = C'$. The electrometer is voltage biased with V at the Coulomb gap e/C' and charge biased near $e/4$ with U_0. Under these conditions, the electrometer current I varies linearly with the small excursions of the charge $< Q_c >$ on the coupling capacitance C_c, which, to a good approximation, is given by $< Q_c > = < Q > C_c/C$. By measuring I as a function of U, one has thus access to the variations of $< Q >$ with the bias charge $\tilde{Q}$.

The electron box and the electrometer were fabricated using e-beam nanolithography and shadow evaporation as in Ref. [8]. The resulting pattern on the chip is shown on Fig. 3(b), in which the numbers and letters labeling the aluminum electrodes refer to the corresponding nodes of the circuit shown in Fig. 3(a). The shape of the electrodes and their guards at larger scale were designed to minimize cross-talk capacitances. Before a run, the junctions were checked at room temperature by measuring the resistance between pads 1 and 3 and between pads 4 and 6. Since all four junctions have the same nominal area 50×50 nm^2, these two resistances should have the same value. The electron box was designed with a parallel combination of two junctions instead of one in order to be able to perform this test. Immediately after this test, pads 1 and 3 were connected together using a strip of silver paint. The chip was then placed in a copper shield thermally anchored to the mixing chamber of a dilution refrigerator and the filtered leads to the room temperature electronics were connected. The temperature of the copper shield was monitored by a combination of a Germanium resistor and a carbon resistor calibrated previously by nuclear orientation thermometry and superconducting fixed points. The electrometer current was measured as in Ref. [8]. Experiments were performed in both the 0.5 T field of a superconducting magnet to drive the sample in the normal state, and in zero magnetic field, in which case the sample was superconducting. The I-V characteristics of the electrometer, both in the normal [Fig. 4(a)] and superconducting state [Fig. 4(b)], were similar to those reported by Fulton et al. [13]. In Fig. 5 we show the electrometer current I as a function of the electrometer gate voltage U_0 for values of V which are multiples of 25 μV. Note that the position of the maxima of the various curves are slightly V-dependent. This feature can be quantitatively explained by assuming a ratio of 2 between the two junction capacitances of the electrometer. By measuring the voltage ΔU_0 between two adjacent maxima of an $I(U_0)$ curve at fixed V, we determined the capacitance $C_0 = \Delta U_0/e = 73 \pm 1$ aF. From the normal I-V curve asymptotes we inferred the value 0.6 ± 0.05 fF for the total electrometer island capacitance and hence, assuming a relative junction uniformity, the capacitance $C = 0.6 \pm 0.3$ fF for the effective junction of the box. The total normal state junction resistance of the electrometer was 620 kΩ at 4 K.

The experiment in the normal state was performed by setting the electrometer to optimum gain (see point O in Fig. 5) and recording the variations of I with U. The resulting $I(U)$ curve is shown in Fig. 6 where we see a small-amplitude short-period sawtooth modulation superimposed on a large-amplitude long-period one. This latter modulation originates from a small cross-talk capacitance between pads 2 and 5 making the electrometer directly sensitive to the voltage U. A small correcting voltage proportional to U was superimposed on U_0 to compensate for the modulation of I due to this cross-talk. Furthermore, in order to get rid of low frequency noise, we used a lock-in amplifier with a 1 kHz, 40 μV modulation on the U input and recorded dI/dU as a function of U. The resulting curve at 20 mK is shown in Fig. 7. After integration, we finally arrived at the genuine variations of $< Q >$ versus $\tilde{Q}$ (solid curve labeled "N" in Fig. 8). The calibration of the horizontal axis involves the value of C_s while the calibration of the vertical axis involves both the ratio C_c/C and a prior calibration of the electrometer using the voltage U_0 and the capacitance C_0. Assuming that the periodicity of the sawtooth variations is e we found $C_s = 85 \pm 1$ aF and $C_c = 74 \pm 1$ aF which are close to the expected values.

In the superconducting state we followed the same procedure as in the normal state except that the optimum electrometer gain point is located at the superconducting gap edge $V = 0.8$ mV. The results are plotted in Fig. 8 (solid curve labeled "S"); the improved signal-to-noise ratio in the superconducting case originates from the larger electrometer gain. The sawtooth variations of $< Q >$ versus $\tilde{Q}$ shown in Fig. 8 correspond in both the normal and superconducting case to charges of value e tunneling through the junctions. Since the U scan took 50 s per oscillation, the current through the junctions of the box was 3 10^{-21}A. Given the signal to noise ratio of the measured charge variations, the leakage current from the box island and the drift in its offset charge [14] is at least one order of magnitude less than this value. On the other hand, in the superconducting state, this small value implies that the e-periodicity of the variations of Q could be due to the presence of only one quasiparticle in the island. Note also that the downward variations of Q, which should be relatively sharp at 20 mK, look rounded when compared with the theoretical prediction Eqs. (2) and (4) (dashed line in Fig. 8). In order to investigate this rounding we performed measurements at various temperatures. The results in the normal state are shown in Fig. 9 (solid lines) where we also show for comparison the predictions of Eqs. (2) and (4) (dashed lines). Since the electrometer gain is temperature dependent, a calibration was performed at each temperature. The same temperature dependence was found in the superconducting state (data not shown). Although the experimental results are in agreement with the theoretical predictions above 100 mK, there is a discrepancy at lower temperatures between the thermometer temperature and the temperature that would fit the data. At 20 mK this discrepancy is 40 mK. 25 % of this discrepancy can be explained by the back action noise induced by electrometer on the electron box, which we have calculated at finite temperature using numerical simulations. Parasitic rf signals on the U_0 and U lines could induce a broadening of the charge variations, although checks were performed to ensure that direct influence of the background noise in the laboratory had no effect. Another source of error could be that the temperature of the box electrons is higher than the thermometer temperature, although hot electron effects [15] due to the electrometer current seem negligible. Finally a contribution to the apparent excess temperature could come from quantum fluctuations of the electron number n, which is being investigated theoretically [10]. It has been assumed here that n is a classical variable, since the junction tunnel resistance is much greater than the resistance quantum R_K. More experiments are needed to test these explanations of the apparent excess temperature of the box at low temperatures. A possible extension of these experiments is to measure the single tunneling events of electrons or Cooper pairs using two or more junctions in series in the box instead of one. In that case, the variations of n with U are hysteretic and experiments along the line of those performed by Schwartz et al. [16] on the switching of an RF SQUID between two flux states become possible.

In conclusion, we have been able to detect the charge variations associated with the flow of single electrons through a tunnel junction out of a metallic island, in both the normal and superconducting state. These results constitute the first direct evidence of macroscopic charge quantization. They also demonstrate the very low drift of charge from such an island, and the presence of quasiparticles at 20 mK in a superconducting Al electrode.

We thank M. Goldman for suggesting the use of Eq. 3 in the numerical evaluation of $< n >$ in the high temperature limit and A. Cleland for critical reading of the manuscript. Technical assistance from P.F. Orfila and discussions with H. Grabert are gratefully acknowledged.

REFERENCES

[1] D.V. Averin and K.K. Likharev, J. Low Temp. Phys. **62**, 345 (1986).

[2] M.H. Devoret, D. Esteve, H. Grabert, G.-L. Ingold, H. Pothier and C. Urbina, Phys. Rev. Lett. **64**, 1824 (1990).

[3] A.N. Cleland, J.M. Schmidt and J. Clarke, Phys. Rev. Lett. **64**, 1565 (1990).

[4] T.A. Fulton and G. J. Dolan, Phys. Rev. Lett. **59**, 109 (1987).

[5] G.-L. Ingold, P. Wyrowski and H. Grabert, Z. Phys. B **85**, 443 (1991).

[6] L.S. Kuzmin, P. Delsing, T. Claeson and K.K. Likharev, Phys. Rev. Lett. **62**, 2539 (1989); P. Delsing, K.K. Likharev, L.S. Kuzmin and T. Claeson, Phys. Rev. Lett. **63**, 1180 (1989); L.J. Geerligs, V.F. Anderegg, C.A. van der Jeugd, J. Romijn and J.E. Mooij, Europhys. Lett. **10**, 79 (1989).

[7] P. Delsing, K.K. Likharev, L.S. Kuzmin and T. Claeson, Phys. Rev. Lett. **63**, 1861 (1989).

[8] L.J. Geerligs, V.F. Anderegg, P. Holweg, J.E. Mooij, H. Pothier, D. Esteve, C. Urbina and M.H. Devoret, Phys. Rev. Lett. **64**, 2691 (1990).

[9] H. Pothier, P. Lafarge, P.F. Orfila, C. Urbina, D. Esteve and M.H. Devoret, Physica **B169**, 573 (1991); H. Pothier, P. Lafarge, C. Urbina, D. Esteve and M.H. Devoret, Europhys. Lett. **17**, 249 (1992).

[10] W. Zwerger and M. Scharpf, Z. Phys. B **85**, 421 (1991), and references therein.

[11] L.I. Glazman and R.I. Shekhter, J. Phys. Condensed Matter **1**, 89, 5811.

[12] M. Büttiker, Phys. Rev. **B36**, 3548 (1987).

[13] T.A. Fulton, P.L. Gammel, D.J. Bishop, L.N. Dunkleberger and G.J. Dolan, Phys. Rev. Lett. **63**, 1307 (1989).

[14] L.J. Geerligs, PhD thesis, T.U. Delft (1990).

[15] M.L. Roukes, M.R. Freeman, R.S. Germain, R.C. Richardson and M.B. Ketchen, Phys. Rev. Lett. **55**, 422 (1985); F.C. Wellstood, PhD Thesis, Berkeley (1988).

[16] D.B. Schwartz, B. Sen, C.N. Archie and J.E. Lukens, Phys. Rev. Lett. **55**, 1547 (1985).

FIGURE CAPTIONS

Fig. 1 (a) "Electron box" circuit consisting of a capacitor, a junction and a voltage source in series. The intermediate electrode between the junction and the capacitor forms an "island" with n extra electrons.

Fig. 2 (a) Average island electron number $< n >$, (b) fluctuations $\sigma_n = (< n^2 > - < n >^2)^{1/2}$, and (c) average charge $< Q >$ on the junction capacitance. These quantities are all plotted as a function of the bias charge $\tilde{Q} = C_s U$ for $\theta = k_B T(C_s + C)/e^2 = 0.01$ (solid lines), 0.1 (dashed lines) and 10 (dotted lines).

Fig. 3 (a) Schematic representation of experimental set-up. An electron box with two junctions in parallel is coupled to a SET transistor used as an electrometer. (b) Electron beam lithography implementation of circuit shown in (a). Superfluous electrodes resulting from the use of the suspended bridge technique have been omitted for clarity.

Fig. 4 Electrometer I-V characteristics in the normal state (a) and in the superconducting state (b) at 20 mK. Solid lines: minimum Coulomb gap; dotted lines: maximum Coulomb gap.

Fig. 5 Electrometer current I versus electrometer gate voltage U_0 for a set of values of bias voltage V separated by 50 μV. The temperature is 20 mK. Point O is the optimum gain point.

Fig. 6 Electrometer current I versus electron box voltage U at 20 mK. The curve is clipped near $U = 0$ because one attenuator in the U line filtering system becomes superconducting at the lowest temperature when too little current flows through it.

Fig. 7 Lock-in signal as a function of electron box voltage U in presence of a correcting linear ramp signal superimposed on the dc value of U_0. The temperature is 20 mK. Each peak is associated with the charge of the box island increasing by one electron.

Fig. 8 Solid lines: Charge variations in the normal state (N) and in the superconducting state (S) at 20 mK. Dashed line: theoretical prediction.

Fig. 9 Solid lines: Charge variations in the normal state at different temperatures. Dashed

lines: theoretical predictions [Eqs. (2) and (4)].

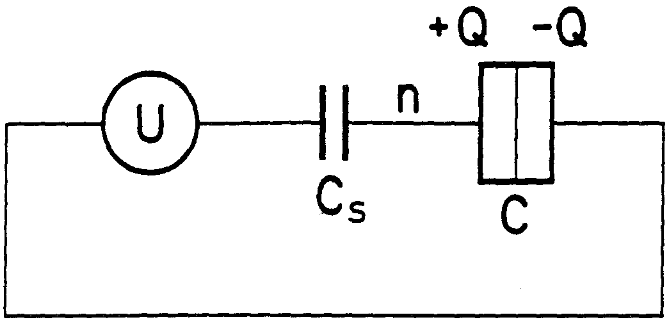

Fig. 1

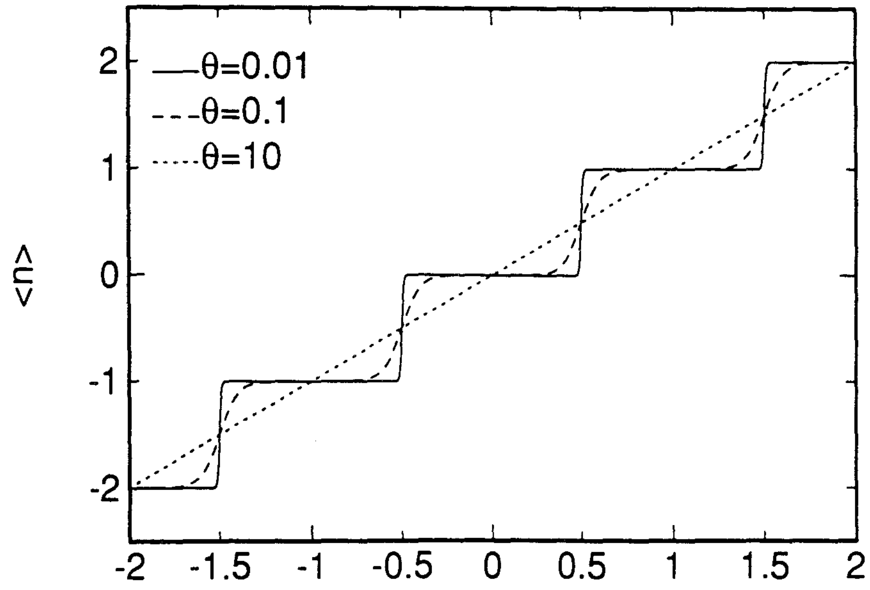

Fig. 2a

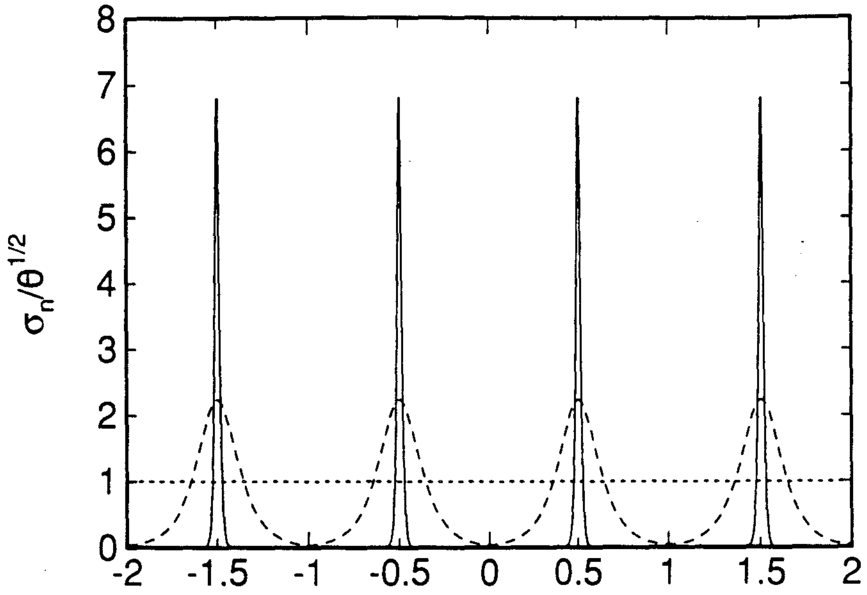

Fig. 2b

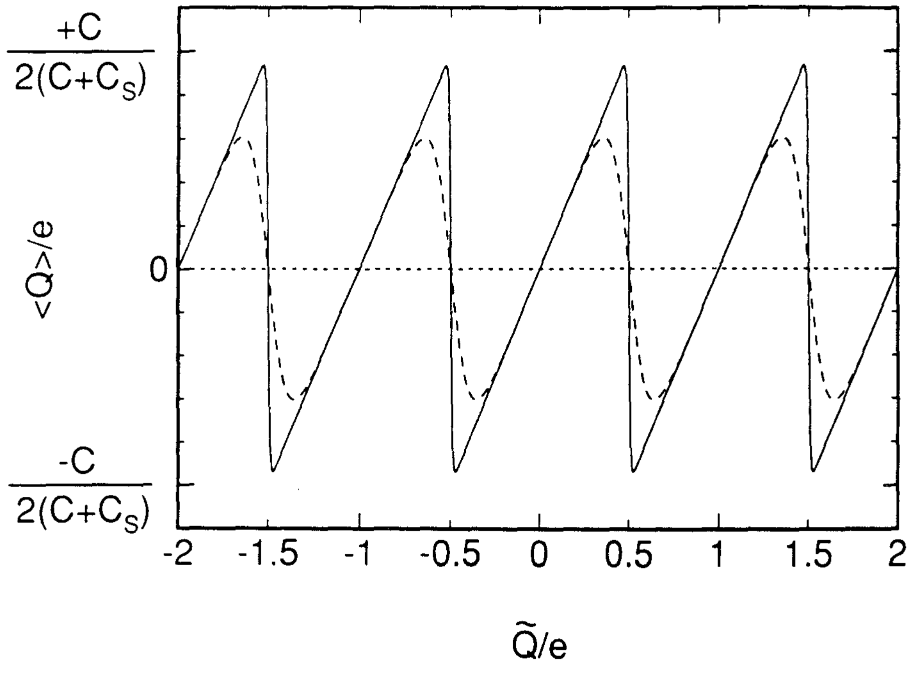

Fig. 2c

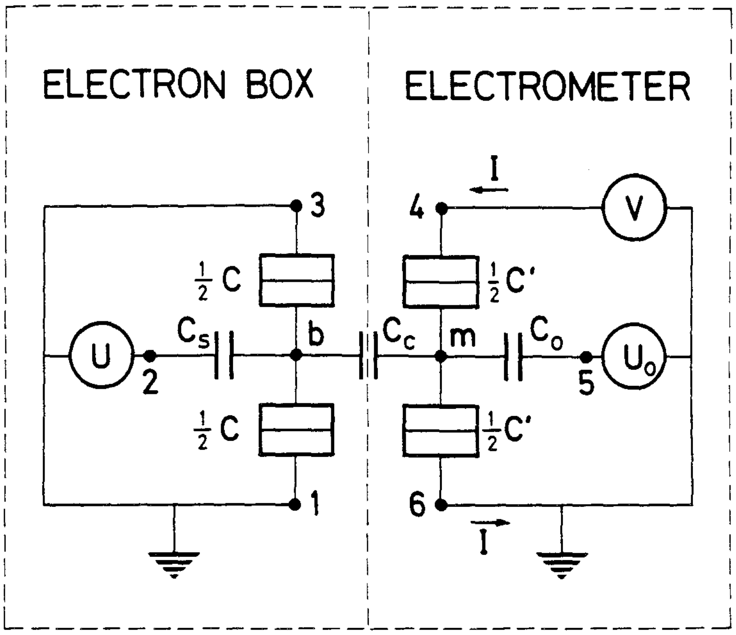
ELECTRON BOX
ELECTROMETER
I
4
V
3
$\frac{1}{2}$C
$\frac{1}{2}$C'
U
2
C_s
b
C_c
m
C_o
5
U_o
$\frac{1}{2}$C
$\frac{1}{2}$C'
1
6
I

Fig. 3a

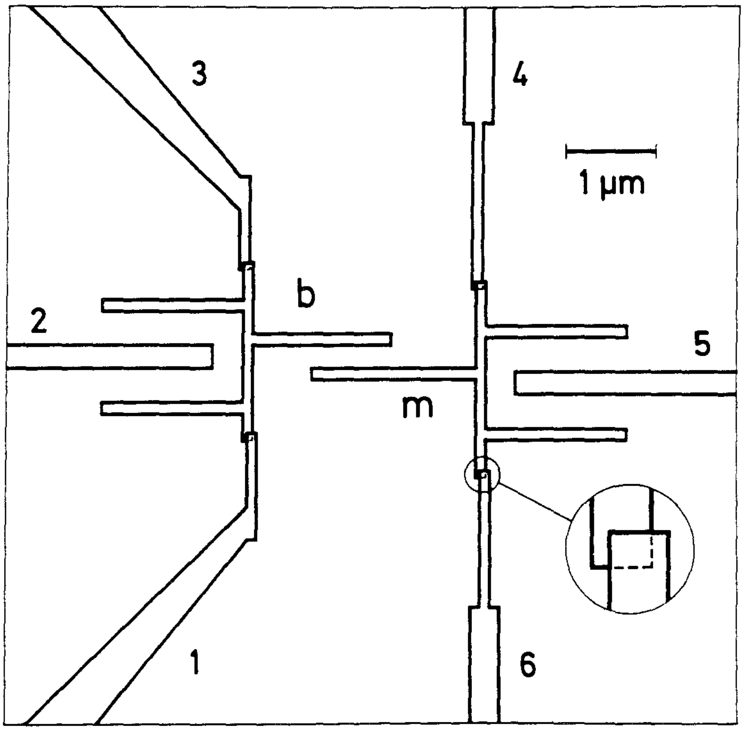
1 µm
b
m

Fig. 3b

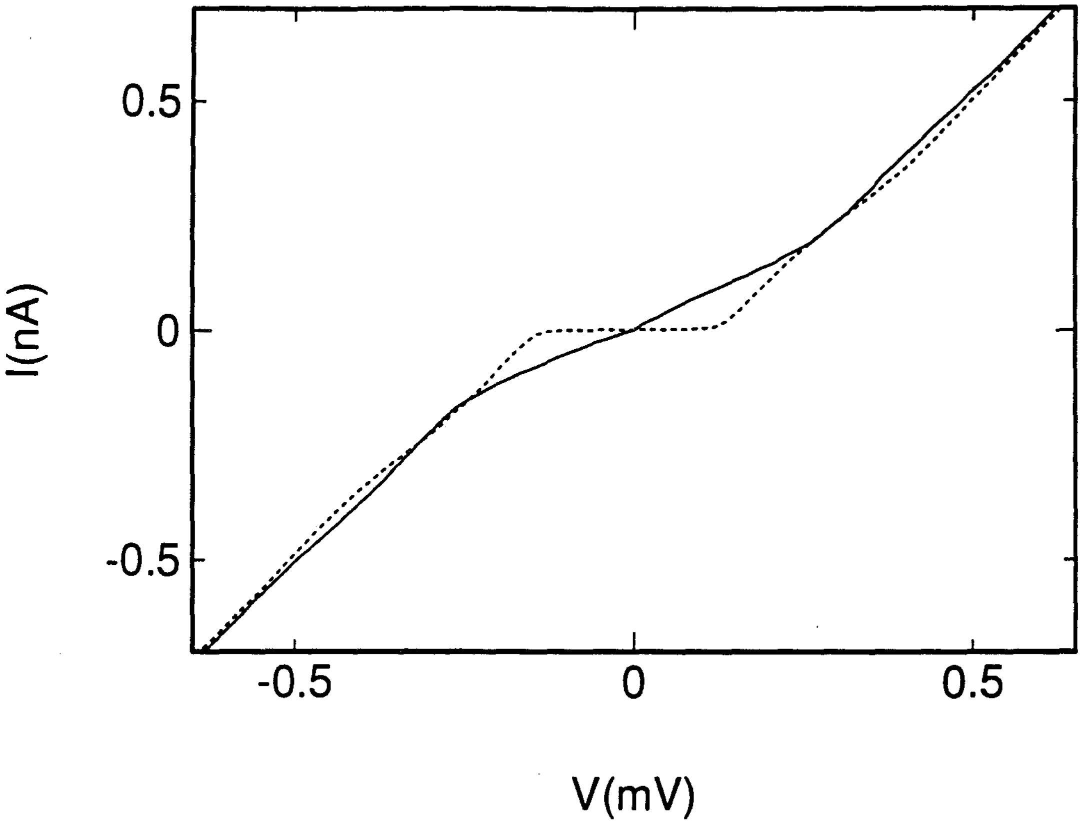

Fig. 4a

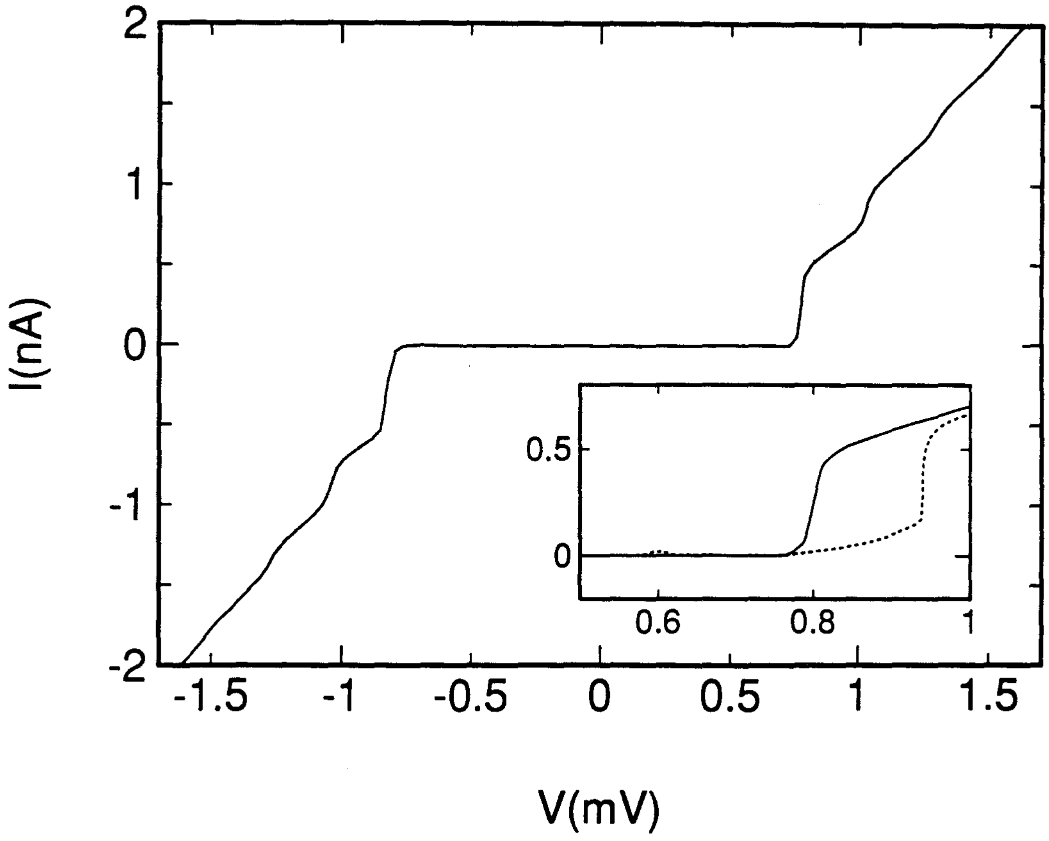

Fig. 4b

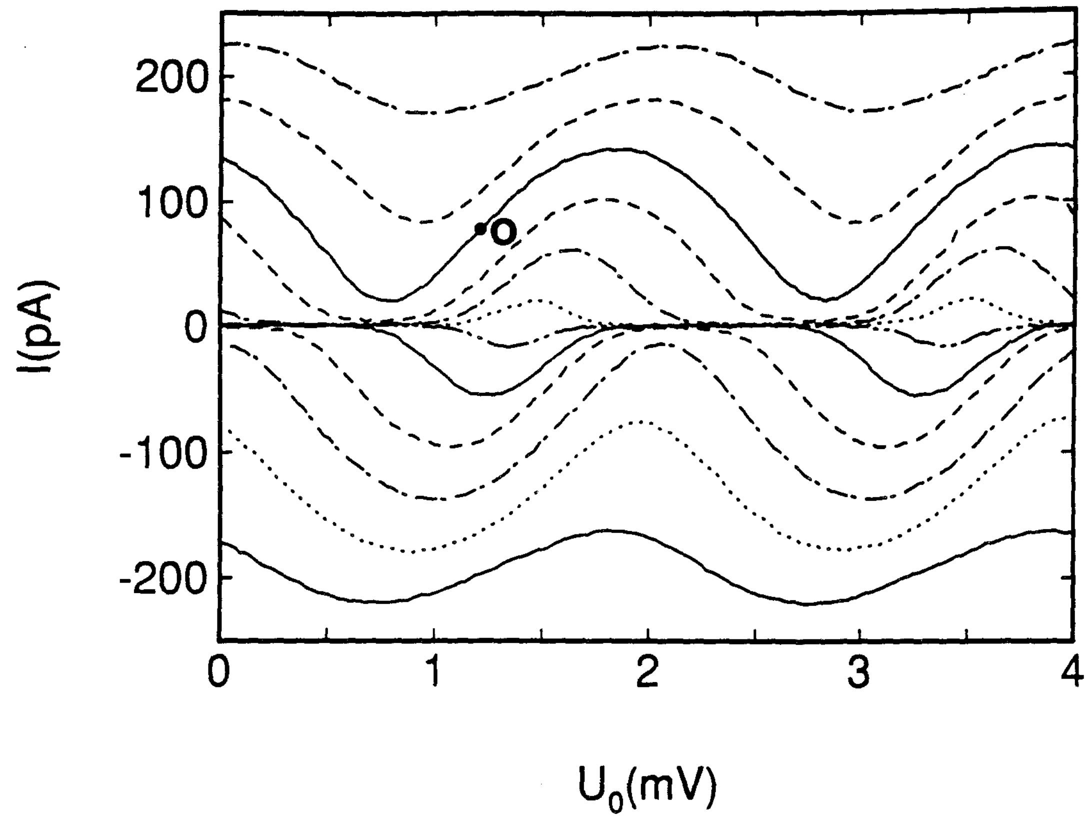
200
100
0
-100
-200
I(pA)
0
1
2
3
4
U0(mV)
O

Fig. 5

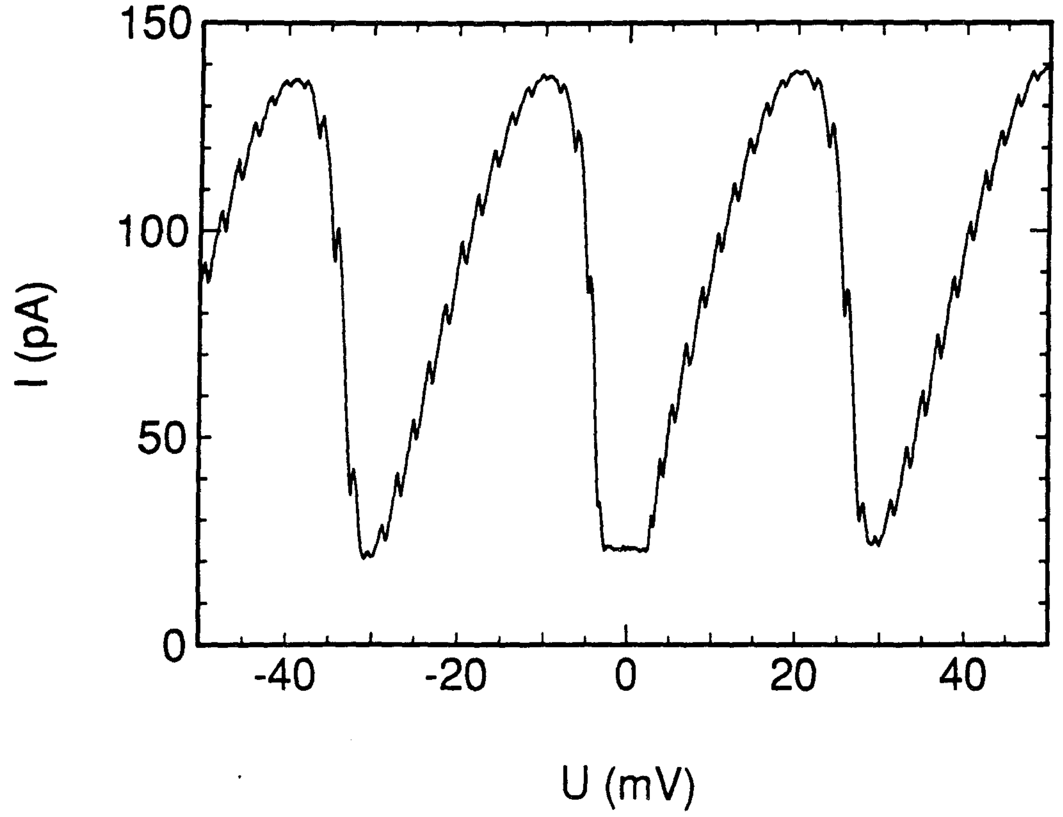
150
100
50
0
I (pA)
-40
-20
0
20
40
U (mV)

Fig. 6

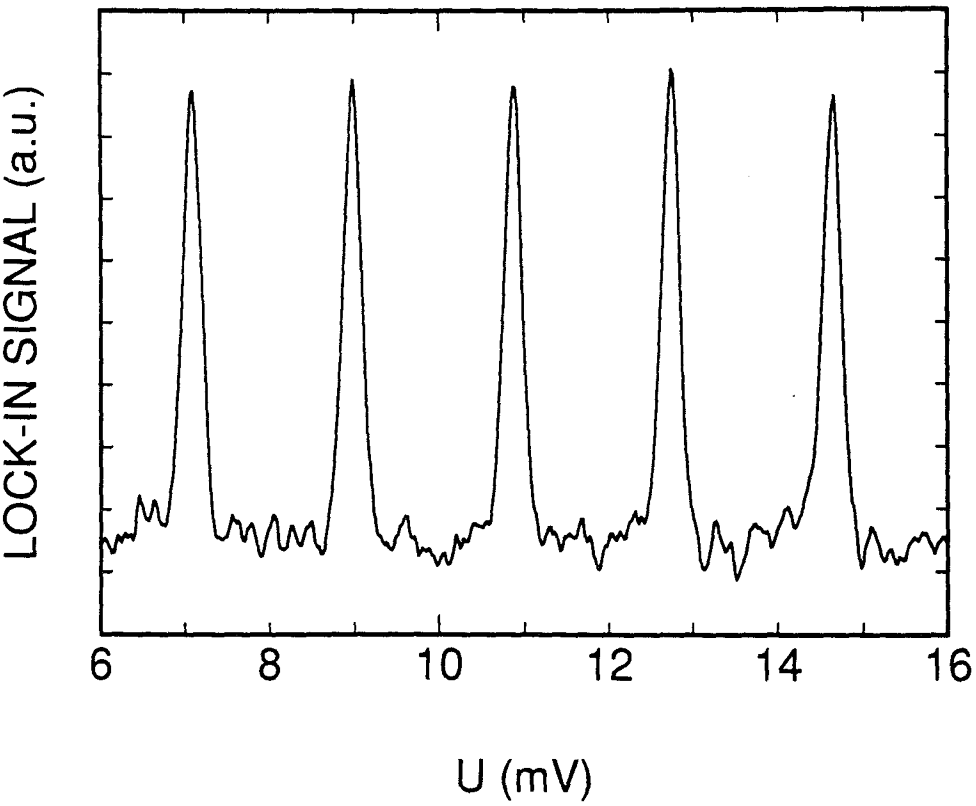
LOCK-IN SIGNAL (a.u.)
6
8
10
12
14
16
U (mV)

Fig. 7

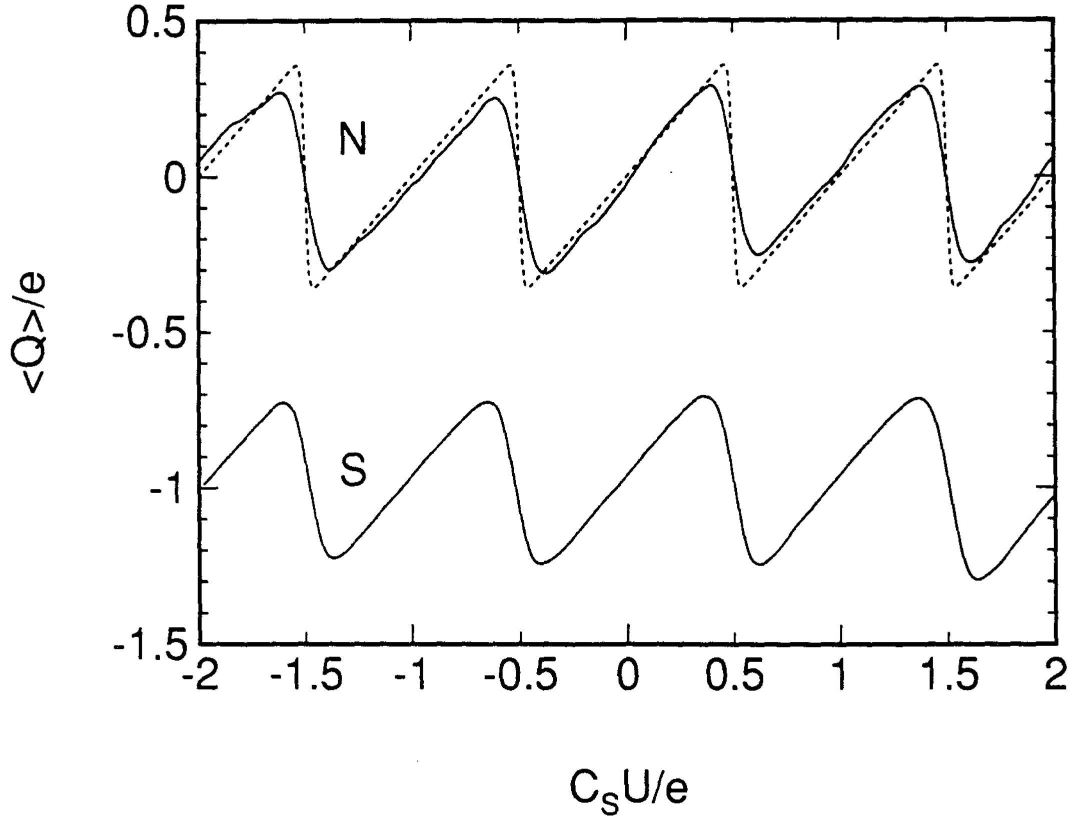
0.5
0
-0.5
-1
-1.5
<Q>/e
N
S
-2
-1.5
-1
-0.5
0
0.5
1
1.5
2
C_SU/e

Fig. 8

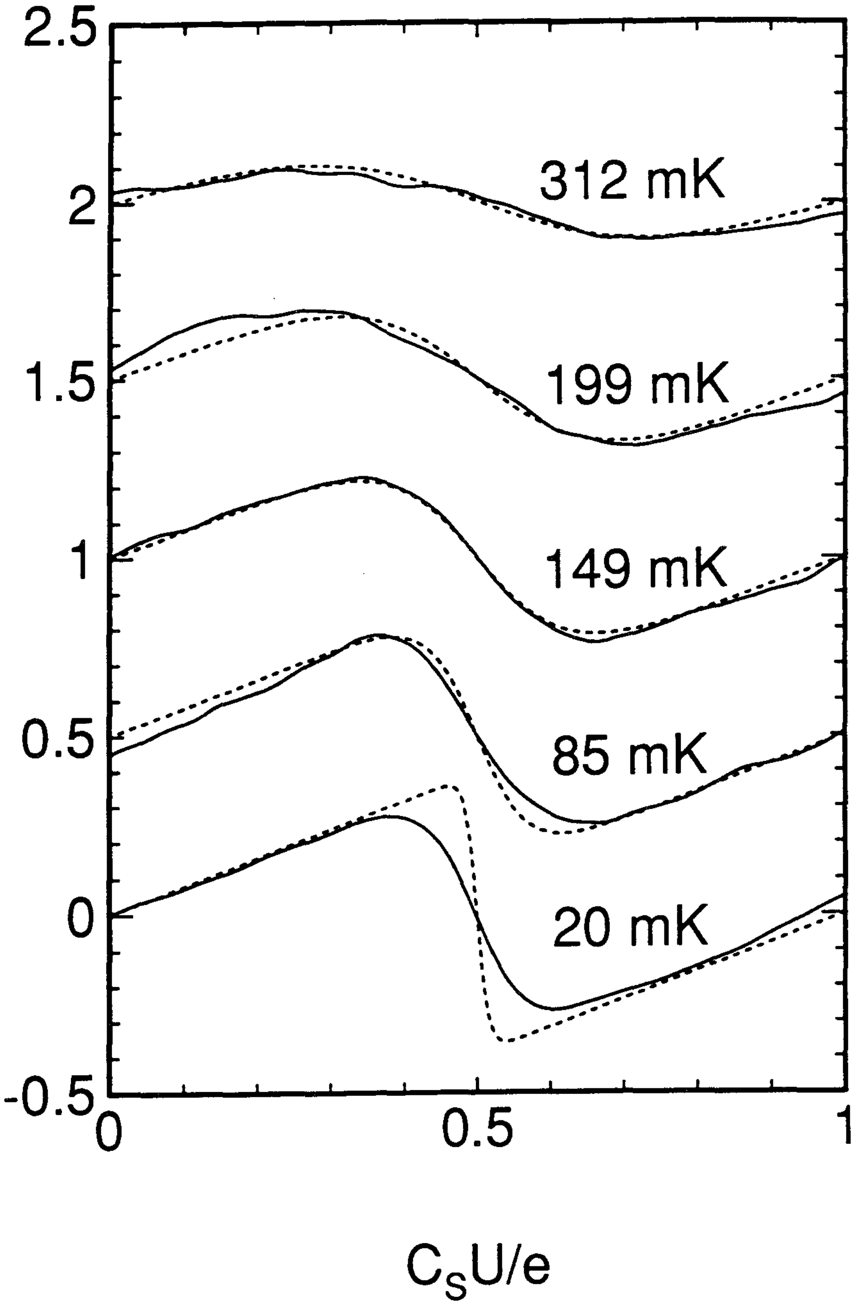

Fig. 9

3.2.1. Paper 2:

Measurement of the Even-Odd Free-Energy Difference of an Isolated Superconductor

Originally published as:

P. Lafarge, P. Joyez, D. Esteve, C. Urbina and M. H. Devoret, Measurement of the even-odd free-energy difference, Phys. Rev. Lett. **70**, 994 (1993).

The paper describes the observation of an asymmetric Coulomb staircase in a normal/superconducting electron box experiment where the superconducting gap Δ at zero temperature and zero magnetic field is smaller than the charging energy E_c (see Sec. 2.2.1). By measuring the staircase asymmetry at various temperatures, we have determined the odd-even free energy difference $D(T,H)$ of the superconducting island at zero magnetic field. The experimental results are in good agreement with the calculation described in Sec. 2.2.3.

Measurement of the Even-Odd Free Energy Difference of an Isolated Superconductor

P. Lafarge, P. Joyez, D. Esteve, C. Urbina and M. H. Devoret

Service de Physique de l'Etat Condensé, CEA-Saclay, 91191, Gif-sur-Yvette, France

Abstract: We have measured the difference between the free energies of an isolated superconducting electrode with odd and even number of electrons using a Coulomb blockade electrometer. The decrease of this energy difference with increasing temperature is in good agreement with theoretical predictions assuming a BCS density of quasiparticle states, except at the lowest temperatures where the results indicate the presence of an extra energy level inside the gap.

PACS: 73.40.Gk, 73.40.Rw

The key concept of the Bardeen-Cooper-Schrieffer (BCS) theory of superconductivity [1] is the pairing of electrons. A surprising feature of the theory appears when one considers a macroscopic piece of superconducting metal with a fixed number N of electrons. If N is even, all the electrons can condense in the ground state. If N is odd, however, one electron should remain as a quasiparticle excitation. In principle, if one would measure the energy required to add one electron to the superconductor, there should be a difference between the cases of even and odd N. This fundamental even-odd asymmetry, which might vanish due to sample imperfections [2], does not manifest itself in conventional experiments on superconductors because these experiments are only sensitive to a finite fraction of quasiparticles. In this Letter, we report a new experiment based on single electron tunneling [3] with which we measured the even-odd free energy difference introduced by Tuominen *et al.* [4].

Consider a superconducting-normal (SN) tunnel junction in series with a voltage source U and a capacitor C_s (see Fig. 1), a basic Coulomb blockade circuit whose normal-normal junction version has been nicknamed the electron "box" [5,6]. The superconducting electrode which is common to both the junction and the capacitor is surrounded everywhere by insulating material. When the junction tunnel resistance R_t is such that $R_t \gg R_K = h/e^2$, the number n of excess electrons on this "island" is a good quantum number [3,7]. The n-dependent part of the ground state energy of the circuit, including the work done by the source U, is given by $E_n = E_c(n - C_sU/e)^2 + \mathcal{E}_n$ where $E_c = e^2/2C_\Sigma$ is the electrostatic energy of one excess electron on the island, C_Σ the total capacitance of the island and where $\mathcal{E}_n$ is the non-electrostatic part of the energy of the island. For a normal island $\mathcal{E}_n = 0$ (Fig. 2a), whereas for a superconducting island, one has $\mathcal{E}_n = D_0 p_n$ where D_0 is the energy difference between the odd-n and even-n island ground states, and $p_n = n \bmod 2$ (Fig. 2c). The BCS theory yields $D_0 = \Delta$ where Δ is the superconducting gap of the island. In equilibrium at zero temperature, n will be determined by the lowest E_n and is therefore given by a staircase function of U (Figs. 2b and 2d). In the normal case, the steps are of equal size, whereas in the superconducting case even-n steps are longer that odd-n steps. For $D_0 > E_c$, the odd-n steps disappear, while for $D_0 \leq E_c$, the ratio ρ between the length of the odd and even-n steps is related to D_0 through $D_0/E_c = (1-\rho)/(1+\rho)$. Thus, from a measurement of the equilibrium value of n as a function of U, which can be done by weakly coupling the island to a Coulomb blockade electrometer [8,5,6] as shown in Fig. 1, one can in principle infer the value of D_0.

In practice, the measurements are performed at finite temperature and the current in the electrometer is directly related to $\bar{n}$, the temporal average of n which we suppose equal to $< n >$, the thermal ensemble average of n. The above analysis must be refined to take into account the thermal population of all the possible states of the circuit. These states are characterized not only by the number n of excess electrons in the island, but also by the filling factors of the various quasiparticle states of the island. One finds that the average value of n is given by

$$< n >= \frac{C_s U}{e} + \frac{C_\Sigma}{C_s \beta e} \frac{\partial}{\partial U} ln \left(\sum_n \mathcal{Z}_n e^{-\beta E_c (n - C_s U/e)^2} \right) \tag{1}$$

where $\beta = 1/(k_B T)$ and where $\mathcal{Z}_n$ is the partition function of the island with n excess electrons. We now follow reference [4]: we assume Fermi statistics for the quasiparticle excitations of this isolated system and we set the parity of the number of quasiparticles equal to the parity of n. We get $\mathcal{Z}_n = [\mathcal{Z}_+ + (-1)^n \mathcal{Z}_-]/2$, with $\mathcal{Z}_\pm = \prod_q [1 \pm \exp(-\beta \epsilon_q)]$, where q denotes a generic quasiparticle state with energy ϵ_q.

At temperatures such that $k_B T \ll E_c$, the $< n >$ vs. U staircase is just slightly rounded. The length of the steps is now defined from the values of U where $< n >$ is a half-integer and D_0 in the expression of the odd-even step length ratio is now replaced by $D(T) = \mathcal{F}_1 - \mathcal{F}_0$, the difference between the free energies $\mathcal{F}_n = -k_B T \ln \mathcal{Z}_n$ of the island with an odd and an even number of electrons [9]. Introducing the transform $\tilde{\rho}(T) = \int_0^\infty \rho(\epsilon) \ln[\coth(\beta\epsilon/2)] d\epsilon/2$ of $\rho(\epsilon)$, the density of quasiparticle states, one can express $D(T) = -k_B T \ln[\mathrm{th}\tilde{\rho}(T)]$. We now suppose that $\exp(-\epsilon_{min}/k_B T) \ll 1$, where ϵ_{min} is the lowest energy for which $\rho(\epsilon)$ is non-zero. In this limit, $\tilde{\rho}(T)$ can be evaluated analytically for mathematically simple ρ's. If we assume a continuous BCS density of states, $\tilde{\rho}(T) = N_{eff}(T) e^{-\beta\Delta}$ where $N_{eff}(T) = N_0 (2\pi k_B T/\Delta)^{1/2} + \mathcal{O}[(T/\Delta)^{3/2}]$ is the effective number of quasiparticle states available for excitation [10] and where $N_0 = \rho_A N_A \Delta$, ρ_A being the normal density of states at the Fermi energy per atom and N_A the number of atoms in the island. Because $\ln N_{eff}$ depends weakly on the sample parameters and on temperature, $D(T)$ is approximately given at temperatures such that $N_0 \exp(-\Delta/k_B T) \ll 1$ by $\Delta(1 - T/T_0)$, with $T_0 = \Delta/(k_B \ln N_0)$ in the range 200-300mK for realistic Al islands. More generally, if there is inside the gap discrete quasiparticle states with energies ϵ_{q_i} and degeneracies g_{q_i}, they each contribute to $\tilde{\rho}(T)$ by $g_{q_i} \exp(-\beta \epsilon_{q_i})$. Their effect is to reduce $D(T)$ which is given in the limit $T = 0$ by $D(T) = \epsilon_{q_0} - k_B T \ln g_{q_0}$, where q_0 is the lowest discrete quasiparticle state. Finally, we must point out that the $2e$-periodic behavior of the SN box is similar to the $2e$-periodicity which has been observed for the current through the SSS [11,4] and NSN [12] Coulomb blockade electrometers as a function of the charge induced on the gate. However, note that when $D(T) < E_c$, the box experiment, in contrast with the transport experiments on Coulomb blockade electrometers, gives access to the ratio $D(T)/E_c$ and not simply to the temperature at which it vanishes.

The sample was fabricated using e-beam lithography and double-angle e-beam evaporation through a suspended mask [13]. First we deposited a 30nm thick aluminium film to form the superconducting island of the box, with lateral dimensions 2.2μm × 0.1μm, as well as the leads of the electrometer. This first layer was then oxidized in 300 Pa of oxygen for fifteen minutes at room temperature. A 50nm thick layer of Cu alloyed with 3% in weight of Al was then deposited to form the normal lead connected to the box and the island of the electrometer. The two nominally identical junctions of the electrometer had an area of $\sim 8 \times 10^{-3}\mu\text{m}^2$, and were much larger than the box junction. The suspended mask was designed so that there was no overlap of the Al island of the box with its Cu-Al copy, which is inherent to the double evaporation technique. The current-voltage curve (inset of Fig. 3) of a single junction fabricated with the same technique showed a sharp current rise at $\Delta/e = 180 \pm 10\mu$V, with the square-root voltage dependence characteristic of NS junctions. Fig. 3 shows a current-voltage characteristic of the electrometer: when the gate charge is adjusted so as to suppress Coulomb blockade for positive voltage, the sharp current rise at $2\Delta/e = 360 \pm 10\mu$V indicates that the electrometer consists indeed of two NS junctions in series. Detailed analysis of these $I(V)$ curves yielded the capacitance parameters of the electrometer. They served as calibrations for numerical electrostatic calculations of the box parameters which gave $C_\Sigma = 0.2 \pm 0.05$fF, $C_s = 25 \pm 5$aF and $C_c = 11 \pm 2$aF. The experiments were done with the sample mounted in a shielded copper box thermally anchored to the mixing chamber of a dilution refrigerator. All voltage and current lines were carefully filtered [14]. When necessary, the sample was put in its normal state by a 1T magnetic field produced by a superconducting coil.

To perform the measurements of $\bar{n}$ versus U the bias and gate voltages V and U_0 of the electrometer were first adjusted to maximize $\partial I/\partial U_0$ (dot on Fig. 3). The electrometer current I was then recorded as a function of U. The resulting sawtooth signal is a measurement, apart from a gain factor, of the second term of Eq. 1. We obtained $\bar{n}$ by adding to this sawtooth signal a linear term whose coefficient was adjusted to null out the slope of the teeth. In Fig. 4 we show the measured equilibrium value $\bar{n}$ as a function of the polarization C_sU/e both for the sample in the normal and the superconducting states, at 20 mK. The even-odd symmetry of the steps in the normal state is clearly broken in the superconducting state. Note that the middle of the steps in the superconducting state coincide with the middle of the steps in the normal state, as predicted from theory (see Fig. 2b and 2d) in the case $D(T) < E_c$. Our previous experiments on a box with an SS junction never showed any even-odd asymmetry [5]. We believe that this was due to the presence of a few long-lived, out-of-equilibrium quasiparticles which in the present experiment are "purged" by the normal metal lead.

Due to the unavoidable electrostatic crosstalk between the U voltage and the electrometer island, which was only partially corrected for in our setup, the gain of the electrometer depends on the U voltage. This leads to the noticeable step height variations as U departs from zero. Nevertheless, these vertical scale distortions do not affect the conclusions we draw from our data, which are based only on the length of the steps along the horizontal axis. The scaling factor used for this axis corresponds to $C_s = 21 \pm 0.5$aF, in good agreement with our numerical estimates. When the temperature was increased the steps became gradually rounded (data not shown). From a fit of the temperature dependence of the data in the normal state using Eq. 1 we obtained a direct measurement of $C_\Sigma = 0.20 \pm .05$fF, also in good agreement with our numerical estimates.

We have measured the odd-even step length ratio ρ as a function of temperature, thereby obtaining $D(T)/E_c$. The experimental results are shown in Fig. 5 together with the theoretical predictions in the case of a continuous BCS density of states (dashed line). Since N_A is known from the sample dimensions, the only adjustable parameters are $C_\Sigma^{fit} = 0.19$fF and $\Delta^{fit}/e = 195\mu$V. The parameter C_Σ^{fit} is in the error range of C_Σ while the uncertainty range for Δ^{fit} is adjacent to the error range of Δ deduced from the electrometer $I(V)$. Apart from this minor discrepancy which may be due to the fact that the island, contrary to the S leads of the electrometer, is not covered by a normal layer, there is good agreement between theory and experiment for temperatures higher than 50 mK. At lower temperatures, the data deviates significantly from theory, in a manner which could be explained by a failure of the box to follow the temperature of the thermometer. However, we find this explanation unlikely. In a previous run on a NN box with parameters adapted to calibration purposes, the staircase sharpness precisely followed the temperature down to 35mK. A more likely explanation is that the density of states of the island may not be a strictly smooth BCS one. To illustrate this point, we show in Fig. 5 a complete fit of the data (full line) using a minimal model: in addition to the continuous BCS density of states, it includes a single, two-fold degenerate, quasiparticle state at 0.8Δ. Even though the number of available states at the gap Δ is of the order of $N_0 \sim 10^4$, the behavior of the box at the lowest temperatures is completely dominated by this single state. This box experiment is thus a very sensitive quantitative probe of the deviations of the density of states from the ideal BCS form, in contrast with transport measurements [11,4,12]. It is remarkable that the sample imperfections like surface states and impurities do not lead to a more severe suppression of the even-odd asymmetry. Additional experiments (data not shown) showed that $D(T = 25\text{mK})$ decreased under the application of a magnetic field applied perpendicularly to the plane of the substrate and vanished at 0.1 T, a reasonable critical field value given the dimensions of the island [15].

In conclusion, we have measured the free energy cost of putting a single extra electron in a superconducting island. We have found that this energy depends on the parity of the total number of electrons in the island and is in good agreement with theoretical predictions based on Tuominen *et al.* [4] assuming a continuous BCS density of quasiparticle states. At the lowest temperatures, though, the experiment is sensitive to indidual discrete states and the results are better accounted for if one incorporates in the theory a single energy level inside the gap.

We acknowledge fruitful discussions with A. Cleland, T. Eiles, J. Martinis, G. Sarma, G. Schön and J. Schrieffer, as well as the technical help of P.F. Orfila.

REFERENCES

[1] J. Bardeen, L.N. Cooper, and J.R. Schrieffer, Phys. Rev. **108**, 1175 (1957).

[2] D.V. Averin and Yu. V. Nazarov, Phys. Rev. Lett. **69**, 1993 (1992).

[3] D.V. Averin and K.K. Likharev, in *Mesoscopic Phenomena in Solids*, ed. by B. Altshuler *et al.* (Elsevier, Amsterdam, 1991); *Single Charge Tunneling*, ed. by H. Grabert and M.H. Devoret (Plenum, New York, 1992).

[4] M.T. Tuominen, J.M. Hergenrother, T.S. Tighe and M. Tinkham, Phys. Rev. Lett. **69**, 1997 (1992).

[5] P. Lafarge, H. Pothier, E.R. Williams, D. Esteve, C. Urbina and M.H. Devoret, Z. Phys. B **85**, 327 (1991).

[6] T.A. Fulton, P.L. Gammel and L.N. Dunkleberger Phys. Rev. Lett. **67**, 3148 (1991).

[7] K.A. Matveev, Zh. Eksp. Teor. Fiz. **99**, 1598 (1991) [Sov. Phys. JETP **72**, 892 (1991)].

[8] T.A. Fulton and G.J. Dolan, Phys. Rev. Lett. **59**, 109 (1987).

[9] This quantity is noted $F_0(T)$ in reference [4].

[10] Over the full temperature range that we consider here, the leading $(T/\Delta)^{1/2}$ term in the expression of N_{eff} is somewhat better than the low temperature approximate form given in reference [4].

[11] L.J. Geerligs, V.F. Anderegg, J. Romijn and J.E. Mooij, Phys. Rev. Lett. **65**, 377 (1990).

[12] T.M. Eiles, J.M. Martinis and M.H. Devoret, Phys. Rev. Lett. **70**, 1862 (1993).

[13] G.J. Dolan and J.H. Dunsmuir, Physica B **152**, 7 (1988).

[14] J.M. Martinis, M.H. Devoret and J. Clarke, Phys. Rev. B **35**, 4682 (1986).

[15] M. Tinkham, *Introduction to Superconductivity*, (McGraw-Hill, New York, 1975), chap 8.

FIGURE CAPTIONS

Fig. 1. Circuit diagram of the experiment. The rectangular symbols represent SN tunnel junctions. The V-shaped marks denote superconducting electrodes. The symbol n denotes the number of electrons in the island of the box (marked by a full dot). The variations of its average $\bar{n}$ with the voltage U are detected by monitoring the current I through the SNS electrometer which is coupled to the box through the capacitor C_c. The bias voltage V and the gate voltage U_0 set the working point of the electrometer.

Fig. 2. Ground state energy of the box in the normal (a) and superconducting state (c) as a function of the polarization C_sU/e, for several values of the excess number n of electrons in the island. E_c is the electrostatic energy of one excess electron on the island for $U = 0$. In an ideal superconductor, the minimum energy for odd n is Δ above the minimum energy for even n. The dots correspond to level crossings where single electron tunneling is possible. Equilibrium value $< n >$ versus C_sU/e is shown in the normal (b) and superconducting (d) state, at $T = 0$.

Fig. 3. $I(V)$ curves for the SNS electrometer at $T = 25$mK, and zero magnetic field, for three values of the gate voltage U_0 corresponding to maximum, intermediate and minimum gap. The minimum gap corresponds to the bare superconducting gap 2Δ of two NS junctions in series. The dot indicates the optimal bias point for maximum sensitivity. Inset: $I(V)$ curve for a single SN junction under same conditions.

Fig. 4. Variations of the average value $\bar{n}$ of the number of extra electrons in the box as a function of the polarization C_sU/e, at $T = 25$mK. Trace N: normal island. Trace S: superconducting island. For clarity, trace S has been offset vertically by 4 units.

Fig. 5. Difference D between the free energies of the island with an odd and an even number of electrons as a function of temperature. Experimental values (dots) are directly measured in units of E_c. Dashed line is theoretical expression of $D(T)/\Delta$ (scale on the right-hand side), assuming a continuous BCS density of states, $\rho_A = 0.572(eV)^{-1}$, $N_A = 38\ 10^7$ and $\Delta^{fit}/e = 195\mu$V (see text). Full line is modified expression corresponding to a single, two-fold degenerate state added at 0.8Δ. The vertical scale factors of theory and experiment coincide for $C_\Sigma^{fit} = 0.19$fF.

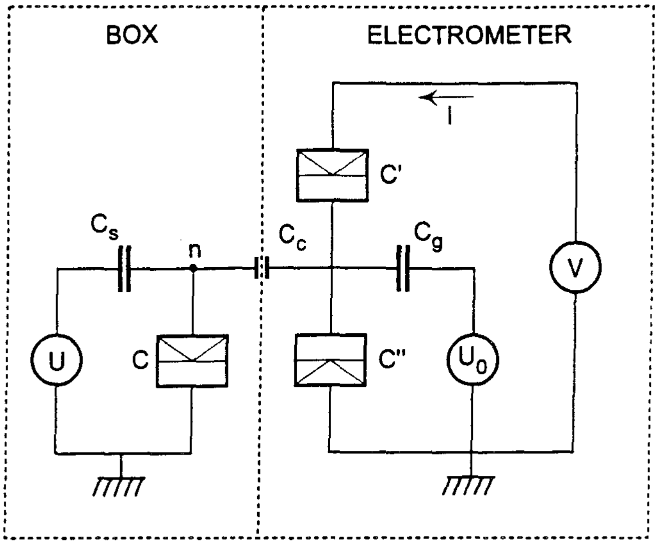
BOX
ELECTROMETER
I
C'
C_s
n
C_c
C_g
V
U
C
C"
U_0

Fig. 1

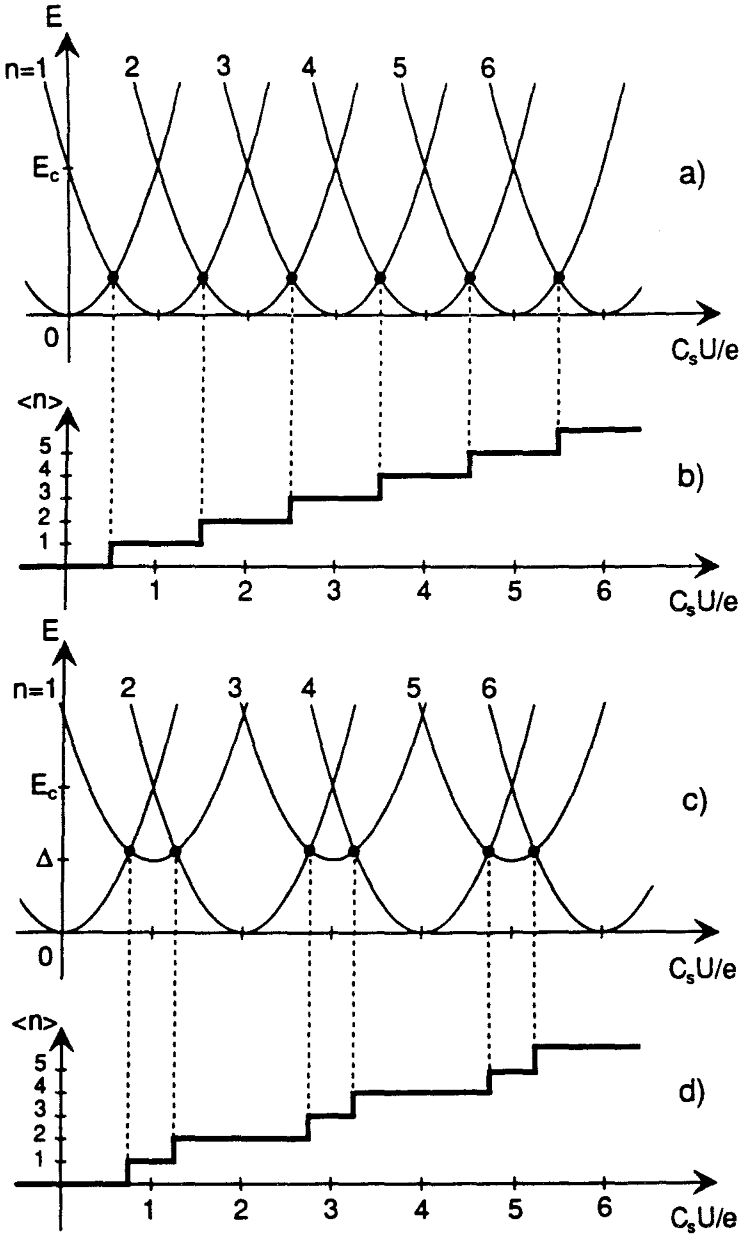
E
n=1
2
3
4
5
6
E_c
a)
0
C_sU/e
<n>
5
4
3
2
1
b)
1
2
3
4
5
6
C_sU/e
E
n=1
2
3
4
5
6
E_c
Δ
c)
0
C_sU/e
<n>
5
4
3
2
1
d)
1
2
3
4
5
6
C_sU/e

Fig. 2

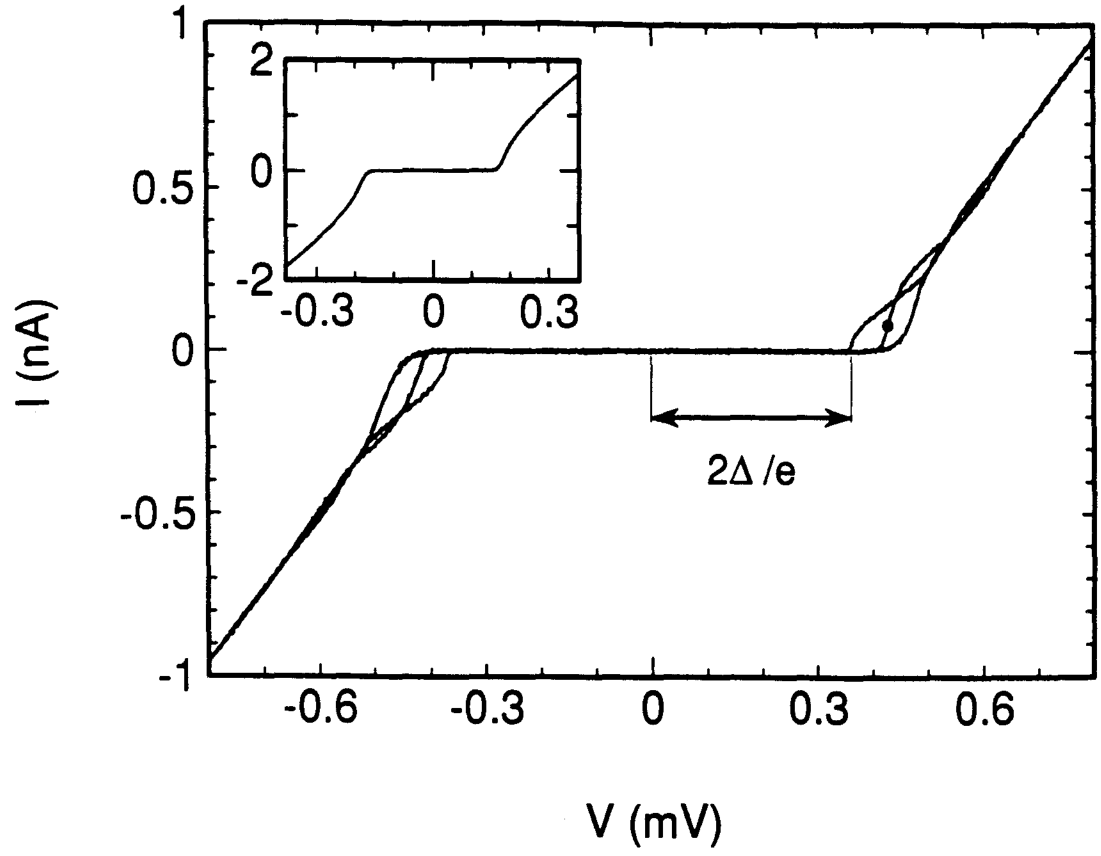
I (nA)
V (mV)
1
0.5
0
-0.5
-1
-0.6
-0.3
0
0.3
0.6
2Δ /e
2
0
-2
-0.3
0
0.3

Fig. 3

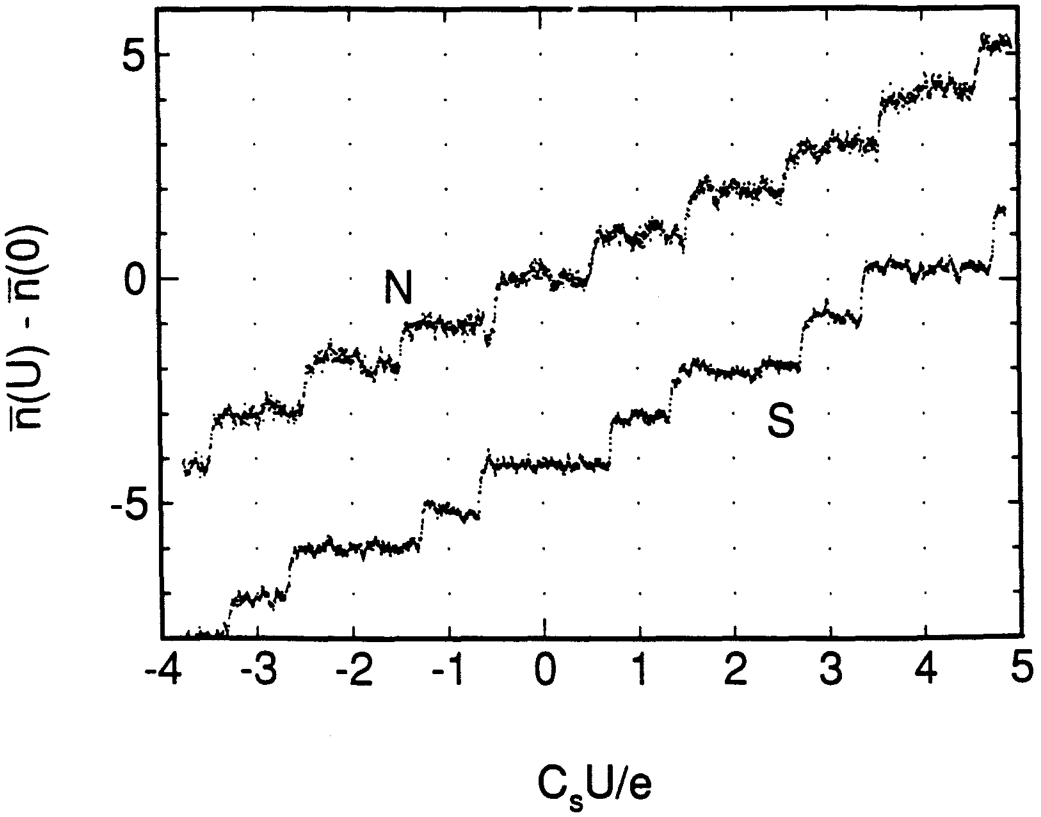
$\overline{n}(U) - \overline{n}(0)$
C_sU/e
5
0
-5
-4
-3
-2
-1
0
1
2
3
4
5
N
S

Fig. 4

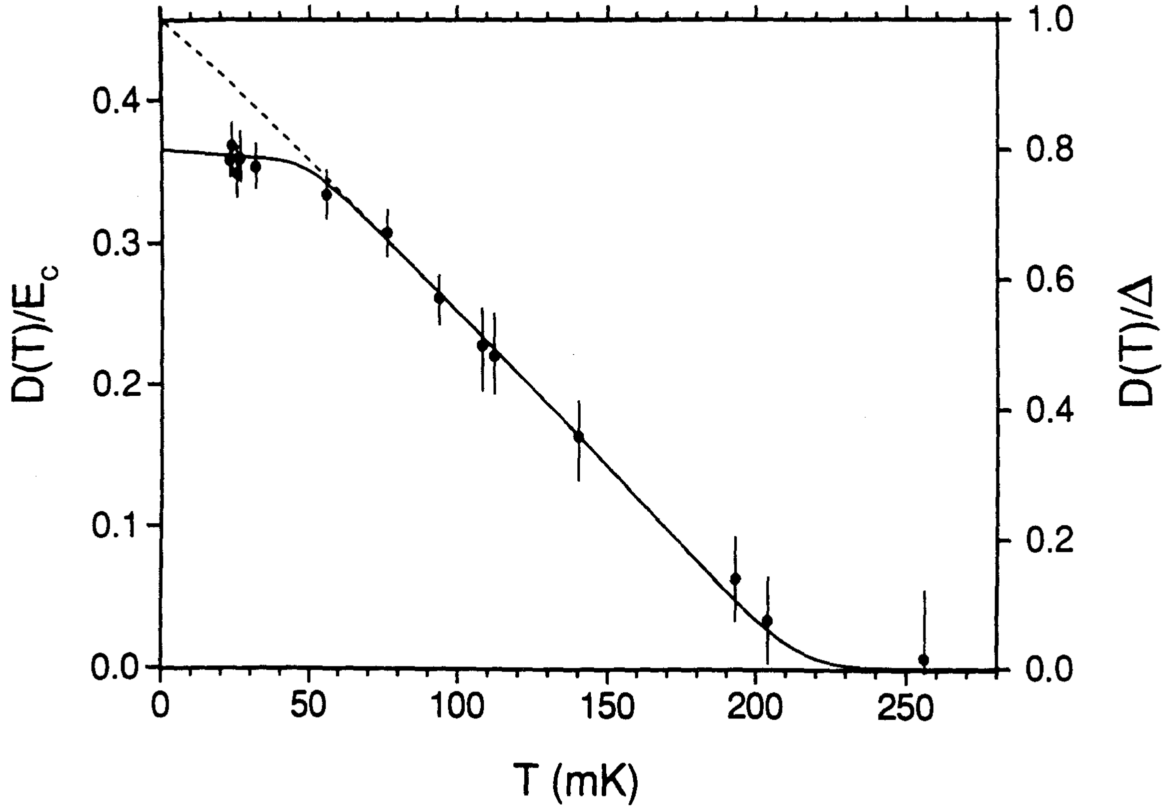

Fig. 5

3.2.2. Paper 3:

2e-Quantization of the Charge on a Superconductor

Originally published as:

P. Lafarge, P. Joyez, D. Esteve, C. Urbina, and M. H. Devoret, Two-electron quantization of the charge on a superconductor, Nature **365**, 422 (1993).

In this paper, we report the first direct observation of the 2e-quantization of the macroscopic charge on a superconducting island. We have measured Coulomb staircases in a normal/superconducting electron box with a ratio Δ/E_c equal to 1.23. The effects of the temperature and the magnetic field are well explained by the theoretical calculation of the odd-even free energy difference developed in Sec. 2.2.3 and 2.2.4.

2e-QUANTIZATION OF THE CHARGE OF A SUPERCONDUCTOR

P. Lafarge, P. Joyez, D. Esteve, C. Urbina and M.H. Devoret
Service de Physique de l'Etat Condensé, CEA-Saclay
F-91191 Gif-sur-Yvette, France

PACS 73.40 Gk, 73.40 Rw

Our theoretical understanding of superconductors is based on the notion of Cooper pair [1]. The first direct experimental evidence for electron pairing was the observation that the flux threading a superconducting ring is always a multiple of a flux quantum given by the ratio of Planck's constant and the Cooper pair charge 2e [2,3]. We report here a direct measurement of the total charge of a superconducting electrode which is free to exchange electrons with a metallic reservoir through a tunnel junction. When the potential of the reservoir is raised with respect to ground, we find that the charge of the superconducting electrode increases in steps of 2e corresponding to the simultaneous tunneling of two electrons. The 2e-steps break into e-steps when the temperature and magnetic field are increased above threshold values, but indicate nevertheless that Cooper pairs could be manipulated in the same way as single electrons in turnstile and pump devices [4].

Figure 1 shows a schematic of the experiment. A $\mathrm{Cu}-\mathrm{Al_2O_3}-\mathrm{Al}$ tunnel junction of capacitance C_j in series with a capacitor C_g is biased by a voltage source U. The Al electrode which is common to both the junction and the capacitor, the "island", is surrounded everywhere by insulating material. Since the junction tunnel resistance R_t is such that $R_t \gg R_K = h/e^2$, the total charge q of the island is a good quantum number and is given by $q = -ne$ [5]. As U increases, electrons will tend to move into the island to minimize the total energy of the circuit, which is the sum of its electrostatic energy and of the internal energy of the island [6]. The fluctuations of n are determined by the ratio between the energy of thermal fluctuations and the Coulomb energy $E_c = e^2/2(C_j + C_g)$, which is the electrostatic energy cost of putting one extra electron on the island when $U = 0$. By nanofabricating the circuit of Fig. 1, E_c can be made of the order of 2K. By lowering the circuit temperature down to 30mK, we can ensure that n has negligible fluctuations and adopts the minimum energy value. This is well demonstrated by the following control experiment. We placed the island in the non-superconducting state by applying a 0.2T magnetic field and measured the variations of the time averaged charge $\bar{q}$ versus U using a Coulomb blockade electrometer [7] operated in a feedback mode. The data are shown on trace (a) of Fig. 2. If q was not quantized, the circuit would achieve an equilibrium charge configuration with no potential difference on the junction capacitance C_j and hence, $\bar{q} = C_g U$. Since q is quantized, $\bar{q}$ can only increase stepwise, with steps located at half-integer values of the reduced voltage $C_g U/e$.

We then placed the island in the superconducting state by suppressing the magnetic field. The results are shown on trace (c) of Fig. 2. There is again a stepwise variation of $\bar{q}$ versus U, but the height and length of the steps have doubled, indicating that only electron pairs are transferred from the reservoir into the island. However, when we applied an intermediate magnetic field, so as to substantially reduce the superconducting gap without suppressing superconductivity, we observed an intermediate staircase pattern which consisted of a succession of long and short e-steps (see trace (b) of Fig. 2) and which was similar to the pattern observed in a previous experiment involving a different sample [8]. The ratio between the length of the short and long steps was observed to decrease as we lowered the field again. Below a threshold field $H = 0.02T$, the short steps disappeared completely and perfect $2e$-quantization was recovered.

These results can be understood by considering the total free energy of the circuit: $E = E_c(n - C_g U/e)^2 + (n \bmod 2)\tilde{\Delta} + \text{terms independent of } n$. The first term is simply the electrostatic energy of the circuit, i.e. the electrostatic energy of C_j and C_g and the work of the voltage source U [6]. The second term is the island internal energy which depends on n only through its parity [9], the parameter $\tilde{\Delta}$ denoting the odd-even free energy difference [10]. Such an odd-even difference is expected for a superconductor, since for an odd number of electrons, one of them cannot be paired and must remain as a quasiparticle excitation whose energy cost is the superconducting energy gap [11]. From this model we can predict the ensemble average $< n >$ which we suppose equal to the temporal average $\bar{n}$ measured in the experiment. In Fig. 3a we show as a function of U the energy of the different n states, for the non-superconducting case $\tilde{\Delta} = 0$. At temperatures T such that $k_B T \ll E_c$, n will adopt the value of the integer closest to $C_g U/e$, which corresponds to the lowest energy state, hence the staircase pattern of Fig. 3b. In Fig. 3e we show the case of a superconducting island such that, at the lowest temperatures, $\tilde{\Delta} > E_c$ in zero magnetic field. In that case, for every value of U, the ground state of the circuit always correspond to an even n, which explains the doubling in Fig. 3f of the step height with respect to Fig. 3b. The energy asymmetry between states with even and odd n has recently been observed through the $2e$-*periodicity* of the gate charge dependence of the current in SSS [10] and NSN Coulomb blockade electrometers [11, 12], and of the asymmetric e-staircase of a superconducting box [8]. It is important to note that although $2e$-quantization implies necessarily $2e$-periodicity, the converse is not true, as shown by Fig. 3d. The present results thus bring a new information: direct transitions between fully paired even states, which do not create a quasiparticle excitation, can be the sole charge transfer mechanism, provided that $\tilde{\Delta} > E_c \gg k_B T$, conditions which could not be satisfied in previous island charge measurements. This perfect $2e$-quantization necessitates that the system finds, as U is increased, its lowest energy state by the coherent tunneling of two electrons from the reservoir into the island to form a Cooper pair. The rate of this process also known as Andreev reflection [13] is proportional to $(R_K/R_t)^2$ [14] and is therefore much weaker than single electron tunneling whose rate is proportional to R_K/R_t. Nevertheless, since the $2e$-steps of Fig. 2c did not display any measurable out-of-equilibrium behavior, the time scale of the Andreev process is shorter than our measurement time scale of the order 10^{-2}s.

At intermediate magnetic fields and temperatures (Fig. 3c), the odd-even free energy difference, while non-zero, is such that $\tilde{\Delta} < E_c$. Odd n states can now exist on a finite U range (Fig. 3d). In this regime, we can measure $\tilde{\Delta}/E_c$ from the length ratio S/L of the short and long steps. This can be done quite accurately because the sharpness of the steps makes S/L insensitive to the long term drift in the electrometer output due to offset charges [7]. The measurement of $(L - S)/(L + S) = \tilde{\Delta}/E_c$ with temperature and magnetic field, which was applied perpendicularly to the strip, is shown in Fig. 4. At a fixed magnetic field, we found we could fit the measured $\tilde{\Delta}(T)/E_c$ using the theory of Refs. [8,10] with the quasiparticle density of state of Skalski *et al* [15] in which enters only one field-dependent parameter, the pair-breaking energy Γ. The other parameter entering in this density of states is the zero-temperature zero-field energy gap Δ. Using the De Gennes and Tinkham prediction $\Gamma/\Delta = (\pi^3/18)H^2 d^2 \ell \xi_0/\Phi_0^2$ for a strip of dirty superconductor in a perpendicular field H [16], we finally arrived at a theoretical expression for $\tilde{\Delta}(T,H)/E_c$ which depends only on three adjustable parameters: the gap Δ, the Coulomb energy E_c and the elastic mean free path ℓ (in the expression for Γ, $d = 110$nm is the width of the strip, $\xi_0 = 1600$nm the coherence length, Φ_0 the flux quantum $h/2e$). The best fit, shown in Fig. 4, yields $\Delta/e = 210\mu$V, $\Delta/E_c = 1.23$, values which are consistent with independent measurements, and $\ell = 6$nm. This latter value is one order of magnitude smaller than the mean free path we extracted from a conductivity measurement of a nanofabricated Al wire with same lateral dimensions as the island. However, this discrepancy may simply reflect the fact that electron diffusion is not isotropic in the island and the main result shown in Fig. 4 is that the 2e-quantization domain occupies only a small portion of the superconductivity domain.

ACKNOWLEDGEMENTS

The technical assistance of P.F. Orfila as well as discussions with T. Eiles and J. Martinis are greatfully acknowledged. This work is partly supported by the Bureau National de la Métrologie.

REFERENCES

[1] Bardeen J., Cooper L.N., and Schrieffer J.R., Phys. Rev. **108**, 1175 (1957).

[2] Deaver B.S. and Fairbank W.M., Phys. Rev. Lett. **7**, 43-47 (1961).

[3] Doll D. and Näbauer M., Phys. Rev. Lett. **7**, 51-55 (1961).

[4] Devoret M.H., Esteve D. and Urbina C., Nature, **360**, 547 (1992) and references therein.

[5] Grabert H., to be published in the proceedings of the LT20 conference, and references therein.

[6] Averin D.V. and Likharev K.K., in *Mesoscopic Phenomena in Solids*, ed. by Altshuler B. *et al.* (Elsevier, Amsterdam, 1991).

[7] Fulton T.A. and Dolan G.J., Phys. Rev. Lett. **59**, 109-113 (1987).

[8] Lafarge P., Joyez P., Esteve D., Urbina C. and Devoret M.H., Phys. Rev. Lett. **70**, 994-998 (1993)

[9] Averin D.V. and Nazarov Yu., Phys. Rev. Lett. **69**, 1993-1996 (1992).

[10] Tuominen M.T., Hergenrother J.M., Tighe T.S and Tinkham M., Phys. Rev. Lett. **69**, 1997-2001 (1992).

[11] Eiles T.M., Martinis J.M. and Devoret M.H., Phys. Rev. Lett. **70**, 1862-1866 (1993)

[12] Tuominen M.T., Hergenrother J.M., Tighe T.S and Tinkham M., to be published in Phys. Rev. B.

[13] Andreev A.F., Zh. Eksp. Teor. Fiz. **46**, 1823 (1964) [Sov. Phys. JETP **19,** 1228 (1964)].

[14] Hekking F.W.J., Glazman L.I., Matveev K.A. and Shekter R.I., Phys. Rev. Lett., **26**, 4138 (1993).

[15] Skalski S., Betbeder-Matibet O. and Weiss P.R., Phys. Rev. **136**, A1500 (1964).

[16] de Gennes P.G. and Tinkham M., Physics, **1**, 107-126 (1964).

[17] Clarke J., in *Non-equilibrium Superconductivity* ed. by Langenberg D.N. and Larkin A.I. (Elsevier, Amsterdam, 1983) chap. 1.

[18] Lafarge P., Pothier H., Williams E.R., Esteve D., Urbina C. and Devoret M.H., Z. Phys. B **85**, 327 (1991).

FIGURE CAPTIONS

Fig. 1. Schematic of the experiment. The superconducting island is a 30×110×2260 nm Al strip containing approximately 10^9 atoms. Its dimensions are such that the electrostatic energy of one extra electron is much larger than the energy k_BT of thermal fluctuations at temperature $T \sim 30\text{mK}$. The island can exchange electrons with a Cu (3% wt. Al) thin film electrode acting as an electron reservoir through a tunnel junction [17]. The total charge q of the island varies under the influence of the externally controlled voltage source U connected between the electron reservoir and a ground electrode. The variation with U of the time average $\bar{q}$ of the island charge is measured by a Coulomb blockade electrometer (not shown) which is weakly capacitively coupled to the island. The nanofabrication and low noise measurement techniques involved in this type of experiment have been described in Refs. [18,8].

Fig. 2. Variations of the average value $\bar{q}$, in units of e, with the polarization C_gU/e, at $T = 28\text{mK}$, for 3 values of the magnetic field applied to the sample. Trace (a): non-superconducting island. Traces (b) and (c): superconducting island. For clarity, traces (b) and (c) have been offset vertically by 2 and 4 units, respectively. The letters L and S refer to the long and short steps, respectively.

Fig. 3. Total energy of the circuit of Fig. 1 as a function of the polarization C_gU/e, for several values of the excess number n of electrons in the island, in the non-superconducting state (a) and superconducting state (c, e). E_c is the electrostatic energy of one excess electron on the island for $U = 0$. The minimum energy for odd n is $\tilde{\Delta}$ above the minimum energy for even n. Panels c and e differ by the relative magnitude of $\tilde{\Delta}$ and E_c. The solid dots correspond to level crossings where single electron tunnel into and from the island. The white dots correspond to level crossings where the only allowed process is the simultaneous tunneling of two electrons into the island to form a pair (Andreev process). The equilibrium value $< n >$ versus C_gU/e is shown in the non-superconducting (b) and superconducting (d, f) states, at $T = 0$. The Andreev process is shown in f by a vertical dashed line to distinguish it from the single electron tunneling process shown in b and d by a vertical continuous line.

Fig. 4. Odd-even step length ratio plotted as $(L - S)/(L + S)$, as a function of the

temperature T and magnetic field H. The fully $2e$-quantized steps are shown as white dots with unit height. The black dots are such that $1 > (L-S)/(L+S) = \tilde{\Delta}/E_c$. The surface corresponding to the grid in full line is the theoretical prediction combining references [10], [8], [15] and [16]. Note that the $2e$-quantization domain is only a small portion of the odd-even asymmetry domain ($\tilde{\Delta} > 0$) which is itself a small part of the superconductivity domain ($\Delta > 0$).

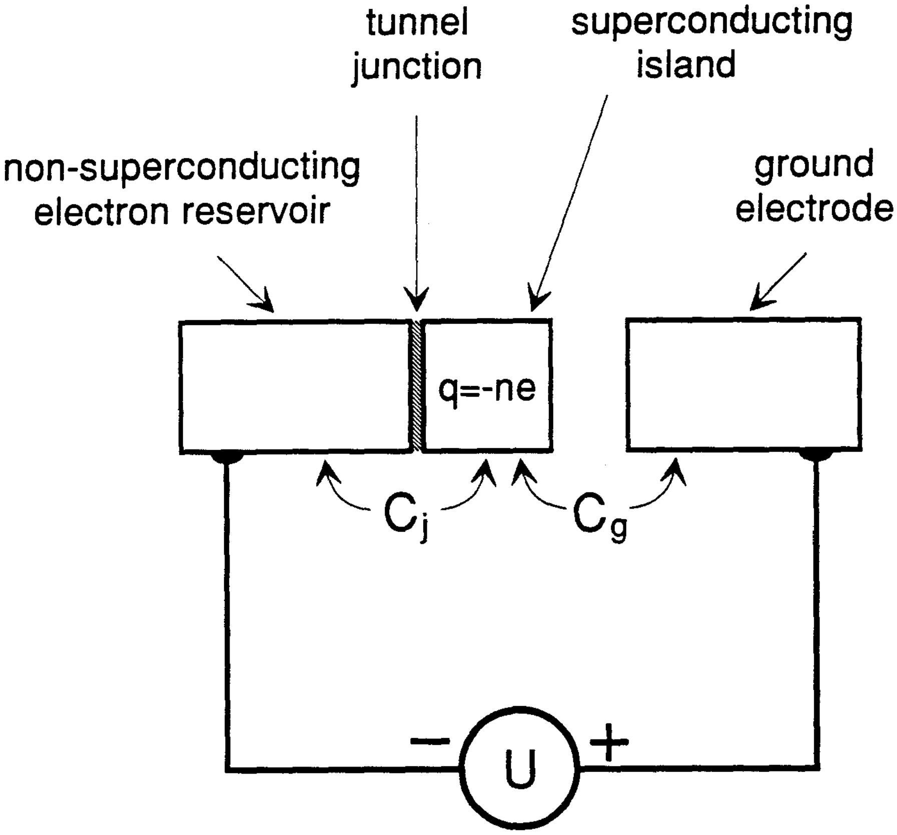
tunnel junction
superconducting island
non-superconducting electron reservoir
ground electrode
q=-ne
C_j
C_g
−
U
+

Fig. 1

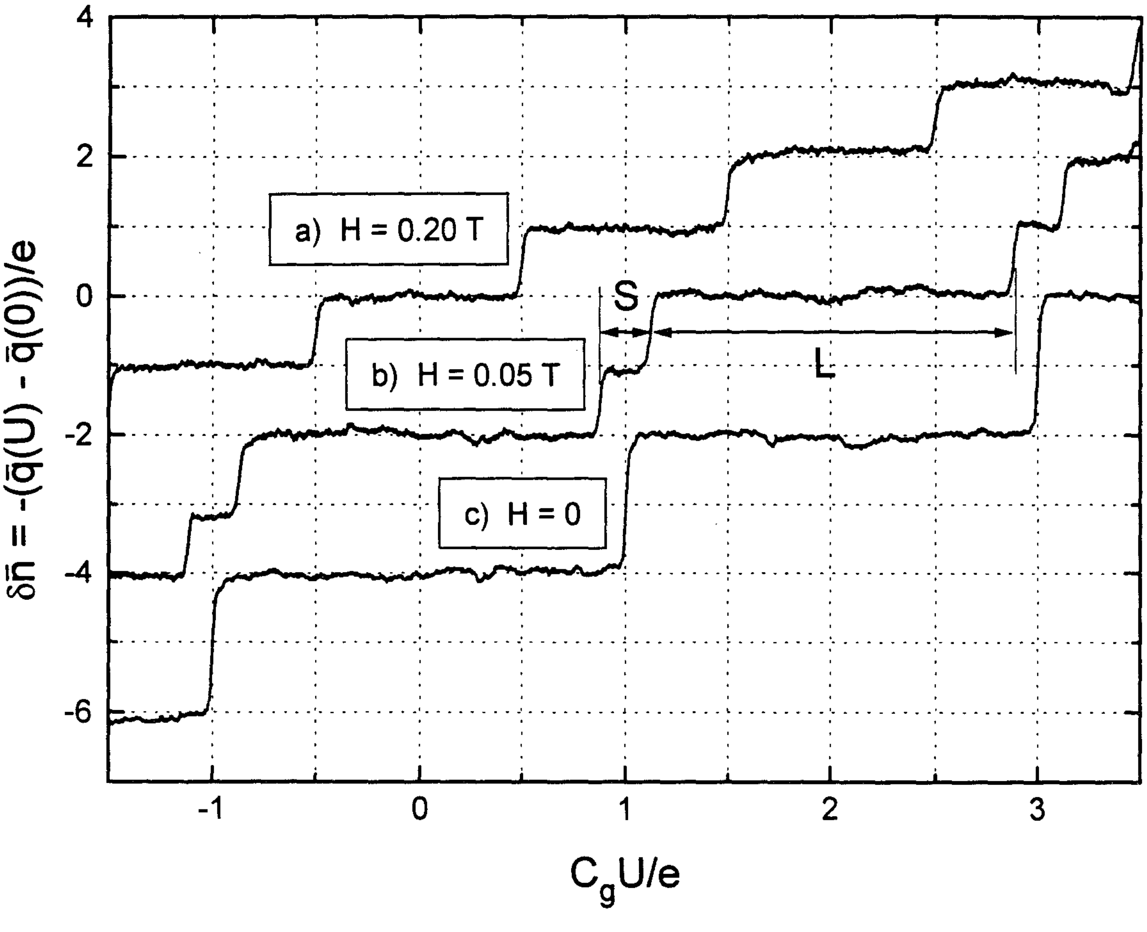

Fig. 2

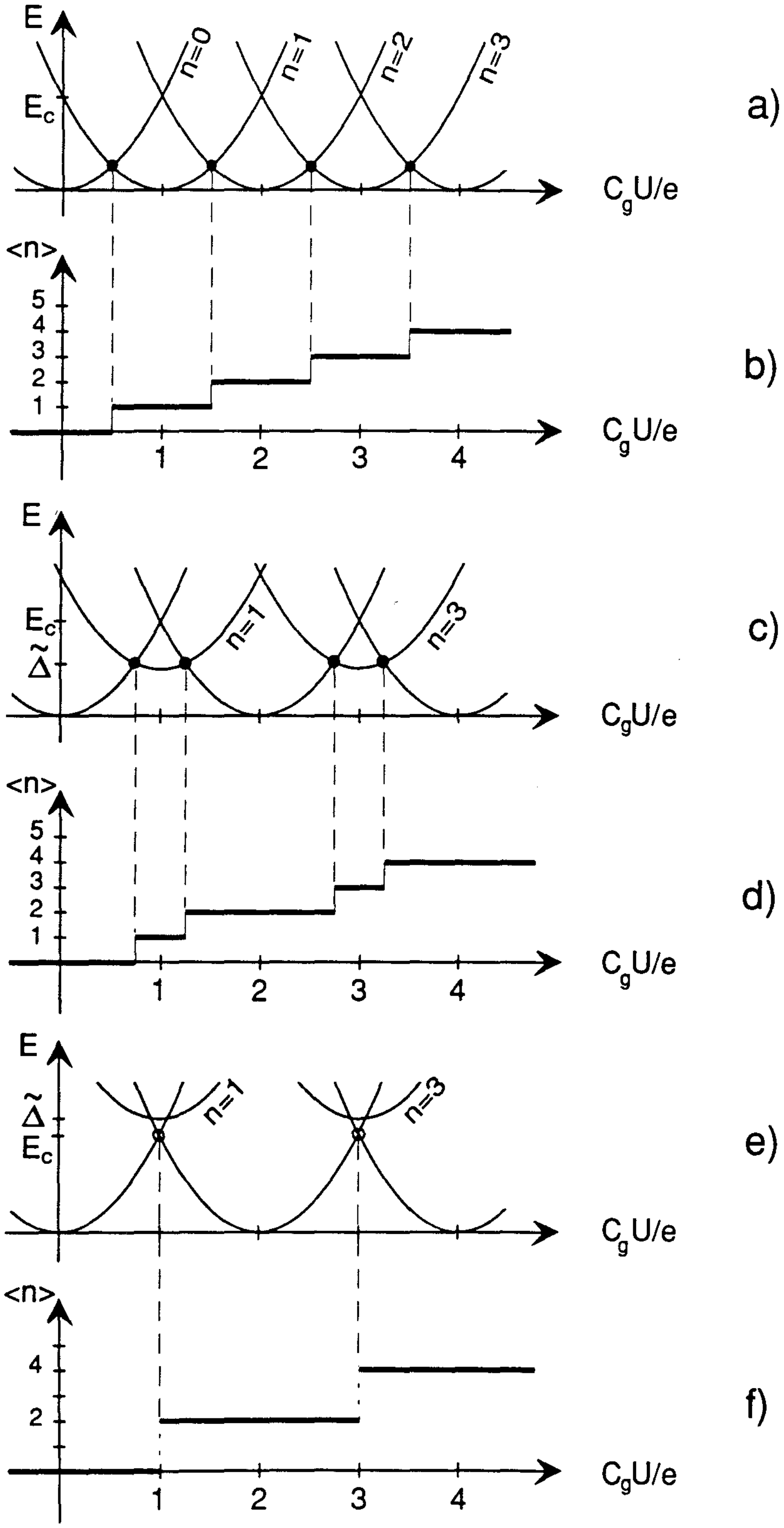

Fig. 3

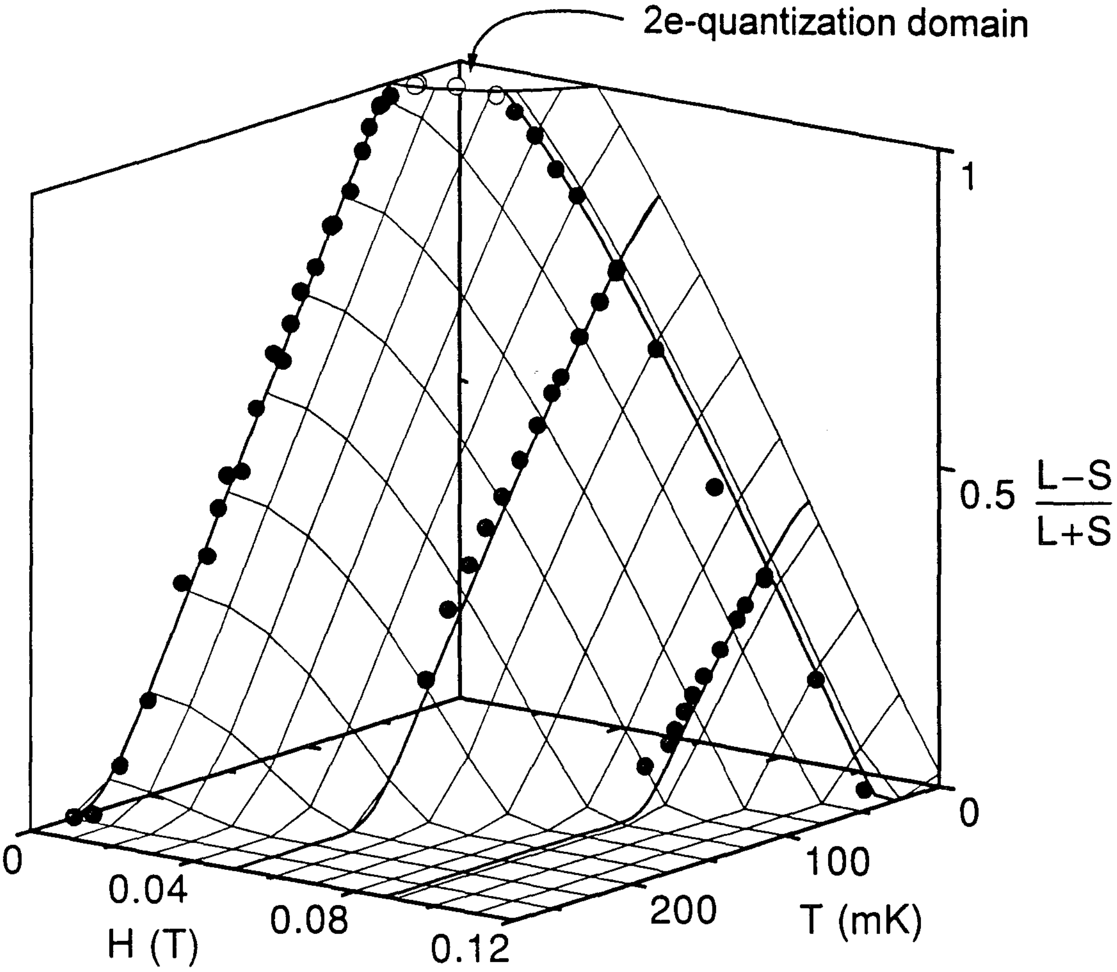
2e-quantization domain
1
0.5
$\frac{L-S}{L+S}$
0
0
0.04
0.08
0.12
H (T)
100
200
T (mK)

Fig. 4

4. Charge transfer accuracy

4.1.1. Paper 4:

Passing Electrons One by One: is a 10^{-8} Accuracy Achievable ?

Originally published as:

H. Pothier, P. Lafarge, D. Esteve, C. Urbina and M. H. Devoret, Passing electrons one by one: is a 10^{-8} accuracy achievable?, IEEE Trans. Instrum. Meas. **42**, 324 (1993).

PASSING ELECTRONS ONE BY ONE: IS A 10^{-8} ACCURACY ACHIEVABLE?

H. Pothier, P. Lafarge, D. Esteve, C. Urbina and M.H. Devoret
Service de Physique de l'Etat Condensé, CEA-Saclay
91191 Gif-sur-Yvette Cédex, France

ABSTRACT

We analyse the error mechanisms of the single electron pump with an arbitrary number of junctions. An upper bound for the error probability is computed analytically at zero temperature. We show that a 10^{-8} accuracy is achievable for devices with five or more junctions.

PACS: 73.40.Gk, 73.40.Rw, 06.20.Hq

1. Introduction

The understanding of single electron effects [1] has led to the design and operation of devices which make electrons pass one at a time in a controlled way in an external circuit [2,3]. The control of single electrons in these devices is achieved using the energy barrier provided by the electrostatic energy of a single excess electron on special electrodes of the device. These electrodes, hereafter referred to as 'islands', are connected to the rest of the device through either tunnel junctions with tunnel resistances large compared to the resistance quantum $R_K = h/e^2$ or pure capacitors. The device will function only if each island has a capacitance C_i such that the Coulomb energy $e^2/2C_i$ is very large compared with the energy $k_B T$ available in thermal fluctuations. In the 'turnstile' and 'pump' devices built using metal-insulator-metal junctions [2,3] or using semiconductor heterostructures [4], the controlled passage of single electrons manifests itself in current plateaus at $I = ne/\tau$ in the current-voltage $(I - V)$ characteristic, where n is an integer and τ the period of the rf modulation on the 'gate' electrodes. These plateaus are analogous to the Shapiro steps in the $I - V$ characteristic of a superconducting tunnel junction irradiated by microwaves [5]. As is well known, these steps are manifestations of the ac Josephson effect which links a voltage to a frequency through the flux quantum $\Phi_0 = h/2e$ and provide the basis for a representation of the standard volt. Thus, the question arises as to whether single electron pumps and turnstiles could be used in metrology to provide a new representation of the ampere. A representation of the ampere is obtained at present from the volt using the quantum Hall effect -discovered by von Klitzing- which links current and voltage through R_K [6]. It is important for metrologists to check if a direct definition of the ampere using the electron charge e is compatible with the 'Josephson + Klitzing' definition which combines Φ_0 and R_K. Another important metrological issue that would benefit from a new access to the electron charge provided by single electron effects is the value of the fine structure constant [7]. This latter application would not necessitate to measure directly the very low current produced by single electron devices. Although the experiments carried out so far to test the precision of single electron devices are chiefly limited by the precision of current measurements, it is necessary to investigate the fundamental limitations of the devices themselves. In this paper we analyse the source of errors and evaluate analytically an upper bound for the error probability of a general device of the pump type. Our goal is to answer the following question: Is it possible to design devices that would achieve an intrinsic accuracy of 10^{-8} which is the level at which the precision of the ampere is questioned by metrologists?

2. Single electron turnstiles and pumps

The devices that transfer electrons one by one in synchrony with an external rf signal consist of a linear array of nominally identical tunnel junctions with capacitance C (see Fig. 1). The array is biased with a dc voltage source V. The metallic islands between the junctions are connected through gate capacitors to voltages that may vary periodically with time at rf frequencies. By convention we will refer to the island placed between the k-th and (k+1)-th junction as the k-th island. We label C_{gk} and U_k the gate capacitance and gate voltage corresponding to the k-th island. We denote by N the total number of junctions. There are two classes of devices: the turnstiles and the pumps.

The turnstiles have an even number of junctions ($N = 2P$, P integer) and necessitate only one rf voltage source. It is connected to the central P-th island. The optimal value of the central gate capacitance is $C_{gP} = 2C/N$. The remaining U_k are fixed and are used only to compensate offset charges on the corresponding islands. Thus, one should have $C_{gk} \ll C$. The action of the central gate voltage is the following: During the first half of the rf period, an electron is attracted onto the central island through the leftmost P junctions, while during the second half of the period, the electron is repelled through the rightmost P junctions. While they were the first devices to be operated successfully, they suffer from the drawback that the current plateaus do not cross the $V = 0$ axis. Because they generate current only at finite voltage, turnstiles dissipate intrinsically more power than pumps and may be difficult to cool at the low temperatures which are required for the suppression of thermal errors.

The pumps necessitate as many independent rf sources as islands but they produce current plateaus that cross the $V = 0$ axis. Their principle can be described as follows: during an rf period, the U_k voltages vary in such a way that a triangular voltage pulse is successively applied to the gate capacitors, in the manner the distributor sends voltage pulses to the spark plugs of an automobile engine (See Fig. 2). The amplitude of the pulse is chosen so that it is energetically favourable for one electron and one electron only to neutralize the pulse. Each traveling pulse is thus accompanied by an electron. Consequently, the direction of current in the pump is not determined by the bias voltage V but by the direction of travel of the pulse, which in turn depends only on the relative dephasing among the gate voltage sources. The accurate reversal of the current produced by the pumps can therefore be performed by purely electronical means.

In the following we will analyze in detail the functioning of the pump and calculate its error probability, i.e. the probability that the pump does not transfer exactly one electron per rf period.

3. Detailed analysis of the N junction pump

The analysis of the pump is greatly simplified by performing a transformation analogous to the circuit transformations of electrical engineers in network theory. The transformation consists in replacing the linear array of Fig. 1(a) by the circular array of Fig. 1(b). In the process, the junctions keep the same parameters but instead of being linked through external leads to the bias voltage, current meter and common ground, the two end junctions are directly connected, thereby forming one extra island. This 0-th island is connected to a corresponding gate voltage U_0 through a gate capacitance $C_{g0} \ll C$. The transport voltage V can now be thought of being applied as a time varying flux through the ring of junctions, which we represent as voltages sources V/N in series with each junction. The electrostatic state of the array of Fig. 1(a) is entirely determined by the "electron configuration" $(n_1, n_2, ...n_{N-1})$, i.e. the set of number of extra electrons on each island, and the set of gate voltages $(U_1, U_2, ..U_{N-1})$. It is easy to show that the junctions in the circular array will adopt the same electrostatic state than in the linear array, if for the circular array, the electron configuration is $(n_0, n_1, n_2, ..n_{N-1})$ and the set of gate voltages is $(U_0, U_1, U_2, ..U_{N-1})$, with n_0 and U_0 satisfying

$$n_0 + \sum_{k=1}^{N-1} n_k = C_0 U_0 + \sum_{k=1}^{N-1} C_{gk} U_k \tag{1}$$

This equivalence is only true in the limit $C_{gk} \ll C$ which is required anyway from other, more practical, considerations. Now, for the circular array, the left hand side of (1) stays constant with time since tunnel events conserve the total number of electrons on the islands. Consequently, condition (1) implies that the number of independent gate voltages in the equivalent circular array is indeed the same as the original linear array. The traversal of the linear array by one electron corresponds to a single electron going around the circular array from island to island in the manner of an arm of a mechanical clock. Ideal pumping of electrons, with period τ, can therefore be described for the circular array as the following time evolution of the electron configuration:

$$n_k(t) = 1 \quad \text{if} k - 1/2 < (Nt/\tau)\text{mod} N < k + 1/2 \tag{2}$$

$$n_k(t) = 0 \quad \text{otherwise} \tag{2'}$$

We can thus index each electron configuration of the pump by an integer n in a natural manner. The integer $n\text{mod}N$ indicates on which island is the electron, while the integer part of n/N gives the number of times the electron went around the array. The ideal time evolution corresponding to (2) and (2') can therefore be described in a more compact form by

$$n(t) = \text{int}(Nt/\tau + 1/2) \tag{3}$$

where $\text{int}(x)$ denotes the integer part of x.

Although the circular pump is not a practical device, its symmetry clarifies greatly the discussion of possible errors and the search for optimal parameters. Once the optimum parameters are established for the circular pump, it is easy to go back to the realistic linear pump.

Obviously, the minimum electrostatic energy of the pump is reached when all the gate voltages and extra island electron numbers are zero. Starting from this state, if one puts one extra electron on island k while raising the k-th gate voltage to e/C_{gk}, one gets an equivalent electrostatic state with the same minimum electrostatic energy as far as the junctions are concerned. The following sequence of gate voltages interpolates between such gate voltage configurations:

$$U_k(t) = e/C_{gk}(x_k + 1) \quad \text{if} \quad -1 < x_k < 0 \tag{4}$$

$$U_k(t) = e/C_{gk}(-x_k + 1) \quad \text{if} \quad 0 < x_k < 1 \tag{4'}$$

$$U_k(t) = 0 \quad \text{otherwise} \tag{4''}$$

where

$$x_k = k - (Nt/\tau \bmod N) \tag{5}$$

This is the sequence which is plotted on Fig. 2 for the case $N = 5$. Note that it satisfies Equ. (1) for the case where there is a single electron in the array. The electron is driven across a junction by the simultaneous decrease and increase of the gate voltages on both side of the junction. The complete cycle requires N such elementary transfer steps. The rotation symmetry of the circular pump shows clearly that the entrance and exit of an electron in the linear pump at the beginning and at the end of a period do not require different pulse shapes than when the electron is traveling inside the array, although the leads seem to play a different role than the islands. However, the absence of these "end effects" only occurs in the limit $C_{gk} \ll C$ on which the equivalence between the circular and linear pump is based.

We will now analyze the error mechanisms of the circular pump containing one electron. We suppose that the temperature is zero. Let us recall the remaining parameters of the system: the number of junctions N, the bias voltage V, the junction capacitance C and the period τ. We suppose moreover that all the junctions have the same tunnel resistance R_T. At this point it is useful to introduce the following dimensionless parameters:

$$r = \frac{R_T}{R_K} \tag{6}$$

$$v = \frac{V}{e/2C} \tag{7}$$

$$x = Nt/\tau \tag{8}$$

$$f = R_K C/\tau \tag{9}$$

where $R_K = h/e^2$. In addition to these parameters which we call reduced tunnel resistance, reduced bias voltage, reduced time and reduced frequency, respectively, the system is characterized by the energy scale $e^2/2C$.

The electrostatic energy of the whole array including the work performed by the bias voltage can be computed for every n, the gate voltages being given by (4). The expression of this total array energy as a function of the reduced time x and the reduced voltage v is given, in units of $e^2/2C$, by

$$E_n(x, v) = -jv - [iv + (N - i)(2(x \bmod 1) - i)]/N \tag{10}$$

where i and j are the integers satisfying

$$n - \mathrm{int}(x) = jN + i \tag{11}$$

$$1 \leq i \leq N \tag{11'}$$

In Fig. 3 we plot the set of values E_n, n running from -7 to +7, in the case where $v = 0.2$, the reduced time x taking the values 0,0.25,0.5,0.75 and 1. The plots of the energy at other reduced times with the same sampling period are obtained simply by a translation along n, as equ. (11) indicates. The energy values plotted in Fig. 3 represent a kind of potential for the discrete configuration variable n. The way this potential evolves with time reflects the gate voltages time sequence of Fig. 2. The evolution of the potential drives the variable n to evolve with time by provoking tunnel events. They always tend, at zero temperature, to lower the total electrostatic energy of the system. If only tunnel events changing n by one unit (single junction tunneling events) were allowed and if τ/N was sufficiently long that these single junction tunnel events would occur essentially as soon as the new configuration with a lower energy became available, n would follow one "potential minimum" (see dot on Fig. 3). The pump would behave ideally, the only difference with (3) being that the $n \rightarrow n+1$ transitions would occur slightly earlier in the cycle because of the bias voltage, and the pump would be error free. To predict the actual error probability of a realistic device we have to take into account i) missed transfer steps which occur when one requires that the period τ should be as small as possible to produce a current as large as possible, as well as ii) higher order tunnel processes involving several junctions, the so-called macroscopic quantum tunneling of the charge, or "co-tunneling" events [8], which allow n to vary by more than one unit if a state with lower energy is found.

4. Error probability calculations

4.1 Errors caused by missed transfer steps

The general expression for the probability of a single junction tunnel event between configuration n and configuration $n+1$ is given using reduced parameters by

$$\Gamma_{n\rightarrow n+1}\mathrm{d}t = \gamma_{n\rightarrow n+1}\mathrm{d}x = (2Nrf)^{-1} \mid \Delta_1 \mid_+ \mathrm{d}x \tag{12}$$

where $\Delta_1 = E_n - E_{n+1}$ and where we have used the notation $\mid y \mid_+ = (\mid y \mid + y)/2$. The probability that the $n \rightarrow n+1$ transition does not occur in the time slot alloted for the n-th transfer step is given by

$$P_n = \exp\left(- \int_{x=n}^{x=n+1} \gamma_{n\rightarrow n+1}\mathrm{d}x \right) \tag{13}$$

In writing (13), we neglect the fact that state $n+1$ is not the only decay channel for state n. This is a very good approximation since, as we will see, the branching ratio for $n+1$ is very close to 1 because co-tunneling rates are much smaller than the single junction tunneling rate. It may happen that the electron which has missed its time slot gets a second chance during the time slot of the next transfer step; however the analysis of this recovery is tedious. By using expressions (10), (12) and (13) a conservative estimate $\epsilon_m = NP_n$ of the probability of losing a cycle because of missed transfers can therefore be calculated:

$$\epsilon_{\mathrm{m}} = N\exp\left(-\frac{(N-1)[1+v/(N-1)]^2}{8N^2rf}\right) \tag{14}$$

4.2 Errors caused by co-tunneling events

It is clear from Fig. 3 that configuration n can always decay into configuration $n+N$ whose reduced energy is lower by v (we suppose for the time being that $v \geq 0$). Such co-tunneling process involving N junctions corresponds to an electron going around the pump in the direction of the bias voltage and returning to its original position. This is why the energy difference between the initial state and final state is constant. However the energy barrier in configuration space is modulated during each transfer step as Fig. 3 indicates. In addition to this N-th order co-tunneling process, we have to consider two (N-1)-th order co-tunneling processes during the n-th time slot. The first one is the $n \rightarrow n+1-N$ transition that has the effect of sending the electron to the island with minimal potential by going around the array in the direction opposite to the normal direction of transfer. This process substracts a transfer cycle to the normal sequence. The second one is the $n+1 \rightarrow n+N$ that has the effect of sending the electron which has tunnelled back to the island it started by going around the array in the direction of transfer. Like the N-th order co-tunneling process, this process adds a transfer cycle to the normal sequence. The three co-tunneling processes are shown schematically in Fig. 4. The thick line with a varying shade represents the probability weight of a given configuration as a function of the reduced time x. The thick vertical dashed line marks the onset of the single junction tunneling process, which is symbolically represented in the figure by a thick arrow. This onset is located $1/2 - v/2(N-1)$ after the beginning of the step. The $n \rightarrow n+1-N$ co-tunneling process is represented by a curved arrow in full line pointing in the direction of decreasing n while the $n+1 \rightarrow n+N$ co-tunneling process is represented by a similar arrow pointing in the direction of increasing n. A thin vertical dashed line located $1/2+v/2$ after the beginning of the step marks the boundary between the domains of existence of the $n \rightarrow n+1-N$ and $n+1 \rightarrow n+N$ processes which are mutually exclusive. Finally the N-th order co-tunneling process is represented by an upward pointing curved arrow in dashed line.

The general expression for the probability of co-tunneling [8] between a configuration n and a lower energy configuration $n+p$ is bounded from above by the expression given here in terms of reduced parameters:

$$\Gamma_{n\to n+p}\mathrm{d}t = \gamma_{n\to n+p}\mathrm{d}x = \frac{2\pi^2}{Nf}(4\pi^2 r)^{-p}\frac{(p!)^2}{(2p-1)!}\frac{{\Delta_p}^{2p-1}}{\prod_{i=1}^{p-1}{\Delta_i}^2}\mathrm{d}x \tag{15}$$

where $\Delta_i = E_n - E_{n+i}$. Expression (12) can be thought of as the $p=1$ case of (15) if the product $\prod_{i=1}^{p-1}{\Delta_i}^2$ is understood as giving the value 1 when the upper bound is 0.

Expression (15) has two drawbacks. First, it is not a piecewise polynomial expression of x like the rate (12) of single junction tunneling. Second, it diverges at the zeroes of Δ_i. The second drawback, however is an artefact of the perturbation theory used to derive (15). The divergences take place where other transitions with a lower p become possible. In the general case, by suitable resummation techniques, it is possible to get expressions yielding a finite value of the transition rate at these singular points [9]. In the particular case of the co-tunneling processes of order $N-1$ we have considered above, we were able, by going back to the original perturbative integral expression of Averin and Odintsov [8], to get an analytical expression for the rate that stays finite during the whole transfer step and its vicinity:

$$\gamma_{n\to n+N-1} = \frac{2\pi^2}{Nf}(4\pi^2 r)^{-N+1}\frac{((N-1)!)^2}{\prod_{i=1}^{N-3}\Delta_i^2}I(x,v) \tag{16}$$

with

$$I(x,v) = \int_0^{\Delta}\frac{\sigma^{2N-7}}{(2N-7)!}[2(\sigma-\Delta)+(2\Delta'+\Delta+\sigma)\ln\left(\frac{\Delta'+\Delta}{\Delta'+\sigma}\right)]\mathrm{d}\sigma \tag{16'}$$

where $\Delta = \Delta_{N-1}$ and $\Delta' = \Delta_{N-2}$.

It is then possible to construct a polynomial expression which is everywhere greater than this complicated expression except at the singular point where the two expressions take the same value. This polynomial expression reads:

$$\gamma_{n+1\to n+N}(x,v) = \gamma_{n\to n+1-N}(-x,-v) \leq \frac{c(N)}{f r^{N-1}} \mid x - v \mid_+^{2N-3} \tag{17}$$

where $c(N)$ is a coefficient that only depends on N. Using expression (17) it is possible to compute the total error probability due to both co-tunneling processes of order $N-1$.

This probability can be written as

$$\epsilon_c = N \int_n^{n+1} [P_n(x)\gamma_{n\to n+1-N}(x) + P_{n+1}\gamma_{n+1\to n+N}(x)]\mathrm{d}x \tag{18}$$

By continuing analytically the integrand outside the time slot alloted for the transfer step and by extending the range of integration to infinity one can get a manageable final expression for the error probability:

$$\epsilon_c = d(N) f^{N-2} F\left(\frac{v}{[8(N-1)rf]^{1/2}}\right) \tag{19}$$

where

$$d(N) = \frac{2^{N-1}N^{2N-3}(N-1)^{N-2}(N-2)^2}{\pi^{2N-4}(2N-5)!(2N-5)(2N-6)(N-3)!^2} \tag{20}$$

and where the function $F(y) = y^{2N-2}/(2N-2) + \int_0^\infty \mathrm{d}t e^{-t^2}(t-y)^{2N-3}$ can be well approximated by

$$F(y) = \frac{(\mid y - a\mid^{\alpha} + b^{\alpha})^{2(N-1)/\alpha}}{2N-2} \tag{21}$$

with $\alpha = 1.4$, $a = 1.1$ and $b = 0.85$. The value of the coefficient $d(N)$ is given in table 1 for values of N relevant to the discussion in the following section.

We have supposed so far that the bias voltage was positive and small compared with $e/2C$. A straightforward analysis carried out for the case of negative bias voltage shows that expressions (19) and (21) are valid in the whole voltage range

$$-(N-1)/N \leq v \leq (N-1)/N \tag{22}$$

where only co-tunneling processes of order $N-1$ and N have to be considered during a transfer step.

We now have to deal with the co-tunneling process of order N. It could be argued that this process is negligible in comparison with the process of order $N-1$ because it has a higher rank in the perturbative expansion of the tunnel hamiltonian. However, one has also to take into account the fact that processes of order $N-1$ are weighted by occupational probabilities which are significantly different from zero only during a small fraction of the time interval alloted for a transfer step, whereas the effect of the process of order N is felt during this whole time interval. As a matter of fact, extensive numerical studies of the relative importance of the two types of processes were needed to show that, indeed, the process of order N was negligible in the voltage range (22). Expressions (19) and (21) can therefore be considered as giving an upper bound of the total error probability due to co-tunneling in the voltage range (22).

5. Optimal parameter space

We can now use expressions (14) and (19) for the error probability due to missed transfers and co-tunneling, respectively, to find the parameters which allow a total error probability less than 10^{-8}. In Fig. 5 we plot the constant error probability curves in the (f, v) plane for the cases $N = 4$ and N=5. We treat ϵ_m and ϵ_c separately, the constant value being 10^{-8}, with a value 5 for the ratio $r = R_T/R_K$ which is easily accessible by conventional nanojunction fabrication. The figure shows that below a certain threshold value of the reduced frequency f, there is a range of reduced voltages for which the error probability is less than 10^{-8}. In the case of $N = 4$, however, the threshold frequency is determined by co-tunneling errors while in the case of $N = 5$ this frequency is determined by missed transfer steps. Consequently, in the $N = 4$ case, the optimal parameter region is a small lentil-shaped domain providing almost no parameter error margin whereas in the $N = 5$ a substantial fraction of the total voltage range (22) can be used at the threshold frequency. In Fig. 6 we plot, in the case $N = 5$, the tongue-shaped domains of the (f,v) plane where the total error probability is below 10^{-8}, for three values of the ratio r. The figure shows that as the tunnel resistance gets smaller, one can reach higher frequencies, and thus higher currents, but at the expense of a smaller voltage range. We have performed numerical calculations to see how finite temperatures shrink these domains. We find that a shrinking by a factor of a half is reached approximately when $k_BT \simeq 0.025e^2/2C$. In conclusion one can summarize our analytical results by stating a rough rule of thumb valid for $N \geq 5$: the product of the maximum voltage range ΔV_{max} by the maximum current I_{max} obeys

$$\Delta V_{max} I_{max} < 10^{-3} \frac{(e^2/2C)^2}{h} \tag{21}$$

For instance, it should be possible to operate a 5 junction pump, with 0.2fF and 100kΩ junction capacitance and resistance respectively, which would deliver at 100mK, over a 100μV voltage range, a 10 pA current accurate to 10^{-8}.

Acknowledgements

We are grateful to D. Averin and J. Martinis who, as our own work was completed, communicated us their results prior to publication [10,11]. By performing somewhat different calculations than us, they also came up to the conclusion that metrological accuracy could be reached with the $N = 5$ pump. We are also indebted to A. Cleland and P.F. Orfila for their help with the figures.

REFERENCES

[1] "Single Charge Tunneling", H. Grabert and M.H. Devoret eds., Plenum, New York (1992) and references therein.

[2] L.J. Geerligs, V.F. Anderegg, P.A.M. Holweg, J.E. Mooij, H. Pothier, D. Esteve, C. Urbina and M.H. Devoret, Phys. Rev. Lett., **64**, 2691 (1990).

[3] H. Pothier, P. Lafarge, D. Esteve, C. Urbina and M.H. Devoret, Europhys. Lett., **17**, 249 (1992)

[4] L.P. Kouwenhoven, A.T. Johnson, N.C. van der Vaart, C.J.P.M. Harmans and C.T. Foxon, Phys. Rev. Lett. **67**, 1626 (1991).

[5] A. Barone and G. Paterno, "Physics and applications of the Josephson Effect", Wiley, New York (1982).

[6] K. von Klitzing, Rev. Mod. Phys. **58**, 519 (1986).

[7] E.R. Williams, R.N. Gosh and J.M. Martinis, J. Res. Natl. Ins. Stand. and Technol. **97** (1992).

[8] D.V. Averin and A.A. Odintsov, Phys. Lett. **A 149**, 251 (1989).

[9] P. Lafarge and D. Esteve, Phys. Rev. **B 48**, 14 309 (1993).

[10] D.V. Averin, A.A. Odintsov and S.V. Vyshenskii, J. Appl. Phys. **73**, 1297 (1993).

[11] H.D. Jensen and J.M. Martinis, Phys. Rev. **B 46**, 13 407(1992).

FIGURE CAPTIONS

Fig. 1 (a) Linear array of N tunnel junctions with the same capacitance C. Each electrode between junctions, called for short 'island', has a sufficiently low self-capacitance C_i that $e^2/2C_i \ll k_BT$ and can be electrostatically acted upon by a gate voltage U_k, $1 \leq k \leq N-1$. The ends of the array are connected to a common ground through voltage sources whose effect is to bias the array by a transport voltage V. (b) Circular array of tunnel junctions obtained by connecting the end junctions of (a), thereby forming an additional small capacitance island electrostatically biased by an additional gate voltage U_0. The transport voltage V around the circular array can be thought of as being produced by a time-varying flux through the array. It is represented by voltage sources V/N in series with each junction.

Fig. 2 Time variations of the gate voltages for the $N = 5$ linear pump (full lines). In dashed line, additional gate voltage for the circular pump. In the circular N pump, the N successive gate signals are shifted in time by τ/N, where τ is the duration of the pumping cycle.

Fig. 3 Array total energy for the $N = 5$ pump biased with $V = 0.1e/C$ as a function of the electron configuration n representing the location of the single electron going around the equivalent circular pump. The energy profile is shown at several instants during a transfer step. For clarity, the $n = 0$ energies at successive instants have been shifted by $e^2/2C$. The dots sitting at an energy minimum represent a possible state of the array and its evolution with time.

Fig. 4 Array configuration versus time diagram showing the various processes affecting the state of the $N = 5$ array. The thick lines with graded shade show the occupation probability of a particular configuration as the gate voltages evolve with time. The thick arrows represent the single junction processes while the curved arrows in full and dashed lines represent the co-tunneling processes of order $N-1$ and N, respectively. The vertical dashed lines indicate the onset of the tunneling processes (see main text).

Fig. 5 Constant error probability curves in the reduced voltage - reduced frequency plane for two values of N. Curves intersecting the vertical axis (marked "c") correspond to a 10^{-8} error probability due to co-tunneling events while the curves intersecting the horizontal axis

(marked "m") correspond to the error due to missed transfer steps, with same probability. The symbol r denotes the reduced tunnel junction resistance R_T/R_K.

Fig. 6 Parameter domains ensuring a probability error less than 10^{-8} in the case of the $N = 5$ pump for three values of the reduced tunnel resistance $r = R_T/R_K$.

TABLE 1

n	$d(n)$
4	84.10
5	78.01
6	44.60

Fig. 1

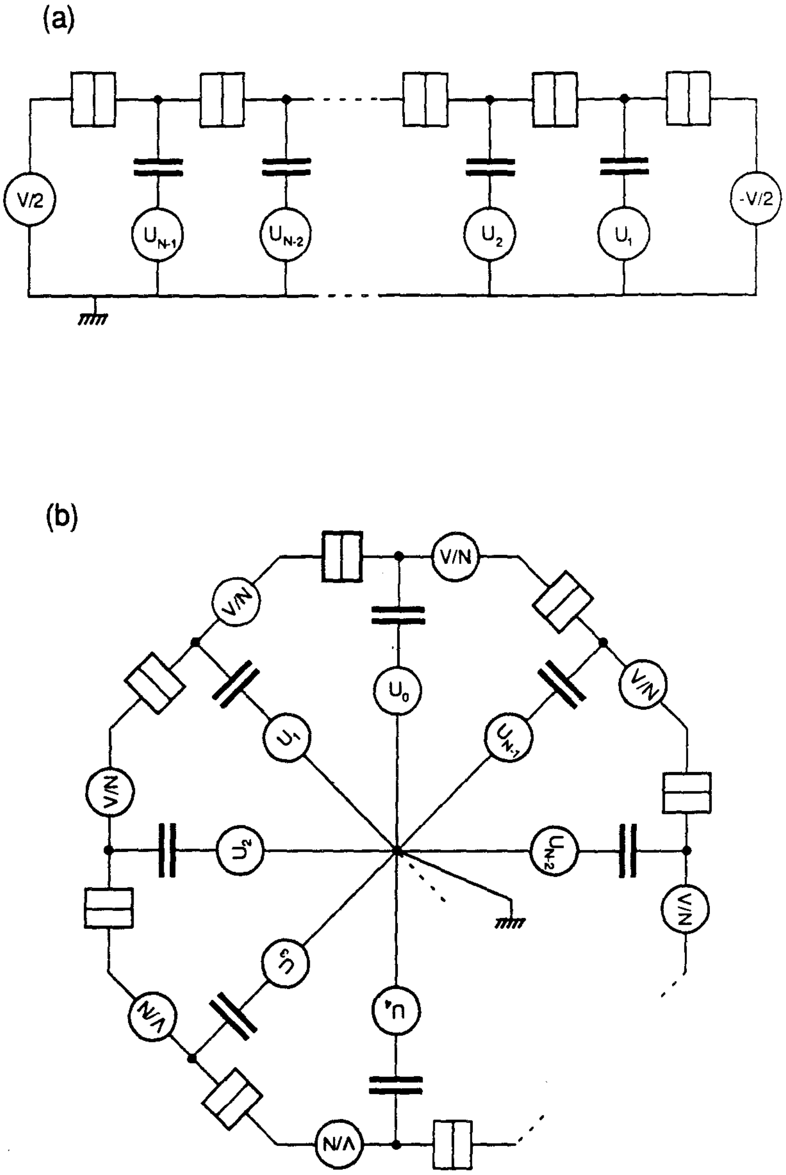
(a)
V/2
U_{N-1}
U_{N-2}
U_2
U_1
-V/2
(b)
V/N
U_0
U_1
U_2
U_3
U_4
U_{N-1}
U_{N-2}

Fig. 2

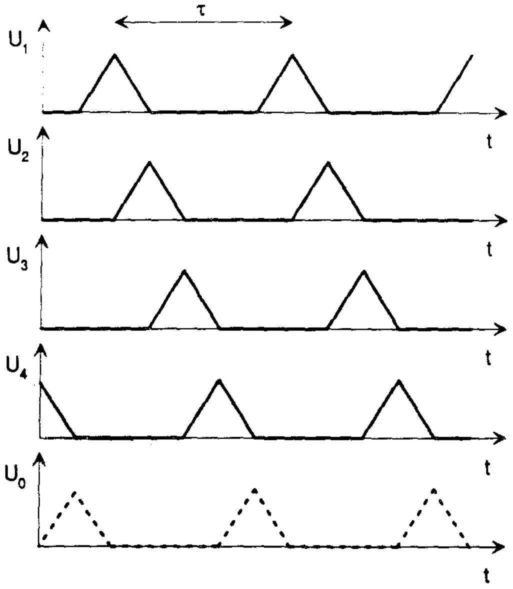
τ
U_1
U_2
U_3
U_4
U_0
t
t
t
t
t

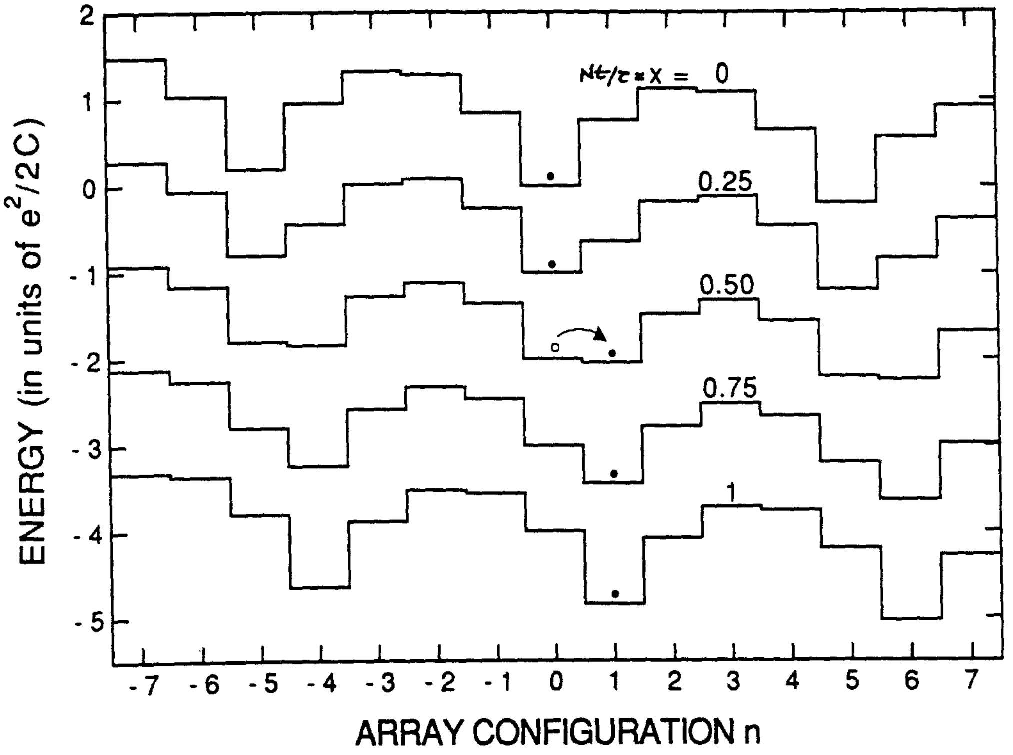

Nt/τ = x = 0
0.25
0.50
0.75
1
ENERGY (in units of $e^2/2C$)
2
1
0
-1
-2
-3
-4
-5
-7 -6 -5 -4 -3 -2 -1 0 1 2 3 4 5 6 7
ARRAY CONFIGURATION n

Fig. 3

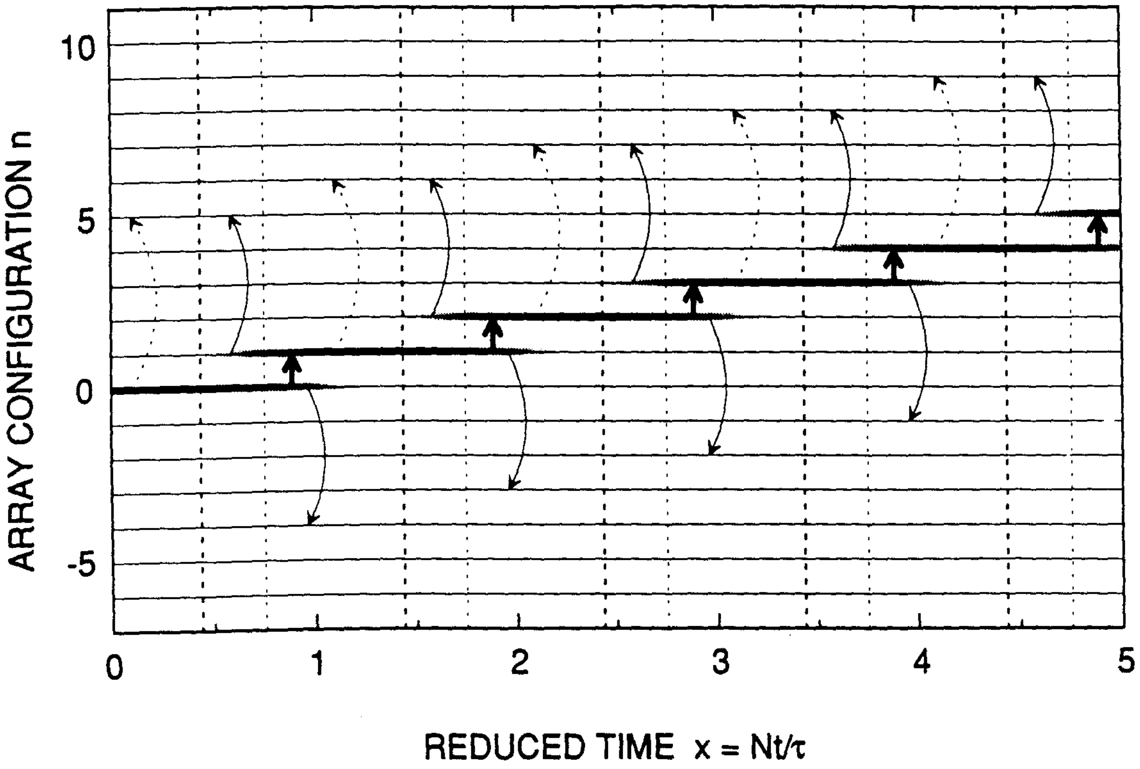

ARRAY CONFIGURATION n
10
5
0
-5
0
1
2
3
4
5
REDUCED TIME x = Nt/τ

Fig. 4

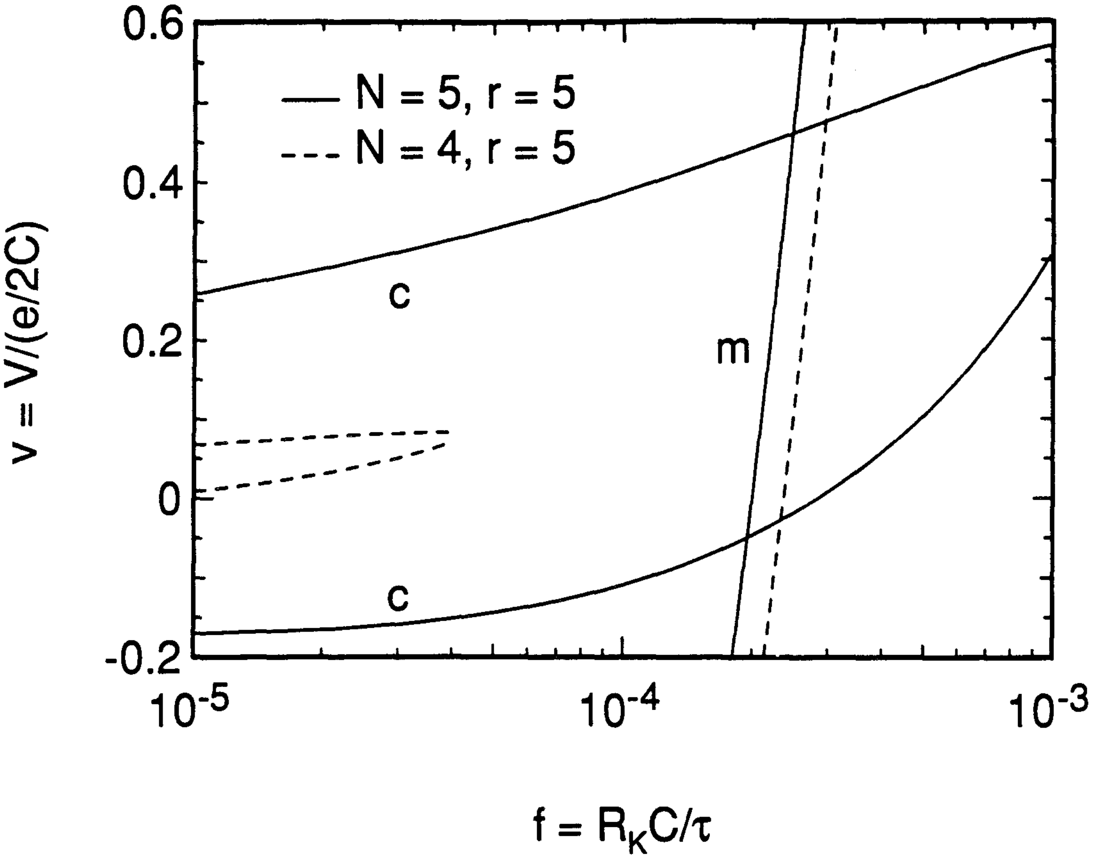

N = 5, r = 5
N = 4, r = 5
c
c
m
$v = V/(e/2C)$
0.6
0.4
0.2
0
-0.2
10^{-5}
10^{-4}
10^{-3}
$f = R_K C/\tau$

Fig. 5

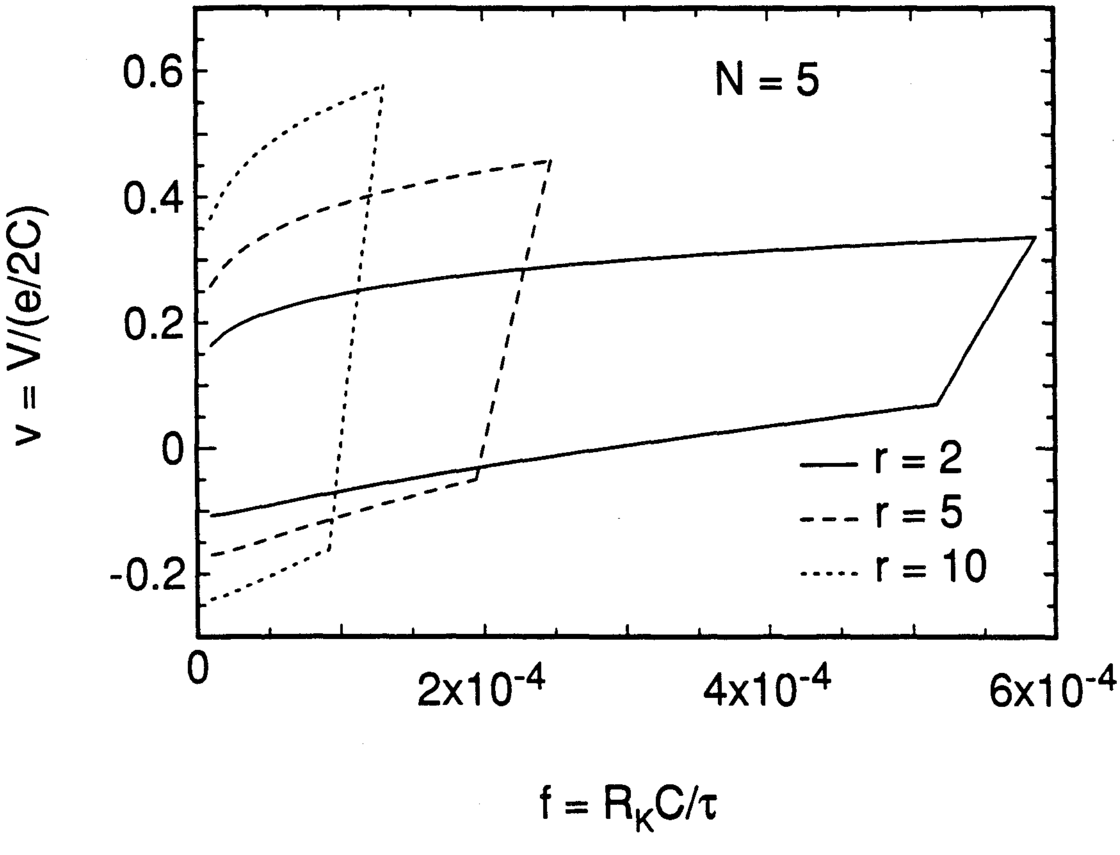

N = 5
r = 2
r = 5
r = 10
$v = V/(e/2C)$
0.6
0.4
0.2
0
-0.2
0
2×10^{-4}
4×10^{-4}
6×10^{-4}
$f = R_K C/\tau$

Fig. 6

4.1.2. Paper 5:

Nondivergent Calculation of Unwanted High-Order Tunneling Rates in Single-Electron Devices

Originally published as:

P. Lafarge and D. Esteve, Nondivergent calculations of unwanted high-order tunneling rates in single-electron devices, Phys. Rev. B **48**, 14 309 (1993).

Nondivergent calculation of unwanted high-order tunneling rates in single-electron devices

P. Lafarge and D. Esteve

Service de Physique de l'Etat Condensé, CEA Saclay
F-91191, Gif-sur-Yvette Cedex, France

Recently developed single electron devices are based on the control of electron tunneling across each tunnel junction of the circuit. However, unwanted higher order tunneling processes, referred to co-tunneling processes, modify this simple picture and reduce the accuracy of the devices. We calculate the co-tunneling rate in a linear array of tunnel junctions beyond the lowest order of perturbation theory by partially resumming the infinite perturbation expansion for the energy of a metastable state. We apply this calculation to the transition between two different tunneling regimes in various single electron circuits.

PACS numbers: 73.40.Gk, 73.40.Rw, 06.20.Hq.

I. Introduction.

In recent years the Coulomb blockade of tunneling has opened a new field of electronics referred as "Single Electronics" [1]. The first realisations are ultra sensitive electrometers [2] or charge transferring devices like turnstiles and pumps [3,4], the latter being a potential candidate for a DC current standard. A single electron device consists of small metallic islands separated by ultra small tunnel junctions with tunnel resistance R_t larger than the resistance quantum $R_K = h/e^2$. Control voltage sources are also applied to the islands through gate capacitors. Each island has a total capacitance C_{island} such that the electrostatic energy of a single excess electron $e^2/2C_{island}$ is larger than the characteristic energy $k_B T$ of the thermal fluctuations. Under these conditions, the number of electrons inside each island is a good quantum number with negligible thermal fluctuations [5]. Single electron tunneling through each junction can be forced or blocked by setting the control voltages to suitable values. However, higher order tunneling processes can directly transfer a single charge across two or more tunnel junctions and therefore compromise the proper operation of the device. This phenomenon, discovered by Averin and Odintsov [6] and called here co-tunneling, allows one electron charge to be transferred through k tunnel junctions although single electron tunneling across each junction is forbidden. The simplest circuit which exhibits co-tunneling is the single electron transistor which consists of two tunnel junctions in series. Co-tunneling is responsible for the leakage current which is observed when this circuit is biased inside the Coulomb gap [7,8]. For the sake of completeness, let us mention that a single junction biased by a current source should also exhibit a Coulomb gap [1]. In this case, subgap leakage can arise from imperfect current biasing [9] or from the transient electronic rearrangement during the tunneling process [10].

In a linear array of N tunnel junctions biased with a voltage source V, a co-tunneling event that transfers one electron across the whole array in the direction of increasing potential is always possible (see Fig. 1). In this paper we will consider the case where another tunneling transition of lower order becomes energetically allowed. A second tunneling process at the P^{th} order, with $P < N$, takes place in the array. Both transitions start from the same initial state and transfer one electron in the same direction but the final states are different. Because it is a perturbative approach, the original co-tunneling theory can only give an expression for the rate of the lowest order decay process which is energetically allowed in the array. In order to describe the behavior of the array when another tunneling transition can occur, we have derived a non-divergent expression of the quantum decay rate of the initial state by partially resumming the perturbation expansion. We will consider here three physical devices where the cross-over between two tunneling transitions with different orders currently appears : i) the single electron transistor consisting of two tunnel junctions in series, the simplest example of a linear array $(P=1,\ N=2)$. Our calculations are in good agreement with results obtained by others approaches [11,12,13], ii) the more general case of a linear array of N tunnel junctions, for which we aim at describing the effect of a finite transport voltage $(P=N-1,\ N>2)$, iii) the charge transferring devices like turnstiles and pumps. In that kind of circuits, every step of a transfer cycle is exposed to an unwanted co-tunneling event through the array $(P=1,\ N>2)$ and the accuracy of the transfer is affected by the rate of this leakage process.

II. The perturbative theory of co-tunneling.

Before examining the case of the single electron transistor, it is worthwhile to describe the general perturbative theory of co-tunneling. Following Averin and Odintsov [6], a co-tunneling transition that transfers one electron through a linear array of N tunnel junctions can be described by an arbitrary sequence of N single tunneling events $\{j_1,\ldots,j_k,\ldots,j_N\}$ where j_k denotes the position in the array of the k^{th} tunneling event. When a tunneling event occurs on the j_k^{th} junction, one electron leaves a filled state at ε_l below the Fermi level on one side of the junction and occupies an empty state at ε_r above the Fermi level on the other side. It creates an "electron-hole" excitation of energy $\varepsilon=\varepsilon_r+\varepsilon_l$. Note however that the electron and the hole are not here in the same piece of metal. In the following, such an excitation will be nicknamed a "tunnelon" of energy ε; the tunnelon density of states is $\rho(\varepsilon)=\lambda\varepsilon$. Within the tunnel hamiltonian approach, λ and the tunnel matrix element t are related to the junction tunnel resistance R_t by

$$\lambda t^2 = R_K/4\pi^2 R_t. \tag{1}$$

Since the final expression of the co-tunneling rates depend on the parameters λ and t of each junction only through the combination λt^2, we use, for the sake of clarity, the same λ for all junctions. The conservation of energy implies that the sum of the energies of all the tunnelons involved in a co-tunneling process must be equal to the electrostatic energy difference ΔE between the initial and the final state of the transition. Therefore, at $T=0$, only transitions bringing the system in a state of lower energy than the initial one are allowed. Let us assume that the energetically allowed transition with lowest order is a co-tunneling transition across M junctions. For a given sequence $\{j_1,\ldots,j_M\}$ of M single tunneling events there are $M-1$ intermediate virtual states $\{s_1,\ldots,s_{M-1}\}$. After k steps in the sequence $\{j_1,\ldots,j_M\}$ the system is in the state s_k and its energy is given by the sum of the electrostatic energy $E(s_k)$ relative to the energy of the initial state and the energies of the tunnelons created by previous tunneling events on junctions $j_1,\ldots,j_k$. The M co-tunneling rate Γ_M calculated by the perturbative theory of co-tunneling [5] is given by

$$\Gamma_M = \frac{2\pi}{\hbar}\left(\prod_{i=1}^{M}\frac{R_K}{4\pi^2 R_{t_i}}\right)\int_0^{+\infty} S^2(\varepsilon_1,\ldots,\varepsilon_M)\delta(\Delta E-\sum_{i=1}^{M}\varepsilon_i)\prod_{i=1}^{M}\varepsilon_i \mathrm{d}\varepsilon_i, \tag{2}$$

$$\text{where } S(\varepsilon_1,\ldots,\varepsilon_M) = \sum_{\{j_1,\ldots,j_M\}}\prod_{k=1}^{M-1}\left(E(s_k)+\sum_{i=1}^{k}\varepsilon_i\right)^{-1}.$$

This integral cannot be analytically calculated except for two junctions in series. In the limit where ΔE is much smaller than the intermediate state energies $E(s_k)$, a useful approximation is obtained by setting the tunnelons energies in the energy denominators to zero. In this approximation the M co-tunneling rate takes the form:

$$\Gamma'_M = \frac{2\pi}{\hbar}\left(\prod_{i=1}^{M}\frac{R_K}{4\pi^2 R_{t_i}}\right)S'^2\frac{\Delta E^{2M-1}}{(2M-1)!}, \tag{3}$$

$$\text{where } S' = \sum_{\{j_1,\ldots,j_M\}}\prod_{k=1}^{M-1}\left(E(s_k)\right)^{-1}.$$

We now consider a linear array of N tunnel junctions biased with a voltage source V. Gate voltages V_{g_i} are also applied to the $N-1$ islands of the array through gate capacitors C_{g_i}. In such a circuit a N^{th} order co-tunneling transition, hereafter called a N tunneling transition, is always possible. Even in the Coulomb blockade regime the transition can occur because the change of electrostatic energy due to the transfer of one electron across the whole array is $-eV$. If under the effect of the gate voltages one of the intermediate state energy $E(s_P)$ with $P<N$ vanishes, then a P tunneling transition becomes possible (see Fig. 1). The perturbative expression (2) can only be used to evaluate the rate of the lowest order transition i.e. a N tunneling rate if $E(s_P)>0$ or a P tunneling rate if $E(s_P)<0$. But the cross-over between N and P tunneling is not properly described. Moreover in the particular case $P=1$, the N tunneling rate diverges at the threshold, while the single tunneling rate is zero at the threshold.

III. Partial resummation of the perturbation expansion in the case of the single-electron transistor.

The simplest example of linear arrays that exhibits the cross-over between two tunneling transitions at different orders is the single electron transistor (Fig. 2). This device consists of two tunnel junctions in series of capacitances C_1 and C_2 and tunnel resistances R_{t_1} and R_{t_2} connected to a transport voltage source V. A gate voltage U is also capacitively coupled to the central electrode by a capacitor C_g. The state of the device is completely described by the number n of excess electrons on the central island and the number n_t of electrons having passed through the voltage source V. For a given state the energy of the whole system including the voltage sources is $E(n,n_t)=(ne-C_gU)^2/2C_\Sigma-(C_gU)^2/2C_\Sigma-n_teV$, where $C_\Sigma=C_1+C_2+C_g$. For

$0 < V < e/C_\Sigma$ and $0 < C_S U < e/4$, we can limit the state space to four states which we denote : (0), (1), (-1) and (0)*. The initial state (0) corresponds to $n = n_t = 0$. The states (1) and (-1) differ from the initial state (0) by a tunneling event on the first and the second junction respectively. The state (0)* differs from (0) by one electron having passed through the device. The energy of (0)* is $-eV$ and the energies of (1) and (-1) are equal to $E_1 = E(1,0)$ and $E_2 = E(-1,0)$ respectively. For $V < V_{th}$ where V_{th} is a threshold voltage dependent of the voltage U and the capacitances C_1, C_2 and C_g, E_1 and E_2 are positive and the tunneling of one electron across each junction is suppressed. Nevertheless, there is a finite current through the device due to the decay of (0) to (0)*. The co-tunneling transition $(0) \rightarrow (0)^*$ can take place through two channels : $(0) \rightarrow (1) \rightarrow (0)^*$ or $(0) \rightarrow (-1) \rightarrow (0)^*$ (Fig. 3). At $V = V_{th}$, one of the intermediate energies E_1 or E_2 vanishes. The co-tunneling rate calculated using Eq. (2) presents at the threshold a logarithmic divergence which can be regularised [11,12]. Above the threshold, electrons can be transferred by a sequence of allowed single tunneling transitions. The limiting single transition rate is proportional to E_1 or E_2 and therefore starts from zero. In order to properly obtain the cross-over between the co-tunneling and single tunneling regimes, we calculate directly the decay rate of the initial state (0) without specifying the final state. This decay rate is a good approximation of the tunneling rate across the whole array if the occupancy probability of the intermediate states (1) and (-1) is much smaller than 1. This condition corresponds to $0 < V \leq 1.5 V_{th}$. At higher voltage, one can use the simplified master equation approach [14] which only considers single tunneling events on each junction and which becomes sufficiently accurate.

To express the quantum decay rate of the (0) state we use the formalism of the energy displacement operator $R(z)$ [15]. The decay rate of the initial state $|i\rangle$ is related to $R(z)$ by

$$\Gamma = -\frac{2}{\hbar} \mathrm{Im}\left[PR(E_i + i\eta)P\right], \tag{4}$$

where $P = |i\rangle\langle i|$, E_i is the energy of the initial state and $\eta \rightarrow 0^+$. The perturbative expansion of $R(z)$ is

$$R(z) = H_T + H_T \frac{Q}{z - H_0} H_T + H_T \frac{Q}{z - H_0} H_T \frac{Q}{z - H_0} H_T + \ldots, \tag{5}$$

where $Q = 1 - P$, H_T is the tunnel hamiltonian and H_0 is the sum of the electrostatic hamiltonian of the whole circuit and of the tunnelon kinetic energy hamiltonian. Each term in the PRP series corresponds to a path in the state space and can be represented by a diagram (see Fig. 4). The construction rules of such a diagram are as follows : an upward curved line represents a "tunnelon" excitation on the first junction and a downward curved line a "tunnelon" on the second junction. Each vertex corresponds to a transition between two different states of the system by absorption or emission of a "tunnelon". In the calculation associated with the diagram, each section i.e. portion of a diagram contained between two dotted lines contributes by an energy denominator and each vertex by a tunnel matrix element. Finally there is an integration over all the "tunnelon" energies $\varepsilon_1,\ldots,\varepsilon_i$ of the diagram with densities of states $\lambda\varepsilon_1,\ldots,\lambda\varepsilon_i$. Only paths starting from the (0) state and coming back to (0) solely at the end give non vanishing terms in the series (5). Each diagram containing one tunnelon (Fig. 5(a)) gives, at $V > V_{th}$, the single tunneling rate through the corresponding junction of the single electron transistor. The set of diagrams containing two tunnelons depicted in Fig. 5(b) give, at $V < V_{th}$, the perturbative expression of the co-tunneling rate. An horizontal segment which is located under or over one tunnelon arc corresponds respectively to the (1) state or the (-1) state (see Fig. 4). In the upper left diagram of Fig. 5(b), a segment (1) appears twice under the tunnelon denoted ε_1. The same situation is reproduced in the upper right diagram of Fig. 5(b) with a segment (-1) over the tunnelon ε_2. In these two diagrams, the horizontal segments corresponding to the (-1) or (1) state are the origin of the co-tunneling rate divergence because the corresponding sections contribute by the square of energy denominators which vanish at the threshold. More generally, for a given number of tunnelons the divergence order of a diagram is proportional to the number of (-1) or (1) segments located under the same tunnelon arc. In order to remove the divergence we will now proceed to a partial resummation of the perturbation series (5) by taking into account the most diverging diagrams at each order in H_T. They are obtained when all the diverging segments belong to the same tunnelon (Fig. 6(a),(b)). However, we want to include in our resummation the four diagrams depicted in Fig. 5(b) in order to recover the perturbative expression of the co-tunneling rate in the limit of small transport voltages. Hence it is necessary to keep also the diagrams with two different possible tunnelons for the (-1) and (1) segments (Fig. 6(c),(d)). One can classify these diagrams in four different types analogous to the four diagrams of Fig. 5(b). The integral corresponding to the first type of diagrams (Fig. 6(a)) is

$$I_k = \int_0^{+\infty} \frac{\lambda t_1^2 \varepsilon_1}{z-(E_1+\varepsilon_1)} \left[\int_0^{+\infty} \frac{\lambda t_2^2 \varepsilon_2 \mathrm{d}\varepsilon_2}{\big(z-(E_1+\varepsilon_1)\big)\big(z-(-eV+\varepsilon_1+\varepsilon_2)\big)} \right]^k \mathrm{d}\varepsilon_1. \qquad (6)$$

With $z = 0 + i\eta$ the resummation yields

$$\sum_{k=0}^{+\infty} I_k = \int_0^{eV} \frac{\lambda t_1^2 \varepsilon_1 \mathrm{d}\varepsilon_1}{-(E_1+\varepsilon_1) + i\pi\lambda t_2^2 (eV - \varepsilon_1)}. \qquad (7)$$

This integral can be calculated explicitly. After taking the imaginary part, we obtain the following contribution to the decay rate:

$$
\begin{aligned}
f(E_1,eV) = {} & \frac{2\pi}{\hbar}\lambda^2 t_1^2 t_2^2\left[-eV + \frac{2E_1+eV}{2}\ln\frac{(eV+E_1)^2}{E_1^2+\left(\pi\lambda t_2^2 eV\right)^2}\right] \\
& -\frac{2}{\hbar}\lambda t_1^2 E_1\left[\pi/2 - \arctan\frac{E_1}{\pi\lambda t_2^2 eV}\right] + O\left(\lambda^2 t_1^2 t_2^2\right).
\end{aligned} \tag{8}
$$

The contribution $f(E_2,eV)$ of the second type of diagrams (Fig. 6(b)) has the same form with E_1 replaced by E_2, t_1 by t_2 and t_2 by t_1. In the third and fourth types of diagrams there are two possible tunnelons for the (-1) and (1) segments. The integrals and the resummation are performed similarly to the previous case. Since the third and the fourth types of diagram (Fig. 6(c),(d)) are symmetric, they give the same contribution to the decay rate:

$$
\begin{aligned}
g(E_1,E_2,eV) = {} & \frac{2\pi}{\hbar}\lambda^2 t_1^2 t_2^2\left[eV - \frac{(E_1+eV)E_1}{2(E_1+E_2+eV)}\ln\frac{(E_1+eV)^2}{E_1^2+\left(\pi\lambda t_2^2 eV\right)^2}\right. \\
& \left. -\frac{(E_2+eV)E_2}{2(E_1+E_2+eV)}\ln\frac{(E_2+eV)^2}{E_2^2+\left(\pi\lambda t_1^2 eV\right)^2}\right] + O\left(\lambda^2 t_1^2 t_1^2\right).
\end{aligned} \tag{9}
$$

Summing the contributions of the four types of diagrams and using Eq. (1), the final expression of the decay rate $\Gamma = f(E_1,eV) + f(E_2,eV) + 2g(E_1,E_2,eV)$ takes the form:

$$
\begin{aligned}
\Gamma = {} & \frac{2\pi}{\hbar}\frac{R_K^2}{\left(4\pi^2\right)^2 R_{t_1}R_{t_2}}\left[\frac{eV}{2} + \frac{E_1E_2}{E_1+E_2+eV}\right]\left[\sum_{i=1}^{2}\ln\frac{(eV+E_i)^2}{E_i^2+(\alpha_i eV)^2}\right] \\
& -\frac{2\pi}{\hbar}\sum_{i=1}^{2}\frac{R_K E_i}{4\pi^2 R_{t_i}}\left[\frac{1}{2} - \frac{1}{\pi}\arctan\frac{E_i}{\alpha_i eV}\right],
\end{aligned} \tag{10}
$$

where $\alpha_i = R_K/4\pi R_{t_j}$, $j \neq i$. This formula provides an expression of the I-V characteristic of the single electron transistor at $T = 0$. In the limit $\alpha_i \to 0$, Eq. (10) reproduces the perturbative expression of the co-tunneling rate across two junctions in series calculated by Averin and Odintsov [6]. One can also treat second order tunneling in any linear array of tunnel junctions if one replaces eV in Eq. (10) by the correct expression for the energy available in the transition. Expression (10) has a form similar to the co-tunneling rate expression of Korotkov et al. [11]. The two formulas, although analytically different, give the same result except in the vicinity of the threshold voltage V_{th}. Recently, Pasquier et al. [13] have explained their experimental results on a 2 DEG electrometer by a temperature dependent co-tunneling rate which agrees with Eq. (10) in the limit $T = 0$.

IV. The general case of a cross-over between N tunneling and $(N-1)$ tunneling in a general linear array.

More generally, the cross-over between N and $(N-1)$ tunneling in larger arrays than the two junctions electrometer can be described by similar non-divergent rate calculation. We now consider a linear array of N tunnel junctions with negligible gate capacitances biased with a voltage source V (Fig. 7). In the case of N identical junctions with capacitance C the set of intermediate energies $(E_1,\dots,E_{N-1})$ is the same for all the sequences. For $V < e/2C$, the N tunneling is the only allowed transition. At $V = e/2C$, E_{N-1} is equal to zero and a $(N-1)$ tunneling transition becomes possible. A N tunneling transition is described at the lowest order in perturbation by $N!^2$ different diagrams containing N tunnelons. If $V << e/C$, the energies of the $N-2$ first intermediate states are always positive and larger than eV. Since the sum of the energies of the tunnelons involved in a co-tunneling transition is equal to eV, we will neglect them in the energy denominators related to the configuration states of the array except for the $(N-1)^{th}$ state and the final one. We can then distinguish only two types of diagrams (Fig. 8). There are $N!(N-1)!$ diagrams of the first type and $N!(N-1)!(N-1)$ diagrams of the second type. For the first type (Fig. 8(a)) the resummation and the integral over ε_N and ε_{N-1} is performed in the same manner as in the first two cases of the single electron transistor. Then one gets the contribution γ_a:

$$\gamma_a = \int\cdots\int_0^{+\infty}\left(\prod_{i=1}^{N-2}\frac{\lambda t^2}{E_i^2}\right) f(E_{N-1}+\sigma, eV-\sigma)\varepsilon_1\dots\varepsilon_{N-2}\mathrm{d}\varepsilon_1\dots\mathrm{d}\varepsilon_{N-2}, \tag{11}$$

where $\sigma = \sum_{i=1}^{N-2}\varepsilon_i$ and where f is the function defined in expression (8).

For the second type of diagrams (Fig. 8(b)) which is similar to the third and fourth types of diagrams in the single electron transistor case, the contribution γ_b is

$$\gamma_b = \int\cdots\int_0^{+\infty}\left(\prod_{i=1}^{N-2}\frac{\lambda t^2}{E_i^2}\right) g(E_{N-1}+\sigma, E_{N-1}+\sigma, eV-\sigma)\varepsilon_1\dots\varepsilon_{N-2}\mathrm{d}\varepsilon_1\dots\mathrm{d}\varepsilon_{N-2}, \tag{12}$$

where g is the function defined in expression (9). The decay rate of the initial state $\Gamma_N = \gamma_a + \gamma_b$ is written:

$$\Gamma_N = \left(\frac{R_K}{4\pi^2 R_t}\right)^{N-2} N!(N-1)!\prod_{i=1}^{N-2} E_i^{-2} F(E_{N-1}, eV), \tag{13}$$

where

$$F(E_{N-1}, eV) = \int_0^{eV}\frac{\sigma^{2N-5}}{(2N-5)!}\left[f(E_{N-1}+\sigma, eV-\sigma) + (N-1)g(E_{N-1}+\sigma, E_{N-1}+\sigma, eV-\sigma)\right]\mathrm{d}\sigma.$$

Eq. (13) allows us to describe any kind of cross-over between two tunneling regimes in a linear array of N tunnel junctions under the effect of a finite transport voltage. Thus one can estimate the I-V curve of the array from the N tunneling regime until the single tunneling regime. In the simplest case $N = 3$, a quantitatively more accurate calculation can be done if one keeps in the energy denominators of expressions (11) and (12) the contribution of the first tunnelon energy ε_1. One obtains the following expression of the 3 tunneling rate:

$$\Gamma_3 = \left(\frac{R_K}{4\pi^2 R_t}\right) 12 K(E_2, eV), \tag{14}$$

where $K(E_2, eV) = \int_0^{eV} \frac{f(E_2+\varepsilon_1, eV-\varepsilon_1) + 2g(E_2+\varepsilon_1, E_2+\varepsilon_1, eV-\varepsilon_1)}{(E_1+\varepsilon_1)^2} \varepsilon_1 d\varepsilon_1$.

This formula Γ_3 correctly describes the 3 tunneling regime and the 2 tunneling regime until the vicinity of the single tunneling threshold. Another expression is necessary to describe the cross-over between 2 tunneling and single tunneling. The 2 tunneling rate Γ_2 is evaluated using Eq. (10) with the correct expression of the available energy difference in place of eV. Because there are three different ways to associate two junctions of the circuit, the tunneling rate across the whole array of three junctions near the single tunneling threshold $CV/e = 1$ is given by $3\Gamma_2$. Results are shown in Fig. 9 for a particular value of the tunnel resistance $R_{t_1} = R_{t_2} = 10 R_K$. For $1/2 < CV/e < 1$ the matching between Γ_3 and $3\Gamma_2$ is sufficiently good to obtain a continuous estimate of the tunneling rate across three junctions over the Coulomb blockade range. Calculation of the tunneling rate across three junctions are shown in Fig. 10 for several values of the tunnel resistance. The cross-over between successive tunneling regimes gets smoother when the tunnel resistance R_t decreases and is hardly noticeable when $R_t < 2R_K$.

V. The cross-over between N tunneling and single tunneling.

The last application of the non-divergent co-tunneling rate calculations we shall consider deals with the accuracy of single electron pumps [4]. A pump consists of a linear array of N identical tunnel junctions of capacitance C where each island $\{k\}$ of the array is connected through a gate capacitor to a time dependent voltage source U_k (Fig. 11). Each gate capacitance is equal to C_g with $C_g << C$. The controlled transfer of one electron across the device is achieved by successively applying to the islands triangular voltage pulses as shown in Fig. 12. These pulses induce a sequence of single tunneling events on the successive junctions of the array : one electron charge follows the pulse propagation through the array. However, an unwanted N tunneling transition is possible at any stage of the transfer cycle. All steps of a transfer cycle in the N pump are equivalent [16] but, for simplicity, let us assume the pump is placed at the beginning of a cycle. There is no excess electron on any island of the array and at small transport voltages ($V << e/2C$) the N tunneling across the array is the only tunneling transition allowed. As in the single electron transistor, the perturbative expression of this N tunneling rate diverges when the energy of the first intermediate state of a co-tunneling sequence becomes equal to zero. This is exactly what happens when, under the effect of the first gate voltage U_1, the pump reaches the threshold of the first step in the cycle. This step will be a single tunneling event across the first junction which puts one excess electron on the first island of the array in the sense of the transfer (Fig. 11). The perturbation theory cannot therefore be used directly to calculate the pump error rate. Using the partial resummation technique we can remove the divergence of the N tunneling rate. The general form of the diverging diagrams is represented in Fig. 13. Introducing the same approximation as in the case of the N linear array of tunnel junctions we neglect the tunnelons energies in the energy denominators except for the first intermediate state. After the resummation and the integration over the tunnelons energies $\varepsilon_2,\ldots,\varepsilon_N$, we obtain the following upper bound of the N tunneling rate γ_{err}:

$$\gamma_{err} = \frac{N!^2}{(2N-3)!}\frac{2\pi}{\hbar}\left(\frac{R_K}{4\pi^2 R_t}\right)^N \left(\prod_{i=2}^{N-1} E_i^{-2}\right)\int_0^{eV} \frac{\varepsilon_1 (eV-\varepsilon_1)^{2N-3}\,\mathrm{d}\varepsilon_1}{(E_1+\varepsilon_1)^2 + \alpha_N^2 (eV-\varepsilon_1)^{4N-6}}, \tag{15}$$

where $\alpha_N = \dfrac{\pi}{(2N-3)!}\left(\dfrac{R_K}{4\pi^2 R_t}\right)^{N-1} \displaystyle\prod_{i=2}^{N-1} E_i^{-2}$.

Using this expression, we have calculated in the particular case of the five junctions pump an upper bound of the N tunneling leakage during a transfer cycle. We have found that this contribution is negligible in the particular parameter range for which metrological accuracy is achievable [17,18,16].

VI. Conclusion.

In conclusion we have shown that in a linear array of tunnel junctions the problem of the cross-over between two tunneling regimes at different orders can be solved by a partial resummation of the perturbation expansion. In the case of the single electron transistor, we have obtained an analytical expression of the co-tunneling rate that remains finite at the conduction threshold. More generally, this approach can be used to calculate the I-V characteristic of an array. Finally, non-divergent calculation of the co-tunneling rate provides a rigorous upper bound of the N tunneling leakage through charge transferring devices like the N junctions pump.

Acknowledgements

We acknowledge fruitful discussions with M. H. Devoret, H. Grabert, P. Joyez, J. M. Martinis and H. Pothier.

REFERENCES

[1] D. V. Averin and K. K. Likharev, in *Mesoscopic Phenomena in Solids*, ed. by B. Al'tshuler, P. Lee, and R. Webb (Elsevier, Amsterdam, 1991), Chap. 6 ; *Single Charge Tunneling*, ed. by H. Grabert and M. H. Devoret, (Plenum, New York, 1992).

[2] T. A. Fulton and G. J. Dolan, Phys. Rev. Lett. **59**, 109 (1987).

[3] L. J. Geerligs, V. F. Anderegg, P. A. M. Holweg, J. E. Mooij, H. Pothier, D. Esteve, C. Urbina and M. H. Devoret, Phys. Rev. Lett. **64**, 2691 (1990).

[4] H. Pothier, P. Lafarge, D. Esteve, C. Urbina and M. H. Devoret, Europhys. Lett. **17**, 249 (1992).

[5] K. A. Matveev, Zh. Eksp. Teor. Fiz. **99**, 1598 (1991) [Sov. Phys. JETP **72**, 892 (1991)].

[6] D. V. Averin and A. A. Odintsov, Phys. Lett. **A 149**, 251 (1989).

[7] L. J. Geerligs, D. V. Averin and J. E. Mooij, Phys. Rev. Lett. **65**, 3037 (1990).

[8] T. M. Eiles, G. Zimmerli, H. D. Jensen and J. M. Martinis, Phys. Rev. Lett. **69**, 148 (1992).

[9] M. H. Devoret, D. Esteve, H. Grabert, G.-L. Ingold, H. Pothier, and C. Urbina, Phys. Rev. Lett. **64**, 1824 (1990).

[10] M. Ueda and F. Guinea, Z. Phys. B **85**, 413 (1991).

[11] A. N. Korotkov, D.V. Averin, K.K. Likharev and S. A. Vasenko, in *Single-Electron Tunneling and Mesoscopic Devices*, ed. by H. Koch and H. Lübbig (Springer, Berlin, 1992).

[12] Yu. V. Nazarov, J. Low. Temp. Phys. **90**, 77 (1993); W. Krech and A. Hädicke, Int. J. Mod. Phys. B **7**, 2201 (1993).

[13] C. Pasquier, U. Meirav, F. I. B. Williams, D. C. Glattli, Y. Jin and B. Etienne, Phys. Rev. Lett. **70**, 69 (1993).

[14] I. O. Kulik and R. I. Shekter, Zh. Eksp. Teor. Fiz. **68**, 623 (1975) [Sov. Phys. JETP **41**, 308 (1975)].

[15] C. Cohen-Tannoudji, J. Dupont-Roc and G. Grynberg, *Atom-photon interactions. Basic processes and applications*, (Wiley, New York, 1992), chap. 3.

[16] H. Pothier, P. Lafarge, D. Esteve, C. Urbina and M. H. Devoret, to be published in IEEE Trans. on Instrum. and Meas.

[17] H. D. Jensen and J. M. Martinis, Phys. Rev. B **46**, 13407 (1992).

[18] D. V. Averin, A. A. Odintsov and S.V. Vyshenskii, J. Appl. Phys. **73**, 1297 (1993).

FIGURE CAPTIONS

Fig. 1. (a) Schematic of a linear array of N tunnel junctions. The rectangular symbols represent ultrasmall tunnel junctions. (b) Energy states of the circuit when the electrostatic energy of the P^{th} intermediate state of a N^{th} order co-tunneling transition is equal to the initial state energy. n_t is the number of electrons which have passed through the array. The arrows indicate co-tunneling events through N or P junctions.

Fig. 2. Circuit diagram of the single-electron transistor which consists of two small tunnel junctions of capacitances C_1 and C_2 biased with a voltage source V. A control voltage source U is capacitively coupled to the island formed between the junctions.

Fig. 3. Energy states of the single-electron transistor when the circuit is in the Coulomb blockade regime. The arrows indicate co-tunneling transitions. A co-tunneling transition between the initial (0) and the final state (0)* can take place through two channels (a) and (b).

Fig. 4. General form of a diagram. An upward (downward) arc represents a tunnelon excitation on the first (second) junction of the single-electron transistor. The solid dots correspond to the absorption or the emission of a tunnelon. Each section of the diagram contained between two dashed lines corresponds to a given state of the device.

Fig. 5. (a) Lowest order diagrams in the perturbation expansion (5) with one tunnelon arc. (b) Two tunnelons diagrams which give the perturbation expression of the co-tunneling rate across the single-electron transistor.

Fig. 6. Diagrams that are taken into account in the partial resummation of the perturbation expansion (5).

Fig. 7. Co-tunneling transition in real space (a) and in state space (b) for a linear array of N identical tunnel junctions with negligible gate capacitances biased by a voltage source V when the energy of the $(N-1)^{th}$ intermediate state of a N tunneling transition is equal to the initial state energy.

Fig. 8. Classes of diagrams for a linear array of N junctions which extend the classification made for the single-electron transistor. (a) Diagrams analogous to diagrams of Fig. 6(a) and

Fig. 6(b). (b) Diagrams analogous to diagrams of Fig. 6(c) and Fig. 6(d). The arcs starting from the horizontal line represent the emission of tunnelons labeled $\varepsilon_1,\ldots,\varepsilon_{N-1}$. The arcs ending on the horizontal line represent the absorption of the previous tunnelons $\varepsilon_1,\ldots,\varepsilon_{N-1}$ in an arbitrary order.

Fig. 9. Tunneling rates across a linear array of three junctions as a function of the transport voltage V. Solid line are Γ_3 (Eq. (14)) for $0 < CV/e < 1$ and $3\Gamma_2$ calculated using eq. (10) with the correct expression of the energy difference available instead of eV. Dashed lines are the divergent tunneling rates across three, two and one junctions obtained by eq. (3) when one retain only electrostatic energies in the energy denominators. All the curves are calculated for $R_t = 10R_K$.

Fig. 10. Tunneling rates across a linear array of three junctions as a function of the transport voltage with $R_t = 2$, 5 and $10 \times R_K$ from the upper to the lower curve. The curves are Γ_3 for $CV/e < 0.8$ and $3\Gamma_2$ for $CV/e > 0.8$ where Γ_3 and Γ_2 are calculated in the same way as in Fig. 8.

Fig. 11. (a) Circuit diagram of the N junctions pump. (b) Energy states of the array at the cross-over between single tunneling across the first junction and N tunneling across the whole array.

Fig. 12. Evolution of the gate voltages in the N pump during a transfer cycle of one electron charge. The amplitude of the voltage pulse is adjusted to transfer only one electron across each junction of the array.

Fig. 13. Diverging diagrams involved in the resummation of the perturbation series in the case of the cross-over between N tunneling and single tunneling in the N junctions pump.

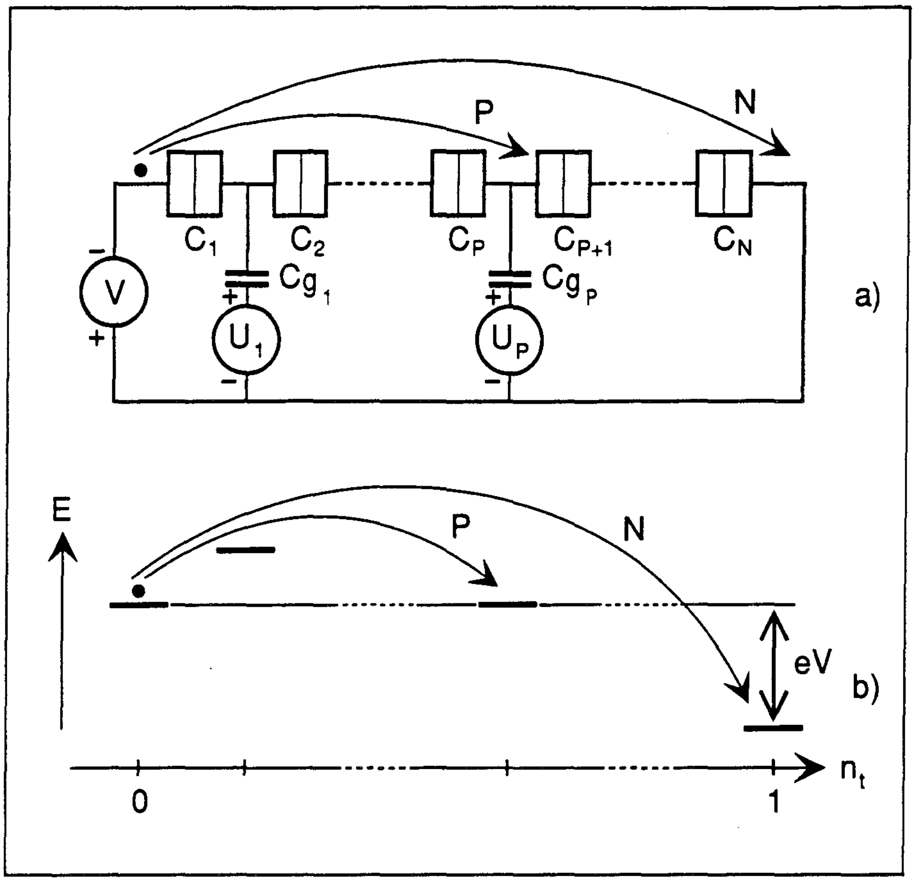
P
N
C1
C2
CP
CP+1
CN
V
Cg1
U1
CgP
UP
a)
E
P
N
eV
b)
nt
0
1

Fig. 1

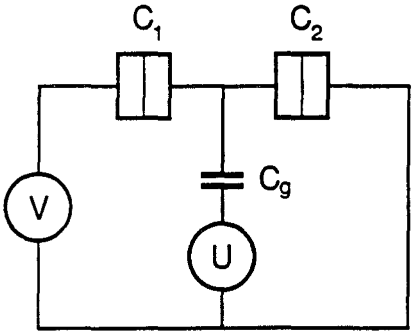

Fig. 2

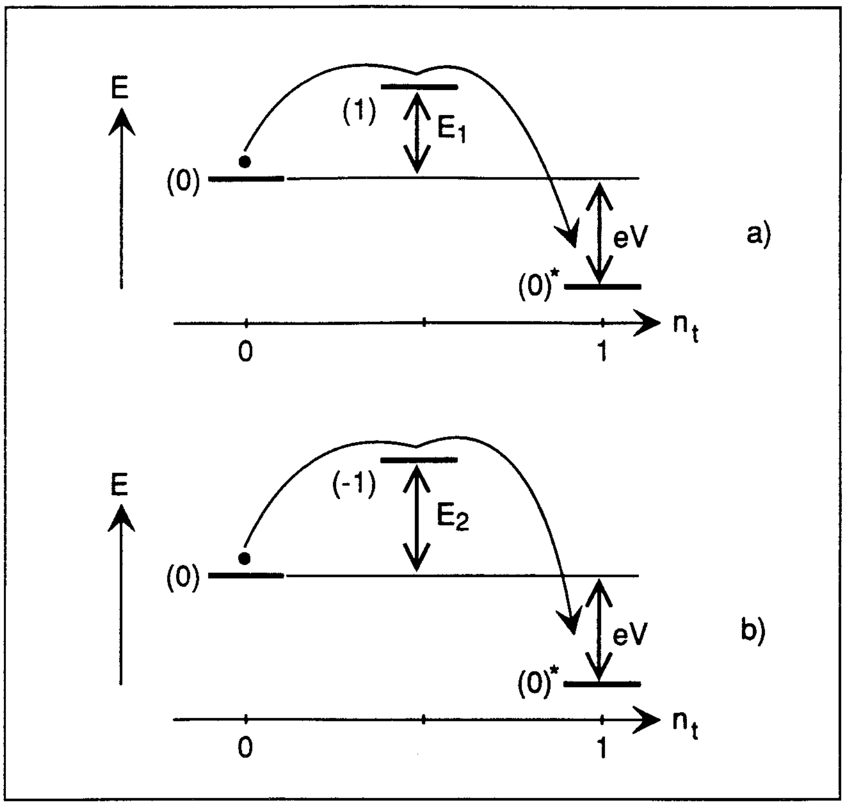
E
(1)
E_1
(0)
eV
a)
$(0)^*$
0
1
n_t
E
(-1)
E_2
(0)
eV
b)
$(0)^*$
0
1
n_t

Fig. 3

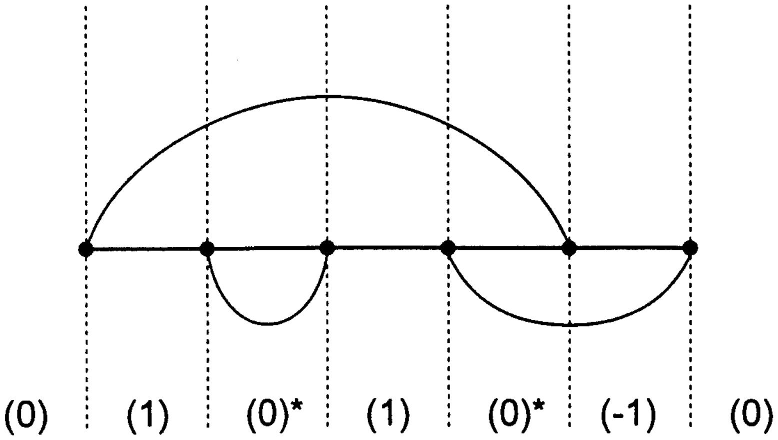

Fig. 4

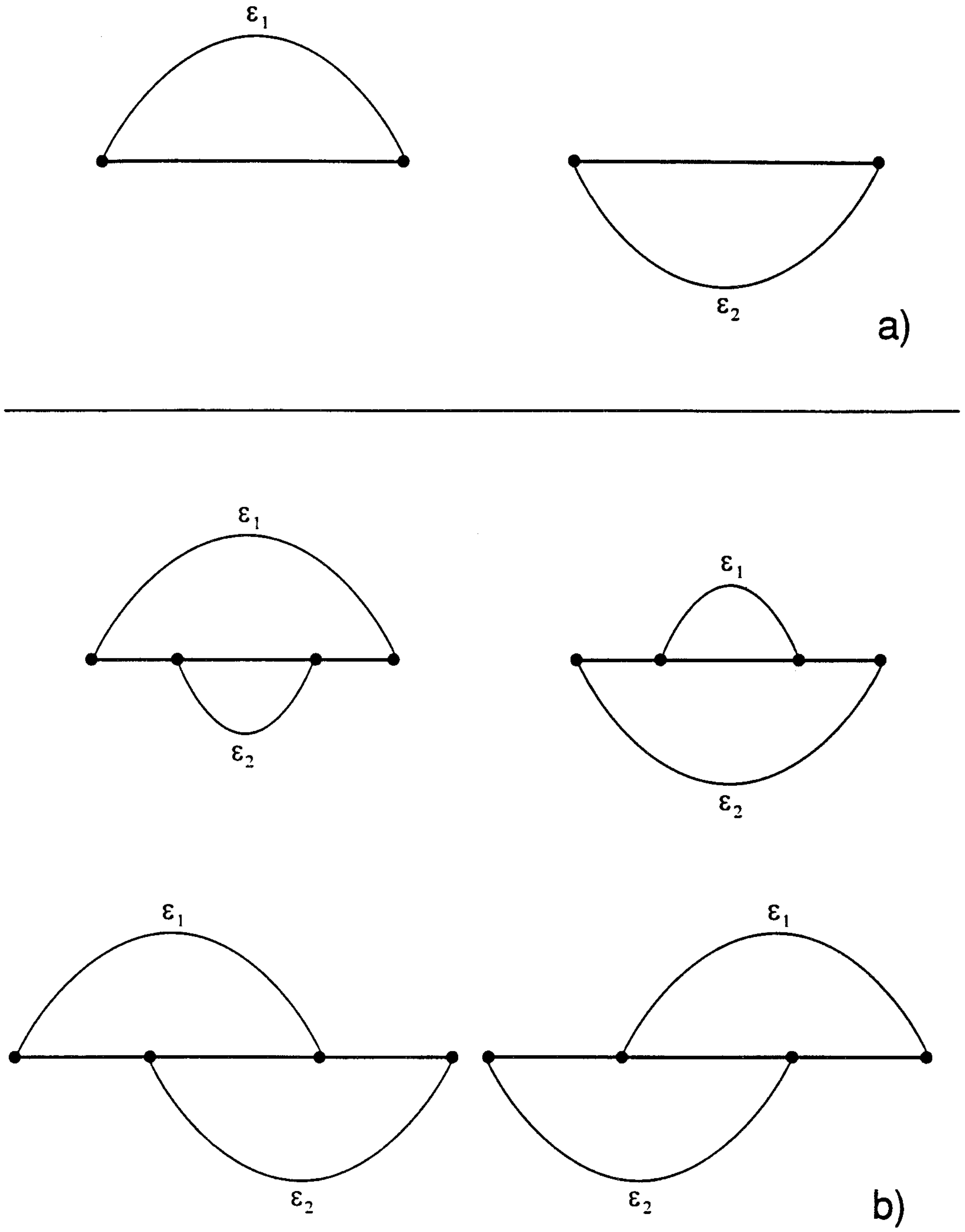
ε_1
ε_2
a)
ε_1
ε_2
ε_1
ε_2
ε_1
ε_2
ε_1
ε_2
b)

Fig. 5

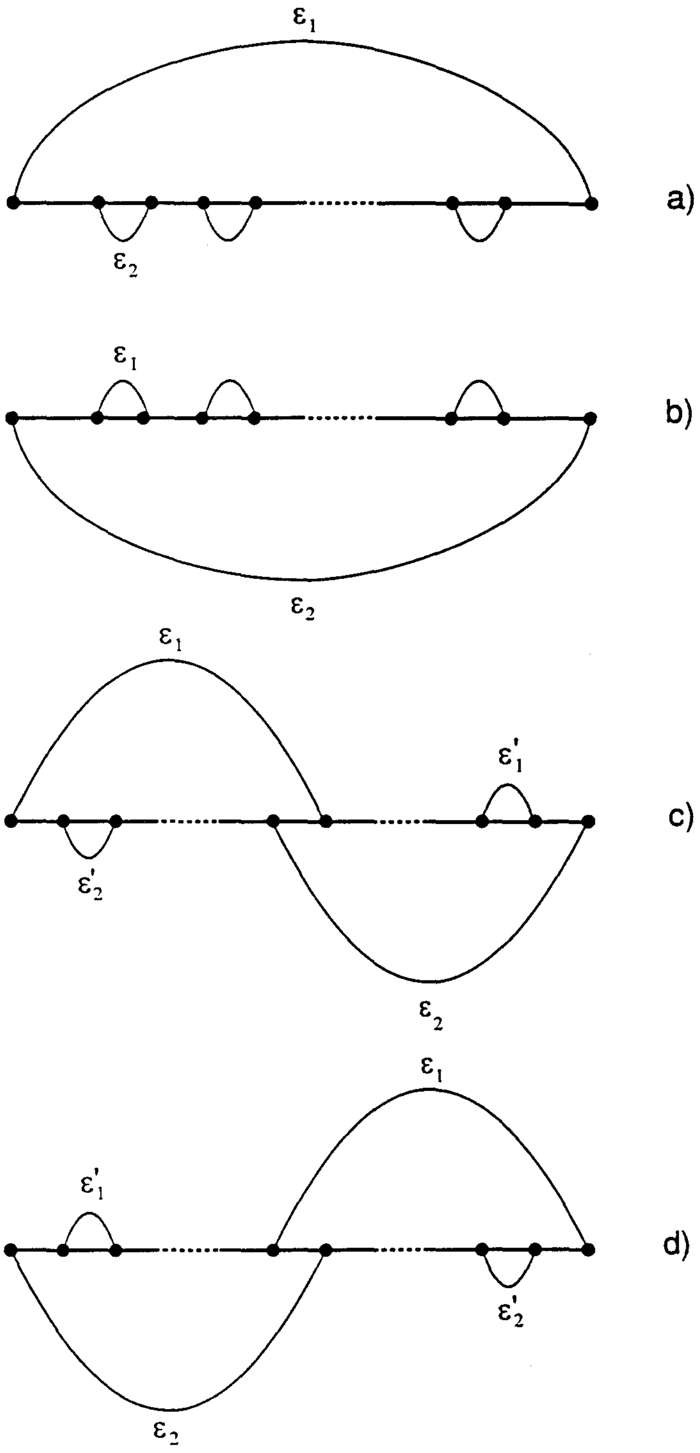
ε1
ε2
a)
ε1
ε2
b)
ε1
ε'1
ε'2
ε2
c)
ε1
ε'1
ε'2
ε2
d)

Fig. 6

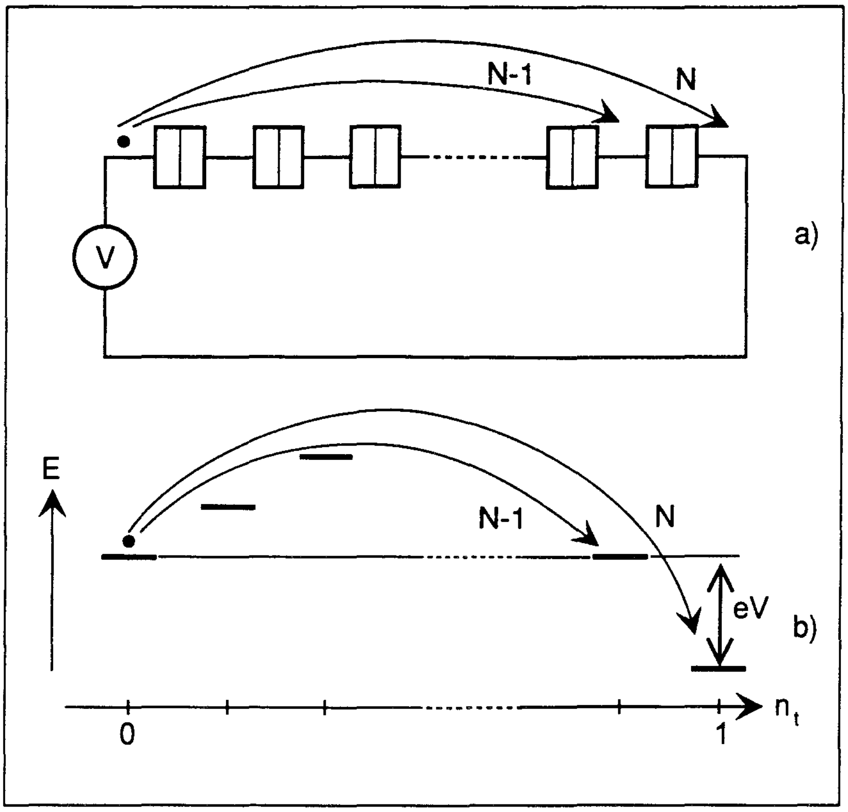
N-1
N
V
a)
E
N-1
N
eV
b)
0
1
n_t

Fig. 7

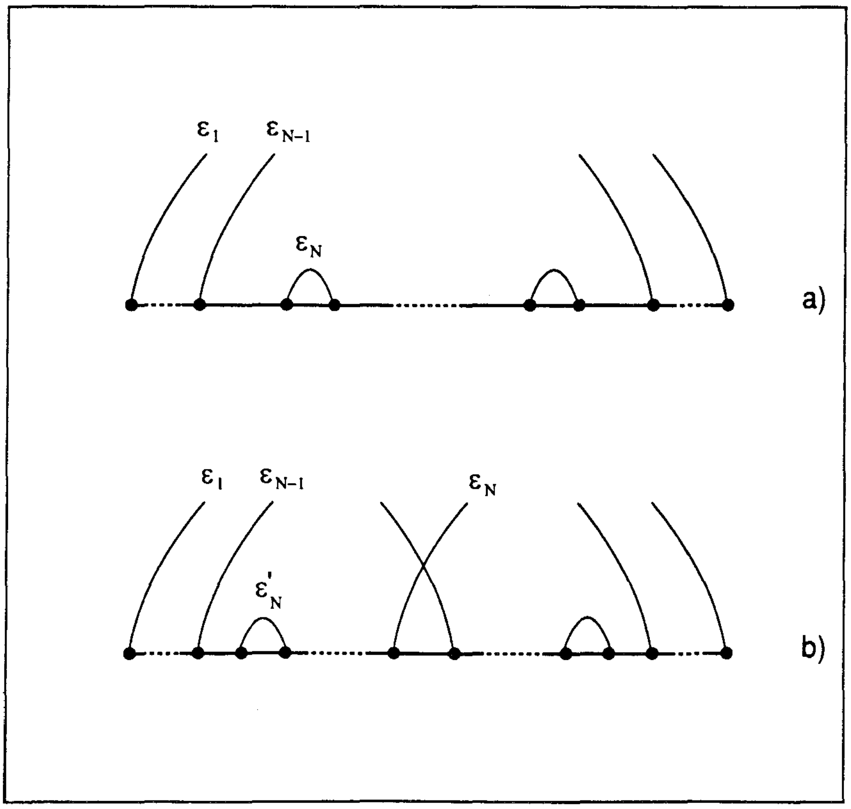
ε_1
ε_{N-1}
ε_N
a)
ε_1
ε_{N-1}
ε_N
ε'_N
b)

Fig. 8

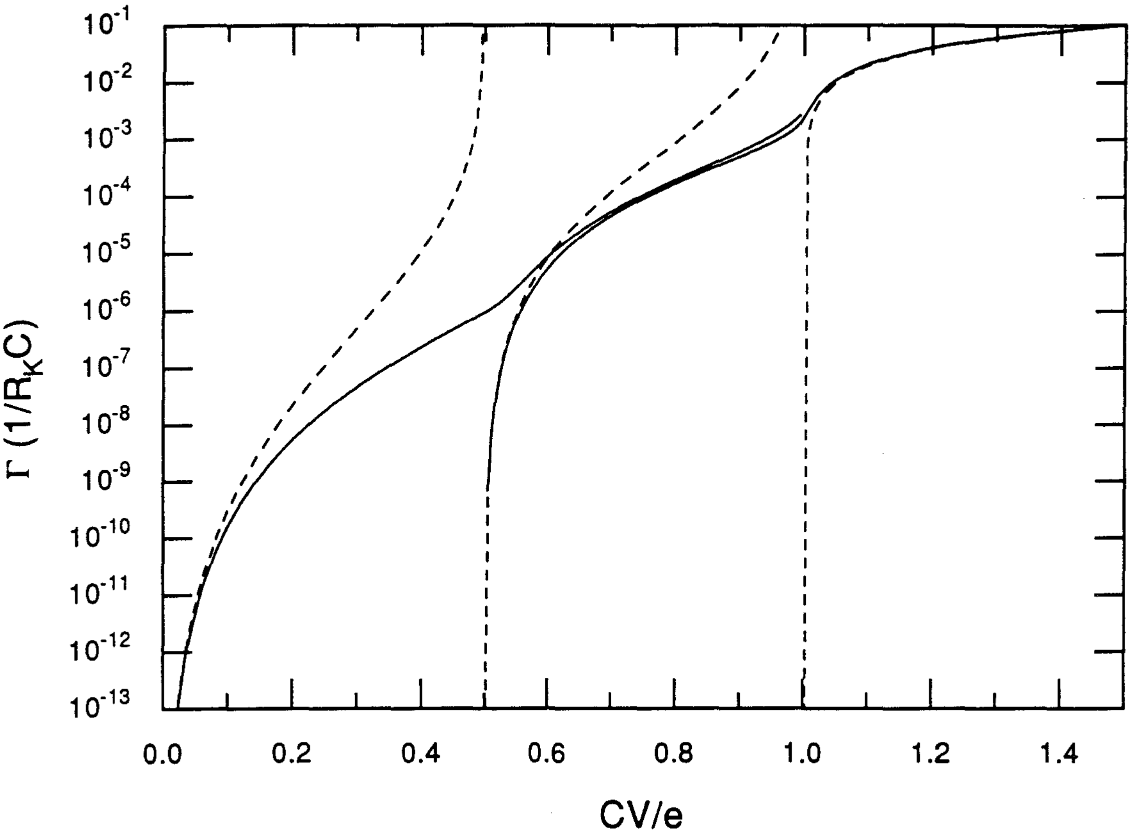

Γ (1/R_K C)
10^-1
10^-2
10^-3
10^-4
10^-5
10^-6
10^-7
10^-8
10^-9
10^-10
10^-11
10^-12
10^-13
0.0
0.2
0.4
0.6
0.8
1.0
1.2
1.4
CV/e

Fig. 9

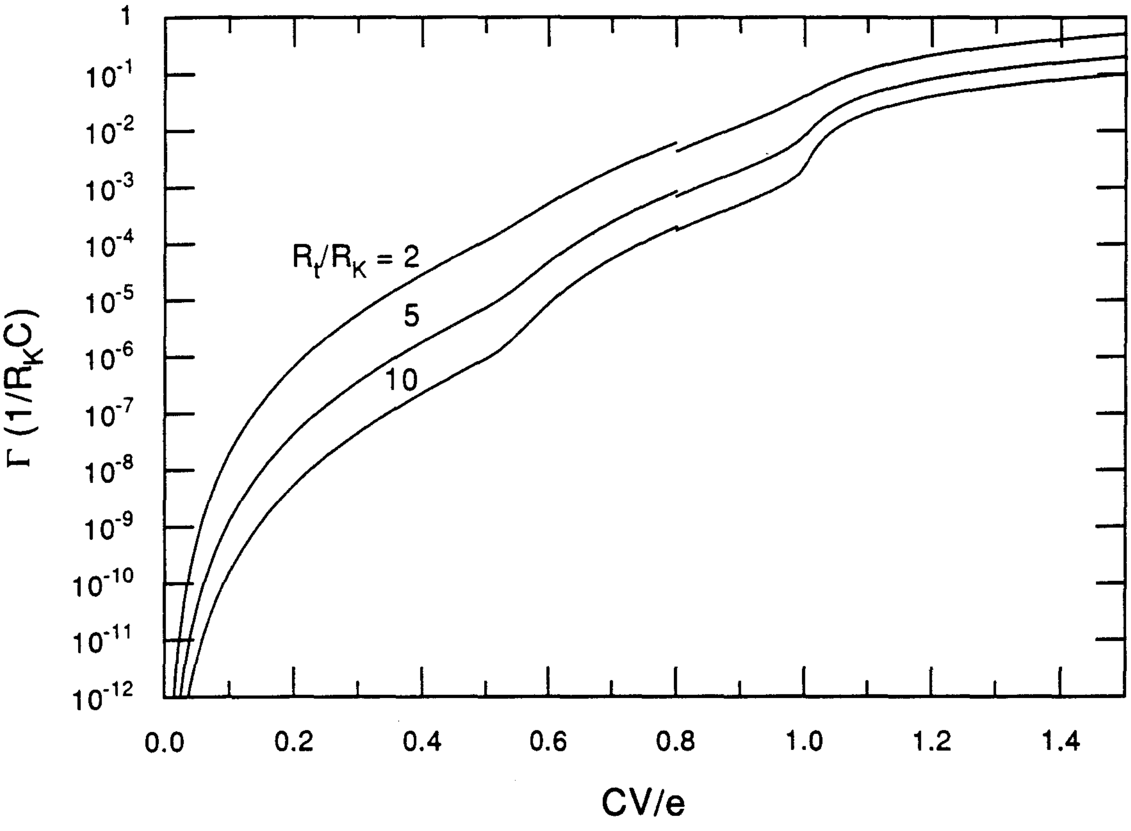

Γ (1/R_K C)
1
10^-1
10^-2
10^-3
10^-4
10^-5
10^-6
10^-7
10^-8
10^-9
10^-10
10^-11
10^-12
R_t/R_K = 2
5
10
0.0
0.2
0.4
0.6
0.8
1.0
1.2
1.4
CV/e

Fig. 10

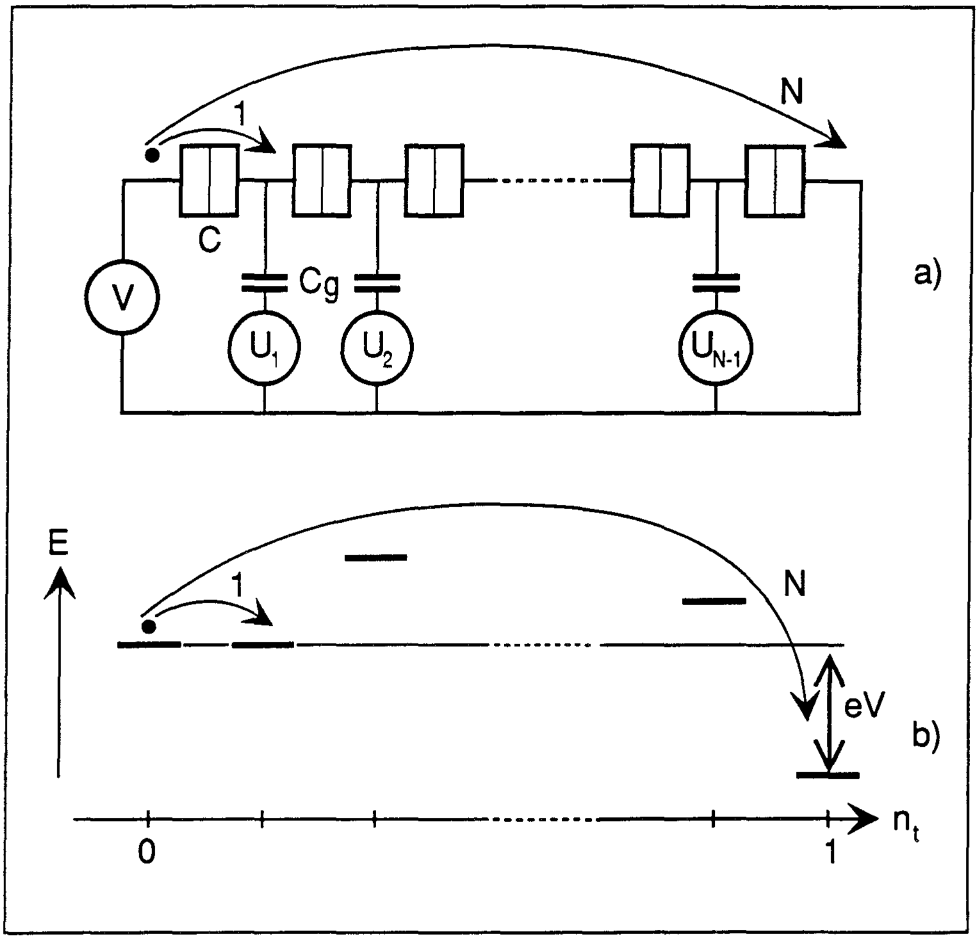
N
1
C
Cg
V
U_1
U_2
U_N-1
a)
E
1
N
eV
b)
0
1
n_t

Fig. 11

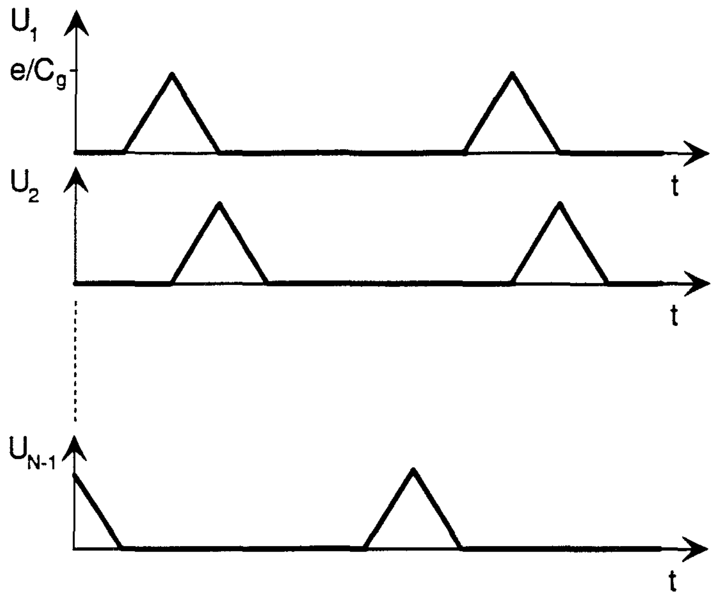

Fig. 12

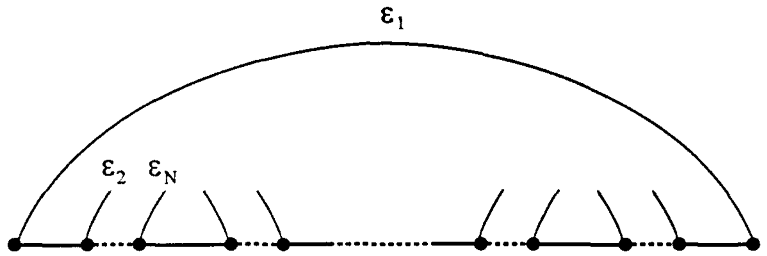
ε_1
ε_2
ε_N

Fig. 13

4.2.1. Paper 6:

Direct Observation of Macroscopic Charge Quantization: a Millikan Experiment in a Submicron Solid State Device

Originally published as:

P. Lafarge, P. Joyez, H. Pothier, A. Cleland, T. Holst, D. Esteve, C. Urbina, and M. H. Devoret, Observation directe de la quantification de la charge macroscopique : une expérience de Millikan dans un dispositif submicronique, C. R. Acad. Sci. Paris **314**, 883 (1992).

In this paper, we report measurements of the instantaneous charge of an electron box island connected to ground by four tunnel junctions in series. The transfer of electrons from the charge reservoir to the island results here from co-tunneling processes whose rate are so low that individual events can be resolved. This circuit can also be seen as a four junctions electron pump in the hold mode [1]. However, the measured rate of the co-tunneling processes which are one of the sources of errors in an electron pump (see paper 4) is several order of magnitude larger than the theoretical value.

[1] J. M. Martinis, M. Nahum, H. D. Jensen, to be published.

Observation directe de la quantification de la charge macroscopique: Une expérience de Millikan dans un dispositif électronique submicronique

Auteurs: Philippe Lafarge, Philippe Joyez, Hugues Pothier, Andrew Cleland, Thorsten Holst, Daniel Esteve, Cristian Urbina et Michel H. Devoret

Résumé: Nous avons mesuré le potentiel d'une électrode métallique couplée à un réservoir de charge par l'intermédiaire d'une chaîne de jonctions tunnel. On observe à basse température les sauts de potentiel associés au passage des électrons individuels à travers les jonctions. Le taux de passage des électrons, bien que suffisamment faible pour que le nombre d'électrons sur l'électrode puisse être connu à tout instant, dépasse la valeur théorique par plusieurs ordres de grandeur.

Direct observation of macroscopic charge quantization: a Millikan experiment in a submicron solid state device

Abstract: We have measured the potential of a metallic electrode which was connected to a charge reservoir by four tunnel junctions in series. At low temperatures, we observe switching events associated with single electrons entering and leaving the electrode. The tunneling rate of electrons through the junctions, although small enough for the number of electrons on the electrode to be known at every instant, exceeds the theoretical value by several orders of magnitude.

Adresse: Service de Physique de l'Etat Condensé
CEA-Saclay, 91191 Gif-sur-Yvette cedex, France

PACS: 73.40G, 06.20H, 73.40R

ABRIDGED ENGLISH VERSION

In his famous experiment, Millikan showed that the total charge on an oil drop was always an integer multiple of a charge quantum e [1], which he determined. Nowadays, the most precise value of e is obtained by a chain of indirect experiments [2]. A more direct determination based on charging effects in nanoscale junction [3] circuits has been proposed [4]. It consists of a purely electrostatic version of Millikan's experiment: an isolated metallic electrode of known capacitance would be charged with $N \simeq 10^8$ electrons using an electron pump [5]. One would determine e with a metrological accuracy by measuring the potential of the electrode with a SET transistor [6], which is able to resolve an increment of charge equal to e. We report here the results of an experiment aimed at testing this idea. We measure the potential variations associated with individual electrons leaving and entering a metallic electrode, both in the normal and superconducting state. Fulton et al. have recently reported a similar result, but only in the superconducting state [7].

Fig. 1 shows the principle of our experiment. The node **p** is the isolated metallic electrode ("island") whose potential is measured by a SET transistor through the coupling capacitor C_c. The charge on island **p** can be varied by means of a voltage source U connected to the island by a capacitor C_s and a chain of four nanoscale tunnel junctions. The total capacitance of island **p** is dominated by capacitance C_p placed in parallel with the chain of junctions. The tunneling rate of electrons through the four junctions at low temperatures [8,9] is small enough that the SET transistor can measure the island potential with a resolution much better than e/C_p. Details concerning the measurement technique of a variable island potential with a SET transistor have been given in a preceding paper [10]. Figure 2 shows the nanolithographic mask with which we implemented the schematic of Fig. 1 on a silicon substrate using the techniques described in reference [9]. Special attention was given to the filtering of the various lines between the sample and the room temperature electronics.

We show in Fig. 3 the SET transistor current I, which varies linearly with the potential of island **p**, as a function of time when U is kept constant. The sample was kept in the normal state with a 0.5 T magnetic field. The random switching events correspond to the tunneling of individual electrons. However, the measured tunneling rate is 10^5 times greater than the predicted rates, even assuming that the temperature of islands **a**,**b**,**c** and **p** is 30 mK higher than the thermometer temperature which was 20 mK. This temperature difference is the maximum one can obtain by considering the various possible heat inputs on the islands.

In Fig. 4, we show the variations of the charge q_p of island **p** as a function of U when U is swept back and forth between +3.5 mV and -3.5 mV in 0.4 s. The hysteresis reflects the ratio between the sweep and tunneling rates. The results in the superconducting state only differ from those in the normal state in that the tunneling rate of electrons is about an order of magnitude higher. No steps corresponding to a

charge variation of $2e$ could be detected.

In conclusion, it is possible, using nanoscale tunnel junctions, to both vary the number of electrons on a metallic electrode and to measure its potential, but the tunneling processes through a series of junction need to be investigated further before metrological applications can be developed.

INTRODUCTION

La charge totale d'un corpuscule isolé est un multiple entier de la charge de l'électron, même quand ce corpuscule est de taille macroscopique. C'est grâce à cette propriété que Millikan a pu mettre en évidence la granularité de l'électricité en mesurant en 1911 la charge de fines gouttelettes d'huile [1]. Quoique très directe, l'expérience de Millikan ne fournit pas une mesure très précise du quantum de charge e car elle consiste en une mesure de force exercée sur la gouttelette d'huile par un champ électrique imposé. Actuellement, la valeur de e la plus précise est obtenue par une chaîne d'expériences indirectes où le quantum de charge intervient avec d'autres grandeurs fondamentales comme la masse de l'électron, la constante de Planck et la vitesse de la lumière [2]. Une détermination plus directe, entièrement électrostatique, pourrait déceler et corriger d'éventuelles anomalies dans cette chaîne. Une telle expérience, qui exploiterait les effets de charge [3] se manifestant dans les circuits à base de jonctions tunnel de taille submicroniques a été proposée [4]. Elle repose sur la mesure du potentiel électrostatique d'une électrode métallique isolée, laquelle a été préalablement chargée par un nombre $N \simeq 10^8$ d'électrons en utilisant la pompe à électrons récemment mise au point par notre groupe [5]. La charge de l'électron serait déterminée à partir de ce nombre N, du potentiel de l'électrode, et de la capacité de cette dernière qui aurait été mesurée par une expérience annexe. Il est indispensable que le nombre d'électrons reste contrôlé à l'unité près pendant toute la durée de la mesure du potentiel. Cette dernière, qui doit évidemment être suffisamment précise pour discriminer N et $N + 1$, s'effectue avec un transistor SET [6]. Au cours de l'expérience décrite dans cette note, nous avons mesuré le potentiel d'une électrode dont la charge moyenne était imposée et nous avons observé les variations discrètes correspondant à l'entrée et à la sortie des électrons individuels. Un résultat préliminaire de ce type concernant une électrode supraconductrice a été présenté récemment par Fulton et coll. [7] . Dans notre expérience, le phénomène de quantification macroscopique de la charge est observé à la fois dans l'état normal et dans l'état supraconducteur.

MONTAGE EXPERIMENTAL

Le schéma électrique de la Fig. 1 donne le principe de notre expérience. Le noeud marqué **p** représente l'électrode isolée ("île") dont on mesure le potentiel et dont on fait varier la charge. L'île **p** est reliée à une source de tension U par l'intermédiaire de deux capacités C_s et $C_p \gg C_s$, lesquelles constituent un diviseur de tension permettant d'utiliser une tension U suffisamment élevée pour que ses fluctuations soient négigeables. On a placé en parallèle avec la capacité C_p une chaîne de quatre jonctions tunnel de taille submicronique. Le potentiel des îles intermédiaires dans la chaîne peut être ajusté à l'aide des sources de tension auxiliaires U_1, U_2 et U_3. Le rôle de cette chaîne de jonctions est de laisser passer les électrons que doit acquérir ou céder l'île **p** pour se mettre en équilibre électrostatique avec la source U. On utilise ici une première propriété-clé: une jonction tunnel de résistance $R_T \gg R_K = h/e^2$ laisse passer la charge de façon discontinue -électron par électron- à la différence d'un fil métallique qui permet de transférer la charge de manière continue. Il faut que les jonctions soient de faibles dimensions pour bénéficier d'une seconde propriété-clé: pour une électrode de capacité totale C_Σ suffisamment petite, l'énergie électrostatique e^2/k_BT d'un seul électron en excès peut être plus grande que l'énergie caractéristique k_BT des fluctuations thermiques. Enfin, quatre jonctions en série sont nécessaires pour que le passage des électrons, qui s'effectue à travers les jonctions en une seule étape [8] à basse température, se produise avec un taux suffisamment faible. En effet, le rapport entre les taux tunnel à tension nulle à travers $\mathcal{N}$ jonctions et 1 jonction est proportionnel à $(R_K/R_T)^{\mathcal{N}-1}(C_\Sigma k_BT/e^2)^{2\mathcal{N}-2}$ [9], où C_Σ est la capacité totale de chaque île intermédiaire.

Grâce à ces effets, une mesure du potentiel de l'île **p** avec une résolution nettement meilleure que e dans l'intervalle de temps séparant deux événements tunnel est réalisable. La mesure est effectuée en utilisant un transistor SET [6] qui comporte deux jonctions tunnel, elles aussi de taille submicronique, et qui définissent une île, notée **m** sur la Fig. 1, couplée à l'île **p** par un condensateur de couplage C_c. Les tensions de polarisation V et U_0 du transistor sont ajustées de manière qu'une variation du potentiel de l'île p produise une variation proportionnelle du courant I qui traverse le transistor. Nous avons décrit cette technique dans un précédent article [10].

La figure 2 représente le motif utilisé pour implémenter le schéma de la Fig. 1 par nanolithographie électronique. Aux zones noires correspondent des fenêtres dans un masque de germanium suspendu à 2000 Å au dessus du substrat de silicium, à travers lesquelles on évapore sous vide de l'aluminium. En séparant deux étapes d'évaporations effectuées suivant des angles différents par une étape de croissance d'oxyde d'aluminium, on forme des jonctions aux zones de recouvrement des pistes métalliques [9]. La capacité C des jonctions est de 0.5 fF avec une dispersion maximale de 50% sur un même échantillon. Les capacités pures du schéma de la Fig. 1 sont réalisées par des pistes interdigitées. Elles sont toutes visibles sur la Fig. 2, sauf la capacité C_p qui, du fait de son plus grand encombrement, sort en grande partie du cadre de la figure. On obtient par cette technique les valeurs $C_0 = C_1 = C_2 = C_3 = C_s = C_c/3 = C_p/25 = 80$ aF.

Après les étapes de nanolithographie et le test des jonctions à la température ambiante, nous avons ancré thermiquement un échantillon dont les jonctions étaient telles que $R_T \simeq 300$ kΩ dans une enceinte de cuivre fixée à la chambre de mélange d'un réfrigérateur à dilution. Les sources de tensions et le préamplificateur pour la mesure du courant I, tous deux placés à température ambiante, ont été ensuite raccordés à l'échantillon par des liaisons électriques filtrées. Enfin, ce dernier est refroidi à 20 mK. On fait transiter l'aluminium des pistes de l'état supraconducteur à l'état normal en appliquant un champ magnétique de 0.5 T à l'aide d'un solénoïde supraconducteur.

RESULTATS

La figure 3 montre le résultat de la mesure du courant I du transistor SET en fonction du temps, lorsque la source de potentiel U est maintenue constante. Le signal se présente sous forme de crénaux dont la durée est aléatoire et dont l'amplitude est fixe. L'amplitude des crénaux, calibrée à l'aide de la tension U_0 et des valeurs des capacités du circuit, est conforme à celle attendue pour une variation d'amplitude e de la charge q_p de l'île. Les tensions U_1, U_2 et U_3 ont été ajustées pour que la durée moyenne des crénaux soit maximale. L'existence de ces conditions optimales est en accord avec la théorie du "co-tunneling" [8] régissant le passage par effet tunnel des électrons à travers les quatre jonctions. Nous attribuons donc les variations aléatoires du potentiel de l'île aux variations aléatoires de son nombre d'électrons dues au passage de ceux-ci à travers la chaîne de jonctions. Il est remarquable que pour des durées allant jusqu'à quelques dixièmes de seconde -durées "macroscopiques" pour des électrons individuels dans un circuit électronique- la charge de l'île reste fixe et donc parfaitement déterminée. La figure 4 montre le résultat d'une mesure de la charge q_p de l'île en fonction de la tension U lorsque cette dernière varie dans le temps de façon triangulaire. On observe les marches successives correspondant à l'entrée des électrons dans l'île lorsque la tension U croît, puis à leur sortie quand la tension U décroît. L'ensemble des marches montantes et descendantes forme un cycle d'hystérésis où se traduit le rapport entre la probabilité par unité de temps de l'effet tunnel et la durée du cycle de variation de la tension U. Cette durée est de 0.4 s dans cette expérience. Des expériences de contrôle ont montré que la largeur du cycle d'hystérésis décroît quand la durée du cycle de variation de la tension U croît. Aucun hystérésis ne peut être détecté lorque la chaine de quatre jonctions est remplacée par une jonction unique [10]. Nous avons répété le même type d'expériences avec quatre jonctions à plus haute température. Elles indiquent alors que le taux tunnel augmente brutalement à partir de 100 mK. Enfin, l'ensemble de ces mesures a été recommencé après avoir replacé l'échantillon dans l'état supraconducteur. La recherche d'incréments de tension correspondant à $2e$ a été infructueuse. Les résultats montrent que les variations de charge du système supraconducteur ne font intervenir que des électrons individuels; les résultats ne diffèrent de ceux obtenus dans l'état normal que par un taux de passage des électrons plus élevé environ d'un ordre de grandeur.

DISCUSSION ET CONCLUSION

Notre expérience démontre qu'il est possible de garder le nombre d'électrons sur une électrode métallique fixe à l'unité près pendant une durée de l'ordre de la fraction de seconde, tout en se réservant la possibilité de faire varier ce nombre électron par électron avec une tension de commande. Ces résultats permettent de donner une borne supérieure pour la valeur expérimentale du taux de passage des électrons à travers quatre jonctions, taux dont la faiblesse est cruciale pour la métrologie de e utilisant les effets de charges dans les circuits à base de jonctions tunnel. Nous trouvons que le taux observé est environ 10^5 fois supérieur à celui que prédit la théorie du co-tunneling [8] en supposant que la température des îles est 30 mK au-dessus de la température du thermomètre, ce qui est une valeur maximum compte-tenu des différentes sources de chauffage possibles. Il est peu probable que ce facteur de 10^5 puisse être attribuée au bruit électromagnétique dans la pièce autour de l'expérience. En effet, si on injecte une irradiation radiofréquence de forte puissance dans la partie du circuit à température ambiante, elle ne produit aucun effet. Nos mesures semblent donc indiquer l'existence d'un bruit intrinsèque qui limiterait, compte tenu des caractéristiques de la pompe à électrons [5], la précision de la mesure de la charge de l'électron à 10^{-5}. Des mesures effectuées sur des échantillons de caractéristiques différentes, tant en ce qui concerne le nombre de jonctions que leur résistance tunnel, devrait permettre de préciser l'origine de ce bruit. Un autre aspect inexpliqué de l'expérience est le taux de passage des électrons plus élevé dans l'état supraconducteur que dans l'état normal. En principe, la température à laquelle se déroule l'expérience est telle que tous les électrons des îles devraient être condensés en paires. Même s'il reste au sein des îles une fraction finie de quasiparticules hors d'équilibre, il est difficile d'imaginer par quel mécanisme elles peuvent traverser les jonctions tunnel avec un taux plus grand que les électrons dans l'état normal.

Références bibliographiques

[1] R.A. Millikan, Phys. Rev. **32**, 1911, p. 349-397.

[2] B.N. Taylor et R.E. Cohen, J. Res. Natl. Stand. Technol. **95**, 1990, p. 497-523.

[3] D.V. Averin et K.K. Likharev, in "Mesoscopic Phenomena in Solids" (Elsevier, Amsterdam, 1991), Chap. 6.

[4] E.R. Williams, J.M. Martinis and R.N. Gosh, à paraître.

[5] H. Pothier, P. Lafarge, C. Urbina, D. Esteve and M.H. Devoret, Europhys. Lett. **17**, 1992, 259-254.

[6] T.A. Fulton et G.J. Dolan, Phys. Rev. Lett. **59**, 1987, p. 109-113.

[7] T.A. Fulton, P.L. Gammel et L.N. Dunkleberger, Phys. Rev. Lett. **67**, 1991, 3148-3151.

[8] D.V. Averin et A.A. Odintsov, Phys. Lett. **A140**, 1989, p. 251-255.

[9] H. Pothier, thèse de doctorat, Université Paris 6, 1991.

[10] P. Lafarge, H. Pothier, E.R. Williams, D. Esteve, C. Urbina, et M.H. Devoret, Z. Phys. B **85**, 1991, p. 327-332.

Légendes des figures

Fig. 1 Schéma électrique de l'expérience. Les jonctions tunnel sont représentées par un symbole en forme de double boîte. Les noeuds marqués d'un point noir correspondent à des électrodes entourées d'isolant. Les noeuds marqués d'un point blanc représentent les électrodes auxquelles sont appliquées les tensions principales.

Fig. 1 Circuit schematic of the experiment. The tunnel junctions are represented by double-box symbols. The nodes marked with a full dot correspond to electrodes surrounded by insulating material. The nodes marked with an open dot correspond to electrodes to which the principal voltage sources are applied.

Fig. 2 Masque nanolithographique réalisant l'implémentation du circuit de la Fig. 1. Les zones marquées avec un chiffre ou une lettre correspondent aux noeuds de la Fig. 1 marqués par le même symbole.

Fig. 2 Nanolithographic mask used for the implementation of the circuit of Fig. 1. The areas marked with digits and letters correspond to the nodes in Fig. 1 marked with the same symbols.

Fig. 3 Courant I dans le transistor SET en fonction du temps pour une tension U constante. La température du porte-échantillon était de 16 mK. La constante de temps d'intégration était de de 1 ms. Les tensions U_0 et V étaient ajustées pour maximiser la sensibilité du transistor. Les tensions U_1, U_2 et U_3 étaient ajustées pour maximiser la durée des crénaux présentés par le signal.

Fig. 3 SET transistor current I *as a function of time. The voltage* U *was held constant. The sample holder temperature was 16 mK. The integration time constant was 1 ms. The voltages* U_0 *and* V *were adjusted to maximize the SET transistor sensitivity. The voltages* U_1, U_2 *and* U_3 *were adjusted to maximize the time between switching events.*

Fig. 4 Charge de l'île **p**, en unités de e, en fonction de la tension U pour une vitesse de balayage $\dot{U} = \pm 35$ mV/s. Les autres conditions sont identiques à celles de la Fig. 3. Les flèches indiquent le sens de variation de U.

Fig. 4 Island p charge, in units of e, as a function of voltage U for a sweep rate $\dot{U} = \pm 35$ mV/s. *Other conditions were as in Fig. 3. The arrows indicate the direction in which* U *was swept.*

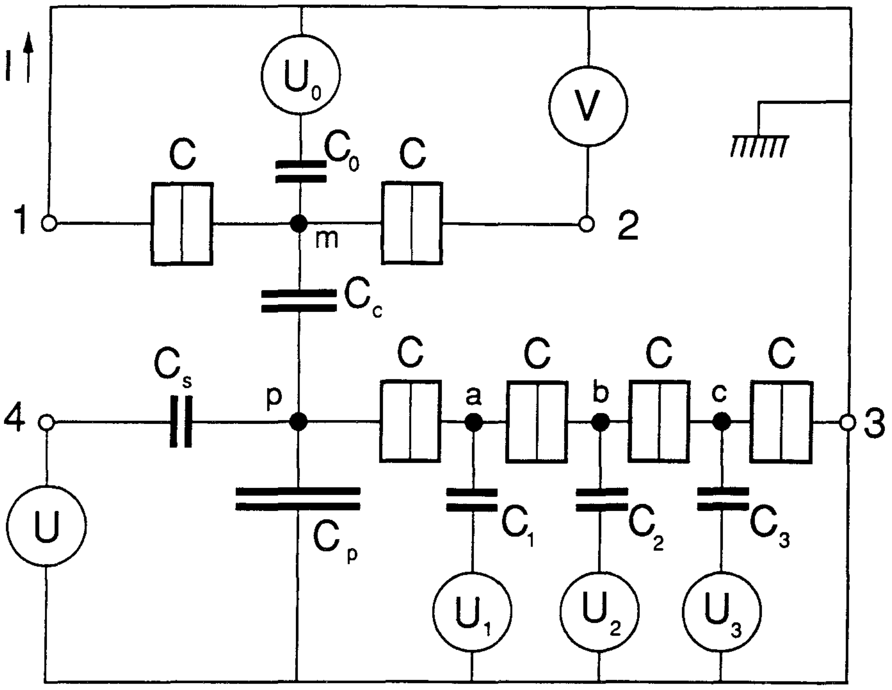
I
U0
V
C
C0
C
1
m
2
Cc
C
C
C
C
Cs
4
p
a
b
c
3
U
Cp
C1
C2
C3
U1
U2
U3

Fig. 1

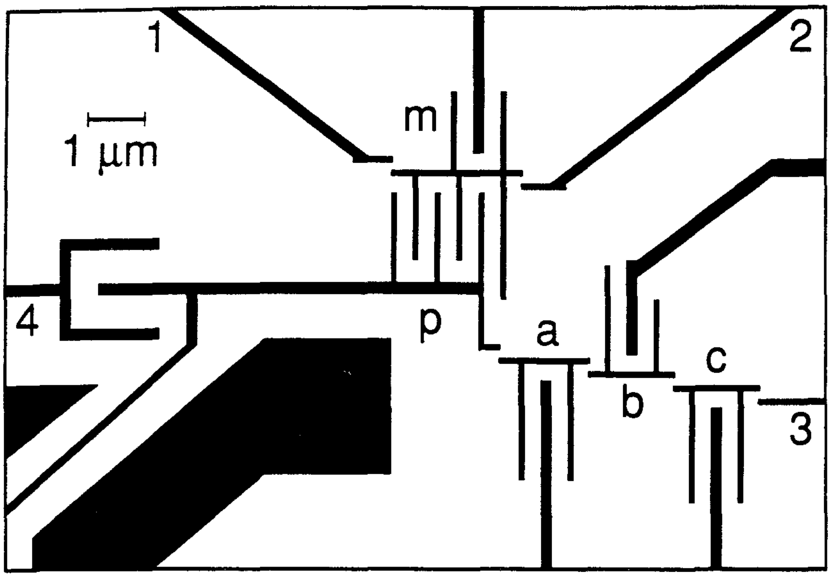
1
2
1 µm
m
4
p
a
b
c
3

Fig. 2

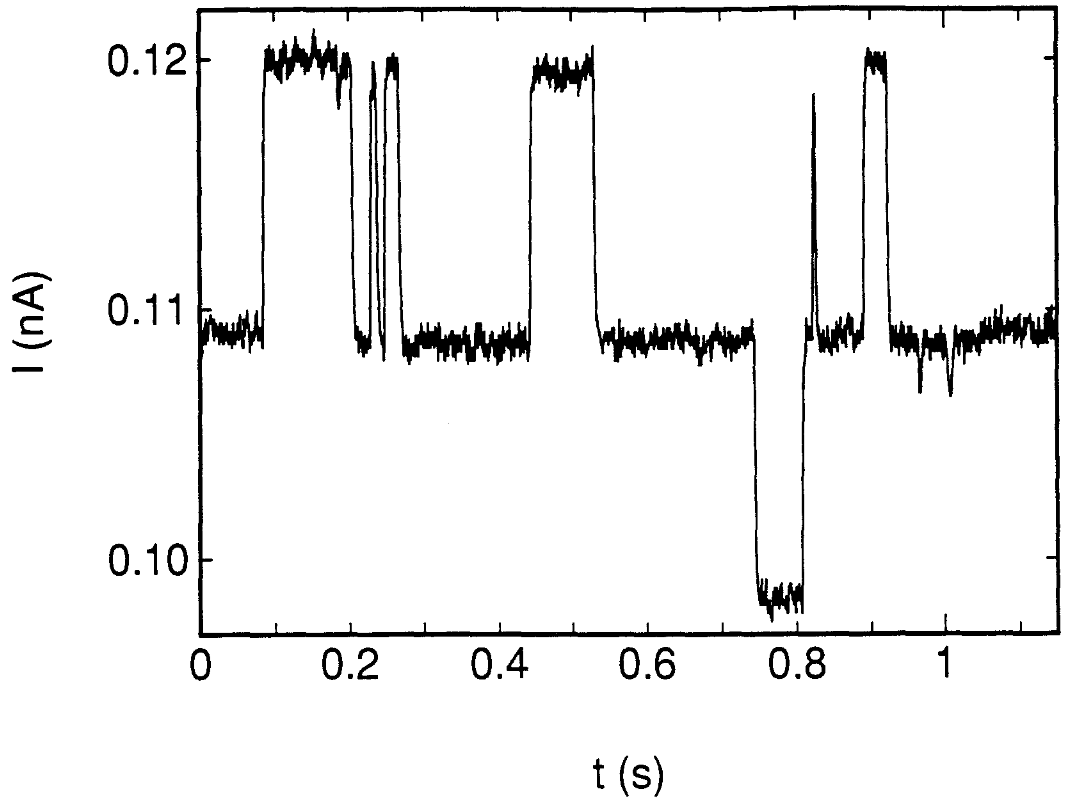

Fig. 3

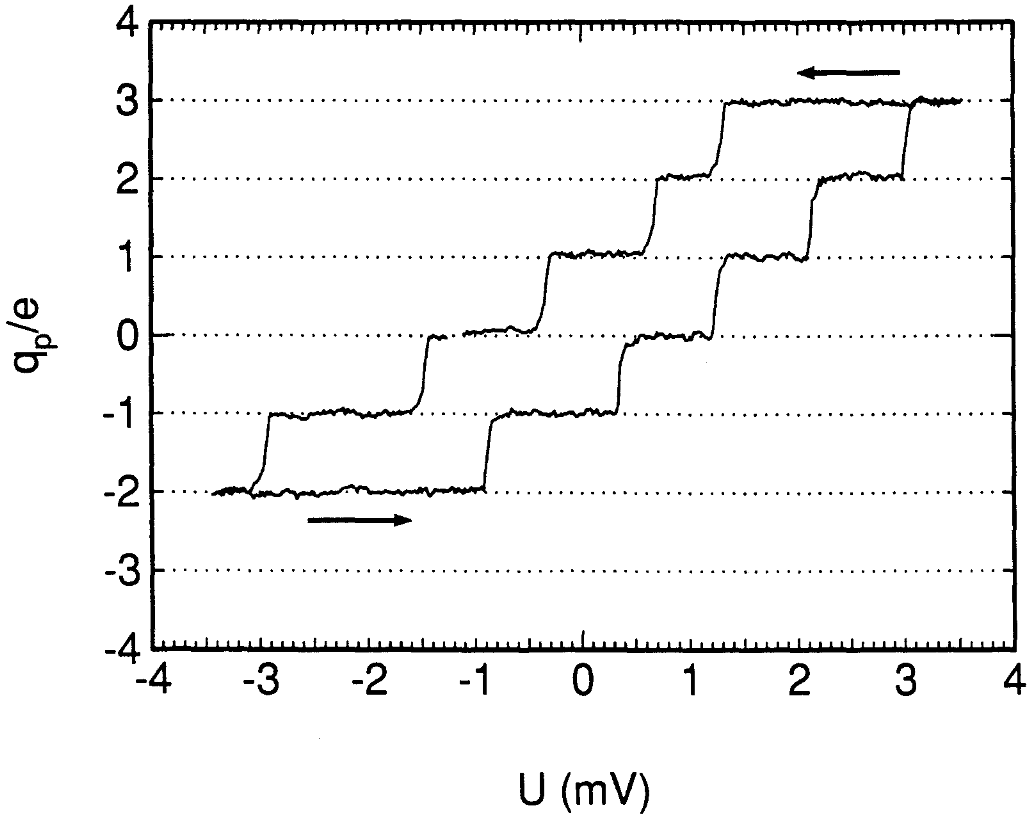

Fig. 4

5. Conclusion

The initial goal of this thesis work was to observe the quantization of the electric charge in a solid state device and to determine if this quantization permits to transfer electrons one by one with metrological accuracy.

Summary of results

We have demonstrated experimentally the quantization of the average charge on a metallic electrode connected to an electron reservoir by a tunnel junction. By using a tunnel junction of nanoscale dimensions we make the electrostatic energy of one excess electron in the island, i.e. the metallic electrode, much larger than the characteristic energy of the thermal fluctuations. We have shown that we can set the average number of excess electrons on the island by an externally applied voltage. The measured variations of the island average charge (macroscopic charge) as a function of this voltage show a staircase pattern and are in good agreement with theoretical predictions taking into account thermal fluctuations. For a superconducting island, our measurements of the macroscopic charge display an asymmetry between the steps corresponding to an odd number of electrons on the island and the the steps corresponding to an even number of electrons. The odd steps are shorter than the even steps. We interpret this effect as a manifestation of electron pairing in the superconducting island. From the steps asymmetry we deduced the free energy difference between the odd states and the even states of the island and we have found a very good agreement between the experimental results and our theoretical calculations. Finally, below a threshold temperature, we have observed that odd steps disappear leading to a strict $2e$-quantization of the macroscopic charge.

The island of electron box experiments appears as the basic element of the design of single electron devices based on macroscopic charge quantization. We have shown that an electron pump device with four islands can theoretically achieve a metrological accuracy of the charge transfer. This analysis is based on a nondivergent expression of high order tunneling (co-tunneling) rates across linear arrays of junctions which we have calculated. Finally, we have performed a measurement of the instantaneous charge of an electrode connected to an electron reservoir by four tunnel junctions in series. In this device, the charge transfer results from co-tunneling processes whose rates are so low that individual tunnel events can be resolved. However, the measured rates are several orders of magnitude higher than expected.

Problems encountered

The influence of the junction tunnel resistance on the macroscopic charge quantization has not been investigated. The observation of the quantum fluctuations of the island charge due to tunneling itself as described in section 2.1.3 would require values of tunnel resistance lower than achievable with our present technique (~ 10 kΩ). Thus, at the temperature of our experiment, we cannot discriminate the effects of thermal fluctuations and the effect of quantum fluctuations. The temperature dependence of the Coulomb staircase at temperature lower than 30 mK and the high cotunneling rate which we have observed in the four junctions box experiment are still unexplained. These problems could be related to the problem of thermal noise filtering. As shown in Sec. 2.1.4, thermal noise at high frequencies coming from part of the circuit at high temperature can indeed activate unwanted tunnel events. Another explanation of the noise problem is the possibility of an intrisic noise coming from the substrate which may contain long lived excited states. The anomalous cotunneling rate across a linear array of junctions (see Sec. 4.2.1) has been observed in several circuits [1,2]. This phenomenon is of crucial importance because it increases the error rate of the devices that transfer electrons one by one and it could severely jeopardize the use of such devices in metrological applications.

Provided the charging energy E_c is smaller than the superconducting gap Δ, the main drawback which can prevent the observation of $2e$-quantization of the macroscopic charge is the presence of single quasiparticle state inside the energy gap of the superconducting island. We may have met this type of defect in the first normal/superconducting electron box experiment (see Sec. 3.2.1). In this experiment, the odd-even free energy difference as a function of the temperature is well fitted below 50 mK if one adds to the continuous BCS density of states a single, two-fold degenerate, quasiparticle state at 0.8Δ. In an other experiment performed with a completely superconducting electron box, the staircase asymmetry increased with decreasing temperature only at high temperature. Below 100 mK, we have observed that the odd-even free energy difference of the island remained constant at a value corresponding to a single quasiparticle state with energy equal to 0.28Δ. The origin of these quasiparticle states inside the gap is still unknown and their presence is not controlled experimentally.

One must now mention the problem of offset charges. As described in appendix 1, the total energy of a circuit made of small tunnel junctions depends on the charge on the islands. Hence, the presence of random offset charges which could be trapped in the substrate or in the oxyde barrier of the junctions affects the tunneling rate across each junction of the circuit and implies the fabrication of a gate electrode for each island. These offset charges prevent to design circuits which require the precise control of the charge on a large number of islands. In particular, it makes impossible to parallelise transfer devices like the electron pump. This problem and the problem of the co-tunneling rate may be connected: the displacement of those charges responsible for offset charges is perhaps the source of noise explaining anomalous cotunneling rates [3].

Possible extensions of these experiments

A possible extension of these experiments would be to use for the island a superconducting material different from aluminum like niobium or high-T_C materials. If the BCS energy gap is larger than in aluminum then the $2e$-quantization domain is extended and the effect of a single quasiparticle state is less important. Since the normal/superconducting box provides a precise measurement of the excitation spectrum of the island, one may in principle investigate the complex form of the density of states of high-T_C superconductors or other exotic superconductors. This experiment would imply of course the fabrication of nanoscale tunnel junctions between metal and the high-T_C material and the control of the spatial orientation of the insulating barrier.

The possibility of controlling the number of Cooper pairs on a superconducting island open the field for experiments taking advantage of both charge quantization and Josephson coupling. One of them is the superconducting single electron transistor [4] consisting of two small Josephson junctions in series. The maximum value of the supercurrent flowing through the device is modulated by the charge induced on the central island and that modulation depends on the parity of the total number of electrons in the island. As we have shown in Sec. 2.3.3, the superconducting electron box with a Josephson junction could constitute an experiment on macroscopic quantum coherence (MQC) [5]. Here the macroscopic degree of freedom involved in the MQC would be the charge on the island and the coupling is due to electron tunneling through the Josephson junction. By using two Josephson junctions in parallel instead of one, the Josephson coupling between the charge state of the system can even be modulated by an externally applied magnetic field. By means of this modulation, one could investigate the effect of dissipation due to the electromagnetic environment.

REFERENCES

[1] T. A. Fulton, P. L. Gammel and L. N. Dunkleberger, Phys. Rev. Lett. 67, 3148 (1991).

[2] T. Eiles and J. Martinis, to be published in Phys. Rev. Lett..

[3] R. Bauernschmitt and Yuli V. Nazarov, Phys. Rev. B 47, 9997 (1993).

[4] P. Joyez, A. Filipe, P. Lafarge, D. Esteve, M. H. Devoret, submitted to Phys. Rev. Lett..

[5] Quantum Tunneling in Condensed Media, edited by A. J. Leggett and Yu. Kagan (Elsevier, Amsterdam, 1992).

APPENDIX 1

TOTAL ENERGY OF A GENERAL TUNNEL JUNCTION CIRCUIT

The most general tunnel junction circuit of practical interest contains only tunnel junctions with high tunnel resistance and pure capacitors. It is biased by voltage sources connected between the nodes of the circuit and ground (see Fig. A1a). In the circuit, an electrode which is connected at least to one tunnel junction while not being directly connected to a voltage source is an "island" containing a well defined number n of excess electrons. At a given instant, the state of the circuit is completely described by its charge configuration given by the set of the numbers of excess electrons on the islands $\{n_1,...,n_M\}$ and by the set $\{p_{M+1},...,p_P\}$ of the numbers of electrons having passed through the voltage sources connected to the junctions. These two sets which enter in the calculation of the total energy are not always independent. In fact, the number of degrees of freedom of the circuit is equal to the difference between the number of junctions and the number of closed loops formed by junctions only. For instance, in the circuit of Fig. A1a, there are 6 junctions and 1 loop. The number of degrees of freedom is thus equal to 5.

The circuit evolves in time by transitions from one charge configuration to another. These transitions are induced by tunneling events (single or multiple) across the junctions of the circuit. The single tunneling rate across a nanoscale junction is proportional to the difference in the total energy of the circuit before and after the tunnel event. The rate of multiple tunneling events (co-tunneling) involves higher powers of this energy difference [1]. We present here the calculation of the total energy for an arbitrary charge configuration.

In the calculation, electron tunneling is viewed as a purely random process which only changes instantaneously the charge of the islands and has no dynamics of its own. Furthermore, because there is no resistive element in the circuit, the charges on the pure capacitors and on the capacitances of the junctions relax instantaneously after a tunnel event. This is why the total energy involved in the tunneling rate calculation is only the sum of the electrostatic energy stored in the circuit and the work done by the voltage sources, with the junctions described as simple capacitors [2].

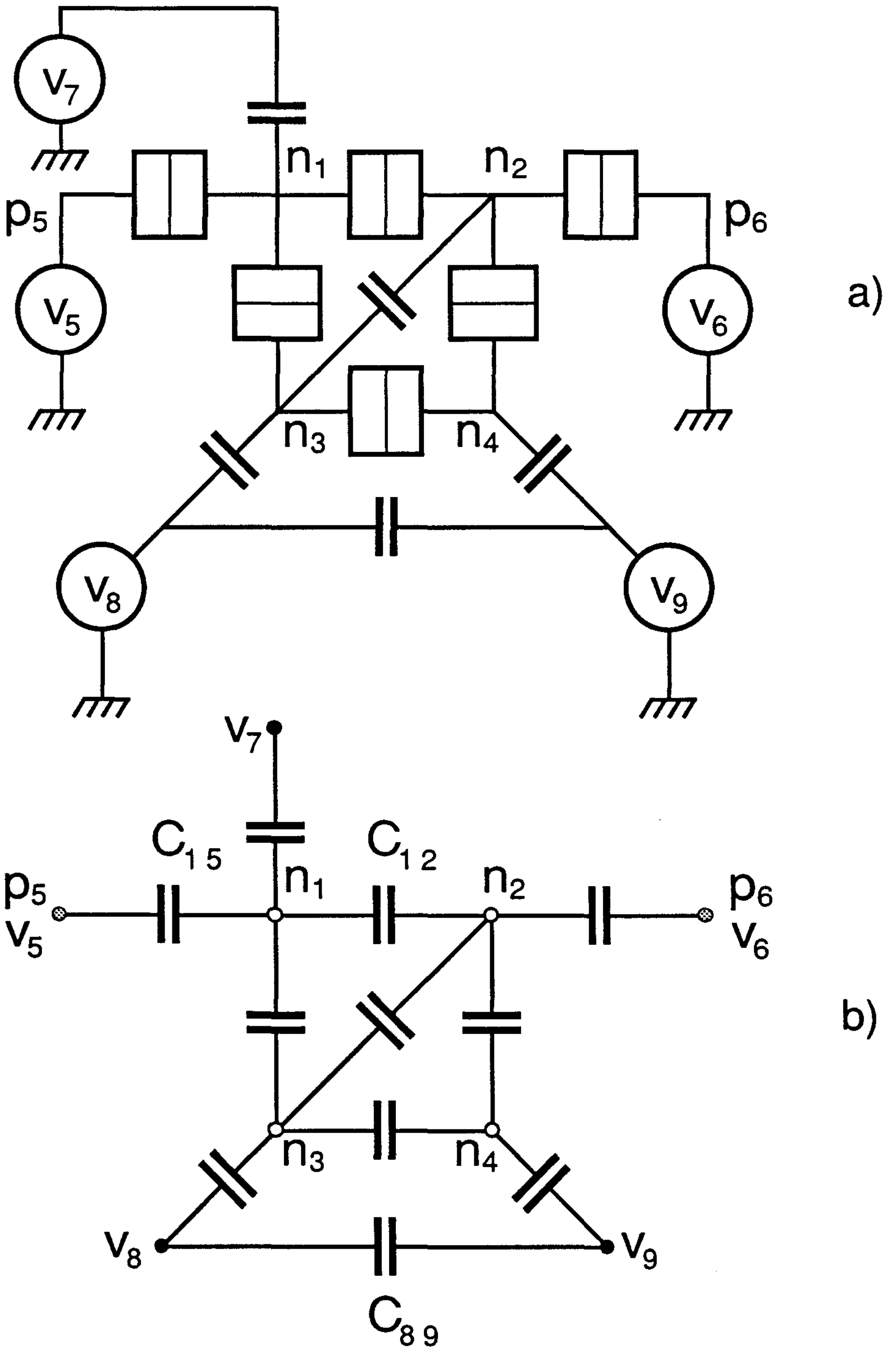

Fig. A1. a) *Example of a circuit consisting of tunnel junctions (rectangular boxes) and capacitances biased by voltage sources. The numbers* n_1 *to* n_4 *denote the numbers of excess electrons on the islands, the number* p_5 *and* p_6 *denote the number of electrons which have passed through the voltage sources* v_5 *and* v_6. b) *Network of capacitances with mixed constraints equivalent to the circuit represented in* a). *This network has 9 nodes. The nodes depicted by open dots (1 to 4) correspond to the islands, the nodes depicted by gray dots (5 to 6) are between voltage source nodes and junctions and the nodes depicted by solid dots (7 to 9) are between voltage sources node and pure capacitors.*

It is useful to represent the circuit as a network of capacitances with mixed constraints (see Fig. A1b). We have to distinguish three sets of nodes in such a network. The first one is the set of nodes corresponding to the islands of the circuit (open dots) which are labeled from 1 to M. For a given configuration, their charge $q_\alpha = -n_\alpha e$ is known but their potential v_α depends on the electrostatic state of the whole circuit. The second set consists of the nodes between a voltage source and a junction (gray dots). These nodes, which are labeled from $M+1$ to P, have a known potential v_i and a known number p_i of electrons which have passed through it but their charge is a priory unknown. We consider that an electron has passed through voltage source i if it has tunneled through a junction directly connected to the source. The number p_i increases (decreases), when one electron passes through voltage source i in the sense of the decreasing (increasing) potentials. Finally the third set consists of the nodes between a voltage source and a pure capacitors (solid dots). For these nodes, which are labeled from $P+1$ to N, only the potential is known. In the following calculation, we will call I the set of the islands nodes, S the set of all the voltage source nodes and J the subset of S corresponding to the nodes between a junction and a voltage source.

For a general network of capacitances, there is a matrix relation which links the vector $\mathbf{q}$ whose elements are the charges of the nodes to the vector $\mathbf{v}$ whose elements are the potentials of the nodes:

$$\mathbf{q} = \mathcal{C}\mathbf{v}. \tag{1}$$

The capacitance matrix $\mathcal{C}$ of the network is a $N \times N$ matrix whose elements are given by

$$\begin{cases} \mathcal{C}_{kk} = \sum_{l \neq k} C_{kl} \\ \mathcal{C}_{kl} = -C_{kl} \end{cases} \quad \text{for } k,l \in \mathrm{I} \cup \mathrm{S}\ , \tag{2}$$

where C_{kl} is the direct capacitance between node k and node l. When applied to island α, Eq. (1) gives the following relation between the charge q_α of the island and the potentials of all the nodes:

$$q_\alpha = \sum_{\beta \in \mathrm{I}} \mathcal{C}_{\alpha\beta}\mathrm{v}_\beta + \sum_{i \in \mathrm{S}} \mathcal{C}_{\alpha i}\mathrm{v}_i\ . \tag{3}$$

We can rewrite this expression as:

$$q_\alpha + \tilde{q}_\alpha = \sum_{\beta \in \mathrm{I}} \tilde{C}_{\alpha\beta} \mathrm{v}_\beta \ , \tag{4}$$

where

$$\tilde{q}_\alpha = \sum_{i \in \mathrm{S}} C_{\alpha i} \mathrm{v}_i \tag{5}$$

is an effective bias charge applied on the island α and where $\tilde{\mathrm{C}}$ is the submatrix of $\mathcal{C}$ which involves the set I of the island nodes only . The matrix $\tilde{\mathrm{C}}$ is a $M \times M$ matrix such that

$$\tilde{C}_{\alpha\beta} = \mathcal{C}_{\alpha\beta}, \ \text{for } \alpha, \beta \in \mathrm{I}. \tag{6}$$

The matrix $\tilde{\mathrm{C}}$ of the island network has an inverse $\tilde{\mathrm{C}}^{-1}$ and we can write the inverse of relation (4):

$$\mathrm{v}_\alpha = \sum_{\gamma \in \mathrm{I}} \tilde{C}^{-1}_{\alpha\gamma} \left(q_\gamma + \tilde{q}_\gamma \right) . \tag{7}$$

The total energy E of the network, which we want to calculate, is obtained by summing the electrostatic energy E_{elec} stored in the circuit and the work done by the voltage sources E_s. Expressed in terms of the capacitances and the nodes potentials, E_{elec} takes the following form:

$$\begin{aligned} E_{elec} &= \frac{1}{2} \sum_{\alpha < \beta \in \mathrm{I}} C_{\alpha\beta} \left(\mathrm{v}_\alpha - \mathrm{v}_\beta \right)^2 + \frac{1}{2} \sum_{i < j \in \mathrm{S}} C_{ij} \left(\mathrm{v}_i - \mathrm{v}_j \right)^2 + \frac{1}{2} \sum_{\alpha \in \mathrm{I}, i \in S} C_{\alpha i} \left(\mathrm{v}_\alpha - \mathrm{v}_i \right)^2 \\ &= \frac{1}{2} \sum_{\alpha, \beta \in \mathrm{I}} \tilde{C}_{\alpha\beta} \mathrm{v}_\alpha \mathrm{v}_\beta + \frac{1}{2} \sum_{i, j \in \mathrm{S}} \mathcal{C}_{ij} \mathrm{v}_i \mathrm{v}_j - \sum_{\alpha \in \mathrm{I}} \tilde{q}_\alpha \mathrm{v}_\alpha \ . \end{aligned} \tag{8}$$

Since for a given charge configuration, we do not know the island potentials v_α but only the island charges q_α, we now need to express the electrostatic energy E_{elec} as a function of the charges q_α. This can be done using the inverse matrix relation (7). From (7) and (8) we get for the electrostatic energy stored in the circuit:

$$\begin{aligned} E_{elec} &= \frac{1}{2} \sum_{\alpha \in \mathrm{I}} \sum_{\beta \in \mathrm{I}} \tilde{C}_{\alpha\beta} \sum_{\gamma \in \mathrm{I}} \tilde{C}^{-1}_{\alpha\gamma} \left(q_\gamma + \tilde{q}_\gamma \right) \sum_{\eta \in \mathrm{I}} \tilde{C}^{-1}_{\beta\eta} \left(q_\eta + \tilde{q}_\eta \right) + \frac{1}{2} \sum_{i, j \in \mathrm{S}} \mathcal{C}_{ij} \mathrm{v}_i \mathrm{v}_j - \sum_{\alpha \in \mathrm{I}} \tilde{q}_\alpha \mathrm{v}_\alpha \\ &= \frac{1}{2} \sum_{\gamma, \eta \in \mathrm{I}} \tilde{C}^{-1}_{\gamma\eta} \left(q_\gamma + \tilde{q}_\gamma \right) \left(q_\eta + \tilde{q}_\eta \right) + \frac{1}{2} \sum_{i, j \in \mathrm{S}} \mathcal{C}_{ij} \mathrm{v}_i \mathrm{v}_j - \sum_{\alpha \in \mathrm{I}} \tilde{q}_\alpha \mathrm{v}_\alpha \ . \end{aligned} \tag{9}$$

The work E_s done by the voltage sources is given by

$$E_s = -\sum_{i\in S}\left(\sum_{\alpha\in I} C_{\alpha i}(v_i - v_\alpha)\right)v_i + \sum_{l\in J}(-p_l e)v_l \,. \tag{10}$$

In this expression, the first term represents the work for charging the capacitances directly connected to the voltage sources and the second term represents the work for furnishing electrons which have been injected in the islands through the junctions. The total energy of the network can then be expressed as

$$E(\{n_\alpha\},\{p_l\}) = \frac{1}{2}\sum_{\alpha,\beta\in I}\tilde{C}^{-1}_{\alpha\beta}(n_\alpha e - \tilde{q}_\alpha)(n_\beta e - \tilde{q}_\beta) - \sum_{l\in J} p_l e v_l - \frac{1}{2}\sum_{i\in S}\sum_{\alpha\in I} C_{\alpha i} v_i^2 + \frac{1}{2}\sum_{i,j\in S} C_{ij} v_i v_j \,. \tag{11}$$

Since we usually want to compare the energies of different charge configurations for the same values of the applied voltages, we are interested in the difference between E and the total energy of the configuration with no electrons on the island and no electrons having passed through the voltage sources. We obtain the following result:

$$E(\{n_\alpha\},\{p_l\}) - E(\{0\},\{0\}) = \frac{1}{2}\sum_{\alpha,\beta\in I}\tilde{C}^{-1}_{\alpha\beta}\left(n_\alpha n_\beta e^2 - \tilde{q}_\alpha n_\beta e - \tilde{q}_\beta n_\alpha e\right) - \sum_{l\in J} p_l e v_l \tag{12}$$

We now apply this calculation to three simple examples:

The Single-Electron Box (Fig. A2)

In the case of the single-electron box there is only one island in the network. This island is connected to a voltage source U through a capacitance C_s and to the ground through the junction capacitance C. Therefore the matrix $\tilde{\mathrm{C}}$ of the circuit has only one element $\tilde{C}_{11} = C + C_s$. We denote by n the number of excess electrons on the island, there is only one bias charge given by $\tilde{q} = C_s U$. The energy of the single-electron box circuit directly follows from (11):

$$E = \frac{1}{2}\frac{(ne - C_s U)^2}{C + C_s} - \frac{1}{2}C_s U^2 \,. \tag{13}$$

We usually consider only the first term of this energy, which is useful for the calculation of the average charge in the junction:

$$E_n = \frac{e^2}{2(C+C_s)}(n - C_s U/e)^2 \ . \tag{14}$$

The Single-Electron Transistor (Fig. A3)

Like the electron box, the single-electron transistor [3] has only one island, whose number of excess electrons is denoted by n. The matrix $\tilde{\mathbf{C}}$ is given by $\tilde{C}_{11} = C_1 + C_2 + C_g$. The direct capacitance between the island and the voltage sources V and U_0 are C_1 and C_g respectively. The number of electrons which have passed to V is denoted by p and the bias charge of the island is $\tilde{q} = C_1 V + C_g U_0$. The total energy is:

$$E = \frac{1}{2}\frac{(ne - C_1 V - C_g U_0)^2}{C_1 + C_2 + C_g} - \frac{1}{2}C_1 V^2 - \frac{1}{2}C_g U_0^2 - peV \ . \tag{15}$$

The *N* junction pump (Fig. A4)

The N junction pump consists of a linear array of N identical junctions [4], and has $N-1$ islands. Each island is connected to a gate voltage source through a capacitor of negligible capacitance and the whole circuit is biased with a voltage source V. The charge configuration is completely described by the number p of electrons having passed through the voltage source and the set $\{n_1, \ldots, n_{N-1}\}$ of the numbers of excess electrons on the islands. The transfer of one charge across the whole array is achieved by N successive single tunnel events across each junction. After i tunnel events in the transfer sequence, the circuit is in an intermediate state given by $\{0\ldots 0, n_i = 1, 0\ldots 0\}$ and $p = 0$. For simplicity, we will calculate the energy of such a state with one excess electrons on island i when there is no gate voltages applied. For this charge configuration, Eq. (12) gives:

$$E(\{0\ldots 0, n_i = 1, 0\ldots 0\}, \{0\}) - E(\{0\}, \{0\}) = E_i = \frac{1}{2}\tilde{C}_{i,i}^{-1} e^2 - \tilde{C}_{i,N-1}^{-1} eCV \tag{16}$$

If we neglect the gate capacitances, the matrix $\tilde{\mathbf{C}}$ is given by $\tilde{\mathbf{C}} = C\mathbf{J}_{N-1}$ where $\mathbf{J}_{N-1}$ takes the following form:

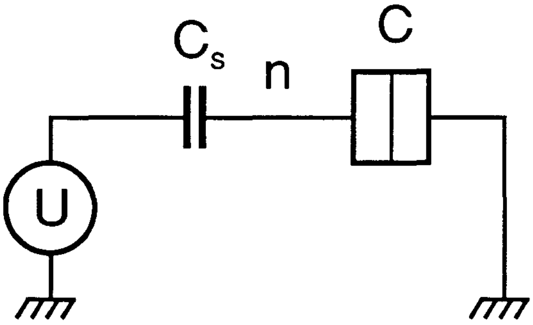

Fig. A2. *The single electron box circuit is the simplest circuit containing one island and consists of a tunnel junction and a capacitor placed in series. The voltage source is connected to the capacitor. The only degree of freedom is the number n of excess electrons on the island.*

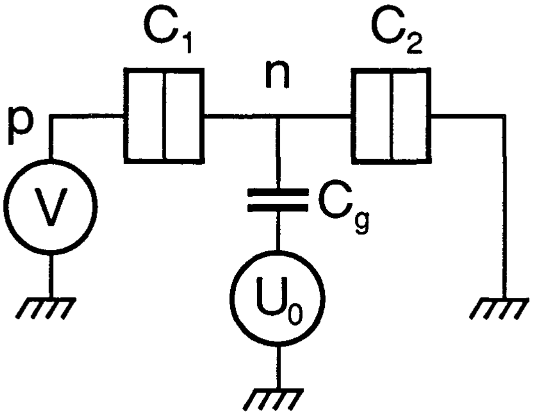

Fig. A3. *The single-electron transistor (SET) has one island and two degrees of freedom: the number n of excess electrons on the island, as in the electron box, and also the number p of electrons which have passed through the voltage source V.*

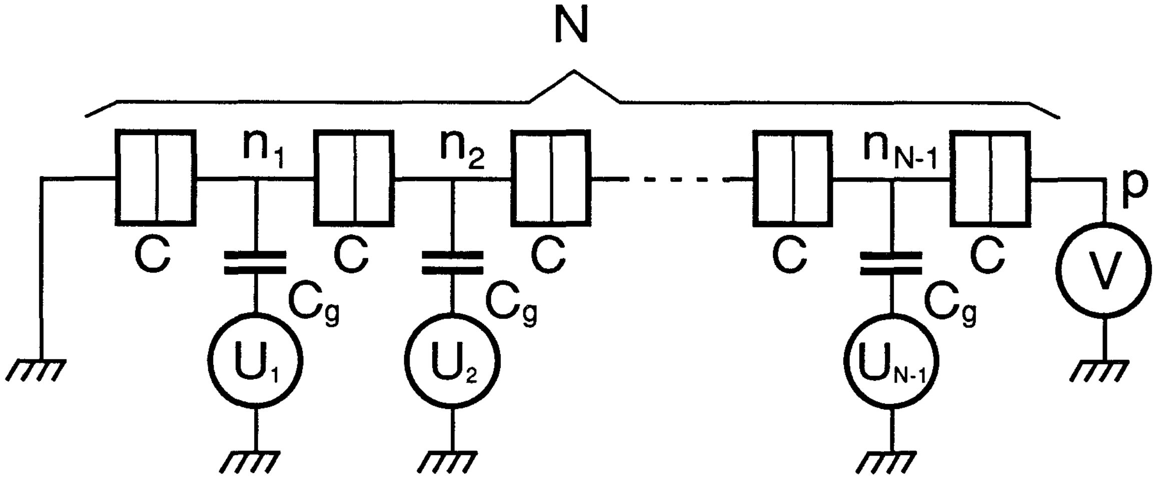

Fig. A4 *Circuit schematic of the N-pump. We assume that the capacitance C_g of the gates is much smaller than the junction capacitance C.*

$$\mathbf{J}_{N-1}=\overbrace{\begin{pmatrix} 2 & -1 & 0 & \cdots \\ -1 & \ddots & \ddots & \ddots \\ 0 & \ddots & & \\ \vdots & \ddots & & \\ & & & \end{pmatrix}}^{N-1} . \tag{17}$$

One can show that $\det \mathbf{J}_{N-1} = N$ and obtain:

$$\tilde{C}_{i,j}^{-1}=\frac{1}{C}\frac{\det\mathbf{J}_{i-1}\det\mathbf{J}_{N-1-j}}{\det\mathbf{J}_{\mathrm{N}-1}}=\frac{i(N-j)}{NC}\ . \tag{18}$$

We finally deduce the energy E_i of the N junction pump after i tunnel events:

$$E_i=\frac{i}{N}\left((N-i)e^2/2C-eV\right)\ . \tag{19}$$

Ideal pumping of electrons would be achieved in the N junction pump by applying successive triangular voltage pulses to the islands through the gate capacitors [5]. In that case, when the gate charge of island k is not zero, it evolves in time in such a way that $\tilde{q}_k+\tilde{q}_{k+1}=e$. Similar calculations can be done in order to obtain the energy difference E_i in that particular case.

REFERENCES

[1] D. V. Averin and Yu. V. Nazarov, in *Single Charge Tunneling*, edited by H. Grabert and M. H. Devoret (Plenum, New York, 1992), Chap. 6.

[2] G.-L. Ingold and Yu. V. Nazarov, in *Single Charge Tunneling*, edited by H. Grabert and M. H. Devoret (Plenum, New York, 1992), Chap. 1.

[3] T. A. Fulton and G. J. Dolan, Phys. Rev. Lett. **59**, 109 (1987).

[4] D. Esteve, in *Single Charge Tunneling*, edited by H. Grabert and M. H. Devoret (Plenum, New York, 1992), Chap. 3.

[5] H. Pothier, P. Lafarge, D. Esteve, C. Urbina and M. H. Devoret, IEEE Trans. Instrum. Meas. **42**, 324 (1993).

APPENDIX 2

FABRICATION OF THE SUPERCONDUCTING/NORMAL TUNNEL JUNCTIONS

Electron box experiments require the use of ultrasmall tunnel junctions with nanometric dimensions. In our samples, such junctions were fabricated by the overlap of two metallic thin films evaporated at two different angles through a suspended mask [1,2]. We describe here the particular technique which we have used to fabricate superconducting/normal tunnel junctions.

The first samples of electron box circuit were fabricated using a metallic suspended mask made out of Germanium [3,4]. The fabrication of such a mask involves depositing three layers on the substrate: an underlying PMMA (Polymethyl Methacrylate) resist layer, a thin germanium film, and a top PMMA layer. The circuit pattern was first defined on the top PMMA layer by electron beam lithography. It was then transferred to the Ge layer by a non-isotropic reactive ion etch. Finally the suspended mask was obtained by an isotropic etch of the bottom PMMA layer. For the fabrication of the normal/superconducting box circuit we have used a fabrication technique which only requires two layers of resist. The spinning of the two resist layers is done following the method of Courtois at CRTBT [5]. The principle of junction fabrication is the same but the suspended mask is directly obtained with the top layer of PMMA.

In our "bilayer", the underlying resist layer is made of PMMA/MAA copolymer resist grade 1660098 solved at 70g/l in 2-ethoxyethanol. The top layer is made of PMMA (Polymethyl Methacrylate) Homopolymer WT 950000 solved at 15g/l in chlorobenzene (Fig. A5a). Just before spinning the resist, we filter it in a 5.0 µm MILLIPORE filter. The support layer is spun at a speed set between 850 rpm and 1000 rpm, yielding a film with measured thickness between 650 nm and 330 nm. After exposure (Fig A5b), the sample is immediatly developed in a solution of MIBK(1) Propanol-2(3) for 40 seconds at 20 °C. The development plays a double role: it precisely reproduces the pattern on the top PMMA layer by removing the exposed areas and simultaneously removes the bottom resist layer around the openings in the top mask yielding an undercut mask profile. Therefore, only the narrow lines of the mask

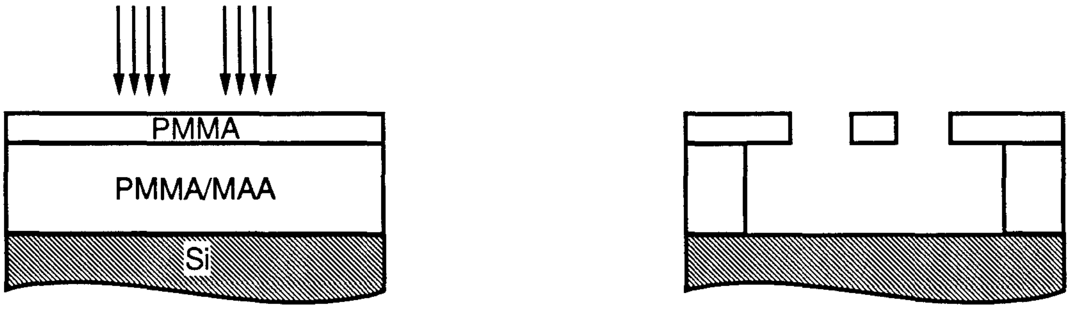

a) e-beam exposure

b) development

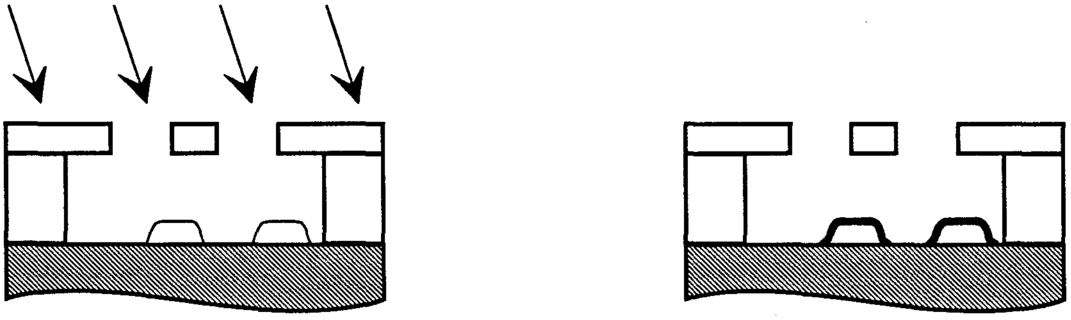

c) first evaporation ex: Al

d) oxidation

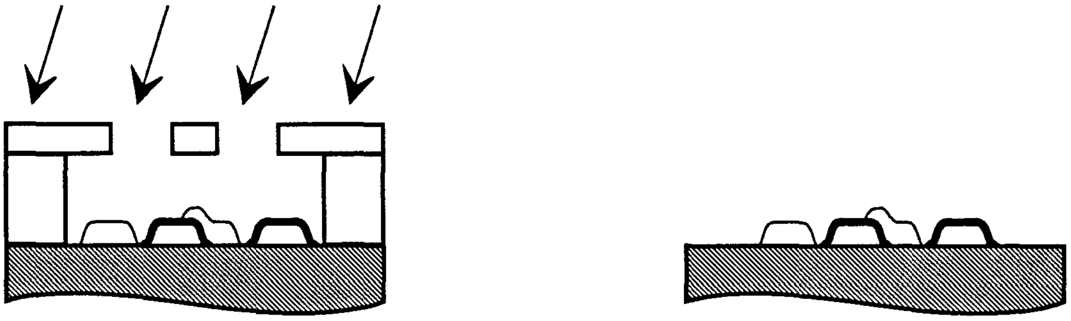

e) second evaporation ex:Cu

f) lift-off

Fig. A5 *Successive fabrication steps of a tunnel junction using a bilayer resist and the shadow mask evaporation technique.*

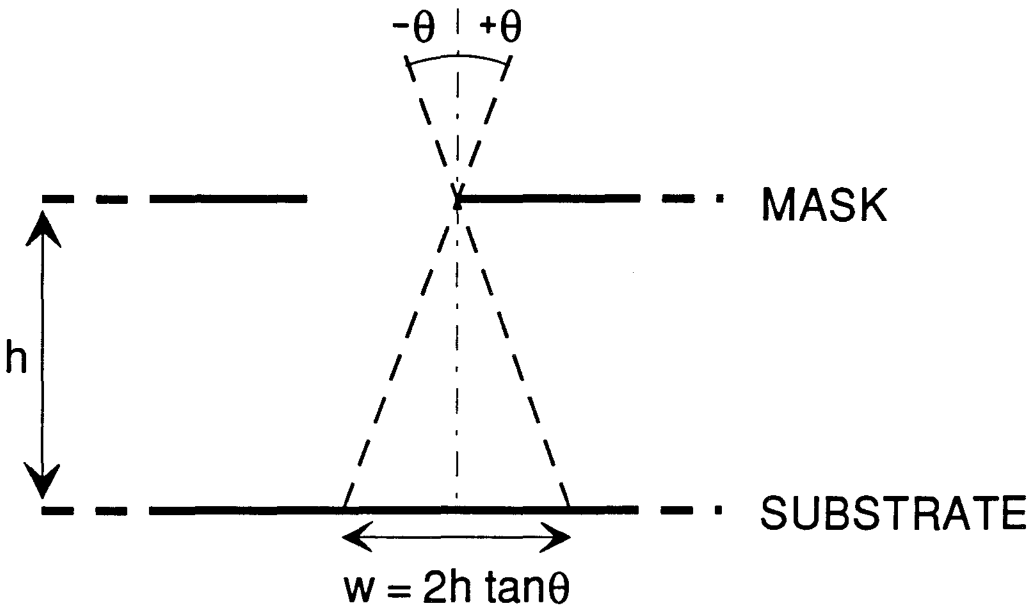
-θ
+θ
MASK
h
SUBSTRATE
w = 2h tanθ

Fig. A6 *Schematic view of the offset between the two images of the suspended mask obtained after a double angle evaporation at angle* $-\theta$ *and* $+\theta$.

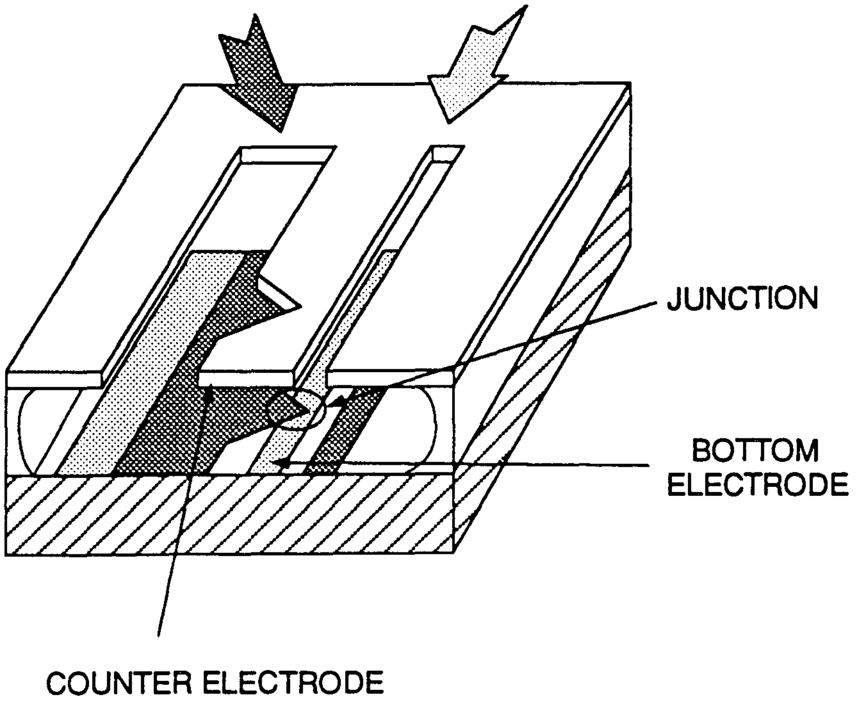
JUNCTION
BOTTOM ELECTRODE
COUNTER ELECTRODE

Fig A7 *Fabrication of a junction by the shadow mask evaporation technique. The junction is obtained at the overlap between the two metallic films produced by two evaporations over a suspended bridge.*

become completely suspended over the substrate, while the other non-exposed parts of the top PMMA layer remain supported by the underlying PMMA/MAA layer (see Fig. A5c). The main benefit of the bilayer process is to suppress the etch step of the Ge layer. It allows a better resolution of the final mask since there is no longer a transfer of the pattern from the resist to the Ge layer. It suppresses also the eventual residues which can be deposited on the Si substrate by etching a metallic film and which can prevent from forming reliable oxyde barriers. However, one has to take into account two undesirable effects: i) on a bilayer resist, the electron beam exposure is non local, ii) the PMMA suspended mask is not so stiff as a metallic mask.

The substrate is an oxidized 2-inch silicon wafer (PURE-SIL, diam 2", thick 275 +/-25, class prime, dope boron, +5000 Å oxyde). After having been covered by the two layers of resist, the wafer is cut in $9\text{mm} \times 9\text{mm}$ chips. Electron beam exposure is done with a modified JEOL 840A scanning electron microscope (SEM). Electrons are accelerated at 35 kV and the standard charge dose is $2\ \text{pC}/\mu\text{m}^2$. The beam blanker and the deviation of the electron beam of the microscope are controlled with a Hewlett-Packard HP 1000 computer through digital-analog converters. The whole pattern, from the submicron junctions until the millimeter size pads, is written by the electron beam of the SEM in four successive magnification steps. The pattern of the mask is generated from a source file by a custom computer program already described by Pothier [3].

In the shadow mask evaporation technique [1], the offset w between two images of the suspended mask, evaporated respectively at $-\theta$ and $+\theta$ from the normal incidence, is given by $w = 2h\tan\theta$ where h is the height of the mask over the substrate (Fig. A6). Typically in our samples, $h \approx 500$ nm, $\theta \approx 15°$, and w never exceeds 200 nm. Therefore, for large scale pattern (> 10 µm), the offset is irrelevant and the result of the evaporation can be considered as a metallic picture of the pattern. At smaller scales, however, the offset becomes relevant. After a double evaporation over a suspended bridge of width d, one obtains under the bridge an overlap region of width $w - d$.

We deposit metallic thin films with an electron gun evaporator. The sample orientation is controlled by the use of a rotating sample holder. We first deposit 30 nm of aluminum

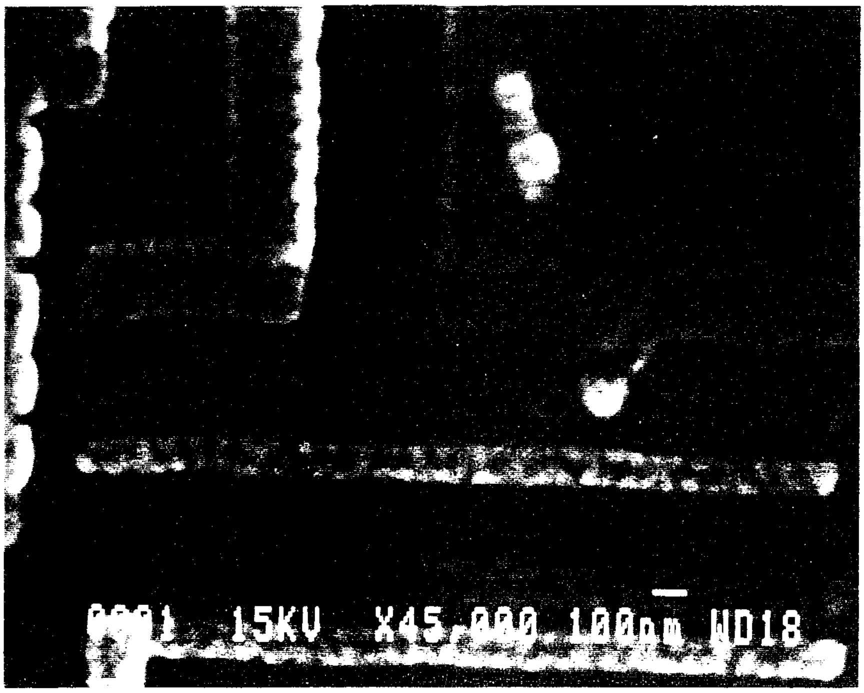

Fig. A8 *Scanning electron microscope photograph of an electron box circuit. Light gray areas correspond to copper covered surfaces and dark gray areas to aluminum covered surfaces. The grain is due to the thin film of gold deposited on the sample in order to enhance the contrast of the photograph. The tunnel junction corresponds to the triangular white dot. The island of the box consists of the single horizontal metallic strip. Note that there is no contact between the two images of the island resulting from the two successive evaporations.*

(99.999 % pure) at 1.0 nm/s at an angle $-\theta$ relative to normal incidence (Fig. A5d). The evaporation angle is adjusted to take into account the thickness of the underlying resist layer. Typically, this angle is set between 11° and 19°. During the evaporation, the pressure does not go above 2.10^{-6} mb. The superconducting electrode of the junction and hence the superconducting island of the box is obtained with this aluminum evaporation. Aluminum can be evaporated at a temperature such that the resist mask is not damaged and can be still used for a second evaporation. A reliable insulating barrier is produced by oxidizing the surface of the aluminum. For that purpose, we introduce few mb of oxygen in the vacuum chamber during 3 mn (Fig. A5e). Depending on the required tunnel resistance, the oxygen pressure is set between 0.5 and 5 mb. Then we deposit 50 nm of copper (99.99 % pure) alloyed with 3 % in weight of aluminum [6] with the same conditions as for the first metallic layer but with an opposite evaporation angle $+\theta$ (Fig. A5f). The superconducting/normal tunnel junction is formed by the overlap of the oxidized aluminum and the copper (see Fig. A7). By varying the angle θ, the width d of the bridge, and the length of the overlap, one can adjust the area of the junction. Areas smaller than 100 nm x 100 nm and tunnel resistances between 25 kΩ and 300 kΩ are commonly obtained. A scanning electron microscope photograph of a normal/superconducting electron box circuit is shown on Fig. A8.

Finally, the resist is lifted-off by placing the sample in a bath of acetone at 50 °C for 10 minutes. Immediatly after the lift-off, the junctions are tested at room temperature. In order to measure its tunnel resistance, the circuit is shunted by a high impedance variable resistor and connected to a multimeter by 1 MΩ resistors.

REFERENCES

[1] G. J. Dolan, Appl. Phys. Lett. **31**, 337 (1977).

[2] G. J. Dolan and J. H. Dunsmuir, Physica **B 152**, 7 (1988).

[3] H. Pothier, PhD. Thesis, Université Paris 6 (1991), unpublished.

[4] L. J. Geerligs, V. F. Anderegg, C. A. van der Jeugd, J. Romijn and J. E. Mooij, Europhys. Lett. **10**, 79 (1989).

[5] H. Courtois, private communication.

[6] J. Clarke, in *Non-equilibrium Superconductivity*, edited by D. N. Langenberger and A. I. Larkin (Elsevier, Amsterdam, 1983), Chap. 1.

Superconducting/Normal Tunnel Junctions Bilayer Processing Sequence:

(1) Substrate

2-inch oxidized silicon wafer.

(2) Resist deposition:

First layer:	PMMA\MAA, 70g/l in 2-ethoxyethanol, filtered. spin at 850-1200 rpm (depending on the thickness required) for 60 s. bake on an hot plate for 15 mn at $T = 160\ ^\circ C$.
Second layer:	PMMA (950 K), 15 g/l in chlorobenzene, filtered. spin at 1000 rpm for 60 s. bake on an hot plate for 15 mn at $T = 160\ ^\circ C$.

(3) Electron beam exposure

Electrons accelerated by a voltage of 35 kV, standard dose 2 $pC/\mu m^2$.

(4) Chemical development

Develop for 40 s in a solution of 1:3 MIBK:Propanol-2 at $T = 20^\circ C$.

Rinse in Propanol-2.

(5) First evaporation

Deposit 30 nm Al at 1.0 nm/s, $P = 10^{-6}$ mb, at an angle $10^\circ < \theta < 20^\circ$ from normal incidence.

(6) Oxidation

Introduce 0.5 to 5 mb of oxygen in the vacuum chamber for 3 mn.

(7) Second evaporation

Deposit 50 nm CuAl (3% in weight) at 1.0 nm/s, $P = 10^{-6}$ mb, at an angle $-\theta$.

(8) Lift off

Immerse substrate in acetone at $T = 50^\circ C$ for 10 mn.

APPENDIX 3

THE SINGLE ELECTRON TRANSISTOR

The SET electrometer

The single-electron transistor (SET) [1] is a device based on ultrasmall tunnel junctions which we have used as an electrometer in order to measure the variations of the island charge of the electron box circuits. The SET consists of two tunnel junctions of capacitances C_1 and C_2 placed in series and biased with a voltage source V. The central island delimited by the two junctions is also connected to a gate voltage U_0 through a capacitor C_g (Fig. A3).

We have described the principle of the SET electrometer in Sec. 4.2.1. The state of this device is described by the number n of excess electrons on the island and by the number p of electrons having passed through the voltage source V. The total electrostatic energy of the device is $E = \left(ne - C_1V - C_gU_0\right)^2 / 2C'_\Sigma - C_1V^2/2 - C_gU_0^2/2 - peV$ (see appendix 1), where C'_Σ is the total capacitance of the island of the SET. At $T = 0$ and $V > 0$, the conduction through each junction of the SET is blocked if the total energy of the two states $(n = -1, p = +1)$ and $(n = 1, p = 0)$ is greater than the energy of the initial state $(n = 0, p = 0)$. The current-voltage characteristic of the SET exhibits thus a voltage gap depending on the induced gate charge C_gU_0. For a given value of the bias voltage V, the current I through the device as a function of C_gU_0 is an e-periodic modulation. Since a small amount of the induced charge, smaller than the charge quantum e, results in a variation of the current I, the SET can be used as an electrometer [2].

The behavior of the SET electrometer has been much investigated both experimentally [1,3,4,5,6] and theoretically [7,8,9,2,10]. The experimentals values of the capacitances and tunnel resistances of the junctions can be deduced from the measurements of the current-voltage characteristics of the device. The voltage gap of the I-V characteristic of the single-electron transistor can be predicted, at $T = 0$, by considering the stability diagram of the charge state $(n = 0, p = 0)$ of the system as a function of the bias voltage V and the gate charge C_gU_0. When $V > 0$, the boundary of the stability domain of the state $(n = 0, p = 0)$ are thus given by the two equations $-(C'_\Sigma - C_1)V + e/2 + C_gU_0 = 0$ and $-C_2V + e/2 - C_gU_0 = 0$. These two equations are sufficient since the stability diagram is e-periodic in C_gU_0 and symmetric with the bias voltage V. The stability diagram of the SET is shown on Fig. A9a. One can distinguish two types of I-V characteristics depending on the gate charge C_gU_0: maximum voltage gap characteristic when $-eC_g/2(C_g+C_2) \bmod e < C_gU_0 < +eC_g/2(C_g+C_2) \bmod e$ and reduced voltage gap characteristic when $eC_g/2(C_g+C_2) \bmod e < C_gU_0 < e/2 \bmod e$. The two quantities $C'_\Sigma - C_1$ and C_2 can be inferred from measurements of the voltage gap of the I-V characteristic at the lowest temperature. The sum $R_1 + R_2$ can be inferred from the measurement of the I-V characteristic at large voltages.

In our normal/superconducting electron box experiment, the SET electrometer is made with normal/superconducting junctions and its island is superconducting. For the states $(n=1, p=+1)$ and $(n=-1, p=0)$ with an odd number of electrons on the island we now must add the energy Δ of a quasiparticle inside the superconducting island (see Sec. 2.2.1) to the electrostatic energy of the circuit. Hence, the boundary of the stability domain of the SET are build with the two following equations: $-(C'_\Sigma - C_1)V + e/2 - C'_\Sigma\Delta/e + C_gV_g = 0$ and $-C_2V + e/2 + C'_\Sigma\Delta/e - C_gV_g = 0$ (see Fig. A9b). From the measurements of the voltage gap of the I-V characteristic one can extract the capacitances of the junction but also the value of the superconducting gap Δ of the island.

Measurement of the island charge

Practically, the SET electrometer is fabricated in situ at the same time as the electron box and its central island is coupled to the island of the electron box circuit by a capacitor of capacitance C_c (see Sec 3.1.1,3.2.1 and Fig. A10).

The chip on which the experimental circuit has been fabricated is glued on a copper sample holder thermally anchored to the mixing chamber of a dilution refrigerator. The contacts between the measurement wires and the circuit pads are done with silver paint. The voltage bias of the electrometer is provided by a voltage dividing bridge. The current I through the electrometer is measured from the voltage drop across a resistor of 12.07 MΩ placed in series with the device. This resistor and the resistor providing the voltage bias are mounted at

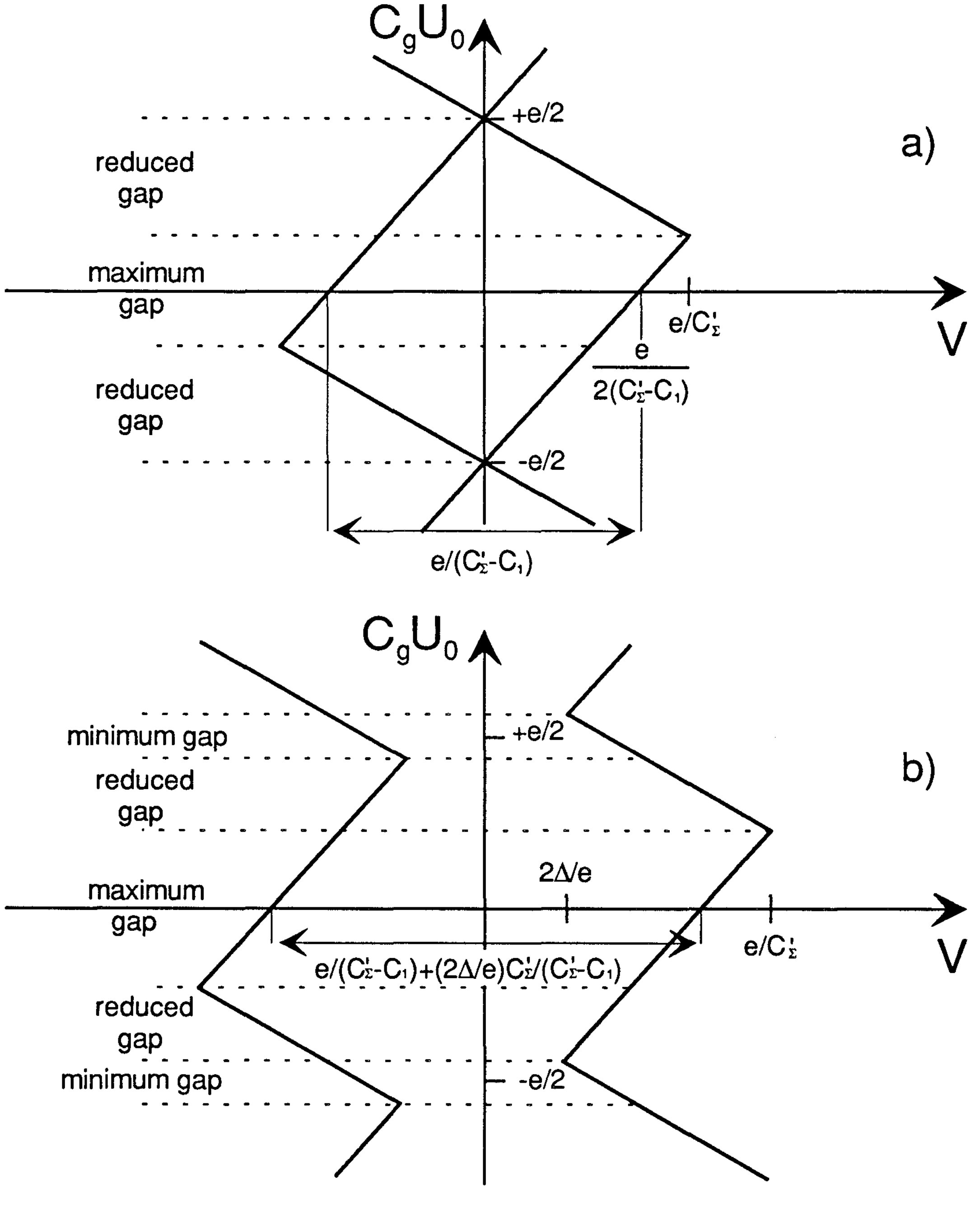
C_gU_0
+e/2
a)
reduced gap
maximum gap
reduced gap
-e/2
e/C'_Σ
e/2(C'_Σ-C_1)
V
e/(C'_Σ-C_1)
C_gU_0
minimum gap
+e/2
reduced gap
b)
maximum gap
2Δ/e
e/C'_Σ
V
e/(C'_Σ-C_1)+(2Δ/e)C'_Σ/(C'_Σ-C_1)
reduced gap
minimum gap
-e/2

Fig. A9 *Stability diagram of the single-electron transistor as a function of the bias voltage V and the induced gate charge* C_gU_0. *Only the cell corresponding to the state* $n = 0$ *is completely represented and we have assumed that* $C'_\Sigma - C_1 > C_2$. *The horizontal dotted lines delimit different regimes of the I-V characteristic of the SET depending on* C_gU_0. a) *Single-electron transistor in the normal state.* b) *Normal/superconducting/normal single-electron transistor. The energy gap of the superconducting island of the SET is denoted by* Δ.

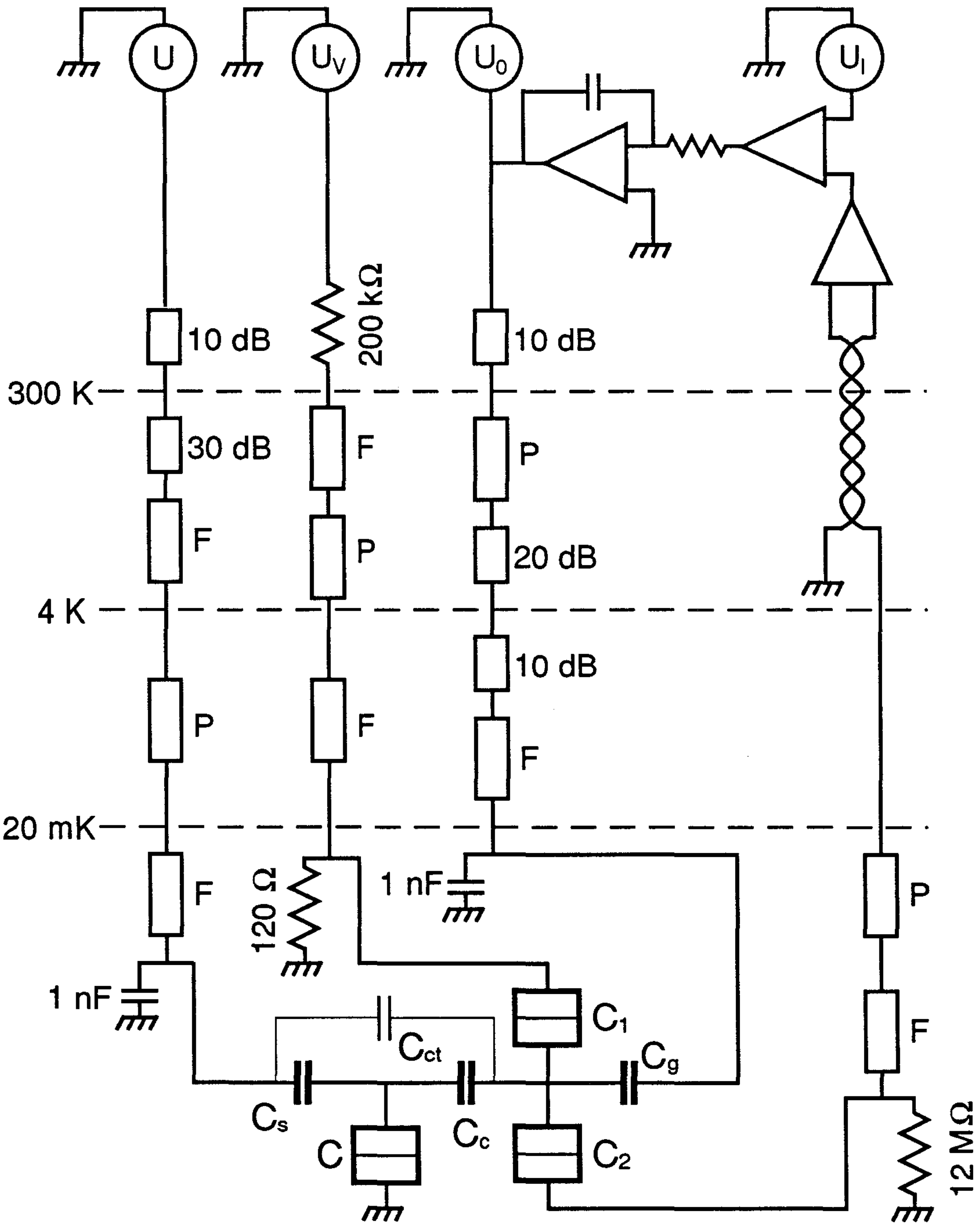
U
U_V
U_0
U_I
10 dB
200 kΩ
10 dB
300 K
30 dB
F
P
P
20 dB
F
P
4 K
10 dB
P
F
F
20 mK
F
120 Ω
1 nF
P
1 nF
C_ct
C_1
C_g
F
C_s
C
C_c
C_2
12 MΩ

Fig. A10 *Schematic of the experimental set up. The capacitance* C_{ct} *is the cross-talk parasitic capacitance coupling the electron box voltage line and the island of the electrometer. The dashed lines represent the intermediate shielding stages. The values in dB's refer to commercial microwave attenuators. The symbols F and P indicate respectively resistive film microwave filters and powder microwave filters described by Pothier [11]. A feed-back loop ensures that the current through the electrometer remains equal to a constant value set by* U_I*. The voltages* U *and* U_0 *implement the corresponding voltages of Fig. 1 in paper 2 (Sec. 3.2.1) while* U_V *sets the value of the transport voltage V in the same figure.*

the lowest temperature stage of the experiment and this circuitry is shielded in a closed copper box. The sample is placed at the center of a superconducting magnet which can produce a magnetic field of 1 T perpendicular to the surface of the sample. The experimental set-up is described in Fig. A10. The electrometer gate line and the electron box voltage line are coaxial lines with filters depicted in Fig. A10.

The average charge $\langle Q_c \rangle$ induced on the coupling capacitor C_c is given by $\langle Q_c \rangle = C_c/C'_\Sigma(-\langle n \rangle e + C_s U) + C_{ct}U$, where C_{ct} is the cross-talk capacitance which directly couples the voltage U the to the island of the electrometer. A variation $\Delta\langle Q \rangle$ of the box island charge $\langle Q \rangle = -\langle n \rangle e$ yields a variation $\Delta\langle Q_c \rangle = (C_c/C'_\Sigma)\Delta\langle Q \rangle$ of the gate induced charge of the electrometer. The coupling coefficient C_c/C'_Σ between the island of the box and the island of the electrometer is determined from the curve which gives the electrometer current I versus the electron box voltage U (Fig. 6 of Sec. 3.1.1). This curve presents a short-period sawtooth modulation superimposed on a large-amplitude one. The former one arises from the discrete variations of the island charge of the electron box and the latter one originates from the cross-talk capacitance C_{ct} which directly coupled the electrometer island to the voltage source U. The period of the large-amplitude "cross-talk" modulation corresponds to a variation of the charge induced on the electrometer island equal to e. On the other hand, each small-amplitude events results from a variation of the charge induced on the electrometer equal to $-(C_c/C'_\Sigma)e$ and is equivalent to a negative voltage offset of the large-amplitude modulation curve. The coefficient C_c/C'_Σ is thus given by the ratio of this voltage offset and the period of the "cross-talk" modulation.

In order to measure the variations of the box island charge $\langle Q \rangle$ as a function of the voltage U applied to the box, we have used two differents methods. In the former one which is described in Sec. 3.1.1, we measured the variations of the current I through the electrometer which are proportional to the variations of the island box charge.

In the latter method, used for the normal/superconducting electron box experiment (Sec. 3.2.2), a feed-back loop acts on the electrometer gate line and maintains a constant current through the electrometer. First the feed-back loop is open and by adjusting the electrometer bias voltage V we maximize the amplitude of the current modulation as a function of the electrometer gate voltage U_0. Then we switch the feed-back loop on and we set the target current to the value corresponding to the maximum of $\partial I/\partial U_0$. Finally, we sweep the voltage U applied on the electron box island and we record the voltage injected by the feed-back loop in the electrometer gate line. The variations of this latter quantity are proportional to the variations of the average charge $\langle Q_c \rangle$ induced on the coupling capacitance. Before recording, we substract to the signal a linear term whose coefficient is adjusted in order to give a signal with a staircase shape defined by horizontal steps. If we have determined the coupling coefficient C_c/C'_Σ, this measurement method does not require any other calibration and thus one can directly compare experimental Coulomb staircases obtained at different temperatures or at different values of the magnetic field.

REFERENCES

[1] T. A. Fulton and G. J. Dolan, Phys. Rev. Lett. **59**, 109 (1987).

[2] A. N. Korotkov, D.V. Averin, K.K. Likharev and S. A. Vasenko, in *Single-Electron Tunneling and Mesoscopic Devices*, ed. by H. Koch and H. Lübbig (Springer, Berlin, 1992).

[3] T. A. Fulton, P. L. Gammel, D. J. Bishop, L. N. Dunkleberger, and G. J. Dolan, Phys. Rev. Lett. **63**, 1307 (1989).

[4] L. J. Geerligs, D. V. Averin and J. E. Mooij, Phys. Rev. Lett. **65**, 3037 (1990).

[5] T. M. Eiles, G. Zimmerli, H. D. Jensen, and John M. Martinis, Phys. Rev. Lett. **69**, 148 (1992).

[6] G. Zimmerli, T. M. Eiles, R. L. Kautz, and John M. Martinis, Appl. Phys. Lett. **61**, 237 (1992).

[7] I. O. Kulik and R. I. Shekter, Zh. Eksp. Teor. Fiz. **68**, 623 (1975) [Sov. Phys. JETP **41**, 308 (1975)].

[8] D. V. Averin and K. K. Likharev, in *Mesoscopic Phenomena in Solids*, ed. by B. Al'tshuler, P. Lee, and R. Webb (Elsevier, Amsterdam, 1991), Chap. 6.

[9] D. V. Averin and A. A. Odintsov, Phys. Lett. **A 149**, 251 (1989).

[10] Yu. V. Nazarov, J. Low. Temp. Phys. **90**, 77 (1993).

[11] H. Pothier, PhD. Thesis, Université Paris 6 (1991), unpublished.